CREATING NEW FOOD MICROSTRUCTURE: AERATED HYDRO AND AEROGELS

Saniye Samanci, M.Sc.

Thesis submitted to the University of Nottingham

for the degree of Doctor of Philosophy

February 2019

To my father and my son

ABSTRACT

Aerated products are common in our daily life and bubbles in aerated products are either created by design or they are formed as a natural result of the processing steps and plays an important role in creating new structure, appearance, texture and giving a different mouthfeel. Aerogels are very light weight materials and can be made from various materials, such as polysaccharides, cellulose and proteins. The term “aerogel” was used to describe the gels that have been dried under supercritical conditions. However, in recent years the gels made by using other drying techniques, such as freeze drying, are also termed aerogels. In this research the main aim was to investigate the inclusion (aeration process), structuring and control of air as an active ingredient to generate a porous structure (air bubbles), which might be used to further control air cells in other formulations. A one-pot approach was used to create aerated hydrogel based on alginate ionic gelation in the presence of calcium carbonate ($CaCO_3$) and glucono-delta lactone (GDL), cellulose derivatives including HPMC-K100M and K4M, MC-A4, non-starch polysaccharide locust bean gum (LBG) and whey protein isolate (WPI). It was recorded that the control of structuring was alginate gelation driven. However, adding MC/HPMC to alginate+ WPI hydrogels improved gel strength significantly with smaller air cells. Aerogels containing LBG had more intact air cells compared to other polymers with slow freezing while fast freezing provided more intact air cells in the final aerogels made of alginate, WPI and K100M.

In this this research, it was also identified that time and temperature control before and also during aeration are important parameters for the formation of self-supporting aerated hydrogels. Optimization of mixing speed was another parameter that had a crucial effect to obtain homogenous gel structure containing more air cells and higher overrun.

ACKNOWLEDGEMENTS

I would like to thank my supervisor Prof Tim Foster, a Division of Food Science, School of Biosciences, the University of Nottingham, for providing this PhD opportunity for me, for his help, excellent guidance, and invaluable contribution throughout this study. I also would like to thank my second supervisor Simon Lawton, PepsiCo UK, for his useful discussions, guidance on data analysis and excellent advice. I would like to thank Christine Grainger-Boultby for Cryo- SEM and SEM, Denise Mclean for TEM microscopic analysis, Craig Sturrock for X-ray computed microtomography imaging and Dr Vinzenzo Di Bari for rheometer training. I would like to thank my dear family and amazing friends who has been with me throughout this challenging study.

Finally, I would like to acknowledgment the financial support that I received from PepsiCo UK.

TABLE OF CONTENTS

CHAPTER: 2

Materials and Methods

CHAPTER: 3

Developing a new method for protein-polysaccharide based aerated aerogels and improvement of hydrogel and aerogels by means of optimising the method of production and material usage

CHAPTER: 4

Understanding effects of physical and chemical parameters on aerated hydrogel and aerogel characteristics

CHAPTER: 5

CHAPTER: 6

CHAPTER: 7

ABBREVIATIONS

ACC	Amorphous calcium carbonate
Ar	Argon
AT:	Aeration time
Ba^{2+},	Barium ion
BET	Brunauer–Emmett–Teller
BSA	Bovine serum albumin
CA	Cellulose acetate
Ca^{2+}	Calcium ion
Ca-alginate	Calcium alginate
$CaCl_2$	Calcium chloride
$CaCO_3$	Calcium carbonate
$CaSO_2$	Calcium hyposulfite
$CaSO_4$	Calcium sulfate
C_g	Critical protein concentration
CMC	Carboxymethylcellulose
CO_2	Carbon dioxide
COLD	Low temperature supercritical drying
DCCA	Drying-control chemical additives
DLS	Dynamic light-scattering
DP	Degree of polymerization
EC	Ethyl cellulose
EtOH	Ethanol
FF	Flow-focusing
G	Guluronic
GDL	Glucono delta- lactone
GG	Guar gum
GMP	Glycomacropeptide
He	Helium
HEC	Hydroxyethylcellulose

HOT	High temperature supercritical drying
HPMC	Hydroxypropylmethylcellulose
I.S	Ionic strength
kPa	KiloPascal
LBG	Locust bean gum
LF	Lactoferrin
LM-pectin	Low-methoxyl pectin
LP	Lactoperoxide
LZ	Lysozyme
M	Mannuronic
MC	Methylcellulose
MC	Microchannel
MCC	Calcium carbonate monohydrate
MCT	Medium chain triglyceride
MEN	Menadione
Mg^{2+}	Magnesium ion
mPa	MilliPascal
N_2	Nitrogen
N_2O	Nitrous oxide
NaCl	Sodium chloride
Ne	Neon
NFC	Nanofibrillated cellulose
NHS	National Health System
nm	Nanometer
OPN	Osteopontin
OR	Ostwald ripening
OR (%)	Overrun
PER	Protein efficiency ratio
pI	Isoelectric point
pKa	Acid disassociation constant
PP	Proteose peptone
RF	Resorcinol–formaldehyde

rpm	Rotation per minute
SA	Sodium alginate
$scCO_2$	Supercritical CO_2 drying,
SE	Spontaneous emulsification
SEM	Scanning electron microscopy
Semi-IPN	Semi-inter penetrating network
SPG	Polymeric and Shirasu Porous Glass
$SrCO_3$	Strontium Carbonate
TAC	Triacetyl cellulose
T_C	Critical temperature
TEM	Transmission electron microscopy
TOC	α-tocopherol
WP	Whey protein
WPC	Whey protein concentration
WPI	Whey protein isolate
WPM	Whey protein microgels
WPSA	Whey protein soluble aggregates
Xe	Xenon
µCT	X-ray computed microtomography

CHAPTER 1

Background

Food aeration: history, methods, stability mechanism and applications

1.1. Introduction

Food aeration is one of the oldest methods in food production and its history goes back to the invention of raised bread in Egypt 6000 years ago. Aerated products are common in our daily life, *e.g*., bread, egg foams, breakfast cereals, chocolates or drinks. Bubbles in aerated products are either created by design as in aerated chocolate, or they are formed as a natural result of the processing steps as in bread making. This depends on the inclusion method used to introduce air into a food system, and plays an important role in creating new structure, appearance and texture.

The main result of aeration is changing texture and rheology of the product and giving a different mouthfeel and appearance. The other aspect of the food aeration, which has been getting great attention, is reduction in the energy density of the product (Campbell and Mougeot, 1999). The effects of aerated foods and drinks on satiety and energy intakes have been studied by many researchers and has been suggested that high volume foods with low energy density can promote satiety and reduce daily energy consumption (Rolls et al., 2000; Rolls and Roe., 2002; Osterholt et al., 2007; Arboleya et al., 2014; Blom et al., 2016; Peters et al., 2015; Murray et al., 2014; Melnikov et al., 2014).

Different techniques (whipping, shaking, steam formation, chemical leavening) are used in order to introduce air or some other gases into a food matrix such as a liquid or viscous solution, where it is entrapped and forms a foam, reducing density and increasing volume. However, aerated materials are thermodynamically unstable due to larger interface between continuous and dispersed phase. In a liquid system, over time they will break down eventually and separate into two phases-gas and liquid (Fameau and Jalmes, 2017; Lazidis et al., 2016,

Campbell and Mougeot, 1999) in order to reach a more stable state that minimizes their interfacial area and their free energy (Amagliani and Schmitt, 2017). The rheology and interfacial activity of the aerated systems usually control the stability. Control depends on stabilisation mechanism, where the lifetime of aerated systems varies from seconds to minutes, as in beer and wine, to years as in extruded, expanded and confectionary products.

Aerogels are extremely light weight materials with nano scale open-cells. They can be made from various materials, such as polysaccharides and proteins. Initially a gel is formed, then the fluid is removed from the hydrogel by various methods (freeze drying etc.) and only the solid structure is left behind. Aerogels were first developed in 1930s by Kistler, who made silica aerogels with a combination of equal volumes of sodium silicate and hydrochloric acid. There are several steps that are involved in making aerogels. These are: gel preparation by sol-gel process, ageing of the gel in its mother solution to prevent the gel from shrinkage during drying, and drying of the gel under special conditions to prevent the gel structure collapsing (Sudhakar et al., 2016).

The term “aerogel” originally was used to describe the gels that have been dried under supercritical conditions. However, in recent years the gels made by using other drying techniques, such as freeze drying, are also termed aerogels. Although there is not any official definition of aerogels, they can only be justified if the pores actually occupy very high percentage of a sample volume, e.g., above 90% (Pierre and Pajonk, 2002).

The traditional drying technique for aerogels is supercritical drying. Principally, during supercritical drying the wet gel is heated in a closed container to exceed the pressure and

temperature above critical point of the liquid entrapped in the pores inside the gel (Pierre and Pajonk, 2002). There are 2 types of supercritical drying: high temperature supercritical drying (or HOT) and in alcohol low temperature supercritical drying (COLD) in CO_2. Freeze drying is also another method and is used widely (Maleki et al., 2016).

In this research, aerated hydro and aerogels with very low dry mass content (0.5%) were created by using a new method based on one pot approach and ionic cross-linking gelation, which are believed to be novel for making food grade aerogels that contain a high level of air (higher overrun) and very low dry mass. In the literature, the concept of "aerated food systems" is well established but "aerated aerogels" is not known yet. The method developed here is based on sol-gel technique, with some modification, and very short processing time (2 hours). It is very easy to apply and can provide high overrun.

The aim of the project is to investigate the inclusion (aeration process), structuring and control of air as an active ingredient to generate a porous structure (air bubbles).

Objectives are:

1. Inclusion (aeration process), structuring and controlling of air as an active ingredient to generate porous structures (air bubbles) by applying designed production, processing parameters and ingredients.
2. Identify and design parameters that may influence and control air cells formation/structure and stability in the final product such as mixing time and mixing speed.
3. Explore ingredient functionality for pre-formulation of excipients- air cell stabilisers- methylcellulose, whey protein isolate and alginate and their effect on stabilisation of air cells.
4. Understanding the effect of the different freezing techniques on the air cell structure, size and shape.
5. Application of the created new aerogel production strategy into real food systems.

The scope of this thesis is as follows: Chapter 1 offers a background about food aeration. It details the history of aerated foods, health benefits of food aeration, food aeration methods and stability of the aerated systems; Chapter 2 provides a background to the experiments conducted, describes the materials and methods; Chapter 3 presents information about creation of a new method for producing aerated hydro and aerogels and followed by improvements of the created hydro and aerogels; Chapter 4 is utilised to understand the effect of physical and chemical parameters on hydrogel and aerogels. It also illustrates the application of the created new aerogel production and formulation strategy into real food systems; Chapter 5 is the overall discussion; Chapter 6 consists of general conclusion and future works and Chapter 7 is the reference list.

1.2. What is food aeration?

Aeration is a very old method and has been used for many centuries in order to include air or some other gases (e.g. CO_2 and N_2) within a food system to produce a gas phase and a condensed phase (solid or liquid). There are several ways of incorporating air into a food matrix including biological, chemical and mechanical process. The abundant structural element of aerated food is air bubbles which give different texture and mouthfeel to a product. Air bubbles within a food matrix not only affect texture and mouthfeel, it also affects the appearance, colour and making the product lighter when sold by volume.

Aeration similarly plays an important role in food rheology by altering flow characteristic of fluids and enables them to be moulded and set into more attractive shapes (Campbell and Mougeot, 1999). Although the bubbles are initially dispersed into a viscous solution or in a bulk of liquid systems, the final continuous phase might be liquid (e.g., beer foam), viscoelastic (e.g., marshmallows) or solid (e.g., meringue) (Zuñiga and Aguilera, 2008). It is thought that aerated foods represent the height of culinary art and it could be the best testimony to a chef's skills (Campbell and Mougeot, 1999).

1.3. History of food aeration

Food aeration is a very old method, may back to later part of the Stone Age (Neolithic). Bread is thought to be the first aerated food and raised in Egypt 6000 years ago caused by fermentation (Campbell, 2008, Table 2.1). Although bread and beer have the longest history, however there is an uncertainty about which one comes first (Campbell and Mougeot, 1999).

According to some archaeological data, Egyptians started to use yeast for leavening and brewing as early as 4000 BC. This date is cited for the discovery of leavened bread and beginning of the brewing industry by many food historians. It is believed that the power of yeast was discovered accidently and brewing began with domestication of first cereals (http://www.foodtimeline, 2018).

Dating the origin of beer making precisely still is a mystery. However, most archaeological evidence suggests that fermentation was being used by around 4000 BC to 3500 BC (http://www.foodtimeline, 2018). Discovery of ale was stimulated by the process of bread making. According to Tannahill (1998), the Neolithic era people started to use the grain that had been sprouted and then dried, which made a bread that kept unusually well.

Tannahill (2009) notes that “something very like this was used in brewing. The Egyptian process was to sprout the grain, dry it, crush it, mix it to a dough and partially bake it. The loaves were then broken up and put to soak in water, where they were allowed to ferment for about a day before the liquor was strained off and considered ready for drinking."

Another ancient aerated drink is wine and made from fermented juice of grape. According to archaeological evidence it is believed that the first production of grape wine was carried out at sites in Georgia and Iran – from as early as 6000 BC. However, the traceable roots of modern age of wine begins with the Greeks. Winemaking was spread around the Mediterranean by Greek, Phoenician and Roman colonisation (http://winehistory.com.au. 2018).

Aerated Food category	4000-1000 BC	1000 BC-0 AD	0-1000 AD	1000-1500 AD	1500-1800 AD
Bakery products	Raised bread from ~4000 BC; leavened bread prohibitions from ~1440 BC		Chinese steamed bread; pretzels	Wafers (11th century); Biscuits, (14th century); Brioche (15th century)	Puff pastries (~1500); Cakes, waffles, choux pastry, profiteroles, hot cross buns, crumpets, bagels; Pumpernickel
Dairy foams	Shaken milk?	Butter		Swiss cheese (Emmental) from ~ 1250, Gruyere a little later; Kumiss (fermented milk, frothed prior to consumption)	Whiped cream (at least <16th Century); Fools (stewed fruit mixed into whipped cream (17th century); Ice cream (17th century); Chantilly cream (17th century)
Egg foams					Meringues (1720); Souffle; Zabaglione
Confectionery					Meringues (1720); Syllabub
Breakfast cereals and snacks				Popcorn (Aztecs)	
Beverages	Beer, wine (~6000 BC) First written recipe, for beer (~2000 BC)	Cacao cultivation, consumed as a foamed chocolate drink			Bubbly beer,~1600; Sparkling winem ~1650; Champagne (Dom perognon, ~ 1700); Soda water (Priestly, 1772; Schweppes, 1783)

Table 1.1. Historical timeline of aerated food categories (adapted from Campbel., 2008).

One of the most popular aerated food is ice-cream and its origin may back as far as the second century BC. It is actually not known when and who invented the ice cream. According to historical evidence Alexander the Great was fond of snow and ice flavoured with honey and nectar. The King Solomon also was fond of iced drinks during harvesting. The Emporer who also had passion for flavoured snow was Nero Claudius Caesar (A.D. 54-86). He was sending

his runners frequently into the mountains for snow, which was then flavoured with fruits and juices (http://www.idfa.org, 2018).

Before 1800, ice cream was a very popular exotic rare desert among the elite. However, around 1800, by the invention of insulated ice houses, the ice cream manufacturing became an industry in America (http://www.idfa.org, 2018). And only in 19th century it reached full commercial potential (Campbell and Mougeot, 1999).

Similar to ice-cream, whipped cream, beaten eggs, cakes and pastries became widely available in the 18 Century (Campbell and Mougeot, 1999). Whipped cream is cream that has been whipped where the earliest recipe related to whipped cream was made during August 1661, which is claimed to be about Crème a la Chantilly. The creation of the Crème a la Chantilly is widely attributed to French chef Vatel who worked in the kitchens of the Château de Chantilly (https://ifood.tv/cream/whipped-cream, 2018).

Carbonated water and drinks became available in 1800. Englishman Doctor Joseph Priestly, created first man-made drinkable carbonated water in 1767 (https://www.thoughtco.com, 2018). In 1793 Schweppes Company was founded by Schweppe, who made a big contribution to popularity of the carbonated soft drinks in 1850 and then, the first ever Coca-Cola was sold in Jacob's Pharmacy in 1885, USA, (htpp://brandstories.net, 2018). The aerated chocolate (Aero, Milky Way and Kitkat) was introduced in 1935. However, the production of chocolate actually dates back to 1800 (Campbell and Mougeot, 1999). Cornflakes were discovered by W.K. Kellogg, and his brother, Dr. John Harvey Kellogg in 1898, who accidently flaked wheat

beer. In 1906 W.K. Kellogg opened his “Battle Creek Toasted Corn Flake Company”, after 1914, the cornflakes became a world-wide product (https://www.kelloggs.com, 2018).

1.4. Health benefits of food aeration

Obesity is an emerging health issue of many countries. According to National Health System (NHS) UK, obesity level of the adults in UK is 27 %. The United States has the highest adult obesity level of 38 %. Childhood obesity is also a serious health threat where it is reported to be 10% in reception year (2016/17) and 20% in year 6 (https://files.digital.nhs.uk, 2018). Obesity is generally caused by over-eating and limited physical activity. High energy intake because of high-fat snacks is said to be a major contributor of the obesity.

Bertéus et al. (2005) founded that there is a parallel relationship between energy intake increases and more snacking, which was more frequent in obese subjects than in reference subjects. It is obvious that there is an urgent need to develop a strategy for decreasing the level of energy intake which, in return may reduce the obesity.

There are several ways of developing low caloric foods, to help reduce energy intake, for example use of non-caloric ingredients, immobilizing high quantities of water (Zuñiga and Aguilera, 2008). Increasing satiety of food by incorporating zero-calorie fillers, i.e., water or air is also another approach for controlling daily energy intake (Melnikov et al., 2014).

The effects of aerated foods and drinks on satiety and energy intakes have been studied by many researcher (Rolls et al., 2000; Rolls and Roe. 2002; Osterholt et al., 2007; Arboleya et al., 2014; Blom et al., 2016; Peters et al., 2015; Murray et al., 2014; Melnikov et al., 2014).

Rolls et al. (2000) increased the volume of yogurt-based milkshakes by incorporating different amounts of air and served as preloads 30 min before lunch. The volume of the milk shake significantly affected energy intake at lunch ($P < 0.04$) such that intake was 12% lower after the 600-mL preload (2966 ± 247 kJ) than after the 300-mL preload (3368 ± 197 kcal). They concluded that, the volume of a preload independent, of its energy density can, influence satiety (Rolls et al., 2000).

In similar studies Rolls and Roe (2002), Osterholt et al. (2007), Arboleya et al. (2014) and Blom et al. (2016) also studied the effect of food volume on energy intake and satiety. Rolls and Roe (2002) reported that high volume preload decreased energy intake at lunch of 77 kcal (13%) compared to low volume preload. However, increasing the energy content of infused food, but not the volume, did not have any effect (Rolls and Roe, 2002).

According to Osterholt et al. (2007) the energy and weight consumed was significantly affected by the degree of aeration of the snacks, and there was reduction by 70 kcal (21%) in a subject's energy intake when they were served the more-aerated snack rather than the less-aerated snack. Arboleya et al. (2014) also reported similar findings to Osterhalt et al. (2007), indicating that the degree of product aeration had a significant effect on the intake and volume of the food consumption by means of affecting the expected satiety (Arboleya et al., 2014).

Blom et al. (2016) hypothesised that creaming (forming a layer) of the foams in the stomach may delay digestion, which in turn can lead to delayed emptying and stimulation of an 'intestinal phase' appetite mechanism. In the study they tested if normal energy food foams can demonstrate higher satiating effects compared to very low energy food foams. It was reported that the energy level of foams did not play crucial role in sustained satiety. Even very little energy in a food foam increased satiety. Energy content appears therefore not to be a prerequisite for the satiating properties of foamed food (Blom et al., 2016).

Although the effect of aerated food on satiety has been studied widely, little evidence is available to show mechanisms whereby aerated foods compared to nonaerated foods reduce appetite and sustain satiety. Several mechanisms have been suggested to contribute to observed effects such as sensory and cognitive response, rate of ingestion, oral processing time (Melnikov et. al. 2014), increased gastric volumes and delayed emptying (Murray et al., 2014).

Murray et al. (2014) hypotheses that "1) an aerated drink will generate more gastric distension than a nonaerated isocaloric control; 2) an aerated drink that is stable in the stomach will generate more or longer gastric distension than an aerated drink that is less stable in the stomach; 3) an aerated drink will reduce appetite more than a nonaerated isocaloric control; and 4) an aerated drink that is stable in the stomach will reduce appetite more than an aerated drink that is less stable in the stomach" (Murray et al., 2014). They used MRI to visualize foams in the stomach after oral ingestion. Therefore, they managed to measure separate volumes of intra- gastric foam, liquid and air layers serially and in turn, total gastric volumes. The hunger suppression induced by aerated drinks could largely be explained

by effects on gastric volumes and emptying, which may be further enhanced by foam stability (Murray et al., 2014).

Inclusion of air into a food system also affects salt and aroma perception has been reported by Chiu et al. (2015). The delivery and perception of salt and aroma was reported to be increased by air inclusion in an aqueous solution with 80 % reduction in total sodium content. The data suggest that samples containing air inclusion were perceived to be significantly saltier compared to the sample containing no air. It was suggested the work might be of interest to food industry and academics looking for new approaches to reduce salt levels without loss of taste quality (Chiu et al., 2015).

The results of many studies suggest that high volume foods with low energy density can promote satiety and reduce daily energy consumption. Several mechanisms have been suggested to explain such effects i.e. sensory and cognitive response, rate of ingestion, oral processing, increased gastric volumes and delayed emptying (Melnikov et al., 2014 and Murray et al. 2014). However, there is need to understand in detail the effect of an aerated structure on the rate of breakdown in the gastrointestinal tract (Zuñiga and Aguilera, 2008).

1.5. Food aeration methods and aerated foods

Food aeration helps to create new structures within foods resulting in different texture, mouthful, appearance, functionality, nutritional benefit and digestibility etc. Aeration can be achieved by different methods including mechanical (whipping) chemical (baking powder) or biological (fermentation by yeasts). During aeration air is introduced into a food matrix such as a liquid or viscous solution, where it is entrapped and forms foam.

Food aeration techniques has been divided into three main categories by Campbell and Mougeot (1999) as "(i) processes in which the liquid is actively forced around external gas (e.g. whipping, shaking, entrapment between layers); (ii) sparging in which gas is actively forced through the liquid (e.g. gas injection); or (iii) in situ generation of gas (e.g. biological or chemical leavening, steam formation by application of heat and/or pressure reduction, CO_2 evaporation on pressure release)". With a slightly different approach, the aeration methods have been categorised as "Conventional and Novel methods" by Zuñiga and Aguilera (2008). The novel methods include, (i) dispersing gases with membranes, (ii) micro engineered devices, (iii) electrochemical reactions and (iv) ultrasound (Zuñiga and Aguilera, 2008). The most common aeration methods for food are shaking, whipping, and fermentation, with CO_2 and steam the most common gases generated within foods (Campbell and Mougeout, 1999).

Food type	Beverages	Baked products	Other cereal products	Dairy products	Egg products	Chocolate and confectionery products	Others
Aeration Process							
Fermentation	Beer Wine, Ginger beer	Breads Crackers Crumpets Pikelets Stollen	Fermented extruded products	Swiss cheese			
Whipping or shaking		Batters Yorkshire puddings		Cream Mousses Milk shakes Sherbet Frozen desserts	Meringue Soufflé Omelette Sponge cake Angel cake Chiffon cake Zabaglione	Frappé Marshmallow	Fruit fool Sorbet Meat foams Fish foams
Dough and paste mixing		Bread dough Biscuit dough		Soft butter Cream cheese Creaming of butter and sugar for cakes	Choux pastry	Fondant Nougat Chocolate	Crèmes Icings Peanut butter Snack preparations Meat doughs
Steam generation, thermal expansion		Unleavened bread Pancakes Doughnuts Pizza base Wafers Yorkshire puddings					Micronized wheat, lentils
Entrapment, pulling		Puff pastry Croissants Vol au vents				Pulled taffy Flaked chocolate Boiled sweets	
Frying		Poppadoms	Snacks				Potato crisps Bubble and squeak
Raising agents		Cakes Waffles Soda breads	Extruded products with added bicarbonate			Honeycomb Brittles Boiled sweets	
Rapid dry heating			Cornflakes Micronized wheat				Crisps
Gas injection	Carbonated drinks			Instant whipped cream		Boiled sweets Bubble gum	
Extrusion		Crispbreads	Breakfast cereals			Marshmallow Chocolate	Snacks Pet food
Pressure beating				Ice cream		Chocolate Toffee Caramel Fillings	
Puffing			Breakfast cereals				Snacks

Table 1.2. Primary aeration methods used with different food types (adapted Campbell and Mougeout, 1999).

1.5.1. Conventional methods

1.5.1.1. Fermentation

Fermentation is an ancient food processing technique and has been developed to increase storage stability of perishable foods and also improve organoleptic and textural properties of raw materials. The most known fermented products include dairy products, such as yoghurt, cheese, buttermilk and soar milk; alcoholic drinks, such as wine, beer, and cider; fermented vegetables, such as sauerkraut and pickles; and fermented meats, such as sausages and salami (Charalampopoulos and Webb, 2013). In general, lactic acid bacteria (e.g., cheese, yogurt) and yeasts (ethanol fermentation, e.g., wine, beer, cider, bread) carry out fermentation, in which carbohydrates are converted to alcohol or preservative organic acids and carbon dioxide. More specifically, in wine and beer conversion of sugars into ethanol takes place. However, in bread yeasts produce CO_2, which is responsible for leavening of bread (Campell and Mougeout, 1999).

In bread making, air is one of the most important ingredients. It arises either from air entrapped in the bulk volume of the flour mass or from entrainment during mixing process (Scanlon and Zghal, 2001). During fermentation CO_2 diffuses into that existing air bubbles (Campbell and Mougeout, 1999). Size and distribution of air cells (Vyakaranam and Kokini, 2008), presence or absence of interconnections between the air pockets and density of them are important parameters affecting bread texture (Scanlon and Zghal, 2001). In beer fermentation CO_2, which is excreted by yeasts during fermentation, is attached to particles within the beer (Bokulich and Bamforth, 2013; Campbell and Mougeout, 1999).

1.5.1.2. Gas injection

This is used in large scale ice cream production, and also for aeration of some cereal-based bread and confectionary products (Ranken et al., 1997). In ice cream, air or nitrogen injection, for soft drinks carbon dioxide and for whipped cream nitrous oxide (N_2O) injection is used (Campbell and Mougeout, 1999). Use of nitrous oxide (N_2O) and hydrogen (H_2) in yogurt has also been reported. In addition, noble gases like helium (He), argon (Ar), neon (Ne), and xenon (Xe) have also been described in the dairy manufacturing (Adhikari et al., 2017).

The nature of the used gas can have a significant impact on structure, texture and flavour perception of aerated food (see table 3). According to Haedelet et al. (2007), who tested the effect of different gases (carbon dioxide, nitrogen, nitrous oxide, and argon) on the sensory properties of chocolate, chocolates made from the 4 gases could be divided into 2 groups on the basis of bubble volume and gas hold-up. Compared to argon and nitrogen chocolate that produced by using N_2O and CO_2 was reported to have higher gas holding capacity with larger bubbles. In terms of sensory characteristics, CO_2 and N_2O were found to be more soluble in chocolate and caused formation of larger voids, which led to the chocolate melting very fast in the mouth and being perceived to be less hard, more aerated, and less creamy. However, nitrogen and argon caused the formation of smaller bubbles and a lower gas hold-up, with creamier mouthfeel and harder texture.

Gas	Used product	Purpose
Air	Butter	Fat coalescence; phase conversion; better overrun
	Cheese	Enhance softness
	Chocolate	Improve stability
	Dairy Foam	Stabilize foaming
	Ice cream	Increase softness, melting properties, control the size of ice-crystals; increase overrun
Carbon Dioxide	Butter	Improve functionality; enhance overrun; reduce time
	Cheese	Enhance rennetability; eye formation
	Cappuccino/coffee foam	Generate foam
	Chocolate	Improve sensory properties/charateristics
	Fat fractionation	Extraction of fat fractions, enhance the process
	Ice cream	Improve texture
	Milk beverage	Improve sensory quality; reduce growth rate of microbes
	Milk Powder	Plasticizing effect; Improve solubility
	Raw milk	Extend shelf life; antimicrobial effect; delay fermentation
	Yogurt	Improve sensory quality and extension of shelf life
Nitrogen	Anhydrous milk fat	Improve oxidative stability
	Butter	Reduce calorific value
	Cheese	Improve physical property
	Chocolate	Improve sensory property
	Cappuccino	Encapsulate foamer ingredient, assist foam formation
	Margarine	Enhance consistency
	Powder	Improve drying
	Yogurt	Enhance shelf life
Hydrogen	Beverage	Improve sensory properties/charateristics
	Yoghurt	Control syneresis, aroma compounds
Nitrous oxide	Coffee foam and cream	Assist whipping process
	Chocolate	Enhance sensory character
Argon	Beverages	Suppress bacterial growth, neuro-protectant component
	Coffee Foam	Enhance foaming
	Chocolate	Enhance Sensory
	Milk powder	Increase droplet size

Table 1.3. Gases used in the manufacturing of dairy products (adapted from Adhikari et al., 2017).

1.5.1.3. Whipping

Whipping is a very common and practical aeration method. It is usually used for aeration of creams, toppings and smal scale production of ice-cream, where fat crystals aid incorporation of air into ice cream and cake batter. By whipping spherical gas bubbles can be formed with approximately 50 µm for normal whipping cream and 20 µm for homogenized whipping cream, while air bubbles in ice cream can be varied between 50 and 100 µm (Aken, 2001).

It was shown by Aken (2001) that during whipping the maximum achievable volume of gas bubbles that can be incorporated depends on the effectiveness of the introduction of gas during the first stage of whipping, but it is limited by packing constraints the thickness of the coating of emulsion droplets at the bubble surface, the ratio between the droplet and bubble radii, and the fat type and content of the emulsion.

The whipping of the dairy cream was reported to consist of three stages. In the first stage, most of the air is incorporated by the formation of a foam that is basically protein-stabilized. In the second stage of whipping, the bubbles are coated by a layer of fat globules. The main feature of the second stage was hypothesised to be close packing of the fat globule-coated gas bubbles, which was depend on adjusted bubble size and overrun by the dynamic of bubble break-up and coalescence. At the third stage, because of high packing density of fat globule-coated gas bubbles, further incorporation of gas is inhibited (Aken, 2001).

1.5.1.4. Frying

Frying has different functions in food processing including cooking, colouring, and dehydration. It also helps aeration due to very fast internal steam formation such as frying in very hot oil, which causes the product to puff (Ranken et al., 1997, Campbell and Mougeut, 1999). Some aeration methods are specific to a food type (e.g., puffing of cereals), however some others are used across several groups, (see Table 2.2), (Campbell and Mougeout, 1999).

1.5.2. Novel methods

1.5.2.1. Dispersing gases with membranes

A membrane is a thin-selective barrier between two fluids and 95 % of them are formed from a polymer either by spinning, or by coating tubes or flat sheets, or by casting a film. It can be divided into two groups: porous and nonporous. Porous membranes are used for separation of particles with diameters in the range of μm to nm. Application of membranes in food and beverage industry is very wide, from production (e.g. in wine production) to processing (e.g. fruit, vegetable juice, sugar and starch processing) (Field and Lipnizki, 2017). However, membrane foaming is a relatively new method (Bals and Kulozik, 2003a), which is based on using applied pressure to force the gaseous phase through the membrane into the continuous liquid phase (Zuniga and Aguilera, 2008). With membrane foaming it is possible to incorporate small gas bubbles into a liquid directly. However, it is crucial to control instantaneous bubble detachment from the pores in order to avoid large bubble or filament generation (Müller-Fischer et al., 2007). There are two mechanisms by which bubble formation is achieved by using using orifices which include, shear-induced detachment from the surface of the

membrane by flow of the continuous phase and spontaneous formation by interfacial tension, without continuous-phase flow (Zuñiga and Aguilera, 2008).

When it is compared to conventional rotor-stator whipping, in which the gas is dispersed by acting turbulent flow forces in gaps between fixed and moving pins (Müller-Fischer et al., 2007), foaming using membranes offers more benefits such as, the structure of the membrane foaming system is technically simple, it is cheap and stabiles the formed bubbles with a relatively low energy input. It is also useful for materials that are sensitive to shear in the mixtures to be foamed. Mean bubble diameter can be controlled by membrane pore size and gas flow rate (Bals and Kulozik, 2003; Müller-Fischer et al., 2007).

There are different types of membranes such as ceramic, metallic, polymeric and Shirasu Porous Glass (SPG) (Zuñiga and Aguilera, 2008). SPG membranes, despite their high porosity, are most preferred because they have high water resistance due to their relatively high aluminum oxide content and a sufficiently high mechanical strength for practical use (Kukizaki and Goto, 2006). Although the use of membranes appears to be promising for the production of monodispersed bubbles and also suitable for large scale production due to easy to scale up by adding more membranes to a module, it encounters several downsides. The main limitation is a low dispersed phase flux through the membrane which is associated with monodispersed bubbles (Zuñiga and Aguilera, 2008), high induced process costs and a delicate maintenance (Laporte et al., 2016).

Methods	Process conditions	Continuous phase	Bubble diameter (μm)
Membranes	Membrane pores, 7–140 nm Continuous-phase flow, 6.2 L/h Shear-induced detachment	Whey protein isolate solution, 10% wt 180–370	180–370
	Membrane pores, 43–85 nm Transmembrane/bubble point pressure ratio, 1.1–2.0 Shear-induced detachment	Sodium dodecyl sulfate (SDS), 0.3% wt	0.36–0.72
	Membrane pores, 3.07 μm	SDS, 0.3% wt	27.8
	Transmembrane/bubble point pressure ratio, 1.1	Tween 20, 1.0% wt	31.3
	Spontaneous formation by interfacial tension	Sodium caseinate solution, 1.0% wt	39.5
		Bovine serum albumin (BSA), 1.0% wt	41.1
Microchannel arrays	Microchannel dimension (16 μm width × 4 μm depth) Spontaneous formation by interfacial tension	SDS, 0.3% wt	33.6
		Tween 20, 1.0% wt	39.1
		Sodium caseinate solution, 1.0% wt	48.9
		BSA solution, 1.0% wt	51.1
Flow-focusing devices	Orifice diameter, 100–210 μm Liquid flow rate, 24–310 μL/s Gas flow rate, 0.2–40 μL/s	Water/ethanol and water/glycerol solutions	5–120
	Exit channel with square section (100 μm width × 500 μm length × 30 μm height) Liquid flow rate, 20 mL/h Gas flow rate, 46 mL/h	Glycerin solution, 50% volume	~46
	Orifice diameter, 250–500 μm	Gelatin solution 1–5% wt	70–200

Table 1.4. Diameters of air bubbles produced by membranes and microengineered devices (from Zuñiga and Aguilera, 2008).

1.5.2.2. Microengineered devices

Microengineering is a new and generic technology. It involves the miniaturisation of mechanics and has grown out of the microelectronic industry. Microengineered devices and systems are mostly applied in the automotive, aerospace, telecommunications, bioscience and ecology (Haskard et al., 1995). Microengineered devices, such as microfluidics, prompted the use of nanotechnology in food industry and changed the way of processing dispersed food systems. In food and agricultural industries microfluidics are generally used for food safety, food processing, and animal sciences (Kim et al.,2016) and have appeared as early as the 1940s (Kolfschoten, 2011).

Microfluidics is the science of designing, manufacturing, and operating devices and processes that deal with small volumes of liquids, typically ranging from nanoliters to attoliters. It uses channels with dimensions of tens of micrometers -at the scale of a human hair. The substances flowing through such microchannels appear as gases, liquids and solids and combinations thereof (Skurtys and Aguilera, 2008; Kim et al., 2016; Kolfschoten, 2011).

Microfluidics have the advantages of low cost, short reaction and analysis time, high sensitivity, small footprints, and high throughput. Microfluidics can be divided into continuous-flow microfluidics and droplet microfluidics (Chen et al., 2013).

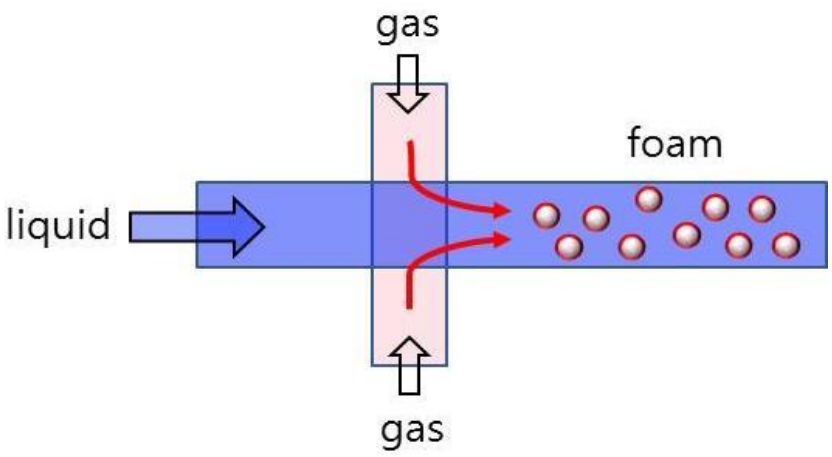

Figure.1.1. Schematics of a microfluidic mixing device for uniform foam generation (from Kim et al., 2016).

In the food industry inclusion of air or gas in a liquid matrix is carried out in batches, through traditional methods, such as whipping mixers or also in continuous rotor-stator systems. Nevertheless, traditional systems possess some disadvantages of being high energy cost and unable to control rate of air flow into the foam. However, with microfluidics devices it is possible to generate mono-dispersed size distribution of bubbles.

Laborte et al. (2016) reported that, a microchannel device produced stable foams by allowing mastering the foams structural properties, especially the bubble size which was down to 75 µm and leads to stable foams even with void fraction of 0.55 (Laporte et al., 2016). Highly porous calcium alginate foams were prepared by using a microfluidic–T junction device. The T-junction device generated monodisperse microbubbles (meandiameter, ~154 µm) and produced stable porous foams (Ahmad et al., 2012).

Microchannel (MC) arrays and flow-focusing (FF) devices are microfluidics techniques and have been used in the food industry. They have different operational principles. MC drives the dispersed-phase-fluids to pass through a micro-channel structure. It can generate uniform

droplets of macro and nanosizes. In a microfluidic FF device, two immiscible phases flow through separate channels (one central for the dispersed phase and on or more outer channels for the continuous phase) that meet at the junction of these channels upstream of a small orifice. By controlling flow rate ratio of the continuous phase and dispersed phase uniform bubbles with tunable size can be created (Zuñiga and Aguilera, 2008; Fu et al., 2007).

There are two disadvantages of FF, being difficult to scale it up due to the three - dimensional centering of the injection needles with the exit orifices and also the gas fraction is very limited to very small values (Zuñiga and Aguilera, 2008).

1.5.2.3. Ultrasound

Ultrasonic technology has been used in the food industry widely and is receiving much attention. Ultrasound is an acoustic wave with a frequency > 20 kHz (Xiong et al., 2018). There are four different acoustic waves; longitudinal/compressional waves: transverse/shear waves, surface/Rayleigh waves, and plate/Lamb waves. They are classified based on the mode of vibration of the particle in the medium, with respect to the direction of the propagation of the initial waves. Ultrasound is divided into three categories based on the frequency as power ultrasound (20–100 kHz), high frequency ultrasound (100 kHz–1 MHz), and diagnostic ultrasound (1–500 MHz).

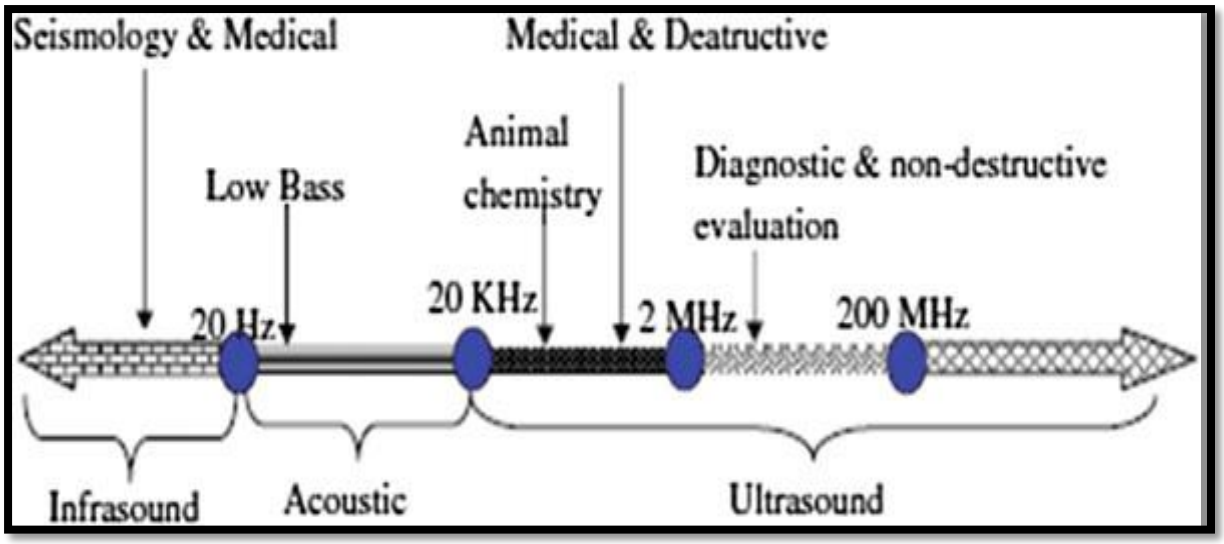

Figure 1.2. Diagram of ultrasound range (from Wu et al., 2013).

Ultrasound ranging from 20 to 100 kHz is used to change physical and chemical properties and/ or structure and functional properties as it has the ability to cause cavitations of bubbles (Wu et al., 2013; Hu et al., 2013).

During sonication a very high shear energy waves and turbulence in the cavitation zone are produced due to extreme temperatures (5000 K) and pressures (1000 atm) which is created by formation of cavitation bubbles and their rapid and violent collapse (Hu et al., 2013). Once a bubble is created, two different cavitation phenomena, stable or transient cavitation, could take place in the liquid. The size of bubbles, ranging from nanometer to micrometers in diameter, depends on the liquid and conditions used. Bubbles may arise from gas nuclei formed in in the bulk of the liquid or in the vessel walls or from ion present in the solution (Zuñiga et al., 2008).

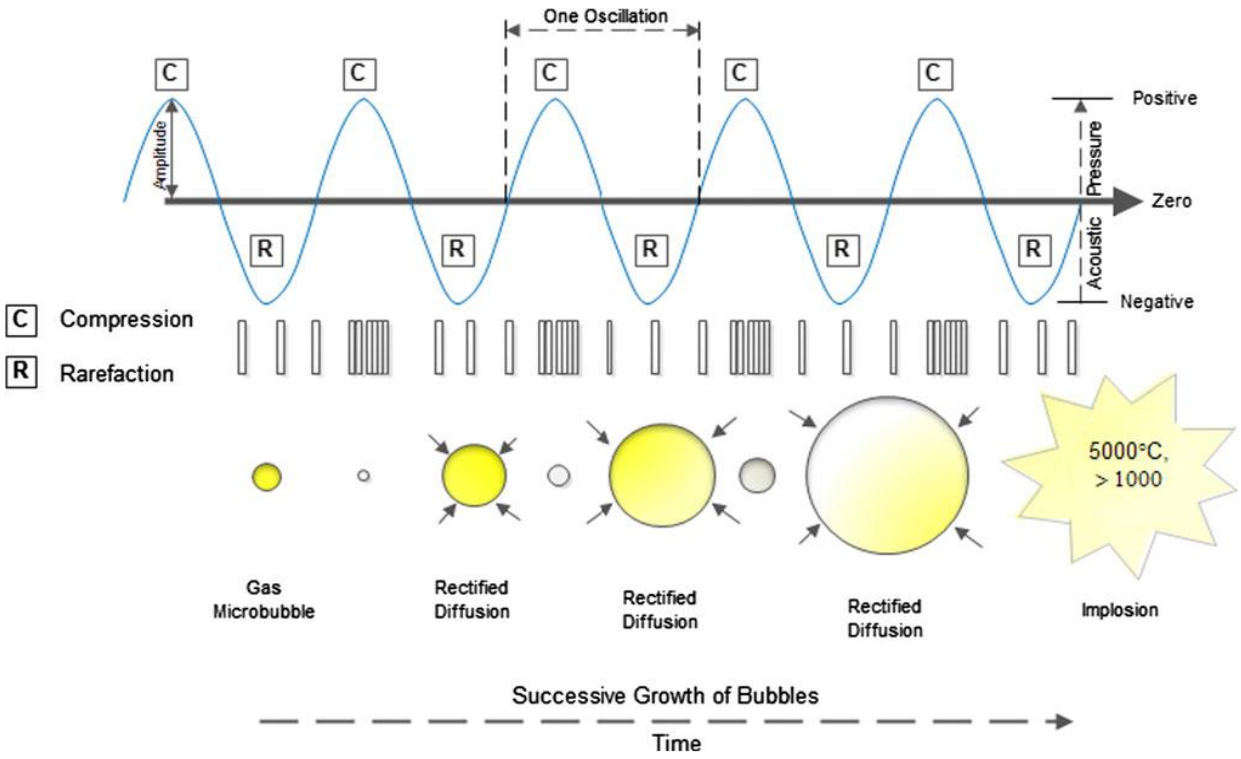

Figure 1.3. Schematic depiction of growth and collapse of bubble in acoustic cavitation process (from Abbas et al., 2013).

The effect of ultrasound has been studied extensively e.g. on whey protein foams (Tan et al., 2015), on faba bean protein (Velasco et al., 2018), on pea protein isolate (Xiong et al., 2018), on egg white (Sheng et al., 2018; Arzeni et al., 2012), on soy protein Isolate (Tang et al., 2009; Morales et al., 2015) , on animal and vegetable proteins (O'Sullivan et al., 2016), on black bean protein isolate (Jiang et al., 2014), on sunflower protein isolate (Malik et al., 2017).

The high intensity ultrasound treatment of various proteins resulted in changing protein functionality, such as foaming capacity. Xiong et al. (2018) reported that foaming properties of pea protein (PPI) isolate was increased from 58% to 73.3% due to partial unfolding of PPI, reductions of particle size and increase in surface hydrophobicity (Xiong et al., 2018).

Tan et al. (2015) reported that ultrasound treated whey protein foam showed a slight increase in gel strength compared to the untreated one. High intensity ultrasound treatment increased foaming ability of faba bean protein isolate, changed the secondry structure of optimized faba bean protein, producing a significant increase of β-conformation and decrease on inter-molecular aggregates (Velasco et al., 2018). Foaming ability of whey protein significantly increased under 120 W high intensity ultrasound probe pretreatment, and foaming ability reached to 232.67 % and was 4.4-fold to the control group (Sheng et al., 2018).

Using ultrasound allows reduction in the size of bubbles (<1 μm) but it is associated with a risk of denaturing fragile food constituents, production of locally increased temperature due to collapse of bubbles in multibubble cavitation. Free radicals, which can promote undesirable chemical reaction, may also be formed because of cavitation of microbubbles (Kim et al., 2016; Zuñiga and Aquilera al. 2008).

Electrochemical reactions (Zuñiga and Aquilera al., 2008), static mixers (Talansier et al., 2013; Laporte et al., 2016) and narrow gap unit (NAGU) (Souidi et al., 2012) are other methods that can be used for forming bubbles.

1.6. Instability of aerated food systems

Aerated foods are widespread in our daily lives. They own different texture, mouthfeel and appearance due to their high air content and low density. Whipped cream, ice cream, beer, confectionaries, extruded and expanded cereal products, meringue, foam based meat and vegetables constitute are some examples of aerated foods (Campbell and Mougeout 1999; Narchi et al., 2009).

Most aerated materials are thermodynamically unstable. In a liquid system they will break down eventually and separate into two phases-gas and liquid over time (Fameau and Jalmes, 2017; Lazidis et al., 2016, Campbell and Mougeot, 1999) to reach a more stable state that minimises their interfacial area and their free energy (Amagliani and Schmitt, 2017). The high instability of the aerated systems is due to larger interfacial area, which is also called film, between continuous and dispersed phase (Lazidis et al., 2016). When interfacial tension is lowered, the droplets became more deformable and easy to disperse (Wilde, 2000).

The rheology of the aerated systems usually controls the stability. The lifetimes of aerated systems vary from seconds to minutes as in beer and wine, to years as in extruded, expanded and confectionary product, depends on stabilization mechanism of the bubbles (see Figure 2.4). In a baked product the aerated structure is fixed by heating and subsequent matrix properties. In most confectionary products, expanded and extruded products the stability is provided by fixing air bubbles in a solid matrix. Meringues are stabilized by drying while stability of ice cream is due to freezing and a destabilised fat matrix (Campbell and Mougeot, 1999).

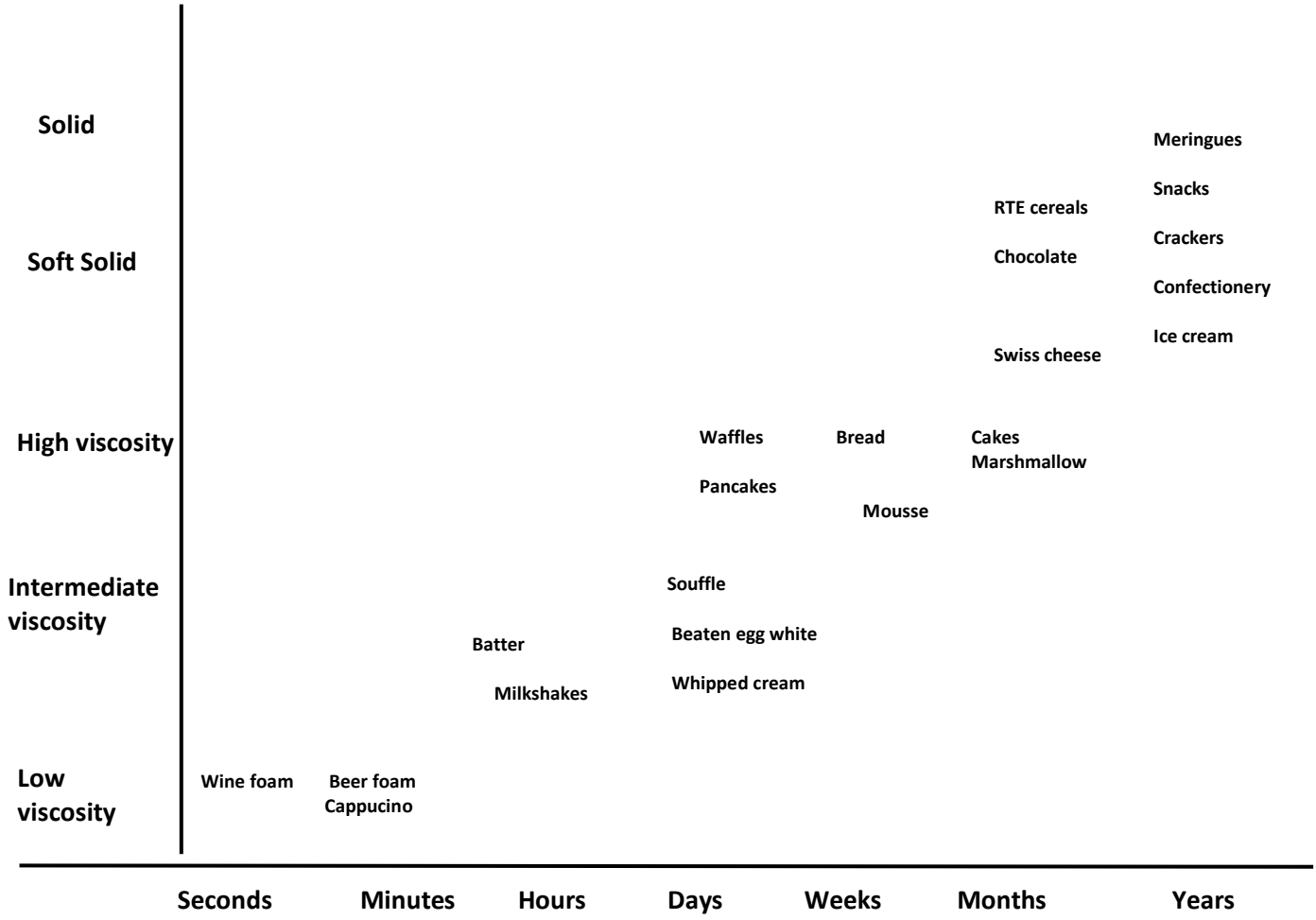

Figure 1.4. Lifetime and rheology of aerated foods (adapted from Campbell and Mougeot, 1999). RTE: Ready to Eat.

Stability of the aerated systems is affected by a range of naturally occurring physical processes. These physical phenomena can be classified into the following categories: (i) **bubble coalescence** (due to rupture of interface within the foams), (ii) **drainage** (liquid drainage from foam to the bulk), **(iii) disproportionation-coarsening** (smaller bubbles disappear while bigger bubbles grow in size and it is equivalent of Ostwald ripening in emulsion) and (iv) **creaming** (the air bubbles separate into a foam layer on top of the liquid), (v) **evaporation** of liquid from the foam (Kokini and Aken, 2006; Foegeding et al., 2006; Lazidis et al., 2016; Pei and Schmidt, 2010; Magrabi and Dlugogorski, 2002).

However, in some cases several destabilisation mechanisms may take place simultaneously in protein foams and therefore it is not easy to detect individual destabilisation mechanisms (Foegeding et al., 2006).

Among aerated foods, foams play an important role in the food industry. They are colloidal dispersions (two-phase media) where a gas or atmospheric air is dispersed into a continuous phase, which in most cases is aqueous, in the form of tiny bubbles (Fameau and Jalmes, 2017; Narchi et al., 2009; Lazidis et al., 2016). In another definition, foam is a macroscopic (i.e.>10 μm) gas dispersion whose existence and properties are controlled by colloidal and surface forces and interactions across the films that separate individual gas bubbles (Bergeron and Walstra, 2005). Foams can be divided into two categories as solid and liquid. Solid foams are made from liquid foams and also referred to as dry foams, xerogel or sponge i.e. bread, marshmallows (Bureiko et al., 2015).

There are three main structural elements of a foam: the (i) lamellae or films, which separate bubbles, (ii) Plateau borders, which are formed where three films meet, each pair forming an angle of 120^{o} and (iii) vertices are the nodes where four Plateau borders meet (Lee et al., 2005). Films provide great surface area to the foam, do not contain high amount of liquid while the plateau borders hold most of the liquid as a result of having more sharply curved and surface tension, have a lower pressure than the bubbles. Therefore, in most cases, liquid moves out of the films into the Plateau borders until the films are thin enough to counter the Plateau border drag through the disjoining forces between the film interfaces (Lee et al., 2005).

In terms of foamability and foam stability surface viscoelasticity, which is related to the non-equilibrium state of the adsorption layer, play important roles. The link between surface viscoelasticity and foam properties are summarised as follows;

a. The foam film can stretch less, and can rupture less by disturbances if a large dilational surface elastic modulus results in a small strain for a given applied stress,
b. The interface can be restored by the film elasticity as a result of bringing back surfactants and by limiting the stretch of the interface.
c. Liquid film rupture can be minimized if the Marangoni effect draws surfactants back to the interface and liquid into the film.
d. If surface viscoelasticity is low, it stretches interfaces and therefore causes liquid film rupture. However, when surface viscoelasticity is high, it creates a solid-like response of the interface, and causes fracture,
e. The process of drainage in foam films and Plateau borders are modified by surface elasticity, which also controls the appearance of bell-shaped liquid drops that have a destabilizing effect on films (Wang et al., 2016).

The Marangoni effect is known as a surface tension gradient on a liquid and first described by Italian physicist Carlo Giuseppe Matteo Marangoni who investigated the spreading of oil drops on a water surface, in the 1860s. He explained this behavior as the macroscopic manifestation of a liquid flow as a result of local gradients in interfacial tension (Fyen and Mertens, 2008) .

1.6.1. Drainage

Foam drainage is the flow of liquid from the lamellae (or films) to the Plateau borders and nodes (intersections of four channels), which transfer liquid through the network of vertices and then finally out of the foam (Figure 2.5). Drainage occurs due to gravity and low surface tension (Magrabi and Dlugogorski, 2002; Hilgenfield et al., 2001; Kinsella, 1981). It is driven by two different phenomena: gravity and capillary pressure. The gravity-driven drainage takes place through the network of Plateau borders and it is very much dependent on the viscosity of both the capillary fluid per second and the surface, if the interfacial film materials are exposed to the aqueous phase (Kinsella, 1981).

The capillary pressure-driven drainage takes place from the films to the Plateau borders due to the lower pressure in the Plateau borders compared with the films. The difference in curvature of the film surface causes the pressure gradient that drives film drainage (Magrabi and Dlugogorski, 2002; Lioumbas et al., 2015).

Due to gravity, the large bubbles bigger than a few microns rise and the liquid will be collected at the bottom (Rio et al., 2014). The rate and extent of drainage from the films strongly affects the foam stability. Owing to drainage the films that separate the bubbles get thin and eventually break, which causes foam collapse. However, Gibbs- Marangoni effects can restore the thickness and prevent further thinning by influencing the surface elasticity of the films.

Any liquid surface that has a surfactant adsorbed onto it is described by a dynamic phenomenon called ‘The Marangoni Effect’, while ‘Gibbs’ is an adsorption isotherm and describes the equilibrium concentration of the surfactant in the film. Hence, the equilibrium concentration is reestablished as a result of the surfactant molecules will diffuse to or from

the bulk liquid. Therefore, the Marangoni and Gibbs phenomena take place simultaneously; and thus, the hyphenated phrase, the Gibbs-Marangoni effect, is often used (Magrabi and Dlugogorski, 2002).

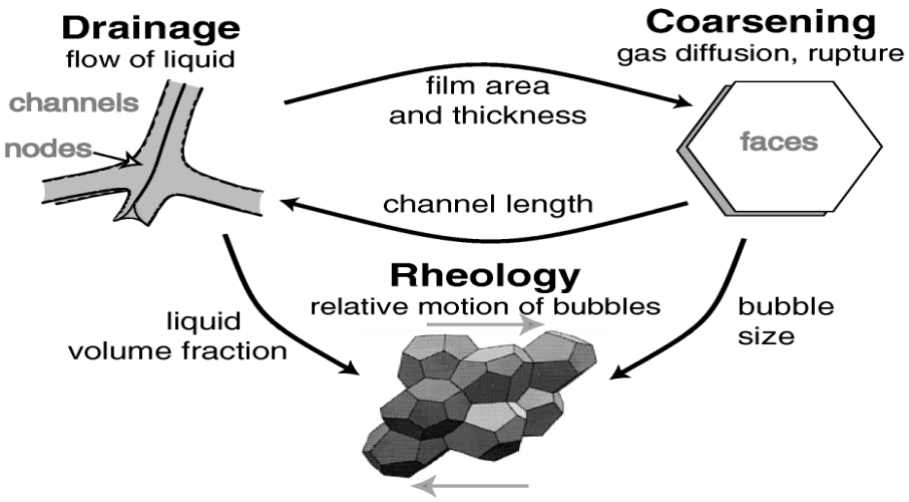

Figure 1.5. Schematic of the interdependence of drainage, coarsening, and rheology of foams. For example, drainage results in a drier foam with increased shear modulus and accelerated coarsening. Coarsening in turn enhances drainage, but also decreases the shear modulus (from Hilgenfeldt et al., 2000).

Bulk density and viscosity of the lamellar fluid influence the drainage directly. Viscoelasticity allows the foam films to respond to stresses by expansion and compression of area, where necessary. Therefore, the viscoelasticity of the films is crucial to form more stable foams because when films are more viscous but rigid tend to be brittle (Kinsella, 1981). Therefore, in order to prevent gravity deformation of the film high viscosity, bubble size reduction and increase of gas content of liquid phase is desirable (Lau and Dickinson, 2005; Pei and Schmidt, 2010).

1.6.2. Coalescence

Once drainage nears completion and the equilibrium liquid volume fraction profiles reached (below about 30 %), the films that separate bubbles get thin then rupture, leading to bubble coalescence (Rio et al., 2014). Coalescence involves the irreversible binding of two or more bubbles forming a single larger bubble (Hunter et al., 2008). Although the film rupture is the driving force of coalescence, the reason behind the film rupture is still not clear. It has been reported that coalescence takes place in foams when: (i) the bubbles reach a critical size, (ii) once the liquid fraction has reached a critical value, or (iii) when the applied pressure or the capillary pressure reaches critical value. In particle stabilised foams film rupture might be promoted by the particles, which depends on the interfacial tensions between the three phases (air, water, and particle) (Rio et al., 2014). Experimentally it is not easy to discriminate between them since capillary pressure, liquid fraction and bubble sizes are linked and change with time due to drainage and coarsening (Langevin, 2017).

The stabilisation of foams against coalescence requires different surface properties. The close approach of the dispersed phase can be prevented by long-range repulsive force, which can be in the form of electrostatic or steric repulsion (Wilde, 2000). Film rupture can be avoided by delaying drainage as long as the foam is wet by use of very viscous liquids and by using surface active stabilising agents. In a food product, this means the use of some functional proteins, especially ones derived from milk or eggs (Adler and Weaire, 2008; Lau and Dickinson, 2005).

1.6.3. Coarsening/ Disproportionation

Disproportionation (diffusive coarsening) involves the transport of gas between bubbles of different sizes and bubbles that contain gases with different solubility, and rupture of the liquid films between bubbles (Hilgenfeldt et al., 2000). It is equivalent of Ostwald ripening in emulsions, where the gas diffuses from the smaller to the larger bubbles because of difference in Laplace pressure (Lau and Dickinson, 2005; Rio et al., 2014), which is higher in the smaller bubbles. Therefore, foam with small bubbles tend to coarsen quickly and drain slowly (Hilgenfeldt et al., 2000). As a result, diffusion flux generally results in the shrinking of smaller but growth of larger bubbles with time (Hunter et al., 2008).

The diffusion rate of the gas between different sizes of bubbles determines the foam stability. Foams with gases of high solubility (like CO_2) and diffusivity coarsen rapidly (Hilgenfeldt et al., 2000). A gas that is soluble in water such as CO_2 gives less stable foams than less soluble ones, such as N_2, because CO_2 diffusion through the water film is faster. If small amounts of N_2 are added to CO_2 foams, it improves their stability (Rio et al., 2014). The gas mainly diffuses through the thin films between bubbles for which the diffusion path is the smallest (Rio et al., 2014).

Although, the coarsening does not affect the foam lifetime directly, it has been noted that the coarsening and drainage has a very close relationship because coarsening rate is sensitive to the liquid fraction that is controlled by foam drainage (Figure 2.6). Equally, foam drainage is strongly dependent on bubble size, which is controlled by coarsening (Wang et al., 2016). As a foam becomes drier from drainage, the rate of gas diffusion increases as the average bubble size becomes larger from coarsening, the rate of drainage increases (Vera and Durian, 2002).

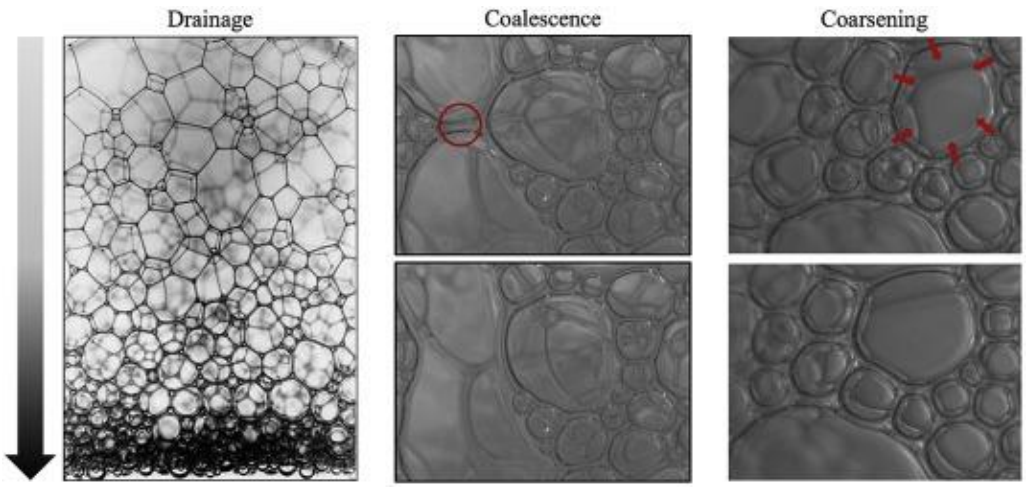

Figure 1.6. The three main mechanisms responsible for destabilization of foams. The arrow shows the direction of flow of the liquid continues phase and the intensity depicts the concentration gradient of liquid within the foam. The circle shows the point where two bubbles come close to each other and coalesce. The arrows show the direction of gas diffusion from the smaller bubbles to the larger on which increases in size over time (from Lazidis et al., 2018).

Vera and Durian (2002) quantified the coarsening/free-drainage connection by imaging and novel use of multiple light scattering. They concluded that coarsening is unavoidable for freely draining foams. Hilgenfeldt et al. (2000) reported that coarsening has a strong influence on foam drainage for gases of large solubility, such as CO_2, and bubble sizes (diameters <1mm). Strong bubble coarsening leads to shorter drainage time (accelerated drainage) which is independent from the initial liquid content and reduced gas permeability.

Coarsening of foams is a very complex process and depends on number of parameters not only on the bubble size. It has been reported that gas diffusion coarsening stops if the continuous phase becomes solid; it is reduced if surface elastic modulus (visco- elasticity) of

bubbles is very high and resistant to collapse (Pei and Schmidt, 2010; Dutta et al., 2004; Rio et al., 2014); or it can be delayed by generating foams with equal bubble size (Adler and Weaire, 2008).

Interfacial rheology of adsorbed films was reported to be effective against rate and extent of bubble shrinkage. In order to shrink, bubbles have to work against the interfacial elasticity and viscosity, which provide an energy barrier that could inhibit bubble shrinkage (Murray and Ettelaie, 2004).

Although coarsening and disproportionation is used interchangeably, they refer to different processes. The change (usually widening) in bubble size distribution in the foam is related to disproportionation. However, coarsening refers to the growth in the average bubble diameter (Magrabi and Dlugogorski, 2002).

1.7. Stabilization mechanisms of aerated systems

Aerated systems are stabilized by high molecular weight surfactants, by polymers-amphilic macromolecules (the most commonly used are proteins) that can adsorb at the air/water interface and reduce the surface tension (Lazidis et al., 2016; Wilde 2000; Dickinson 2010) or by particles (Rio et al., 2014). Bubbles are also stabilized by solid crystals of fat (as in whipped cream), or ice (as in ice cream), in viscous liquid phase, or by a semi-solid or solidified continuous matrix (Table 2.5).

In some cases, a combination of stabilisation mechanisms acts together; for example, in bread dough proving, the viscoelastic protein matrix stabilises bubbles against coalescence, but added surfactants can give some extra stability, while fat crystals contribute to stability during baking. However, in some other cases stabilisation mechanisms act one after the

other, e.g. in cake making, entrained bubbles are retained due to high viscosity of the creamed butter and sugar, but during baking the egg protein stabilises the air bubbles (Campbell and Mougeot, 1999).

Aeration method	**Liquid forced around external gas (whipping, shaking, dough mixing, layering)**	**Gas forced though liquid (sparging)**	***In situ* generation and/or expansion of gas (steam, CO_2, thermal expansion, vacuum expansion)**
Stabilisation mechanism			
Proteins	Milkshakes, soufflé, zabaglione, marshmallow, egg foams	Widgets in beer, carbonated drinks, Cappuccino	Beer foam, wine foam, carbonated drinks, proving bread dough, sponge cake, angel cake, soufflé
Fat crystals	Whipped cream, puff pastry	Instant whipped cream	
Ice crystals	Ice cream, frozen desserts		
High viscosity/semi-solid	Batters, bread dough, pastries, cake batters, creamed butter and sugar, dairy desserts, soft butter, peanut butter, meat doughs, fruit fool, sorbet, fondant, Yorkshire pudding		Pikelets, pancakes, baked goods, Swiss cheese, gums
Solid matrix			
Starch	Bread, crackers, crumpets, cakes, waffles, pastries, poppadoms		Bread, crackers, crumpets, cakes, waffles, crispbreads, snacks, potato crisps, cornflakes, breakfast cereals, popcorn, pastries, poppadoms
Sugar	Meringue, taffy		Honeycomb, boiled sweets
Fat	Chocolate bars		Chocolate bars

Table 1.5. Stabilization mechanisms for aerated foods produced by different methods (from Campbell and Mougeot, 1999).

1.7.1. Surfactant stabilized aerated products

Foams and aerated structures require stabilisers to prevent separation between two phases (continues and dispersed) and improve stability**.**

Surfactants are surface active materials; contain a polar (hydrophilic) head group and a non-polar (hydrophobic) chain tail. Therefore, they can adsorb to the air/oil-water interface and reduce interfacial surface tension (Hunter et al., 2008). The interfacial surfactants should adapt and reinforce a stressed area and in a viscous but fluid film flow into thinned area of higher surface tension and reinforce it (Marangoni effect). However, the surfactants may not be effective at preventing rupture and leakage when the film becomes too thin or if surfactant is too viscous because of slow rate of diffusion of the film material. Therefore, during initial foam formation high surface viscosity is not desirable, since it restricts mobility (i.e migration to the interface), solubility, and molecular flexibility, which are required for foam formation and stability (Kinsella, 1981).

In the presence of surfactants foam is formed when bubbles are dispersed into a surfactant solution, with an air volume fraction higher than the volume fraction of closely packed spheres. The bubbles are separated by thin, plane-parallel films and stabilized by surfactant adsorption layers (Denkov et al., 2009).

In a foam, surfactants may influence both the gas–liquid interfacial properties (e.g., surface tension, surface dilatational viscosity, surface shear viscosity, surface elasticity) and the bulk liquid viscosity. It has been reported that the foam drainage rate was significantly altered by surfactant concentration; larger surfactant concentrations result in dryer foams with a more packed structure. At high surfactant concentrations (2000 ppm), the foams become more

stable because at such a surfactant concentration not only the Plateau border walls become more rigid and oppose drainage but also the curvature of interstitial films gets higher due to the much smaller bubbles. In contrast, coarsening and coalescence was favoured due to reduction in bubble sizes (Lioumbas et al., 2015).

To summarise, the stabilising effect of surfactants is reported to be due to: (i) improved elasticity of liquid films between bubbles and therefore their resistance to deformational breakages and (ii) increased disjoining /conjoining pressure inside the liquid film because of electrostatic and or steric repulsion between adsorbed at liquid-air interface (Bureiko et al., 2015). However, surfactants stabilise foams most effective if they form a fluid adsorbed layer, which allows them to migrate to regions with reduced surfactant concentrations, as a result of perturbation during creation, mixing or transport processes-Marangoni mechanism (Wilde, 2000).

1.7.2. Protein stabilised aerated products

Proteins are amphiphilic macromolecules (having both hydrophilic and hydrophobic parts) and widely used in food industry in order to stabilise aerated food systems (Dickinson, 2017). This is mainly due to spontaneous adsorption of proteins from solutions to the air /aqueous interface (Foegeding et al., 2006) and their ability to unfold and rearrange their secondary and tertiary structure exposing the hydrophobic regions to the hydrophobic phase at the interface and form viscoelastic interfacial films by means of intermolecular interactions (hydrogen bonding, electrostatic and hydrophobic interaction), between adsorbed proteins (Amagliani and Schmitt, 2017; Lazidis et al., 2017; Foegeding et al., 2006).

According to Kinsella (1981), the physical requirements for stability in a protein foam are: "the interfacial film should be structurally stable and relatively impermeable to the entrapped air; at a critical distance contiguous bubbles should be repelled to minimise coalescence; the outward projecting polar polypeptide loops or segments should retain the lamellar liquid against gravity and the protein in the film should possess both rigidity and flexibility to withstand local shocks while permitting sufficient mobility of component molecules to strengthen localized stress thinning" (Kinsella, 1981).

The interfacial rheology, which involves measuring the forces encountered upon shearing, and protein adsorption is affected by electrostatic interactions. The protein foaming ability and stability is optimum near their isoelectric points and protein adsorption to the interface is very fast at this pH because electrostatic repulsion is minimized for the net neutrally charged proteins (Foegeding et al., 2006).

Environmental and processing factors, such as temperature, pH, protein concentration, salts, composition of the continuous phase etc., alter the configuration and stability of proteins and also may retard film formation or cause destabilisation in foams (Patino et al. 1995). It has been reported that a very stable foam can be created when the adsorbed protein forms a coagulated solid network (Murray and Ettelaie, 2004). However, excessive denaturation leading to coagulation and aggregation may destabilises the foam. Therefore, limited surface denaturation is required to impart viscosity and rigidity to the interfacial film for foam stabilization (Kinsella, 1981).

The applied forces affect functionality of proteins, under the high shearing conditions it is possible to breakdown the large particles. Nevertheless, high shearing may induce excessive heating which causes undesirable protein aggregation and destabilize the aerated systems

(Dickinson, 2017). However, under modest shearing conditions whey protein fluid gels (gel-like particles) are formed (Norton et al., 1999). It has been reported by Lazidis et al. (2016) that whey protein fluid gels were very effective at stabilising foam due to reduced local liquid drainage by large protein particles which filled the free space between the air bubbles and increased the bulk viscosity. The smaller and mobile protein particles increased foam stability by their fast diffusion rate to the interface and reducing interfacial tension (Lazidis et al., 2016).

Alternatively, the ability of proteins to stop disproportionation due to their interfacial elasticity mechanism was reported not to be effective. Dickinson et al. (2002) reported that the rates of shrinkage with the different proteins were not significantly different except in the case of gelatin, which at any given bubble size appeared to give a slightly higher rate, probably because the surface tension is higher for this system. None of the tested proteins were capable of stopping disproportion completely, just slowing it down by a factor of 2-3, compared to an interface with zero dilatational elasticity (Dickinson et al., 2002).

Large protein particles are the most useful in foaming and as foam stabiliser agents (Bureiko et al., 2015). However, protein fibrils and hydrophobins have been receiving great attention from the researches as a foam stabilisers.

Protein fibrils (aggregation of proteins; especially whey proteins forming fibrils upon heating) also have been used as thickener, stabiliser and gelling agent (Dickinson, 2017) due to their capacity to generate space-filling networks at low volume fraction, which is a characteristic more traditionally associated with food polysaccharides than with food proteins (Dickinson, 2016).

Protein fibril networks were reported to be very effective at inhibiting coalescence due to formed viscoelastic layers at liquid interfaces and steric structural barriers between neighbouring liquid droplets or gas (Dickinson, 2017). To add, globular proteins were also founded to be very effective against coalescence due to stronger intermolecular actions (Wilde, 2000).

Hydrophobins, are small proteins with molecular weight of 4 kDa, are reported to be very effective for arresting bubble shrinkage due to the adsorbed elastic films. Hydrophobins can pack together very closely at the interface and form an adsorbed solid like layers at the surface of water which has a highest surface shear viscosity and rigidities reported of any protein, and do not collapse upon compression. The hydrophobins have a very stable structure, due to four intramolecular disulfide cross links. This structure makes hydrophobin highly surface active – at least as surface active as many low molecular weight surfactants at the air–water interface (Murray, 2007; Rio et al., 2014).

1.7.3. Particle stabilised aerated products

The colloidal particles have been used to stabilise aerated systems for long time. They have an ability to accumulate at the interface of two immiscible fluids and to be adsorbed irreversibly if they are small and hydrophobic (Bournival et al., 2015).

Particles act on foams in different ways depending on their size which affects their capture by bubbles, wettability, hydrophobicity, shape (affecting contact angle), concentration and also on the use of surfactant type. Particles provide long-term stability to air bubbles by forming an interfacial layer that is sufficiently rigid to arrest the destabilising processes of droplet coalescence and bubble shrinkage (Bournival et al., 2015; Dickinson, 2016).

In some cases, hydrophobic particles enter the air/water surfaces of the foam and destabilise aqueous foams by a bridging-dewetting mechanism. There is a series of events that take place during the bridging-dewetting mechanism. Initially, the solid particle contacts with the two opposite interfaces of the liquid film during the film thinning and form a solid bridge between them. Then the particle surface is dewetted, and the three-phase contact lines come in direct contact with each other, which makes liquid film rupture. Evidently, for solid spheres the film rupture happens when the contact angle is larger than 90^{o} (Wang et al., 2016). Therefore, for efficient foam formation the contact angle is needed to be highly favourable towards the strong particle attachment at the new liquid interface (Dickinson, 2017). According to literature particles with a contact angle between 50 and 85^{o} are more effective at stabilising foams (Bournival et al., 2015).

However, in other cases, hydrophilic particles decrease the foam drainage by clogging up the Plateau border network or by increasing the liquid apparent viscosity. If they are nano-metric

and equal sized, hydrophilic particles form layers that remain trapped inside the films, preventing excessive film thinning and rupture (Binks, 2002; Adler and Weaire, 2008).

There are several mechanisms which are thought to be important for an explanation of the foam drainage behaviours in the presence of hydrophilic particles, which are rheology of the powder suspension and clogging in the confined regions of the Plateau borders. The hydrophilic particles become trapped in the network of aqueous foams either by the mechanism of collective trapping—jamming of the suspension for the confinement parameter <1, or by the individual capture of the particles by the foam constrictions for confinement parameter >1. Confinement parameters relates the size of the particle and to the maximum diameter of the circle inscribed in the Plateau border cross-section (Figure 2.7).

Additionally, the volume fraction of particles in the interstitial liquid of the foam is another parameter that affects performance of the hydrophilic particles on foam drainage. It has reported that the foam drainage velocity is reduced when liquid of the foam is sufficiently high even if the confinement parameter is <1 (Wang et al., 2016).

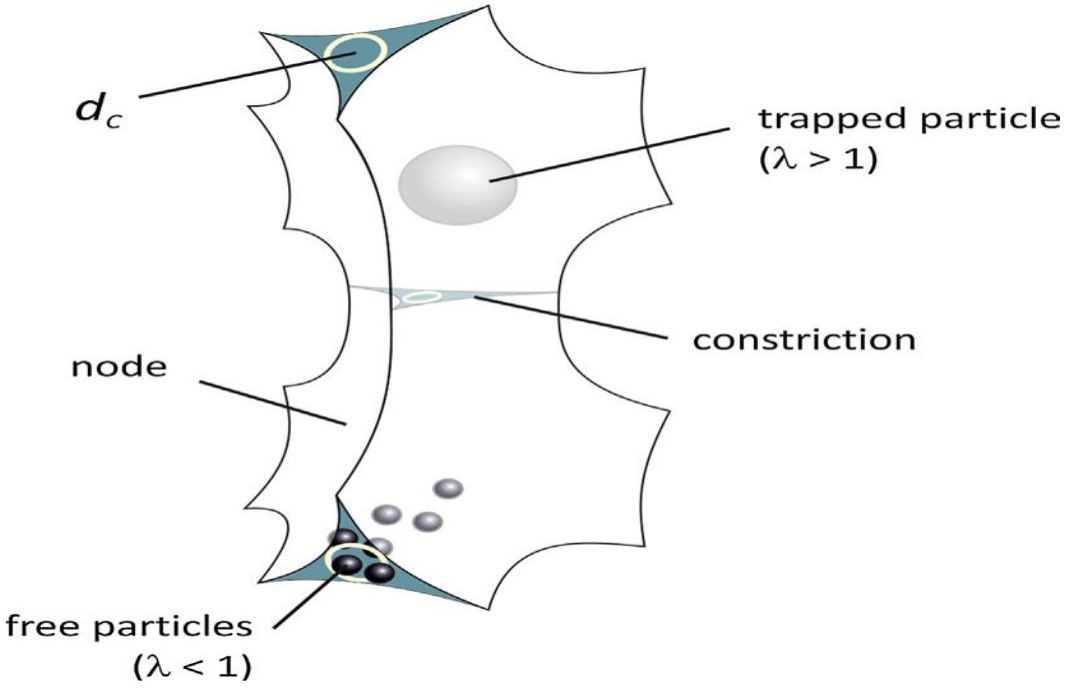

Figure 1.7. The interstitial network of aqueous foams consists in nodes connected by constrictions. Particles suspended in the interstitial fluid can be either freely transported or trapped by constrictions. This behavior is described using the so-called confinement parameter, λ, which compares the particle size to the size of passage through those constrictions, (from Haffner et al., 2015).

Individual gas bubbles need some kind of interfacial barrier to prevent coalesce with neighbouring bubbles. Surface active particles are reported to be very effective against coarsening and coalescence and can improve the foam stability due to irreversible attachment of the particles to the air/water interface and to the formation of rigid elastic layer at the bubble surface. (Rio et al., 2014; Gonzenbach et al., 2006; Adler and Weaire, 2008; Dickinson., 2017).

The complete irreversible adsorption of particles is reported to be related to the size of particles (usually around 10 nm), and their correct surface energy or contact angle with the

interface (Murray and Ettelaie, 2004). At a contact angle of 90°, the maximum capillary pressure for rupture of the film with a bridging monolayer is zero. Therefore, a particle with contact angle equal to or greater than 90° should not be able to stabilize water films by a bridging monolayer mechanism (Horozov, 2008). When the contact angle is greater than 90° foams will collapse, upon opposing bending energies, as there is no ability for foams to invert (Hunter et al., 2008).

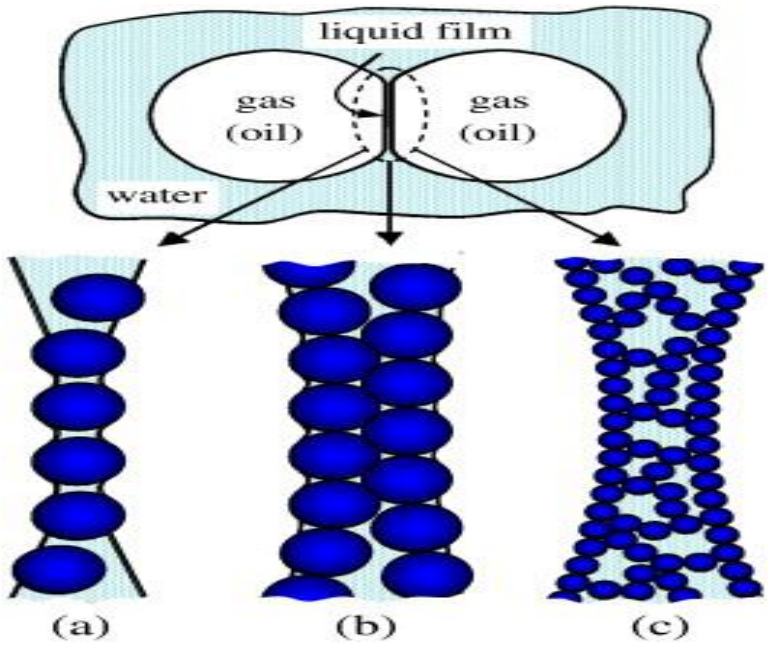

Figure 1.8. Possible mechanisms of liquid film stabilization by: (a) a monolayer of bridging particles; (b) a bilayer of close-packed particles and (c) a network of particle aggregates (gel) inside the film (from Horozov, 2008).

It has been reported by Gonzenbach et al. (2006), that foam stability can be improved significantly if particles are used instead of surfactants. They reported that the particle-

stabilised foams did not show significant bubble growth for more than 4 days. However, surfactant-stabilized foams were very unstable and coarsening was observed within the first 4 hours after foaming. Bubble shrinkage and coalescence was mechanically prevented due to forming an interfacial armour by adsorbed particles around the bubble surface. They concluded that irreversible absorption of the partially hydrophobised particles at the air-water interface played crucial role in the high foam stability (Gonzenbach et al., 2006).

According to Dickinson (2017) the stabiliation of air bubbles or droplets by Pickering particles requires a complete monolayer of closely packed particles around each bubble interface. Coalescence is prevented by the physical barrier associated with this particle bilayer arrangement.

1.8. Aerogels

Aerogels are extremely light weight materials with nano scale open-cells, low density (0.003-0.15 g/mL) and high surface areas (500-1000m^2/g). They can be made from various types of gels by removing the fluid and leaving behind only a solid structure. Aerogels have very flexible chemistry and their pore size and surface area can be tailored (Sudhakar et al., 2016; Smirnova and Gurikov, 2018).

Aerogels can be produced by different methods; traditionally aerogel production includes three main steps. Initially a gel is formed (chemical reaction, crosslinking, sol-gel transformation), followed by solvent exchange (if required by the following drying) and then the fluid is removed from the hydrogel by various methods (freeze drying etc.) and only the solid structure is left behind (Smirnova and Gurikov, 2018).

The aerogels developed by Kistler are washed with water and subsequently transferred to an alcohol bath. The process to create them could take several days. Subsequently, various researchers have found new methods for making aerogels (see Figure 2.9) (Sudhakar et al., 2016).

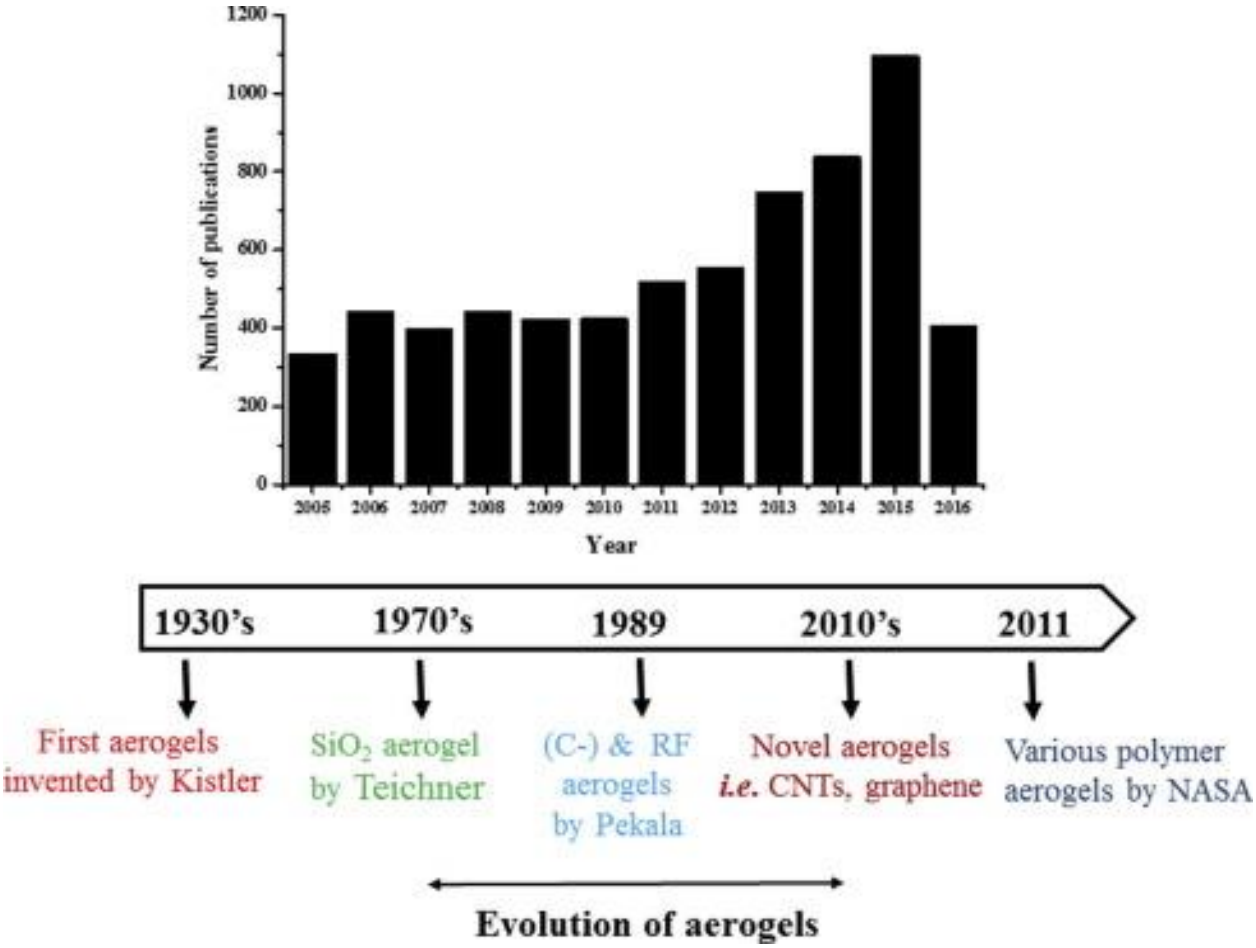

Figure 1.9. Number of publications (Science Direct record) during the last ten years containing "aerogel" in the content along with the evolution pattern of aerogels after invention (Date of search: 13 Feb. 2016) (from Maleki, 2016).

Depending on the pore-filling solvent type, aerogels can be named in different ways; alcogel and acetogel, and pore solvent is exchanged for alcohol and acetone, respectively. Also, if the aerogel is prepared from the natural polymer - based precursors that are subjected to a

physical or chemical gelation in an aqueous solution, they are named as 'hydrogels' (Maleki, 2016).

The sol-gel route is the main method that has been used for production of aerogel polymer blends (Figure 1.10). Sol-gel processing is typically performed in the liquid state and at low temperature in which solid materials are synthesised (T<100 ^{0}C) (Pierre and Pajonk, 2002).

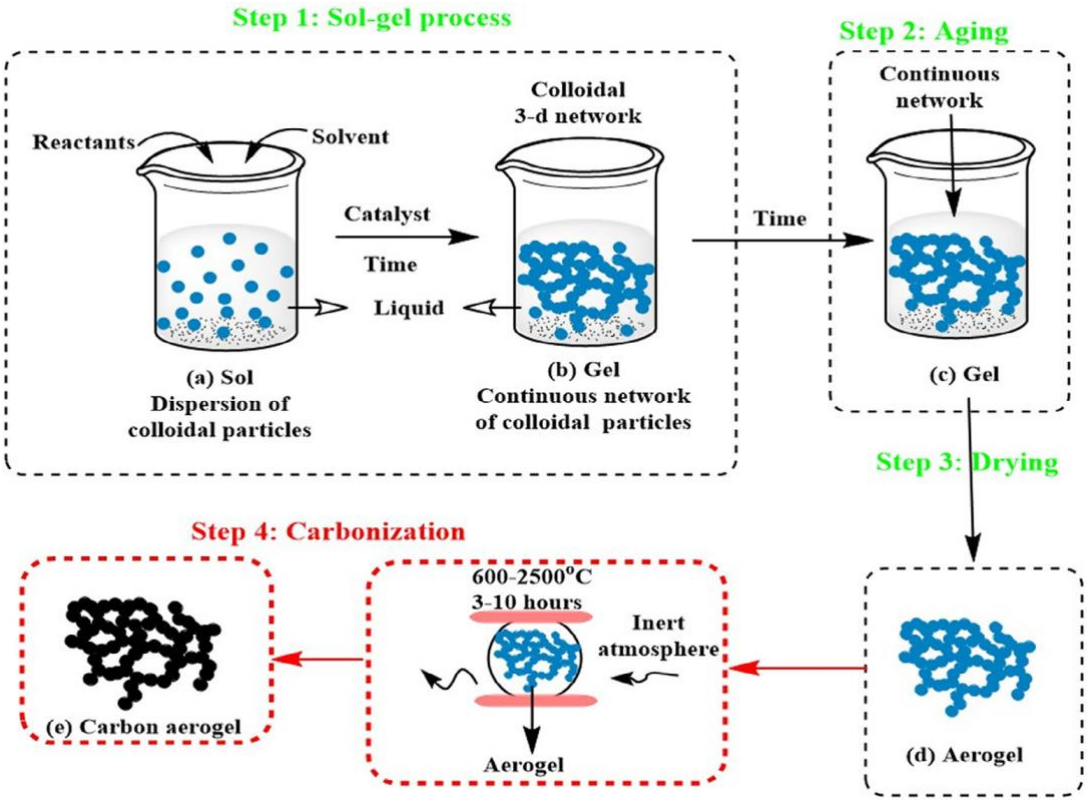

Figure 1.10. General preparation route to prepare aerogels, which begins by preparing a dispersion of colloidal particles which are then induced to gel. Carbonization is only specific for carbon based aerogels, which are synthesized at room temperature by a sol-gel polymerization route using resorcinol and formaldehyde as precursors, acetonitrile as solvent and hydrochloric acid as catalyst, followed by CO_2 supercritical drying and carbonization, in which biomass is converted into a highly carbonaceous, charcoal-like material as a result of slow pyrolysis process (from Maleki, 2016).

A sol can be defined as a dispersed solution of colloidal primary particles/monomers that are prepared from a mixed solution of precursors, water, solvents and catalysts as a consequence of hydrolysis and polycondensation reactions. The colloidal particles are cross linked to form three-dimensional porous networks by the addition of a chemical cross-linker or by changing the physical conditions of the reaction (e.g. pH, temperature). During the sol-gel reaction it is possible to tailor the gel nanostructure by adjusting key reaction parameters, which influence the sol–gel reactions, namely pH, temperature, solvent type, the concentration of precursors, relative concentrations of the precursors to the solvent, ratio of water to silica precursors (Maleki, 2016).

Ageing is an important aerogel processing step which involves formation/ further growth of gel network in the gelation solvent. Ageing improves the mechanical strength of the aerogel network and might take place from hours to days by soaking the gel in the initial sol or suitable solvent and under the controlled conditions. During the ageing process, the network particles undergo several phenomena. In emulsions “Ostwald ripening” and in foams “coarsening” are the most important ones. The kinetics of the ageing procedure is very much dependent on pH, time and temperature. To add, during ageing some important changes take place in pore size, porosity, and surface area of synthesized gels (Maleki, 2016).

1.8.1. Aerogel drying techniques

Drying is a crucial step for producing an aerogel that retain its original porous structure that is created in the wet gels. Supercritical drying (using i.e. alcohol, acetone, or CO_2), freeze drying, and ambient pressure drying are the most common ways of drying, which lead to creating a monolithic sample (Maleki, 2016). These drying techniques are explained in detail

in the following sections and summarised well in the Table 2.6 by Smirnova and Gurikov (2018).

	Conditions	**Preparation steps prior to drying**	**Limitations for the gel matrix**	**Main energy costs/Risks**
Ambient drying	Ambient pressure, room or slightly elevated temperature	Chemical hydrophobization of the matrix is often needed	Compaction of the matrix: mainly aerogels with density >0.1 g/cm^{3}are reported; Not possible for fragile and hydrophilic matrices	Low energy costs; well established process; extensive use of hydrophobization agents
Freeze drying	Vacuum (P <100 mbar); −70 < T <−20 ^{0}C	Addition of modifier (e.g. tert-butanol) to avoid structure compaction	Target density below 0.03 g/cm^3 hardly achievable; pores partly destroyed	High energy costs to maintain low temperature; batch process
Direct supercritical drying (high temperature)	Over critical point of organic solvent used for gel formation T > 100 ^{0}C P > 30 bar	No solvent exchange needed; direct conversion of the solvent to critical conditions	Temperature >100 ^{0}C often not compatible with the organic gels; possible side reactions with the solvent	Moderate energy costs to reach critical conditions (heating); batch process, High explosion and toxicity hazards
Supercritical drying by CO_2 extraction	T > 31 ^{0}C P > 74 bar Typically 40 ^{0}C, 100–150 bar	Solvent should be reasonably mixable with CO_2 at process conditions; For hydrogels solvent exchange needed	Drying kinetics depend on the CO_2/solvent transport in/out the matrix; Well compatible with all kind of gels	Significant energy costs due to CO_2 compression (may be improved by process optimization); so far bath process; lower explosion risk due to low T and CO_2 nature

Table 1.6. Drying technologies for aerogel production (from Smirnova and Gurikov, 2018).

Removal of the liquid from a wet gel is very complex and it involves different stages. Shrinkage is the first stage; the gel shrinks by the volume that was previously occupied by the liquid. The liquid flows from the interior of the gel body to its surface. During the drying process the pore

radii become smaller and therefore the network becomes increasingly stiffer and the surface tension in the liquid rises correspondingly.

The second stage starts when the surface tension is no longer capable of deforming the network and the gel body becomes too stiff for further shrinkage, whichs is the "critical" point. The probability of cracking is at its highest at this stage due to the very large tension in the gel. At this second stage of the drying, the liquid/gas interface retreats into the gel body. The third stage of the drying involves the rupture of the drying film and as a result only isolated pockets containing liquid can leave the network only by diffusion into the gas phase (Hüsing and Schubert, 1998).

There are two processes which play important roles in the collapse of the network. The first one is the formation of a pressure gradient due to slower shrinkage of the network in the interior of the gel body, which causes cracks. The second is the pores size, because during drying larger pores empty faster than smaller ones. Therefore, if pores with different radii are present, the meniscus of the liquid drops faster in larger pores. As a result, uneven stress and crack can be put on the walls between pores of different size (Hüsing and Schubert, 1998).

1.8.1.1. Super critical drying

As mentioned above, one of the traditional drying techniques for aerogels is supercritical drying. Formation of a liquid-vapour meniscus, which recedes during the emptying of the pores in the wet gels, is prevented by supercritical drying method. There is no liquid/gas interface in the pores during drying. As a result, supercritical evacuation of the wet gel permits the recovery of a kind of “dry solid image” of the wet material. By avoiding collapse of pores, the intact porous texture is also maintained. Principally, during supercritical drying

the wet gel is heated in the closed container to exceed the pressure and temperature above critical point of the liquid entrapped in the pores inside the gel (Pierre and Pajonk, 2002).

For supercritical drying different organic solvents can be used. However, CO_2 is the most commonly used solvent. Due to the mild critical temperature (T_C = 31 ^{0}C) in supercritical CO_2 drying, the implementation of this drying technique is safer and convenient compared to the supercritical fluid drying with alcohol (T_C, ethanol = 240 ^{0}C) (Maleki, 2016).

There are 2 types of supercritical drying; high temperature supercritical drying (or HOT) with organic solvents (methanol, ethanol, acetone, 2- propanol, H_2O), and low temperature supercritical drying (COLD) in CO_2 or N_2O.

Drying in organic solvents requires very high temperature and high pressure (about 250 ^{0}C and 5-8 MPa respectively) to put a solvent in the supercritical state. Nevertheless, the very high pressure and temperature combination creates problems while the flammability of these solvents is very high. To add, due to the sensitivity of the organically modified aerogels to temperature, organic groups might be destroyed during drying (Hüsing and Schubert, 1998).

Liquid carbon dioxide (CO_2) is an alternative to drying in organic solvents and is developed by biologists for electron microscopy. It has some advantages of being safe due to the very low temperature and a moderate critical pressure. However, solvent exchange step is necessary, which is very time consuming. The exchange rate of the original pore liquid for liquid CO_2 is determined by the diffusion of CO_2 into the gel. The miscibility of the pore liquid with CO_2 is also required. For instance, water and CO_2 are immiscible, and therefore an intermediate solvent exchange (e.g. water for acetone) is necessary. Similar to supercritical drying with alcohols, structural changes also take place during cold super critical drying. However, it is

minor with CO_2, so the network of the wet gel can be preserved almost unchanged (Hüsing and Schubert, 1998).

There are some dissimilarities between both (HOT and COLD) methods; during hot method which is accompanied by a kind of a rather poorly controlled ageing process, the temperature and pressure increase in order to attain the chosen supercritical conditions. Therefore, the formed aerogel is usually hydrophobic because its surface is covered by alkoxy groups. Alternatively, the materials produced in the cold method are more hydrophilic because the cold method does not favour any reaction of the silanol groups with alcohol (Pierre and Pajonk, 2002).

Silanols are compounds that analogous to alcohols and contain one or more the Si-OH group which are found in nature, for example in silicic acid, $Si(OH)_4$, found in low concentration in the aqueous environment, and on the surface of silicate rocks. Silanols are very high acidic group and therefore they tend to form strong hydrogen bonds both to themselves and to organic molecules containing suitable hydrogen bonding sites. The silanol group is important in some industriel application such as the manufacture of silicones, sol-gel processes, and as silane coupling agents for use in the functionalisation of surfaces (Baxter et. all., 1997).

1.8.1.2. Freeze drying

Freeze drying is another most applied drying technique due to it being simple, economic and environmentally friendly producing a porous structure (Maleki, 2016). During freeze drying, the gel liquid is first frozen and later the gel is dried by a sublimation process under very low pressure. Therefore, the formation of a liquid-vapour meniscus is prevented. The materials

that are obtained through this drying method are termed "cryogels" providing maximum 80% porosity with only half of the surface area compared to its aerogel counterpart (Maleki, 2016).

Due to the nucleation and growth of solvent crystals the gel network may be destroyed, which tends to produce very large pores. A rapid freezing process known as flash freezing has been used in order to prevent formation large ice crystals. However, it is also vital to have a solvent with a very low expansion coefficient and high pressure of sublimation. Ambient-pressure drying, the addition of drying control chemical additives (DCCA), solvent evaporation are other drying methods that can be applied (Pierre and Pajonk, 2002).

The main disadvantages of the freeze drying are: high shrinkage rate, low surface area, the high volume of macroporosity, are developed more in cryogels compared to their $scCO_2$ counterparts. However, this technique is more favourable for aerogels processed from a hydrogel or a gel prepared from an aqueous solution (e.g. cellulose, pectin), although the porous microfibrillar structures may fail due to the large ice crystals creating the pores (Maleki, 2016).

1.8.1.3. Ambient pressure drying

Ambient pressure drying is an alternative and safe drying method especially for the mass industrial productions. However, irreversible shrinkage is a major problem and therefore the surface of the pore walls inside the gel must be chemically treated with some non-polar groups in order to prevent additional condensations in neighbouring surface functionality after being compressed by capillary stresses. In order to avoid the capillary stresses endured by the pore walls, the pore-filling solvent must be exchanged with a hydrocarbon or a solvent with less surface tension (Maleki, 2016).

The contact angle between the liquid and the pore walls has to be influenced by deliberate modification of the inner surface and variation of the solvent to minimize the capillary stresses. Once the drying process is completed, the dried gel recovers its original dimension by a spring-back effect as a result of the repulsion of the neighbouring non-polar groups. In the untreated gels, the main reason for the shrinkage is mainly the creation of the new bonds between the two neighbouring functionalities (Maleki, 2016; Hüsing and Schubert; Pierre and Pajonk, 2002).

1.8.2. Aerogel applications

Aerogels have very extensive application areas; from construction to tissue engineering and from food to cosmetics to cleaning and drug delivery (Table 2.7). In the biomedical industry, aerogels have been used mostly for drug delivery (Mehling et al., 2009; Ulker and Erkey, 2014) and scaffolds for tissue engineering (Kang et al., 1999). Especially polysaccharide based aerogels are promising carriers for drug delivery systems due to being biodegradable and biocompatible and having large variety of chemical functionalities. Biocompatibility and biodegradability are two important parameters for applications of an aerogel in life sciences. Silica aerogels are biocompatible but they are not biodegradable. In addition, application of the organic aerogels is also limited in life sciences because synthesis of organic aerogels such as resorcinol–formaldehyde aerogels involves toxic elements (Stergar and Maver, 2016).

A good review of aerogel applications in different areas can be found in Maleki (2016), Smirnova and Gurikov (2018) and in Stergar and Maver (2016), for biomedical applications.

Although, aerogel application in the food industry is not well established yet, it has been receiving great attention. Aerogels possesses some advantages as a novel approach for

processing different food materials for various purposes. Recently, it has been reported by Plazzotta et al. (2018) that they obtained porous materials by supercritical-drying of vegetable wastes, which can be regarded as a bioaerogel-like material and would allow its use in food systems as adsorbents and carriers. Pectin based nanocomposite aerogels for potential insulated food packaging was produced by Neśic et al. (2018). They concluded that the nanocomposite aerogels can be considered as a promising alternative bio- and short-life packages for temperature-sensitive food, such as a food delivery package.

Application	**Type of aerogel involved**	**Decisive aerogel properties**
Drug delivery	Native silica; biopolymers: alginate, pectin, starch, chitosan, cellulose, and hybrids thereof	High surface area, accessibility of the pores for the drugs (micropores may be a hindrance), affinity to specific drugs (surface modification may be needed)
Tissue engineering	Mainly biopolymers: alginate, pectin, starch, chitosan, cellulose, and hybrids thereof	Combination of meso- and macroporosity in the same material, biocompatibility
Medical implants	Polyurea crosslinked aerogels, natural biopolymers: alginate, alginate-starch, gellan gum, hybrids with gelatin	Pore structure suitable to applications (usually micropores to be avoided), biocompatibility, stability in liquids, biodegradability
Biosensors	Au-carbon aerogel (doped with nanoparticles), graphene, silica, zirconium phosphate--carbon, carbon/metal hybrids, N-doped graphene, graphene/alginate, tungsten oxide, graphene-ZnO, resorcinol-formaldehyde aerogels, MoS_2/graphene, boron nitride aerogel	Surface functionalization to ensure the selectivity to target molecules, open porosity

Table 1.7. Main aerogel applications (adapted from Smirnova and Gurikov, 2018).

1.8.3. Aerogel types

Aerogels can be classified based on their appearance, microstructure and composition (Figure 2.11). However, the most commonly used classification is based on their composition, which in general describes four aerogels categories: inorganics, (*i.e*. SiO_2 derived from various alkoxysilanes, TiO_2, $Al2O_3$, ZrO_2, etc.), organic (*i.e*. resorcinol–formaldehyde (RF), polyurethane, polyimide, polystyrene, etc.), hybrid (based on organic-inorganic compounds) and bioaerogels (Stergar and Maver, 2016; Maleki, 2016).

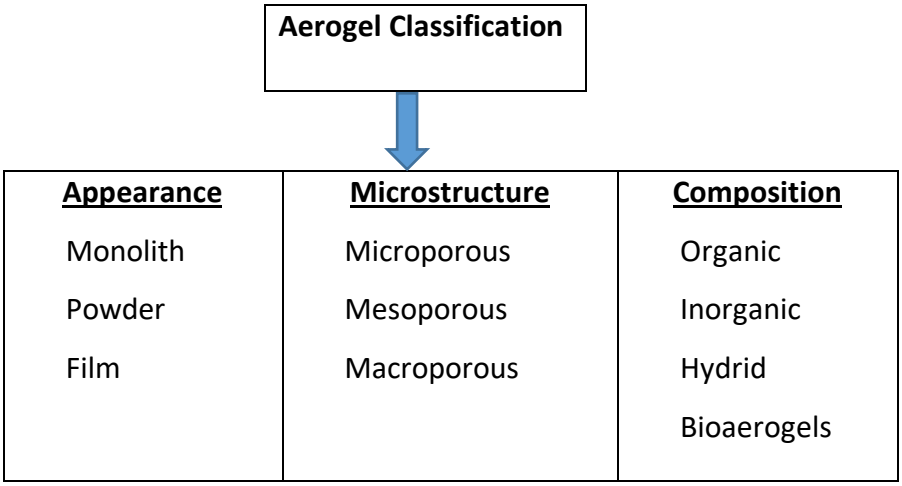

Figure 1.11. Aerogel clasification based on appearance, microstructure and composition (Adapted from Stergar and Maver, 2016; Maleki, 2016).

The organic aerogels were first developed in 1987 by polymerization of multifunctional organic monomers in dilute solution which was followed by supercritical drying (Hüsing and Schubert, 1998). Preparation of hybrid aerogels are based on both organic and inorganic components. It is reported that the combination of the high surface area of the inorganic components with the biodegradable organic constituents resulted in novel materials with interesting properties (Hüsing and Schubert, 1998).

Bio-aerogels have received great attention due to being produced from natural sources such as protein, starch, cellulose/cellulose derivatives, and marine polysaccharides. They are widely used in medical engineering, sustainable packaging production and novel food development due to being biocompatible, biodegradable and food-grade. In addition, they can absorb large amounts of liquids by capillary forces and therefore they are also used as carriers for different solvents. In addition, it has been suggested that bioaerogels can act as templates for liquid oil structuring and innovative carriers of nano-sized biochemicals and also as food bulking agents (Plazzotta et al., 2018; Neśic et al., 2018).

For the purpose of this research only protein (whey protein, egg white protein) and polysaccharide (cellulose, alginate, starch) based bioaerogels will be explored in detail.

1.8.3.1. Protein based aerogels

Food grade aerogels made of proteins attract attention in various applications especially as a carrier system or as an encapsulation material due to their high surface area (up to 400 m^2/g), biocompatibility and digestibility. Whey protein isolate (Chen et al., 2013; Betz et al., 2012) and egg white protein (Kleemann et al., 2018; Selmer et al., 2015) are commonly used proteins to create aerogels

Betz et al. (2012), investigated the applicability of thermal whey protein hydrogels for the generation of highly porous water-insoluble aerogels as drug carriers. It was reported that whey protein aerogels showed a high drug loading capacity of up to 9.5% (w/w) (cryogels: 0.4–0.8%, w/w) and whey protein-based matrices were applicable for a pH-controlled drug

release with regard to their swelling behaviour. Similar to whey protein isolate, egg-white protein based food grade aerogels were developed by Selmer et al. (2015). The pH and the ionic strength of the solution was reported to be important for tailoring the porosity and surface area of the gelation process. The pH values above the isoelectric point (pI) (at alkaline pH) was recommended for producing mechanically stable aerogels with high surface areas (Selmer et al., 2015). For the formation of the egg white protein (pI:4.54) hydrogels ionic strength and pH was reported to be key parameters to influence the structure of the egg white protein hydrogels (Kleemann et al., 2018).

1.8.3.2. Polysaccharide based aerogels

Polysaccharides as aerogel-forming materials has many advantageous aspects in food and non-food for being natural and sustainable. Nevertheless, food applications of polysaccharide-based aerogels do not currently exist on the market.

Among biopolymers, particular attention has been given to cellulose, which occurs in all plants, some animals and certain bacteria. Cellulose aerogels are very porous materials with a solid structure. There are three steps in cellulose aerogel preparation: dissolving/dispersing cellulose or cellulose derivatives, forming a cellulose gel by the sol–gel process, and drying cellulose gel (Long et al., 2018).

When compared to traditional silica aerogels and synthetic polymer aerogels, the cellulose aerogels have the specific surface area (10–975 m^2/g), porosity (84.0–99.9%), and density (0.0005–0.35 g/cm^3). Cellulose aerogels are more biodegradable and have a higher compressive strength (5.2 kPa–16.67 MPa). Therefore, they have a great potential in the application of adsorption and oil/water separation, heat insulation, biomedical materials,

metal nanoparticle/metal oxide carriers, the preparation of carbon aerogels, and many other areas (Long et al., 2018).

Among cellulose types, cellulose derivatives are used for aerogel production due to being soluble in water and in some organic solvents; for example, carboxymethylcellulose (CMC), hydroxypropyl methylcellulose (HPMC) are both soluble in water, triacetyl cellulose (TAC) is soluble in dioxane/isopropanol, ethyl cellulose (EC) is soluble in dichloromethane, and cellulose acetate (CA) is soluble in acetone. Since acetone and some other organic solvents are soluble in the case of supercritical CO_2 drying ($ScCO_2$), the time-consuming solvent exchange process can be omitted. However, for the gelation, a cross-linking agent is needed because the molecular chains of cellulose derivatives have a reduced number of hydroxyl groups (Long et al., 2018).

In the aerogel field, nanofibrillated cellulose (NFC) has been studied widely. When it is used to reinforce other materials, these biofibrils show excellent mechanical properties. In addition to NFC, hemicelluloses, which are structurally different polysaccharides and also exist in plant cell walls, are consumed in the human diet within cereals, fruit, and vegetables. Of the hemicelluloses, xylans (occurs in in various plants and agricultural products), β-glucan (are highly viscous, gel-forming bioactive polysaccharides- especially in oat), and xyloglucan have been studied in the aerogel field so far (Mikkonen et al., 2013).

Alginate and chitosan are marine origin polysaccharides and utilised in aerogel research widely. Two other marine polysaccharides studied as potential aerogel components are also of algae origin. Carrageenan and agar are obtained from red seaweeds, while alginate from brown seaweeds (Mikkonen et al., 2013).

Although starch is a most abundant plant polysaccharide after cellulose, it is not as widely studied as an aerogel matrix as alginate and cellulose (Mikkonen et al., 2013). However, there are some studies of application of starch in aerogel fields. Ubeyitogullari and Ciftci (2016) have reported that biodegradable nanoporous aerogels were obtained from wheat starch, which can be promising carrier systems for bioactive and drugs in food and pharmaceutical industries. Aerogels made of corn starch were developed for an anti-fungal volatile release. Crosslinked starch aerogel was reported to be a convenient reservoir for loading and succeeding release of the volatile compound *trans-2-hexanal* (Abhari et al., 2017). Maize starch aerogel was prepared by using supercritical gel drying as porous support for the adsorption of α-tocopherol (TOC, vitamin E) and menadione (MEN, vitamin K_3). It was concluded that incorporation of poorly water-soluble vitamins into starch aerogel by the supercritical fluid adsorption can be considered an effective possibility (Marco and Reverchon, 2017).

The polysaccharide aerogels could represent innovative approaches as advanced materials in food packaging industry, in a form of wraps, internal food packaging layers or as oxygen/humidity sachet scavengers. Polysaccharides are edible and have good film-forming properties. They have an ability to form gels by changing the pH or temperature, as well as in the presence of divalent cations, which make them suitable for production of bio-materials of any size and shape (Neśic et al., 2018).

CHAPTER 2

Materials and methods

2.1. Materials

The materials used as aerogel matrices were whey protein isolate-WPI (Myprotein, Cheshire, UK), Sodium alginate (SA) powder (Danisco, Landerneau, France), with Mannuronic /Guluronic ratio 0.9, Locust bean gum (LBG 246), (Danisco, Valencia, Spain) and methylcellulose (MC) A4M with a methyl substitution percentage of 27.5-31.5% and Hydroxypropyl methylcellulose (HPMC) K4M and K100M (Dow Wolf, Bomlitz, Germany). For ionic cross- linking calcium carbonate ($CaCO_3$, Sigma-Aldrich, Gillingham, UK), and Glucono delta-lactone (GDL, Sigma-Aldrich, Gillingham, UK) were used. All chemical reagents were of Food grade and directly used unless otherwise mentioned.

The materials that were used as aerated food based aerogel matrices weres whey protein isolate- (WPI), Sodium alginate (SA) powder with M/G ratio 0.9, and methylcellulose A4M with methyl substitution percentage of 27.5-31.5%. For ionic cross- linking calcium carbonate ($CaCO_3$), and Glucono delta-lactone (GDL), were used. Fresh carrot juice (squeezed from carrots which were bought from supermarket), commercial tomato puree and a commercial orange juice. Sodium hydroxide (1M) from Sigma- Aldrich, Australia was also used to adjust pH. All chemical reagents were of food grade and directly used unless otherwise mentioned.

	Alginate	WPI	K100M	K4M	A4M	LBG
Mw	216.120 kDa	18.4 kDa	1150 kDa	400 000 kDa	400 000 kDa	50 000 -3000 000 kDa
Viscosity	N/A	N/A	2% in Water at 20 ^{0}C 75 000-140 000 m Pa.s	2% in Water at 20 ^{0}C 2 663-4 970 m Pa.s	2% in Water at 20 ^{0}C 2.663-4.970 m Pa.s	1% in water yields 3000-3500 cP
Degree of Methoxyl substitution (Ds)	N/A	N/A	19.0-24%	19.0-24.0%	27.5-31.5%.	N/A
Degree of Hydroxypropoxyl substitution (Ds)	N/A	N/A	7.0-12.00%	7.0-12.0%	N/A	N/A
M/G ratio	0.9	N/A	N/A	N/A	N/A	N/A

Table 2.1. Characteristics of used poylmers.

2.4. Methods

Total Solid mass content %	Alginate %	WPI %	HPMC-K100M %	$CaCO_3$ %	GDL %	Mixing (aeration) time minutes	Mixing (aeration) speed- rpm
2.5 %	0.5	1	0.25	0.5	0.25	10	8000
0.875	0.25	0.25	0.125	0.125	0.125	10	8000
0.70	0.20	0.15	0.15	0.10	0.10	10	4000,6000,8000
						4,6,8,10,12,14,20	8000
0.55	0.20	0	0.15	0.10	0.10	10	8000
0.50	0.20	0	0.10	0.10	0.10	10	8000

Table 2.2. Formulation for aerated hydro and aerogel production with varied dry mass content and processing parameters.

2.2.1. Preparation of viscous solutions

Initially WPI+Alginate+ MC/HPMC solutions were prepared by dissolving dry blends of the polymers in deionised water. The powders were hydrated for 2 hours by stirring at room temperature with a magnetic stirrer (IKA, RCT basic at 400 RPM). The dry blend of polymers were added to water gradually in order to prevent lump formation. After 2 hours of hydration, calcium carbonate ($CaCO_3$) was gradually added and mixture was stirred for 5 more minutes for complete $CaCO_3$ dispersion. GDL was added in the same manner and the mixture was stirred for another 5 minutes. The mixture was taken to an overhead mixer immediately (Silverson, L5M) for aeration (within less than a minute) in order to prevent any gelation that might take place before such an aeration step (Refer to Figure 2.1).

For preparation of LBG aerated hydrogels, the dry blend of WPI+Alginate+LBG was dissolved in deionised water at 40 ^{0}C by 2 hours stirring using a magnetic stirrer IKA, RCT basic) at 400 rpm. Calcium Carbonate ($CaCO_3$) and then GDL was added as it was explained above and then it was aerated.

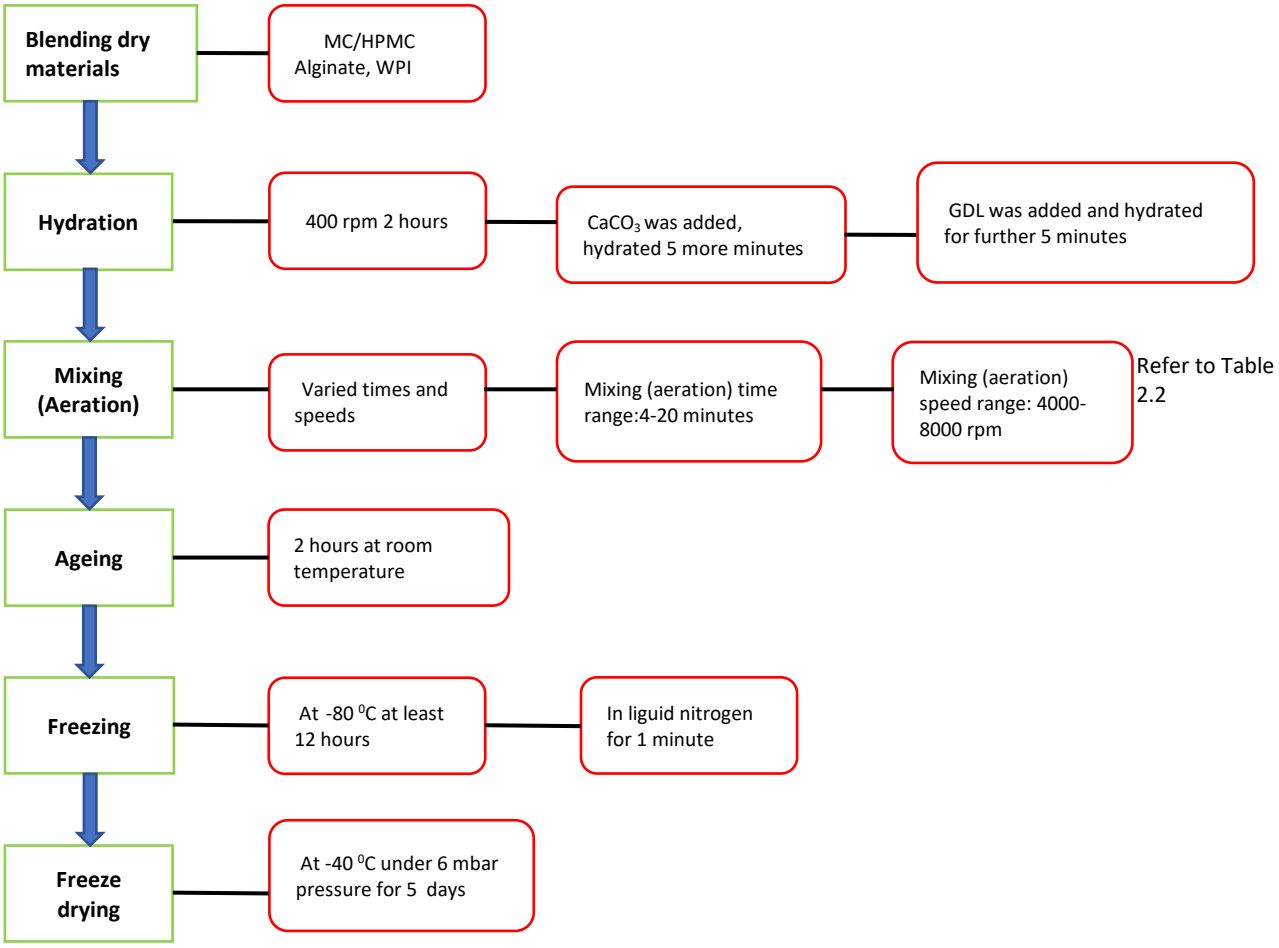

Figure 2.1. Process flow diagram for production of aerated hydro and aerogels.

2.2.2. Aeration of the viscous solution (gel preparation/foaming)

Formation of aerated hydrogels was induced using overhead mixer (Silverson, L5M). Solutions were aerated for varied time periods from 4 minutes to 20 minutes, and at varied speeds from 4000 rpm to 8000 rpm (refer to Figure 2.1)**.** During aeration, the solutions were kept in a cold water bath (10 ^{0}C) in order to prevent excess temperature increase. After completion of the aeration step, samples were kept at room temperature for 2 hours in order to promote full gelation.

2.2.3. Freezing of the hydrogels

The aerated hydrogel samples were frozen either by fast freezing in liquid nitrogen at -196 ^{0}C or at -80 ^{0}C. For liquid nitrogen freezing, 20 ml of aerated hydrogel samples were transferred into 50 ml plastic tubes and keept at room for inducing complete gelation. Later, the samples were immersed in liquid nitrogen for 1 minute and then than kept at -80 ^{0}C prior to freeze drying.

2.2.4. Freeze Drying of hydrogels (formation of an aerogels)

The aerated frozen hydrogel samples were dried by sublimation of liquid at -40 ^{0}C under 6 mbar pressure for 5 days using a freeze dryer (Edwards, Freeze Dryer Modulo).

The materials used as aerated food based aerogel matrices were whey protein isolate - WPI (Myprotein, UK), Sodium alginate (SA) powder (Danisco- Denmark), M/G ratio 0.9, and methylcellulose A4M with methyl substitution percentage of 27.5-31.5%. For ionic cross linking calcium carbonate ($CaCO_3$), (Sigma, UK) and Glucono delta-lactone (GDL), (Sigma, UK) were used. Fresh carrot juice (squeezed from carrots that were bought from supermarket), commercial tomato puree and a commercial orange juice. Sodium hydroxide (1M) from Sigma Aldrich, Australia was also used to adjust pH. All chemical reagents were of food grade and directly used unless otherwise mentioned.

2.2.5. Preparation of aerated edible hydrogels

Initially WPI+Alginate+A4M solutions were prepared by dissolving the dry blend in deionised water for 2 hours by stirring at room temperature using a magnetic stirrer (IKA, RCT basic at 400 RPM. After 2 hours, calcium carbonate ($CaCO_3$) was gradually added to the solution and was stirred for further 5 minutes for complete $CaCO_3$ dispersion. GDL was added in the same manner and the mixture was stirred for another 5 minutes. After 5 minutes of adding GDL, the desired amount of fresh carrot, commercial tomato puree or commercial orange juice was added. The mixture was sheared using an overhead mixer (Silverson, L5M) for aeration immediately (within less than a minute) in order to prevent any gelation that might take place before aeration step. There was not any heat treatment during preparation of all viscous solutions. The final total dry mass content was 0.80% (alginate 0.20%, WPI 0.15 %, A4M 0.15%, $CaCO_3$ and GDL at 0.15% w/w.). The pH measurements were performed with a Delta 320 pH-meter (Mettler Toledo Instruments Co., Ltd.). Each sample was measured three times, and the results shown are the mean pH value.

2.3. Characterisation of aerated hydro and aerogels

2.3.1. Overrun measurements

The overrun represents the amount of air that was able to incorporated after foaming by mixing, and is defined as follows;

$$\text{overrun } \% = \frac{(WBA \div VBA) - (WAA \div VAA)}{(WAA \div VAA)} \times 100 \qquad \text{Equation 2.1}$$

Where:

WBA: Weight before aeration

VBA : Volume before aeration

WAA : Weight after aeration

VAA: Volume after aeration

All measurements represent the arithmetic means of three replicates.

2.3.2. Rheological measurements

Viscosity and rheological measurements were performed using a rheometer (Anton Paar Ltd, UK) with cone and plate geometry diameter of (55 mm) with true gap. The rheological properties of the bulk phase were determined by oscillatory rheology (time and temperature sweep) by applying a strain controlled frequency sweep at a strain rate within the linear viscoelastic region of the samples, as defined by an amplitude sweep performed beforehand using a similar sample.

Shear dependent viscosity of the solutions were analysed by using rotational rheology which was then followed by oscillations for time and temperature sweep measurements.

The viscosity of the solutions was measured by the same geometry at increasing shear rate (0.001 to 1000 s^{-1}) at 25 ^{0}C. The solutions were prepared using steps from section 6.1 3 at various concentrations. All rheological measurements were carried out in triplicate.

2.3.3. Texture analysis

Dry and wet gel texture parameters were determined by using a TA. HD Plus Texture Analyser (Stable Micro Systems, UK). The wet aerated hydrogels were compressed with a 5 kg load cell and P/100; 100mm diameter plate to a true strain of 0.4. The force required to compress the foams to a strain of 0.4 was the maximum force exerted on the hydrogels.

The dry gels (aerogels) were compressed with a 100 kg load cell and P/100; 100mm diameter plate to a true strain of 0.7. The force required to compress the foams to a strain of 0.7 was the maximum force exerted on the aerogels. All texture analyser measurements were carried out in triplicate.

2.3.4. X-ray computed tomography imaging

The microstructure of the aerated hydrogels including volume, air cells count, porosity, surface area, were analysed by X-ray Computed Microtomography using a Phoenix Nanotom NF180 X-ray CT System at The Hounsfield Facility, University of Nottingham (GE Sensing &

Inspection Technologies GmbH, Wunstorf, Germany). Samples were scanned in a plastic tube (length 222 mm, width 50 mm). The scan consisted of 2400 projection images collected over a 360° rotation using an electron acceleration energy of 60 kV, a current of 160 µA and a scan resolution of 8.5 µm. Data was reconstructed using Datos REC software (GE Sensing & Inspection Technologies GmbH, Wunstorf, Germany) and analysed for pore characteristics using VG StudioMax V2.0 (Volume Graphics GmbH, Germany).

The porosity ($\emptyset$) can be defined as the ratio between the volume of empty space (V_e) and the total volume of the hydrogel (v_{hg})

$$\emptyset\ (\%) = (\mathrm{Ve} \div \mathrm{Vhg})\ \mathrm{X}\ 100 \qquad \text{Equation: 2:2}$$

2.3.5. SEM and CRYO -SEM imaging

The aerogel microstructure and pore images of the freez dried specimens were obtained using SEM at Nanoscale and Microscale Research Centre, University of Nottingham. The samples were cut with a scalpel and placed on a specimen holder. They were coated with gold using Leica EM SCD005 Sputter Coater (Leica Microsystems, UK) for 240s at 25mA to prevent charging on the sample surface from electron beams. JEOL 6060LV Variable Pressure Scanning Electron Microscope (JEOL UK Ltd.) analysed the sample under vacuum using 10kV of electrons.

The microstructure and pore images of the aerated hydrogels were obtained using CRYO-SEM (JEOL UK Ltd) at Nanoscale and Microscale Research Centre, University of Nottingham. CRYO-

SEM allows for samples to be rapidly frozen, manipulated and then imaged. This enables preservation of the initial substrate morphology and chemistry of a fully hydrated or liquid specimen.

For CRYO-SEM the samples were cut with a scalpel and placed on a holder which was transferred into an Oxford HT 1500F Cryo System chamber attached to the microscope (JEOL Scanning Microscope 6320F, Tokyo, Japan). Once the sample was inside the chamber, a fracture of the sample was made to get a fresh clean surface to be examined. The temperature of the sample was raised by heating the holder to −92 ^{0}C for 30 seconds in order to sublimate free water in the solid state, followed by a temperature decrease to −130 ^{0}C to stabilise the sample. The surface of the frozen preparation was then coated with platinum/palladium to obtain a good relation between signal and noise. The coated sample was thereafter transferred into the microscope chamber where it was analysed. Digital images were collected at 5 kv and computer stored (JEOL SemAfore software, Sollentuna, Sweden) before being further assessed by image analysis.

Cryo preparation of samples were prepared in same manner of SEM. However, the samples were frozen in the nitrogen slurry. Reduced pressure caused the liquid nitrogen to solidify at successively higher temperatures until it changed into a solid state.

At this point, the pressure was returned to atmospheric in the chamber and the sample was immersed in the nitrogen slurry. This process allowed for immediate freezing of the sample without disruption of delicate structures in the sample. Then the sample was fractured after freezing, exposing an undisturbed surface for examination.

2.3.6. Inverted light microscopy imaging (EVOS)

The images of aerated systems were taken using EVOS-Inverted light microscopy. In this way light passed through the samples and outline of whole bubbles can be visualised.

2.3.7. Particle size analyzer

Particle size distribution of the $CaCO_3$ solution after mixing at varied speeds with overhead mixer (Silverson, L5M), were determined using a Beckman Coulter, LS 13 320 Laser Diffraction Particle Size Analyzer. All size measurements were carried out in triplicate.

2.3.8. ImageJ

The diameter of air cells in the aerated hydrogels was analyzed using the scientific image-analysis program, ImageJ software. The images of the aerated hydrogels were taken by using light microscope (EVOS). The images were processed and analyzed by using principal functions of ImageJ as follows:

1. Set the Scale.
2. Calibrate images.
3. Select most evenly illuminated part and duplicate it.
4. Chosing right filter (Ban fast).
5. Thresholding
6. Analyze particles, “size=0- infinity circularity=0.00-1.00
7. Count: between 1000 and 1200

8. The individual work steps were recorded as a macro in imageJ.

The data was saved as a table (File > save as) in an ms excel file (file extension. Xls) or directly copied into the previously created excel analysis file. The distribution of individual data from one measurement was shown on a histogram.

2.3.9 Statistical analysis

All the data of the replicated measurements of the study that are plotted in this thesis include the average of the measurement accompanied by error bars that consist of the standard deviation (SD) of the mean. In the case where mean values of an observation are compared between samples the data have been subjected to analysis of variance (one-way ANOVA-Fisher) in order to determine significant differences between the samples. Data where checked for following normal distribution and equality of variance prior to carrying out the ANOVA. The level of significance of $p < 0.05$ was chosen.

CHAPTER 3

Developing a new method for protein-polysaccharide based aerated aerogels and improvement of hydrogel and aerogels by means of optimising the method of production and material usage

3.1. Introduction

Proteins and polysaccharides are natural biopolymers and are used in food products as thickening, stabilising, gelling and emulsifying agents etc. The control of their molecular interaction adds diversify to their functionality, which is therefore of high interest for the development of novel food products (Le et al., 2017).

Alginate is a natural polysaccharide extracted from seaweed. The main applications of alginates are based mainly on their gel-forming ability and used as food additives in jams, jellies to improve and stabilise the structure of food (Rinaudo, 2014). It also used in the areas of tissue engineering, controlled drug release, cell encapsulation/immobilization and wound healing (Lee and Mooney, 2012). Similar to alginate, whey proteins are widely used in many food formulations. They have ability to form thermally induced gels, which capable of holding large amounts of water, emulsions and gelled emulsions (Chen and Subirade, 2006; Barbut and Foegeding, 1993).

In the food industry different biopolymers are used to produce gels with different textural characteristics, appearance and gel point. There are some internal and external factors that determine functionality of the biopolymers namely type of the biopolymer, formation conditions (e.g., heating), chemical conditions (e.g., pH), and interactions with other food ingredients (Barbut and Foegeding, 1993).

Depending on the characteristics of the biopolymers used and the environmental conditions, gelation of protein-polysaccharide mixtures has usually been associated with different

interactions, which can be classified into three types: interpenetrating, coupled and phase-separated networks (Le and Turgeon, 2015).

When proteins and polysaccharides are mixed in water two different interactions can take place, depending on pH and ionic strength, either being thermodynamically incompatible or thermodynamically compatible (Le et al., 2017).

Interpenetrating networks can be formed when the two components gel separately and form independent networks which are continuous throughout the sample only topological. Coupled or complex coacervate networks are formed in the presence of favourable intermolecular interactions between the different types of polymers. In contrast, incompatible polymers, where interactions between the different polymers are repulsive and/or when the two types of polymers show varying affinity toward the solvent, form phase-separated gels (Turgeon and Beaulieu, 2001). When calcium ions are presented, interpenetrating network has been observed in bovine serum albumin (BSA)/LM-pectin mixtures. A very weak protein aggregate network formed by heating and then it was interpenetrated by a LM-pectin network formed with calcium ions upon cooling. Therefore, both biopolymers form two independent gelled networks (Le et al. 2017).

Protein-polysaccharide hydrogels, which can be defined as two- or multi-component systems consisting of a three-dimensional network of polymer chains and water that fills the space between macromolecules, could be micro/macroporous. The state of the water inside hydrogel play important in pore structure of hydrogels. According to literature in hydrogels water exists in three states: (i) free water, which is not interacting with polymer and behaves as pure water; (ii) weakly bound water weakly interacting with the polymer and freezing at

subzero temperatures and (iii) water strongly bound to the polymer through hydrogen bonding and unfrozen at T < -15 ^{0}C (Savina et al., 2011).

The drying method is crucial for retaining the structure of wet gels. Freeze drying and supercritical CO_2 drying are two methods that are mostly used. Air drying is not a very common way of drying a hydrogel, as it leads to shrinkage, deformation, and closure of pores and even collapse of the network due to the high surface tension of the water. Alternatively, freeze-drying, by which water from hydrogels is removed through sublimation of frozen hydrogels, also has some drawbacks such as formation of ice crystals within the hydrogel network, and as result expanding and distorting the polymer chain network. On the other side supercritical CO_2 drying which is actually not suitable for hydrogels due to a large miscibility gap in the CO_2/water since the gelation of polysaccharides usually takes place in an aqueous medium, could be an alternative method for avoiding these problems. However, prior to the supercritical drying water should be substituted by an organic solvent such as ethanol which is very miscible with CO_2 and can evaporate faster (NeŠic et al., 2018).

The aim of the work described in this chapter was to explain in detail how a new method was developed to create low mass content aerated hydro and aerogel, which was followed by the optimisation of physical and chemical parameters in order to improve macro and microstructure of aerated hydro and aerogels made of protein and polysaccharides (WPI, Alginate, MC/HPMC and LBG). Physical parameters investigated include mixing speed, time and temperature of mixing. MC/HPMC was included into the formulation to improve gel strength. As an alternative, the effect of LBG was assessed as a cryo protectant on providing more intact air cells in the final aerogel. Two different freezing regimes (slow and fast) were

used and the effect of fast freezing was compared on aerogels made using the two different polymers (HPMC-K100M and LBG).

The microstructure of hydrogels and aerogels was characterised by Cryo-SEM and SEM respectively, giving qualitative information. Unfortunately, there are limited techniques for the investigation of hydrogels in their hydrated state, such as confocal laser scanning microscopy or multiphoton microscopy. In this study, it was not possible to use techniques that normally used for structural characterisation, e.g. mercury porosimetry, pycnometry, BET (Brunauer–Emmett–Teller) due to very delicate structures which collapsed when they were s subjected to even if very low pressure.

3.2. Developing a new method for protein-polysaccharide based aerated aerogels

After some concept testing and pilot trials for producing aerogels, a new method was developed. Initially an aerogel based on whey protein isolate (WPI) was attempted (Orrego et al., 2015).

Figure 3.1. Image of an aerated whey protein isolate gel (from Orrego et al., 2015).

The method that has been used by Orrego et al. (2015) includes three main steps; (a) formation of whey protein isolate (WPI) dispersion, (b) thermal treatment of WPI dispersions, and (C) formation of aerated WPI gels. In this study, this approach was not successful. There were found to be some reproducibility problems of the published method by Orrego et al. (2015) as explained below:

a. Formation of WPI dispersion was very long and time consuming,
b. Thermal treatment of WPI dispersion was very tedious and it was not practical,
c. Cooling of WPI in ice water was time consuming and difficult to control the internal temperature in the test tubes,
d. Formation of self-supporting gels after the heat treatment was not constant across samples; forming in some tubes, but not in others, although they experienced the same conditions,
e. After cooling it was very difficult to pour the WPI dispersion into a beaker for aeration. It was found that it was not possible to aerate after heat treatment and cooling, 20 ml in 20 ml beaker, as indicated in literature,
f. Aeration step was not successful, as it did not produce a foam,
g. After attempting aeration, samples were stored for 24 hours at 10 ^{0}C to set the aerated gel structure. However, unlike the published method, after 24 hours no gelation was achieved.
h. Overall, the method was very time consuming and long. It took me 3 days to get a result, which was not successful at all.

Figure 3.2. WPI dispersion after thermal treatment. Self-supported gel formed after 21 minutes thermal treatment at a constant temperature of 70 ^{0}C.

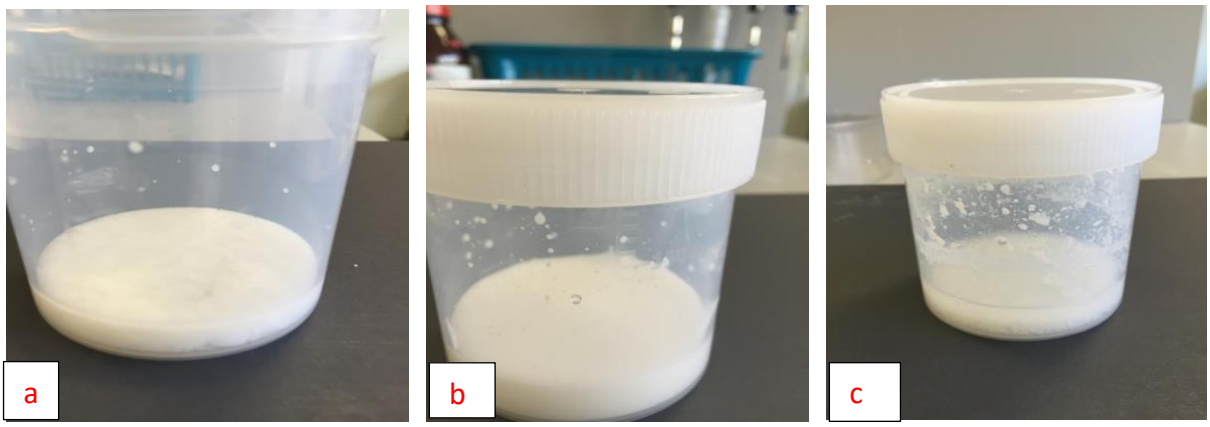

Figure 3.3. Different stages of WPI-based aerogel production; (a) before aeration, (b) After aeration and (c) after storage, no elf-supported gel structure after 24 hours storage.

After unsuccessful adaptation (Figure 3.3) of the published method by Orrego et al. (2015), a new method was developed:

a. One easy to apply.
b. With a shorter process time.
c. Reproducibility.
d. Providing a high overrun.
e. Structure stable with time.
f. Controlled gelation rate.

g. Minimised dry mass content and high in air.

h. Tailored processing conditions before and also after aeration (time, temperature, pH, overrun etc.).

After a very intensive literature review and concept testing, the new method is based on a one -pot approach and ionic- cross linking. The used materials and methods will be explained in detail in section 3.3 and 3.4.

3.3. One-pot approach

A facile “One Pot" approach was chosen for preparing aerated aerogels. The one pot approach involves blending and hydrating all dry materials (except for cross-linking agents; $CaCO_3$ and GDL) in deionised water under the desired conditions.

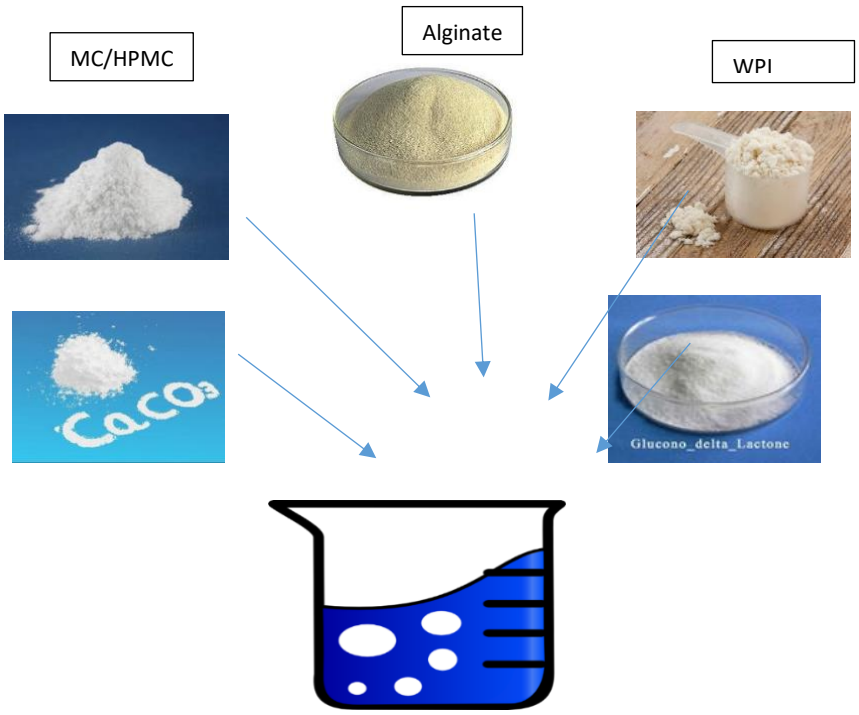

Figure 3.4. One pot approach for creating aerated hdyrogel (Images are sourced from Google)

3.4. Ionic cross linking

The $CaCO_3$-GDL cross-linking system was used. $CaCO_3$ is used as a source of calcium ions to initiate gelation of alginate. In the presence of calcium ions, the gelation rate can be too quick to control in the process, which leads the resulting hydrogel being non-uniform and having a weak mechanical strength (Figure 3.5). However, the $CaCO_3$ –GDL binary system could make the gelation process slow and gives homogenous structure to aerated hydrogel (Cheng et al., 2012).

In the absence of ionic cross- linking agent ($CaCO_3$) aerated WPI and alginate solutions did not form a gel (Figure 3.5a and 3.5b). However, $CaCO_3$-GDL system produced strong, uniform, and three-dimensionally defined gels (Figure 3.5.c- and d).

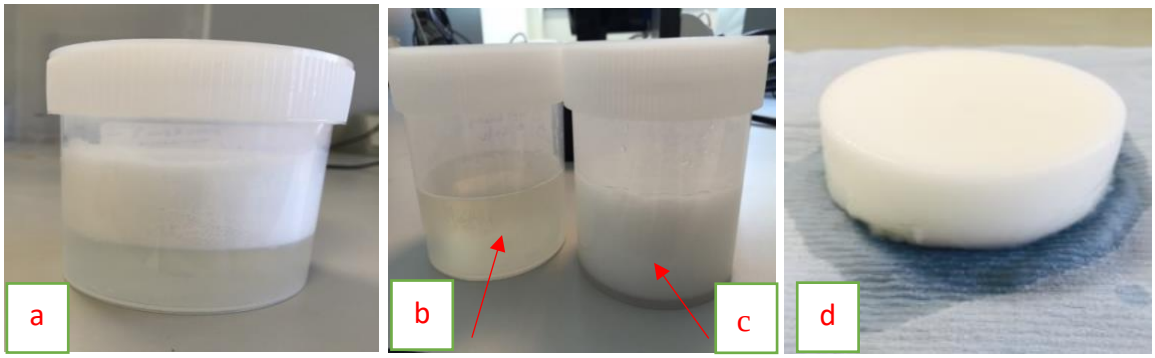

Figure 3.5. Showing formation of hydrogel after aeration with WPI and alginate mixture, no gelation after aeration without $CaCO_3$ and GDL (a) WPI and alginate mixture 2 hours later after aeration (b), WPI, Alginate, $CaCO_3$ and GDL, 2 hours after aeration (c) and formation of aerated gel after adding $CaCO_3$ and GDL (d)

Slow release of Ca^{2+} from $CaCO_3$ provides slower gelation rate, which was advantageous to form more uniform structures and greater mechanical integrity. Slower gelation rates were also advantageous since longer working time required for effective aeration.

In this study, the formation of 3-D gel structure in the presence of Ca^{+} ions with alginate and WPI might be explained by interpreting them as interpenetrating networks (Figure 3.6).

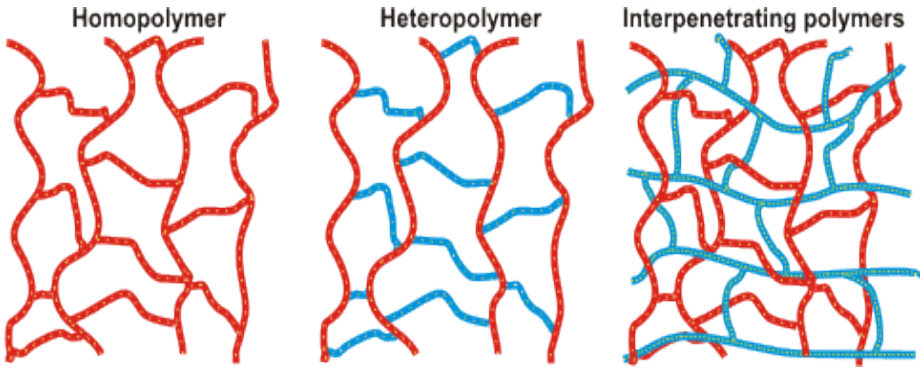

Figure 3.6. The three main types of 3-D hydrogel network Homopolymers are composed of a single polymer type (e.g., poly (2-hydroxyethyl methacrylate); heteropolymers are composed of two or more polymers cross-linked together, and interpenetrating polymer networks comprise two different polymers that are physically entangled but not covalently linked (from Chaplin, 2018).

Interpenetrating networks are a result of independent gelation of two components and formation of independent networks which are continuous throughout the sample. However, any interaction between independent networks is just topological, there is no interaction between them (Turgeon and Beaulieu, 2001). In general when proteins and polysaccharides are mixed in water two different interactions can take place, depending on pH and ionic strength, either being thermodynamically incompatible or thermodynamically compatible (Le et al., 2017).

3.5. Improvement of hydrogels by optimising physical and chemical parameters: Results and discussion

After setting up a method for creating an aerated hydrogel, the optimisation and understanding of the system was required in order to improve hydrogel macro and microstructure. For physical parameters time and temperature control before and during aeration was fundamental for higher overrun. Another physical parameter that was optimised was speed of mixing. Different additional polymers were added to the formulation (e.g. Hydroxypropyl methyl cellulose (HPMC) and LBG) in order to obtain more intact air cells in the aerogels (Table 3.1).

Optimised parameters		**Outcomes**
Physical	Temperature control before and during mixing (aeration) Optimisation of time before and during mixing (aeration) Optimisation of mixing (aeration) speed	Control of hydrogel microstructure Increased overrun
Chemical	Adding new polymers (MC-A4M and HPMC- K100M) to the formulation	Control of hydrogel microstructure Increased overrun

Table 3.1. Optimised physical and chemical parameters for control of hydrogels.

3.5.1. Temperature optimisation

Temperature control before and during aeration was essential for successful aeration, to provide higher overrun and homogeneous gel structure.

3.5.1.1. Temperature control before aeration

There was not any heat treatment of the solutions prior to aeration. Based on some preliminary works (refer to Figure 3.7), it was seen that if temperature of the solution before aeration is high, the increase in temperature during aeration will be higher even if it is held in a cold water bath. Therefore, all solutions were prepared at room temperature because an increase in temperature during aeration was a limitation for creating an aerated hydrogel with a high overrun and desired structure.

3.5.1.2. Temperature control during aeration

During the aeration process, which was carried out using overhead mixer (Silverson), the solution media was placed in the cold water bath (temperature 10 ^{0}C) in order to prevent sudden temperature increase. In the absence of cold water bath an increase in temperature was very high, rising up to 60 ^{0}C after 10 minutes aeration.

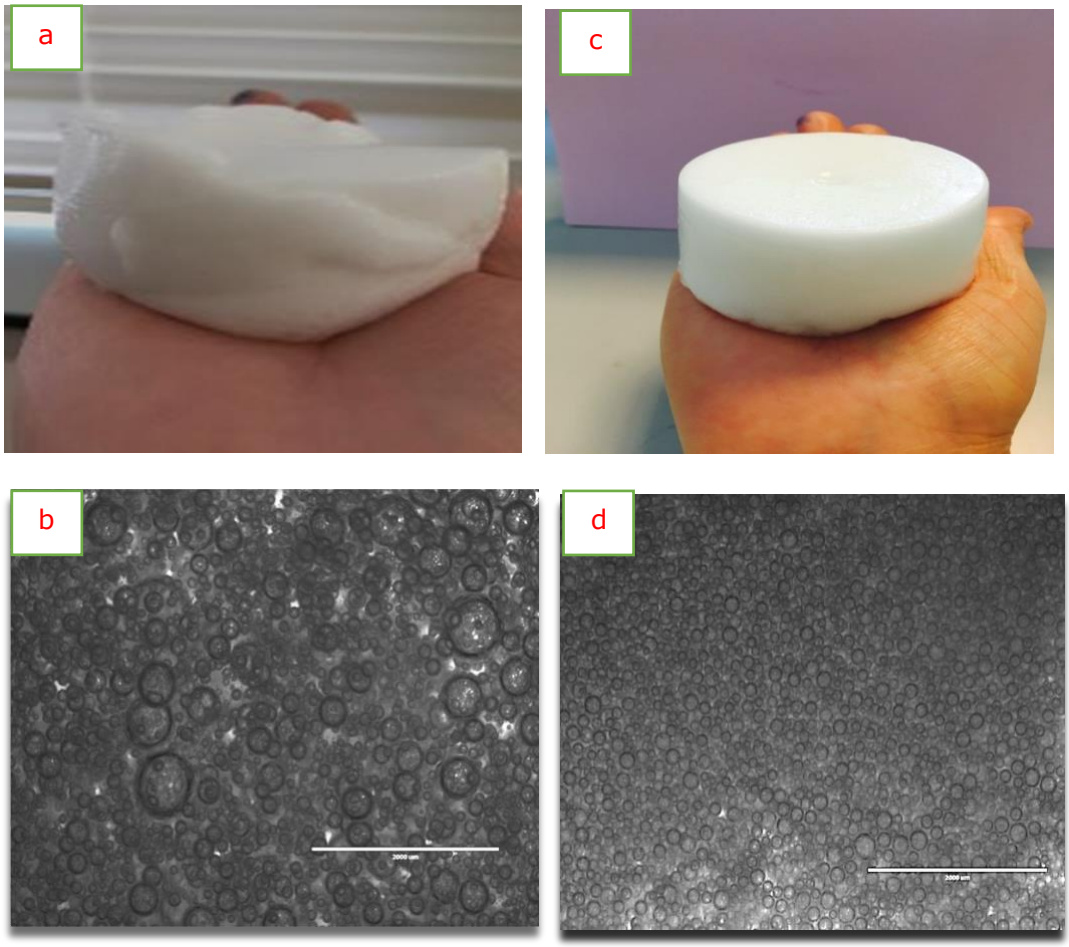

Figure. 3.7. Images of gels formed after aeration under two different processing conditions. Aerated gel without temperature control during aeration process (a-b). Aerated gel with temperature control during aeration (c-d). Scale bar represents 2000 µm.
Due to the cold bath, the increase in temperature was limited.

After 10 minutes aeration at 8000 rpm the final temperature was around 50 ^{0}C. The increase in temperature during aeration had a substantial effect on gel appearance, air cells size and air cells number distribution.

In the absence of cold water bath (high temperature), a very lumpy gel was formed. The gel had a non-homogenous appearance and coarse texture (Figure 3.7a). The microstructure of gels formed under two different temperature conditions was observed under a light microscope (Figure 3.7).

Visually, the air cells formed in the absence of cold water bath appeared to be less uniform, containing few larger bubbles and also large number of small bubbles, which were highly packed and formed cluster of small bubbles (Figure 3.7b). The lamellae, especially around very small bubbles, were poorly defined. Therefore, it was impossible to carry out any geometrical measurements (air cells size etc.). By contrast, via holding the solution media in a cold water bath it was possible to form a gel with smoother appearance (free of lumps), homogenous structure (Figure 3.7c). The air cells appeared to be more regular without with a uniform population of small air cells.

As explained above, an increase in temperature had a significant effect on the final hydrogel properties (e.g. bigger air cells, non-uniform appearance). Because whey proteins undergo some structural changes, commonly known as denaturation when they are subjected to thermal processing, which is accompanied by protein unfolding and an exposure of hydrophobic groups. Temperatures above 41^0C. will break the interactions in many proteins and denature them. At temperatures >60-70 ^{0}C hydrogen, electrostatic and hydrophobic bonds are ruptured or weakened resulting in destruction of secondary structures (Donovan and Mulvihill, 1987).

It has been reported that pre-treatment with heating could cause partial or complete unfolding of the globular protein's tertiary conformation to expose buried hydrophobic amino groups to the surface, hence increasing its additional volume and flexibility (Raikos, 2010) Additionally, the heat-induced aggregation of whey proteins (WPs) could result in excessive turbidity, increased viscosity, phase separation, precipitation, and gelation (Jiang et al., 2018).

Foaming properties of whey proteins are also affected by heating. In a research, Dissanayake and Vasiljevic (2009) showed that the foaming properties of WP were detrimentally affected by heating. None of the non-heat-treated WP samples along with controls showed good foaming ability. When the heating conditions are extreme, protein molecules may not have time to align themselves in an ordered fashion. In these circumstances, poorly hydrated aggregates or precipitates that lack a continuous matrix are formed. Excessive heating of protein dispersions at temperatures far higher than the denaturation temperature can lead to a metasol state, which does not set into a gel (Boye et al., 1997).

In this formulation WPI is not the only compound that goes under structural changes when it is subjected to heat. It has been reported that structural and rheological properties of mixed gels are influenced by internal and external factors such as pH, ionic strength, temperature, polymer concentration, ratio of protein to polysaccharide, the charge of the proteins and polysaccharides (Tolstoguzov, 1991). Although alginate gels are not thermoreversible, it undergoes depolymerisation above 100–120 ^{0}C and viscosity decreases at temperature above 50 ^{0}C. In thermal treated gels, gel strength, as defined by critical compression force (N), peaked at 90 ^{0}C and drop sharply as temperature increased to 120 ^{0}C. As a result, alginate gels tend to be less rigid as temperature increases. Gels subjected to thermal treatment (boiling 100 ^{0}C or steam 121 ^{0}C) resulted in changes in textural attributes being generally softer (mushy) and less brittle but nevertheless maintained gel structural integrity (Leo et al., 1990).

In our case, it is assumed that heat induced aggregation of WPI caused an increase in viscosity, which constrained mobility of air cells and their surface activity. Consequently, a lumpy, non-uniform gel was formed with smaller air cells. According to Kamath et al. (2008), higher

viscosity promotes smaller bubble size, due to decreased rates of coalescence. Therefore, in order to prevent heat-induced aggregation of whey protein, which has a negative effect on final gel structure and overrun, during aeration the temperature of the aerated media was kept to a minimum.

3.5.2. Optimisation of time before and during aeration

For successful aeration, time control was critical either before or during aeration step. Time control before aeration was important to prevent any gelation that might take place before the aeration step, which could have a negative impact on overrun and gel microstructure. Therefore, there was need to set up the correct aeration time in order to create a gel that hold high overrun with desired microstructure.

3.5.2.1. Time control before aeration

In order to avoid any pre-gelation before the aeration step, $CaCO_3$ and GDL was added to the polymer solution in a time- controlled manner. Initially, $CaCO_3$ was added and then exactly 5 minutes later GDL was added. The time for GDL hydration was also exactly 5 minutes. In another words, 5 minutes after adding GDL the solution was aerated.

3.5.2.2. Time control for aeration

The correct aeration time was a key parameter in obtaining aerated hydrogels with desired characteristics (high overrun, higher mechanical strength etc.).

Tested parameters		Effect on gel hydrogel structure	Effect on overrun
Aeration time (minutes)	4	Non-homogenous hydrogel	Very low overrun[a]
	6	Non-homogenous hydrogel	Low overrun[b]
	8	Homogenous hydrogel	Low overrun
	10	Homogenous hydrogel	High overrun[c]
	12	Homogenous hydrogel	Higher overrun[d]
	14	Homogenous hydrogel	Very high overrun[3]
	20	Not self-supporting (weak) hydro gel	Low overrun

Table 3.2. The effect of tested aeration time on hydrogel characteristics. Overrun (%) a: 30-40 b:40-50, c: 70-80, d:80-90, e:100-120.

It was recorded that when aeration time is not long enough the created hydrogel was not stable and there was phase separation (Figure 3.8a). Additionally, when the aeration time was too long the hydrogel had a very weak structure (Figure 3.8b).

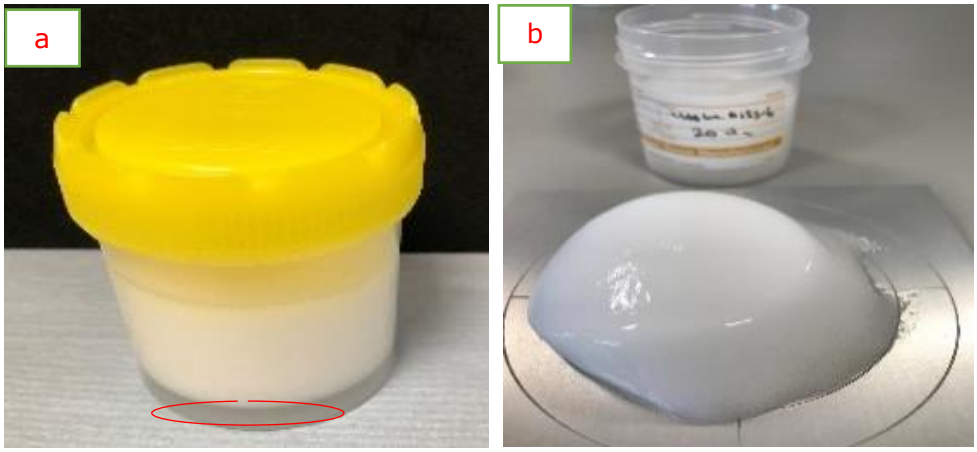

Figure 3.8. Optimisation of aeration time. When aeration time is not long enough (4 minutes) a non-homogenous hydrogel was formed (a) and when aeration is too long (20 minutes) a weak hydrogel was formed (b).

The effect of aeration time on gel characteristics (overrun, microstructure, texture, and rheology) will be discussed in Chapter 4, under 'Physical Parameters' section.

3.5.3. Control of mixing speed

Aeration with overhead mixer was key parameter for forming an aerated hydrogel. Without aeration, it was not possible to form a uniform hydrogel with air cells distributed in. However, similarly the correct speed for the mixer was recorded to be a fundamental physical parameter, which needs to be controlled and set up correctly (Table 3.3).

Tested parameters		Effect on gel hydrogel structure	Effect on overrun
Mixing (aeration) speed (rpm)	4000	Non-homogenous, non-self-supporting hydrogel	Lower overrun
	6000	Non-homogenous, self-supporting hydrogel	Low overrun
	8000	Homogenous, self-supporting hydrogel	Higher overrun

Table 3.3. The effect of mixing (aeration) speed on hydrogel characteristics, AT:10 minutes.

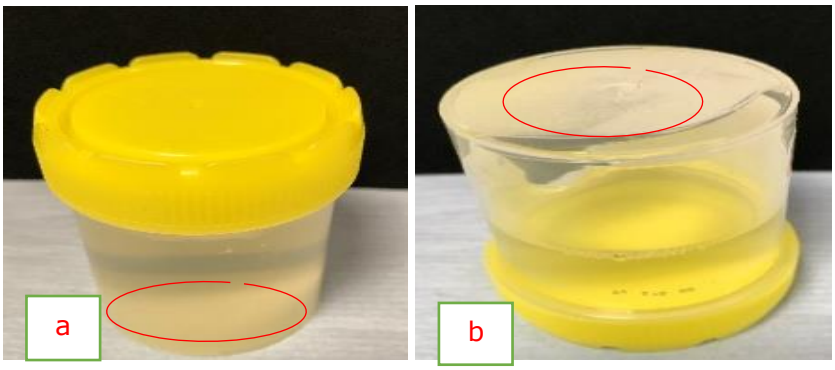

Figure 3.9. When there is no aeartion a non-uniform gel like structure formed with two different phases, gel like structure at bottom and more liquid at top (a and b).

When mixing speed was below 6000 rpm, fast phase separation was observed just after aeration was stopped. A non-uniform gel was formed with air cells on top and liquid at bottom (Figure 3.9a).

Figure 3.10. Showing the effect of aeration speed on gel formation. When aeration speed was very low (4000 rpm- a) a two-phase, unstable gel formed. However, by increasing aeration seed to 6000 and 8000 rpm, a more uniform gel formed (b and c, respectively).

Once the mixing speed was increased to 6000 rpm the degree of phase separation was reduced significantly (p-value 0.011) (Figure 3.10b) and it was almost unnoticeable. However, when the mixing speed was increased further to 8000 rpm, a uniform gel with high overrun was formed (Figure 3.10c).

Refer to Chapter 4 for the effect of aeration speed on gel microstructure, rheology and texture.

3.5.4. Introducing new materials: MC/HPMC

MC/ HPMC was introduced as a viscosifier into the hydrogel formulation containing alginate, WPI, $CaCO_3$ and GDL (0.5%, 1%, 0.5% and 0.25%, respectively) in order to increase strength and stability of aerated hydrogel. Hydrophilic polymers can swell and absorb significant amount of water and increase viscosity, which make significant contribution to gel stability. The initial positive effect of adding 0.25 % (w/w) MC-A4M was seen as an increase of overrun by a further 15 %. Visually, the both gels with and without MC look very similar,

there was not any noticeable difference in their appearance (Figure 3.11b and 3.11d). Figure 3.11a and 3.11c show representative microscopic images of the aerated hydrogel with and without MC immediately after aeration. The air cells of aerated fresh hydrogel made with MC-A4M appeared to be smaller and produced a more uniform microstructure.

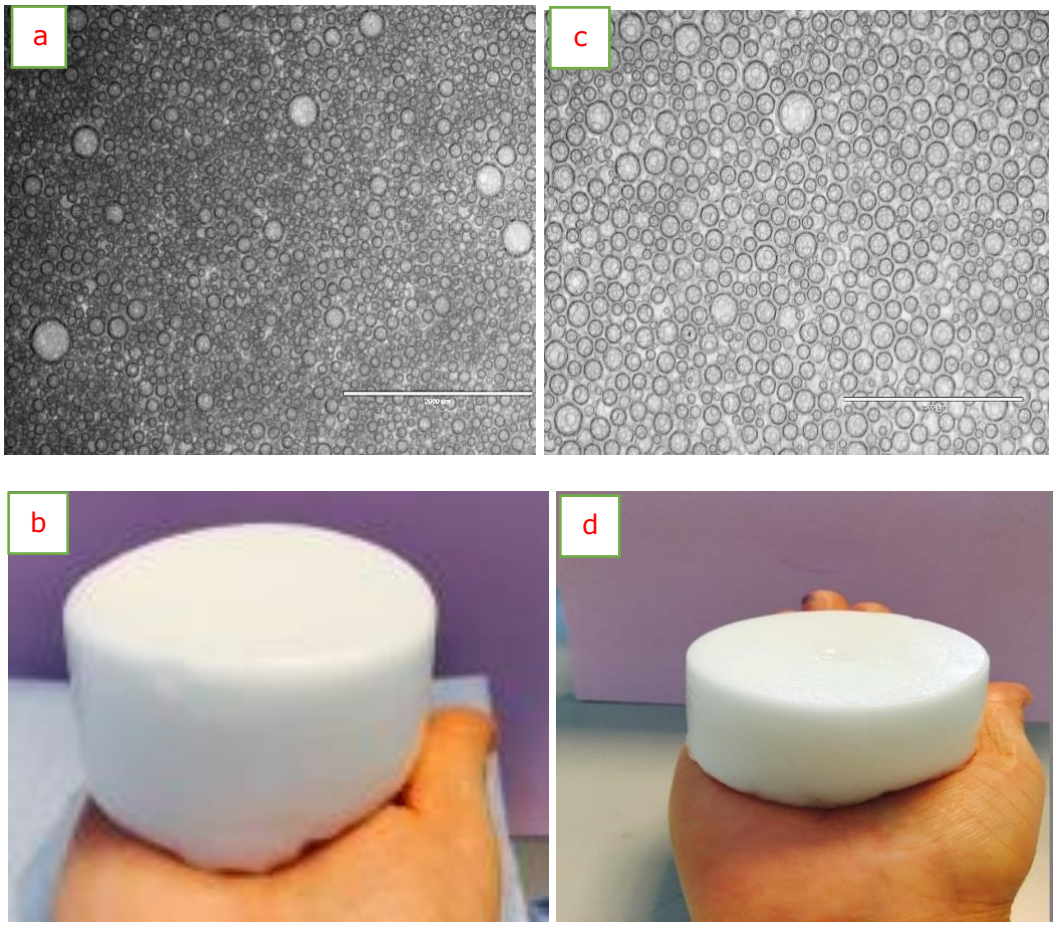

Figure 3.11. Light microscopy images of aerogel with MC-A4M (0.25 %) soon after aeration (time zero) (a) and and self-supporting gel (b), Light microscopy image of aerogel without MC after aeration (time zero) (c) and self-supporting gel (d). Scale bar is 2000 µm.

Air cells in the aerated hydrogel formed without MC-A4M appeared to be larger with well-defined lamellae (Figure 3.11c). These observations were confirmed by the measured sizes of the air cells with ImageJ-image processing program (Figure 3.12).

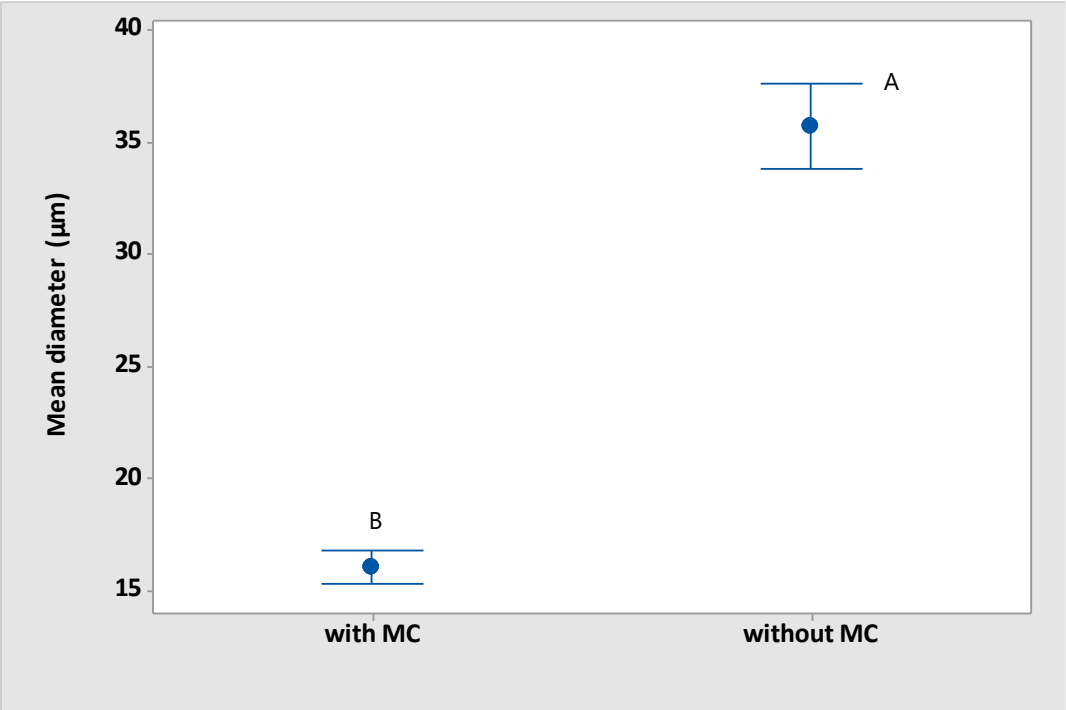

Figure 3.12. Mean diameter (µm) of air cells in aerated fresh hydrogels with and without A4M. Error bar resresents the 95 % confidence interval for the mean

The mean diameter of air cells in fresh hydrogel containing MC-A4M were much smaller (16 µm) compared with those of air cells formed in hydrogels without A4M (Figure 3.12). The smaller air size formed with A4M could be due to the higher viscosity, as a higher viscosity promotes smaller bubble size, due to decreased rates of coalescence (Laakkonen et al., 2005).

However, the effect of MC/HPMC on gel structure was more pronounced when total solid mass content was reduced to 0. 70 %. Additionally, the gel made of only WPI, alginate and cross-linking agents at a reduced solid mass content (0.55 %) had a very weak and heterogeneous structure. Visual phase separation took place soon after aeration was completed. The drained bottom part of the gel was transparent with less air cells, whereas

the upper part of the gel was more like foam with more air cells (Figure 3.13a). By adding either MC-A4M or HPMC-K100M, the gel structure was improved significantly. The formed aerated gel had more uniform appearance and a free-standing structure (Figure 3.13b and 3.11c).

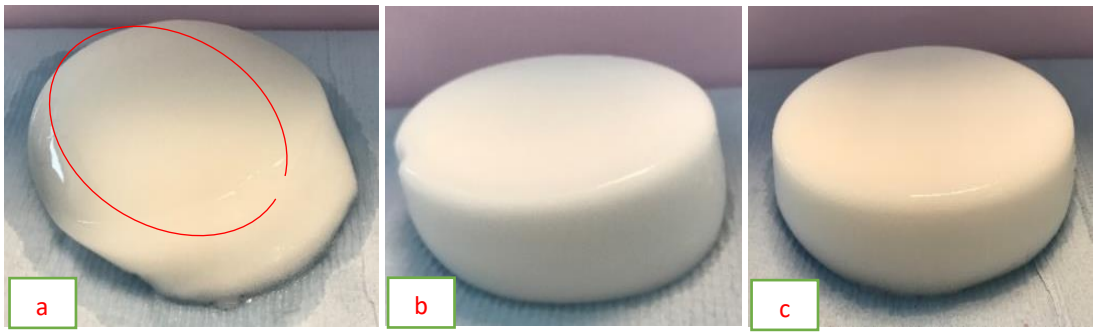

Figure 3.13. Aerated hydrogel without MC (a), with A4M (b) and with K100M (c), respectively.

It is known MC is readily miscible with alginate in all proportions and hence, blending of MC with alginate increases the matrix viscosity (Babu et al., 2007). Therefore, when a small amount of MC/HPMC was added to the solution, it formed a gel with more uniform, self-supported structure even if at very low solid mass content of 0.50 % (w/w).

According to Liang et al. (2004), a semi-interpenetrating network like structure was formed within the methylcellulose/ alginate hydrogel when blended with divalent cations such as $CaCl_2$. As it is illustrated in Figure 3.14, at 37 ^{0}C and above, there is a hydrophobic interaction between methylcellulose molecules, the hydrogen-bond formation between -COOH and –OH groups in hydrogel, and the ionic cross-link between alginate molecules (Liang et al., 2004).

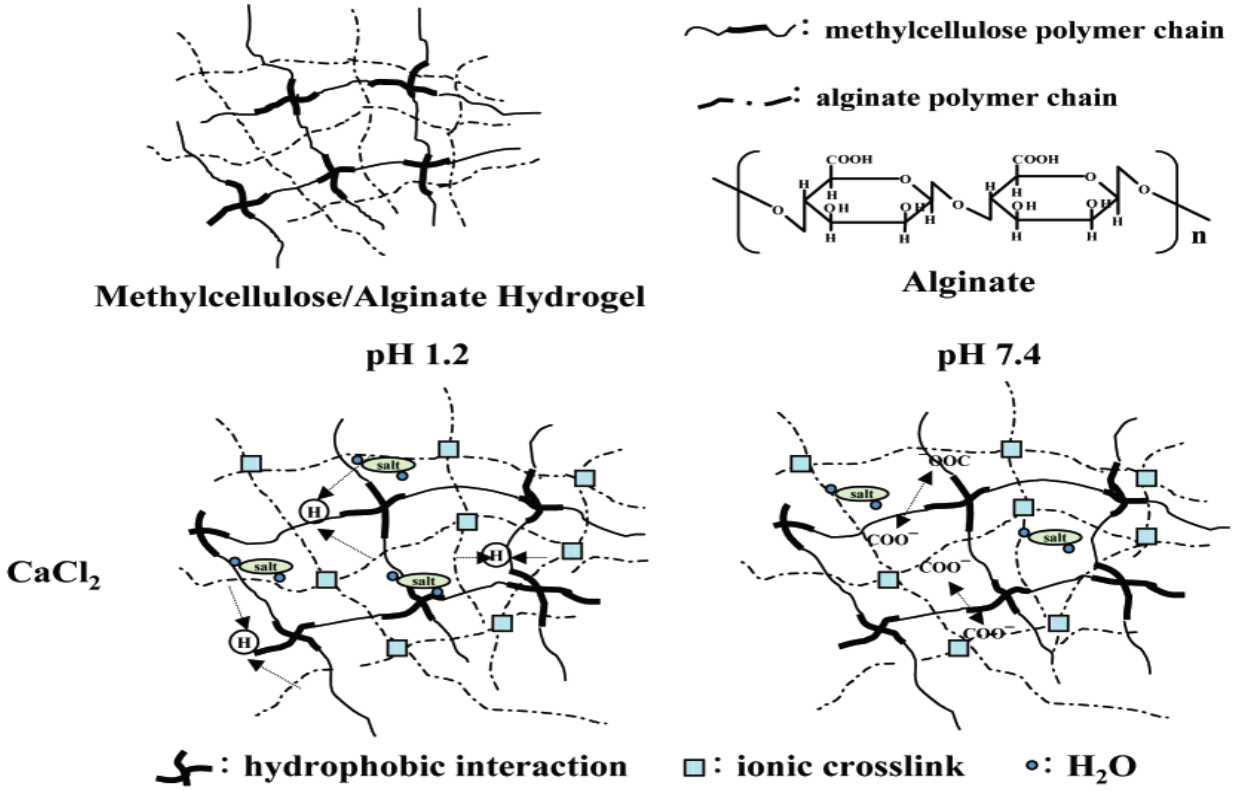

Figure 3.14. Schematic illustrations of the physical structures of methylcellulose/alginate hydrogels blended with $CaCl_2$, 1.2 and pH 7.4 at 37 ^{0}C (From Liang et al., 2004).

Chang et al. (2009) has also reported that macroporous hydrogels were prepared by blending of cellulose and sodium alginate (SA) solution, and then cross-linking with epichlorohydrin. According to Chang et al. (2009) the introduction of sodium alginate into cellulose hydrogel increased significantly the pore size and swelling ratio while cellulose could improve the mechanical properties of cellulose/SA hydrogel. In the hydrogels, cellulose contributed to support the pore wall whereas, alginate acted as an expander of the pore size (Chang et al., 2009).

3.6. Optimisation of materials: Results and Discussion

3.6.1. Solid mass content challenge; from 2.5 % to 0.50 % solid content

The dry mass content of the aerated hydrogels was gradually reduced to 0. 50 % (99.5 % H_2O) from 2.5 % (Table 3.4).

Total Solid mass content %	Alginate %	WPI %	HPMC-K100M %	$CaC0_3$ %	GDL %
2.5 %	0.5	1	0.25	0.5	0.25
0.875	0.25	0.25	0.125	0.125	0.125
0.70	0.20	0.15	0.15	0.10	0.10
0.55	0.20	0	0.15	0.10	0.10
0.50	0.20	0	0.10	0.10	0.10

Table 3.4. Formulation of hydrogels with varied solid mass content.

It was recorded that hydrogels even such a low dry mass content had self-supporting gel structure. However, compared to high dry mass content, it was a weak gel with less uniform structure (Figure 3.15e).

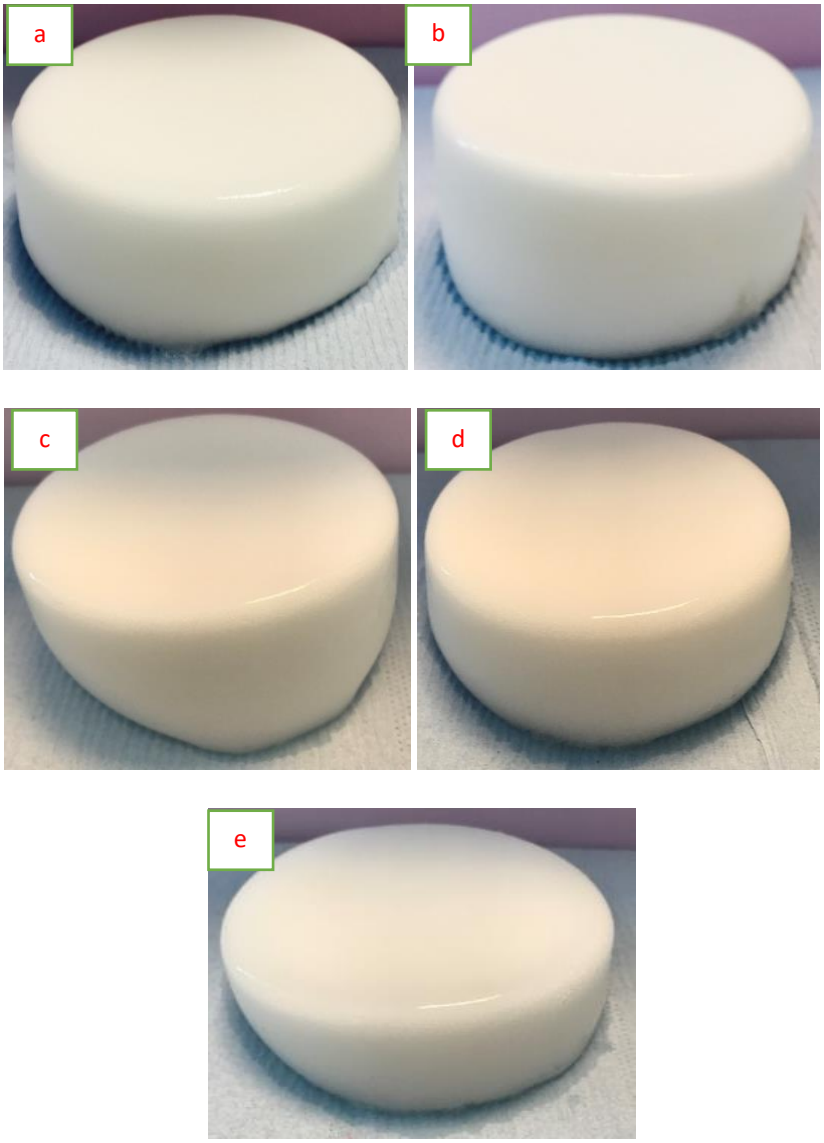

Figure 3.15. Aerated hydrogel with different solid mass content; 2.5 and 0.875, 0.70, 0.55 % and 0.50 % (a-e), respectively; containing alginate, WPI, HPMC-K100M, $CaCO_3$ and GDL.

However, reduction in the dry mass had a negative effect on overrun. The highest overrun was recorded with 0.875 % dry mass while the lowest dry mass (0.50 %) gave the lowest overrun (p value < .001) (Figure 3.16), while the recorded overrun for 2.5 % solid mass content was 91%.

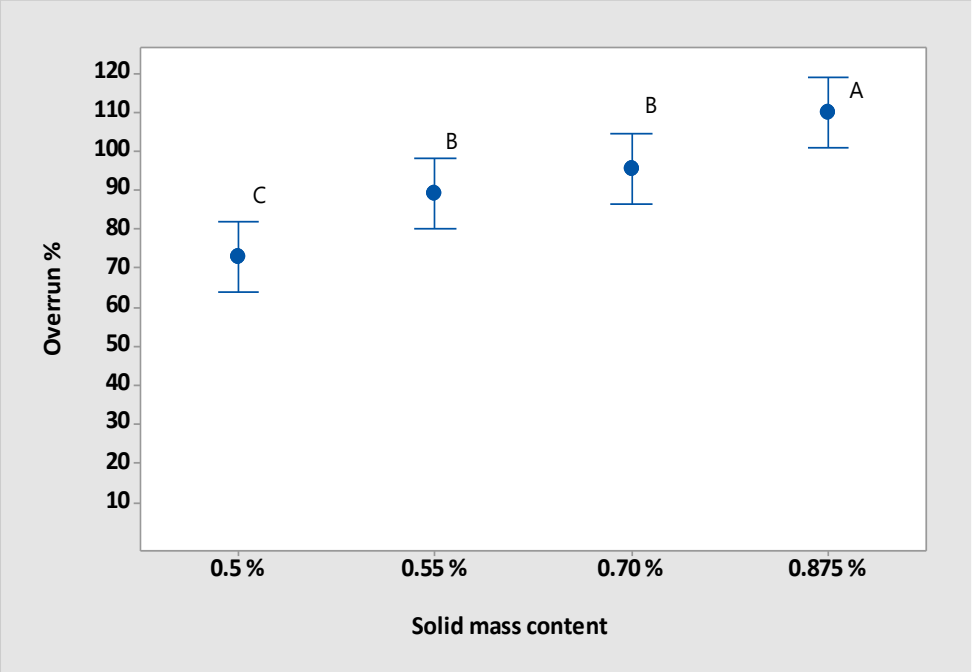

Figure 3.16. The effect of solid mass content on overrun. Means that do not share a letter are significantly different at p-value <0.05. Error bar resresents the 95 % confidence interval for the mean

Cryo-SEM images (Figure 3.17 a-d) show the microstructure of aerated hydrogel with two different dry mass contents (0.875 and 0.50 %). There was a striking difference in the air cell morphology of two hydrogels. The higher dry mass content showed visibly higher amounts of air cells with small pore sizes, therefore appearing to be more porous (Figure 3.17a and 3.17b).

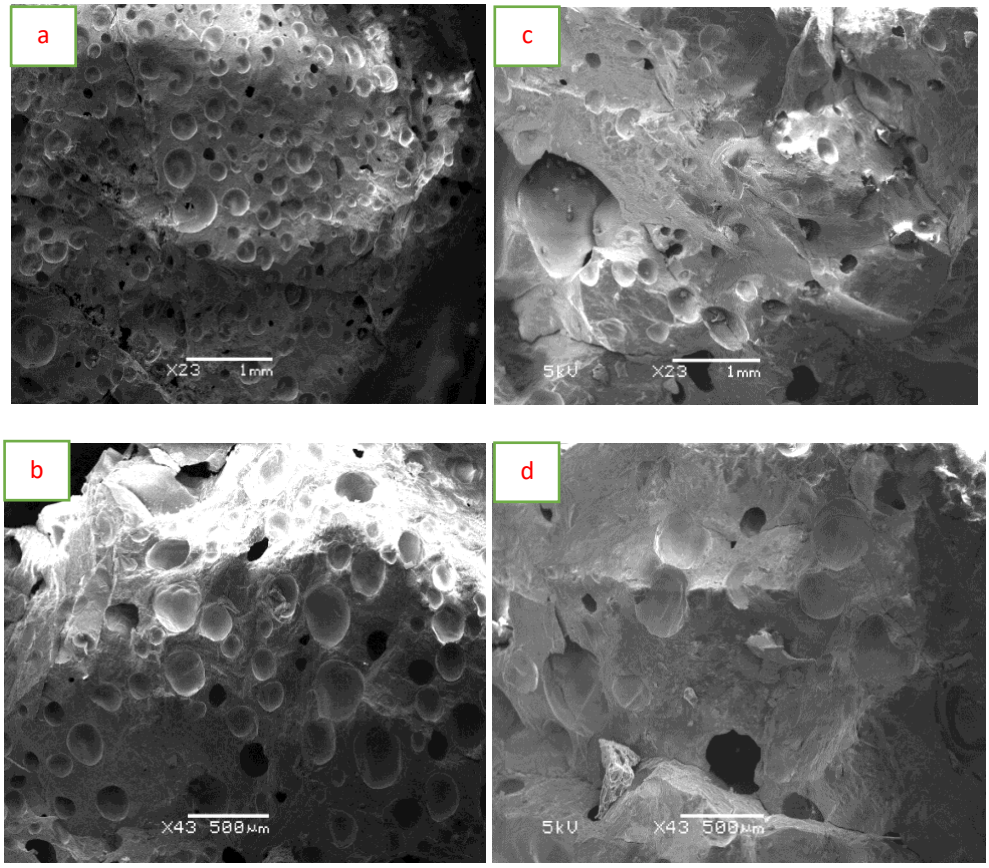

Figure 3.17. Cryo -SEM images of aerated hydrogel with 0.875 % and 0.50 % dry mass content (a-b and c-d, respectively).

The recorded smaller pore size and increased porous microstructure with the higher dry mass sample might be related to the gel density and gel water retention.

It has been reported that there is a linear relationship between gel porosity and syneresis. Larger pore size is associated to higher syneresis values. It is possible to control the gel properties by increasing the biopolymer concentration, with the concurrent gel strength increases with concentration seemingly increasing the ability to aerate (Le et al., 2017).

Additionally, the samples of freeze dried aerogel with the lowest dry mass content appeared to be less dense with a sandy texture with visible air cells (Figure 3.18).

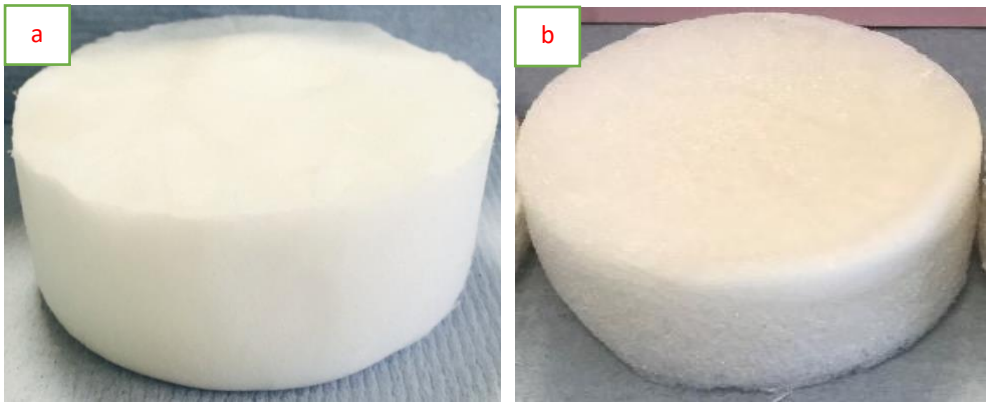

Figure 3.18. Freeze dried aerogels with 0.8750 % (a) and 0.50 % (b) dry mass content.

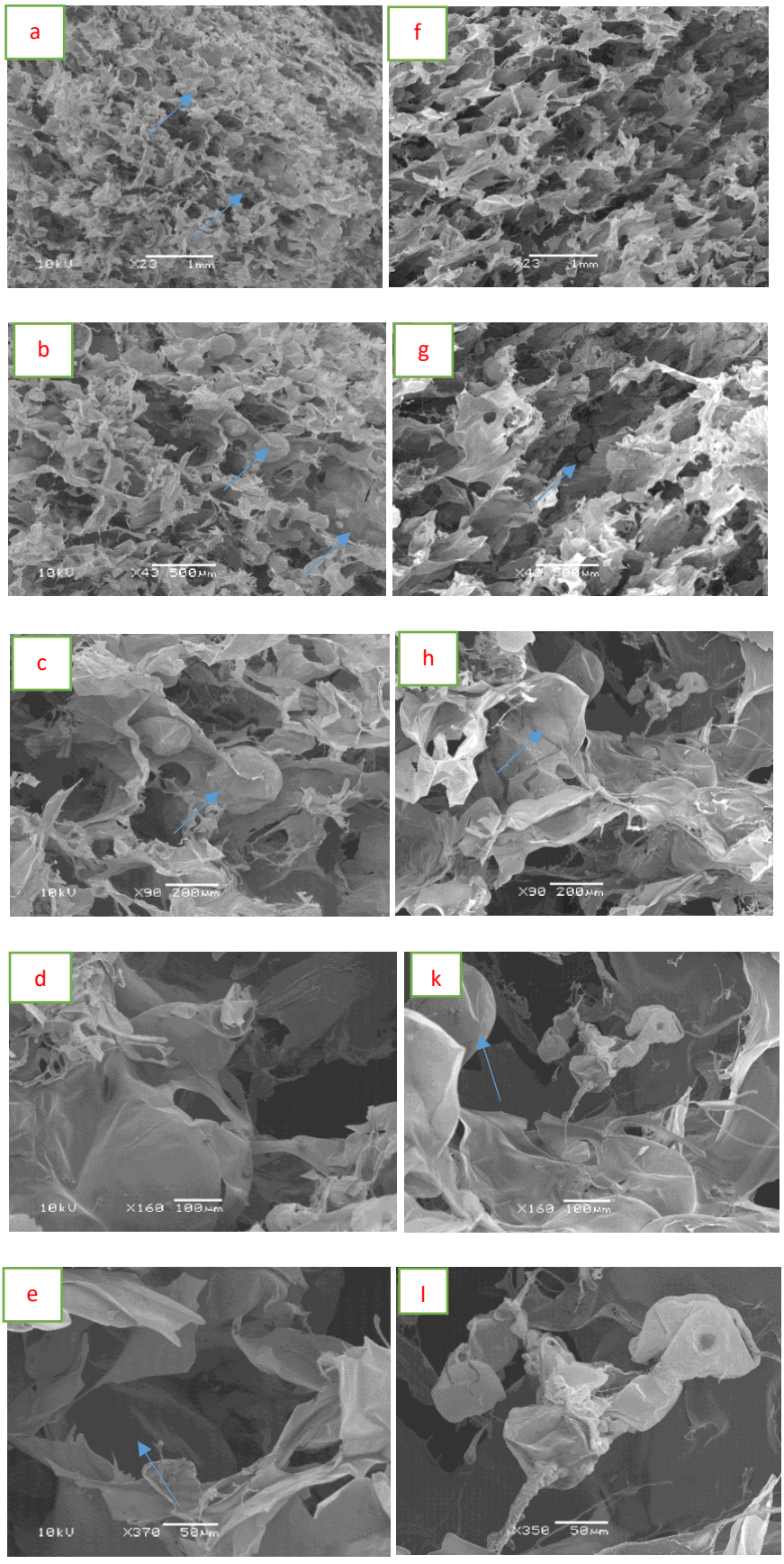

Figure 3.19. SEM images of aerogels with 0. 8750 % (a-e) and 0.50% solid mass content (f-l) from left to right, respectively. Blue arrows are pointing to the intact air cells.

As it is seen above on SEM images (Figure 3.19), the freeze- dried aerogels with higher solid mass content (0.875%) appeared to have more intact air cells and more homogenous structure. Therefore, based on these figures, it can be concluded that the sizes and number of air cells and microstructure formed in both hydrogels was dependent on the dry mass content.

3.7. Improvement of aerogels: Results and Discussion

The aim of this section was to improve mechanical strength of aerated hydrogel during freezing in order to have more intact air cells in the final aerogel. Initially, two polysaccharides HPMC-K100M and LBG were compared for their stabilising effects in aerated hydrogel against freezing treatment (-80 ^{0}C only). Later, the effect of two freezing regimes namely slow freezing (-80 ^{0}C) and rapid freezing in liquid nitrogen (- 197 ^{0}C) on aerogel microstructure made with either HPMC or LBG were compared (Table 3.5).

Methods to improve aerogel mechanical strength	
Chemical	Replacement of HPMC-K100M with LBG
Physical	Different freezing types; fast freezing (Liquid nitrogen-197 ^{0}C) versus slow freezing (-80 ^{0}C)

Table 3.5. The physical and chemical parameters that were used in order to improve aerogel mechanical strength.

3.7.1. Replacement of HPMC-K100M with LBG and its effect on aerogel microstructure

The freeze-dried aerogels obtained from two different hydrocolloid types differed in terms of structure. There was a significant difference between two freeze-dried aerogels. The samples made of LBG showed a less dense appearance and non-uniform structure, forming two layers (Figure 3.20a-c). The bottom of the aerogels was denser and rough while top layer was more like dry foam, less dense with larger and visible pores. The aerated hydro and aerogel samples made with HPMC-K100M appeared to have more uniform structure and denser appearance (Figure 3.20 b-d).

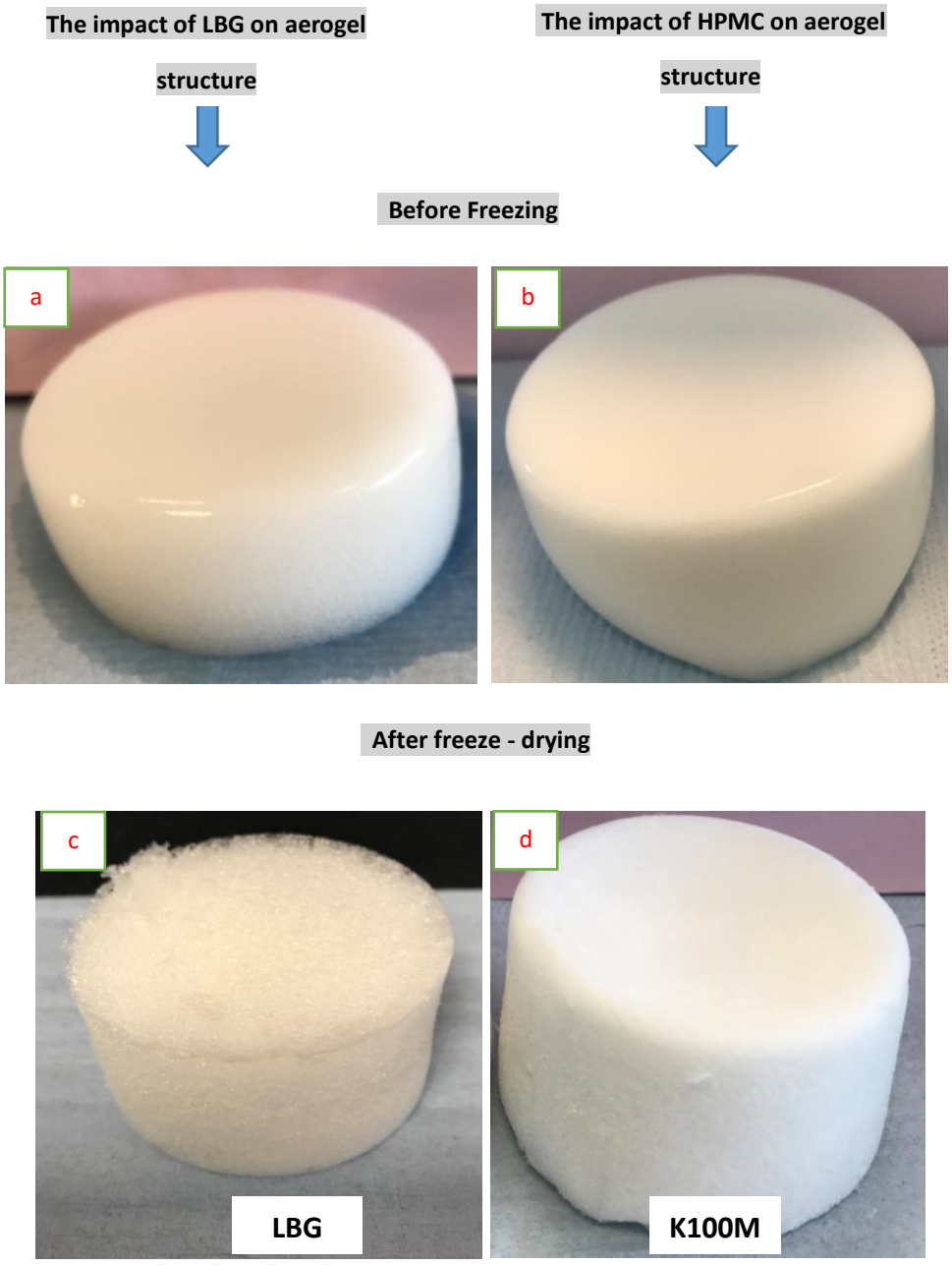

Figure 3.20. The effect of LBG and HPMC on aerogel macromorpholgy before freezing (a and b) and after freeze-drying (c and d).

The morphology of the hydrogels was observed under scanning electron microscope (SEM). Figure 3.21 shows cross-section of the freeze-dried hydrogels. Each of the hydrogels had a highly interconnected porous network structure.

However, the samples containing LBG had an architecture of highly disordered network with irregular pores. Conversely, it appeared to have more intact air cells, (Figure 3.21a-c). Compare to LBG, the aerogel with K100M showed more uniform microstructure with better defined cell walls, but there were very few intact air cells which might have been burst during either freezing or freeze-drying process (Figure 3.21d-f).

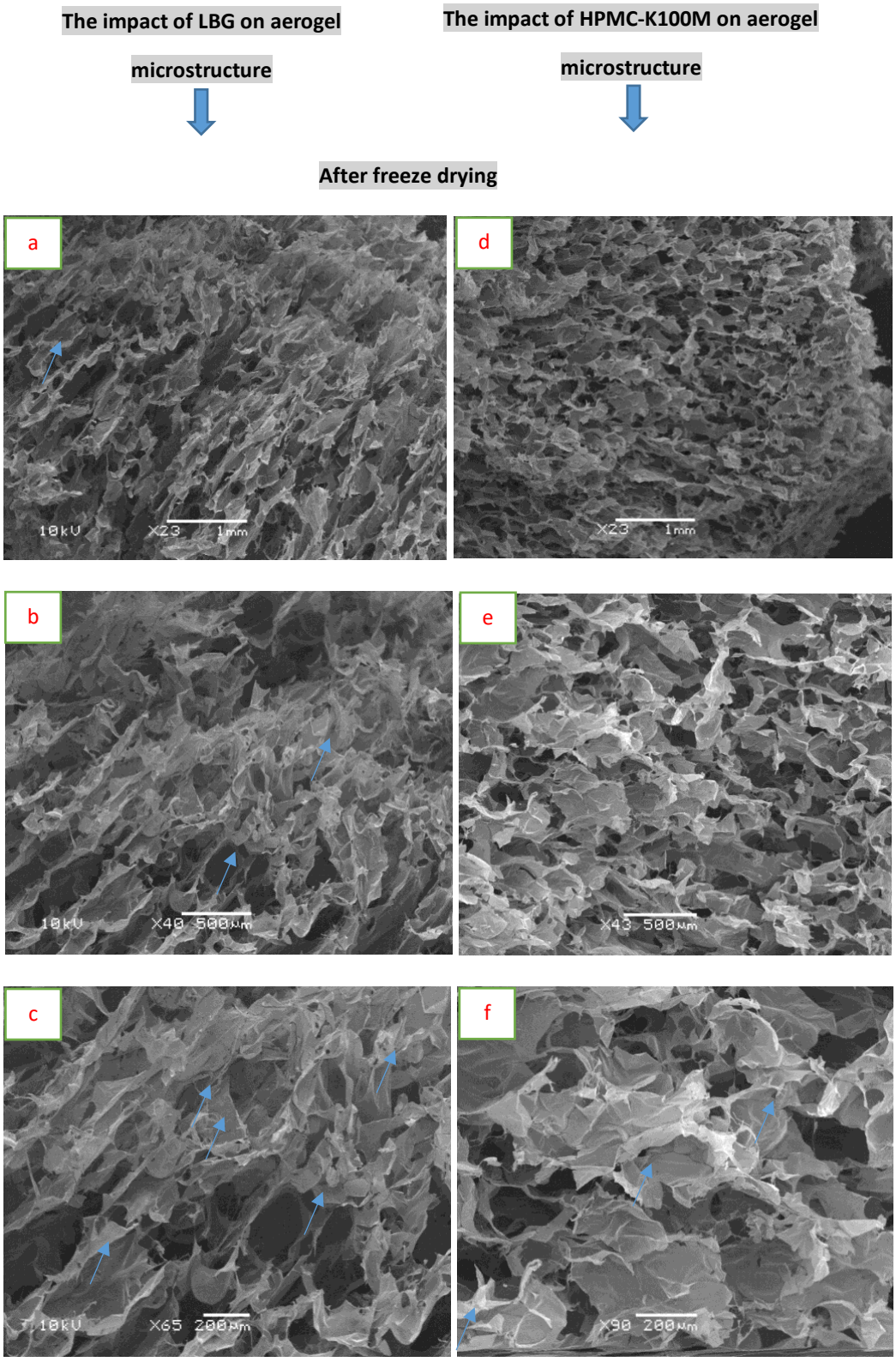

Figure 3.21. SEM images show the effect of LBG and K100M on aerogels microstructure. Arrows are pointing to the intact air cells.

Texture properties are connected to sample structure. Aerated hydrogels (wet) containing LBG had the lowest values of the maximum force during compression (P value 0.023). In contrast, the aerated hydrogel with K00M was harder than LBG, it was characterized by the highest value of compression (Figure 2.22).

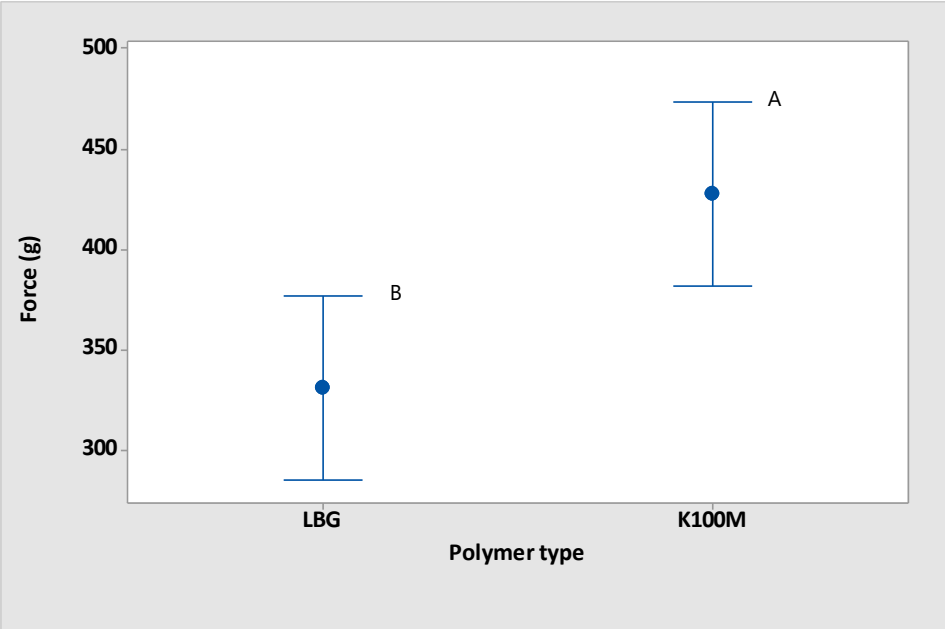

Figure 3.22. The effect of polymers- LBG and K100M on aerated hydrogel (wet) hardness. Error bar resresents the 95 % confidence interval for the mean.

This result is in an agreement with literature, because gel firmness has been connected to inhibition of ice crystal growth and change in ice crystal morphology. This effect has been explained as a mechanical interference with the ice growth. A more elastic gel would probably exert a stronger opposing force for ice front propagation and a firm gel would be more fragile and be ruptured more easily by the ice front. Thus, a firm gel might not be effective at retarding ice crystal growth (Miller-Livney and Hartel, 1997; Bahramparvar and Tehrani,

2011). That may be a reason why aerogels with LBG had more heterogeneous microstructure and showing more intact air cells compare to K100M aerogels.

3.7.1.1. Discussion

Polysaccharides act as cryoprotectants providing stability by minimising the negative effects of freezing and frozen storage (Liehr and Kulicke, 1996). It is commonly used in frozen desserts to retard the growth of ice crytals during fluctuating temperatures (Harper and Shoemaker, 1983).

Compound	**Cryoprotective activity (%)**
Sucrose*	18.2
Galactose*	0
Mannose*	0
Dextran *	17.9
Mannan *	22.0
LBG *	45.3
Crude extract *	100.0
Purified S-LBG**	100.0
Sucrose concentration is 10 mg/ml * Sugar concentration is 100µg/ml. **Sugar concentration is 50µg/ml. S-LBG indicates purified shorten LBG. Mannan is the cell wall component **from *S. cerevisiae.***	

Table 3.6 Cryoprotective activities of various sugars (from Kawahara et al., 2008).

Hydroxypropylmethyl cellulose (HPMC) is a water soluble polymer derived from cellulose. K100M is a high molecular cellulose and can form gel structure with high water holding capacity at higher temperature. However, at low temperature the gels melts, thus the water

molecules could form ice nuclei, and grow freely into large ice crystals with migration and aggregation of water molecules.

The cryo-gelation effect of locust bean gum (LBG) has been reported extensively (Goff et al., 1999; Harper and Shoemaker, 1983; Fernández et al., 2007). The presence of more intact air cell in the sample of the mixture containing LBG could be strengthened by the cryo-gelation effect of LBG. According to Goff et al. (1999) LBG produced a structured gel-like network around the ice crystals, which became more distinct with repeated temperature cycling. Image analysis of the ice crystal size distributions showed that LBG had provided much greater resistance to ice recrystallisation than guar gum (Goff et al. 1999). Similar to Goff et al. (1999) it was also reported by Fernández et al. (2007) that in the presence of the mixture of LBG and xantham gums ice crystals in samples were smaller than in the other samples due to the formation of a gel-like structure by the locust bean and xanthan gums, which would limit water molecule diffusion and hence ice crystal growth (Fernández et al., 2007).

However, Harper and Shoemaker (1983) observed tha locust bean gum in the concentration range of 0.0-0.5% did not act as an effective inhibitor of ice crystal growth in these aqueous solutions, even though it produced a marked increase in the apparent viscosity (Harper and Shoemaker, 1983).

Stabilisers also may adsorb to the ice crystal surface and result in a modified crystal shape in addition to reduced growth rate. Some researchers have proposed that stabilizers inhibit ice crystal growth by binding water, thus leaving less water available to freeze initially or to refreeze during storage (Lee et al., 2002; Park et al., 2006).

As a result, the LBG as a cryo-protectant had influence on the polysaccharide network, and could be used to improve the stability of the hydrogels with better structural uniformity.

3.7.2. The Influence of freezing types on aerogel microstructure; fast freezing (Liquid nitrogen freezing, -197 ^{0}C) versus slow freezing (- 80 ^{0}C)

Freezing is an essential step for freeze-drying of aerated gels. However, during freezing water inside the gel matrix freezes and expands to form ice crystals which cause gel matrix to rupture. It is possible to minimise freezing damage by controlling freezing rate of materials (Lee et al., 2002). As it is known fast freezing results in less destruction of material properties because fast freezing of water results in the formation of smaller ice crystallites. Conversely, slow freezing results in the formation or larger ice crystallites. The slower the freezing rate with consequent larger the ice crystallites, which can destroy pore walls, cellular membranes, whole cells due to a larger volume of ice crystallites (Gun'ko et al., 2013).

3.7.2.1. Influence of freezing types (fast freezing versus slow freezing) on microstructure of aerogels containing HPMC K100M

Aerated hydrogels samples made of alginate, WPI, K100M and cross- linking agents ($CaCO_3$ and GDL) were frozen by two different freezing methods namely fast (-197 ^{0}C) and slow freezing (-80 ^{0}C). The freeze-dried aerogels obtained with fast (-197 ^{0}C) and slow (-80 ^{0}C) freezing differed in terms of structure. The fast- frozen aerogels had some cracks a smooth surface. Slow frozen ones (-80 ^{0}C) did not have any crack formation. They had a more uniform shape with a rough surface (Figure 3.23).

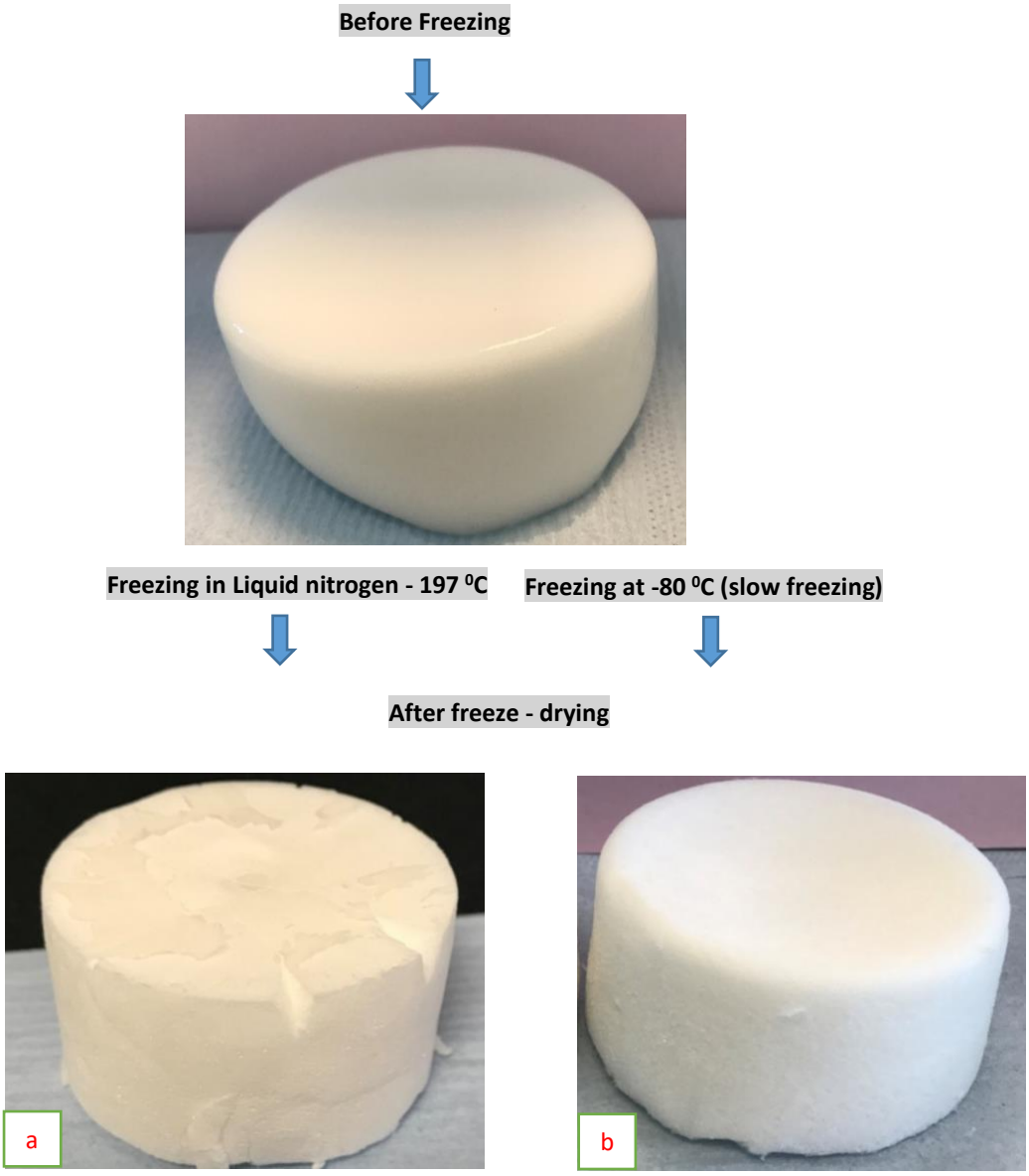

Figure 3.23. The impact of fast freezing (liquid nitrogen freezing) (a) and slow freezing (-80 ^{0}C) (b) on aerogel morphology. The colour difference between rapid and fast freezing was very distinctive.

The microstructure of aerogels was analyzed by scanning electron microscope (SEM). The samples obtained with slow freezing were characterized by heterogeneous structure with more ruptured cells. Visibly intact air bubbles were difficult to discern and matrix cell walls had an irregular shape (Figure 3.24d-f). Alternatively, fast frozen aerogels samples had homogenous structure with more well-defined intact air cells (Figure 3.24a-c).

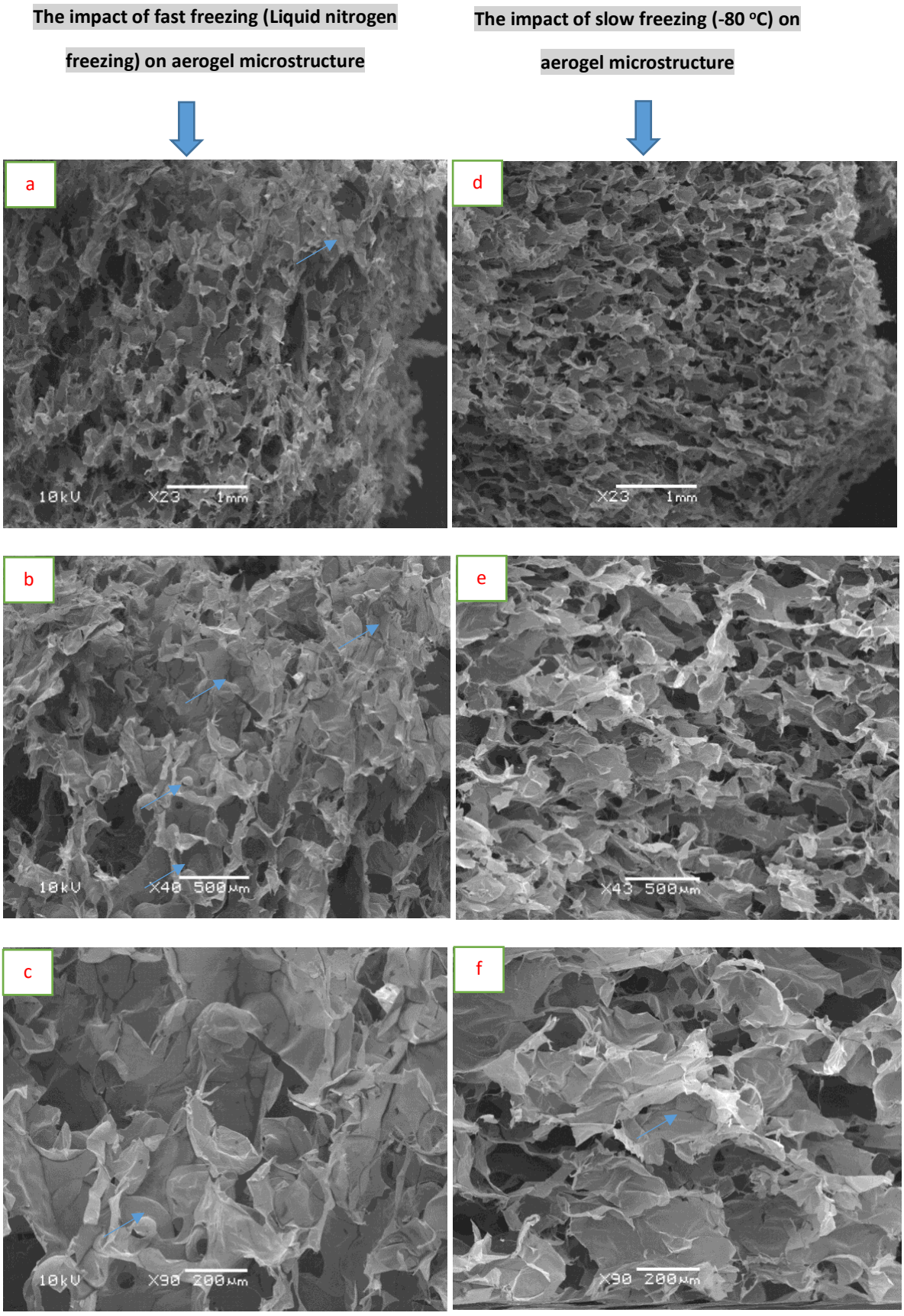

Figure 3.24. SEM images of freeze dried aerogels frozen at -197 ^{0}C (a-c), and at – 80 ^{0}C (d-f).

It can be assumed that faster freezing would result in smaller ice crystals and less damaged cell structure, are in an agreement with literature. The fast frozen samples demonstrated less damaged network with more intact air bubbles.

At slow freezing (-80 ^{0}C), ice cystal growth rate is expected to be greater than the nucleation rate, and thus small ice particles are able grow into large ice crytals. However, at lower freezing temperature (-197 ^{0}C) a larger undercooling led to an increased rate of nucleation of ice crystals, and ice crystal growth rate was less than the nucleation rate, thus water molecules can quickly form a large number of small ice crystals. At slow freezing the ice crystal size can be too big, leading to a disordering aerogel pore structure with uneven ice crystal distribution (Ni et al., 2016; O'Briena et al., 2004). Therefore, it can be concluded that aerogel pore microstructure morphologies were dependent on ice crystal growth characteristics.

3.7.2.2. Influence of freezing types (fast freezing versus slow freezing) on microstructure of aerated aerogels containing LBG

The macro and microstructure of aerated hydrogels made of alginate, WPI, LBG and cross-linking agents ($CaCo_3$ and GDL) were frozen at two different freezing temperature namely fast freezing in liquid nitrogen and slow freezing at – 80 ^{0}C was compared. Similar to all liquid nitrogen frozen aerogels, LBG aerogel frozen in liquid nitrogen had a smooth appearance, compact and uniform macrostructure with some cracks (Figure 3.25-left). LBG aerogels frozen at low temperature appeared to be less dense, sandy texture and with creamy appearance

(Figure 3.25-right). Although it did not have any cracks, it had a non-uniform structure; the upper part of the aerogel formed a foam like layer.

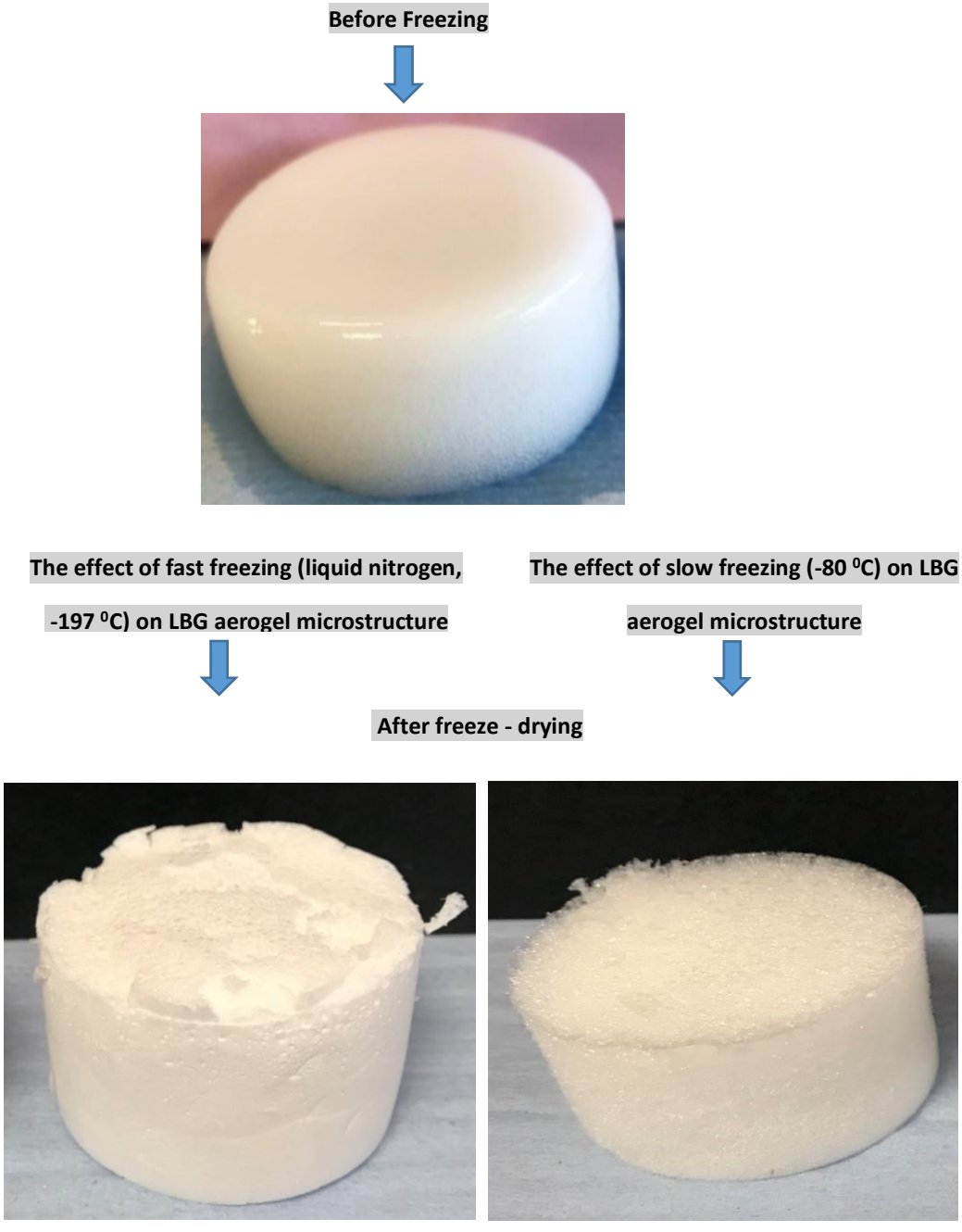

Figure 3.25. LBG aerogels frozen at two different temperature before freeze drying; fast freezing (left) and slow feeezing (right) with very different appeaeance.

Morever, LBG aerogels are frozen at two different temperature showed similar microstructure. Although a both aerogels had irregular structure with damaged cells, the both apeared to have more intact air cells (Figure 3.26).

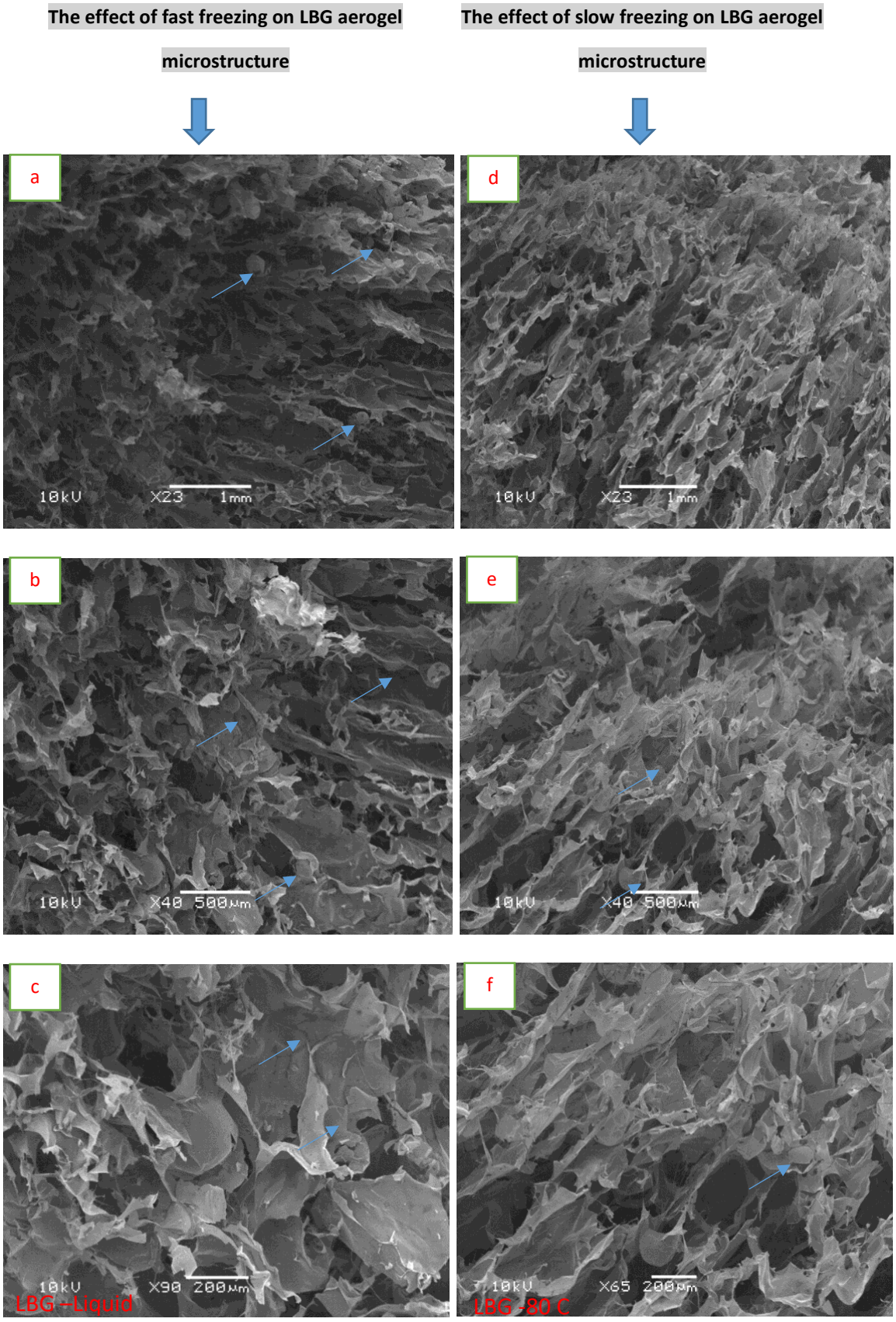

Figure 3.26. SEM images of the LBG aerogels frozen very fast at very low temperature (a-c.) and frozen slow at higher temperature (d-f).

3.7.3. Comparing effect of fast freezing (-197 ^{0}C) on aerated aerogel microstructure containing different polymers; LBG versus K100M

The freeze-dried aerogels containing either LBG or K100M were assessed against their macro and microstructure after fast freezing in liquid nitrogen. Visually, the both aerogels appeared to be homogenous in nature throughout the entire macrostructure but with some cracks. However, compare to K100M aerogel, LBG aerogel had some visible pores around the upper part of the aerogel (Figure 3.27-left).

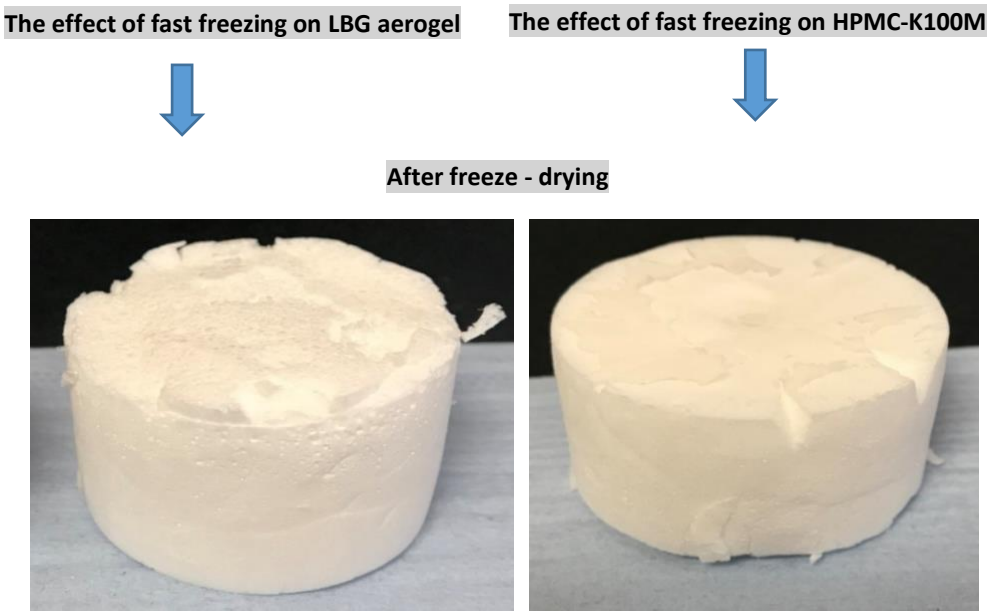

Figure 3.27. The effect of fast freezing on LBG (left) and K100M aerogels (right).

The analysis of SEM images of both aerated hydrogels frozen under the fast-freezing conditions (liquid nitrogen, -197 ^{0}C) indicate that both aerogels had different architecture. According to SEM images, samples containing LBG had least regular microstructure with more delicate appearance (Figure 3.28a-c). Although, microstructure of the both aerogels were destroyed either during freezing or during freeze- drying, the both aerogels displayed large amount of intact air bubbles with thin walls separate the pores. However, compared to LBG, the samples made of K100M seemed to have more distinctive cells walls with more intact air bubbles (Figure 3.28d-f).

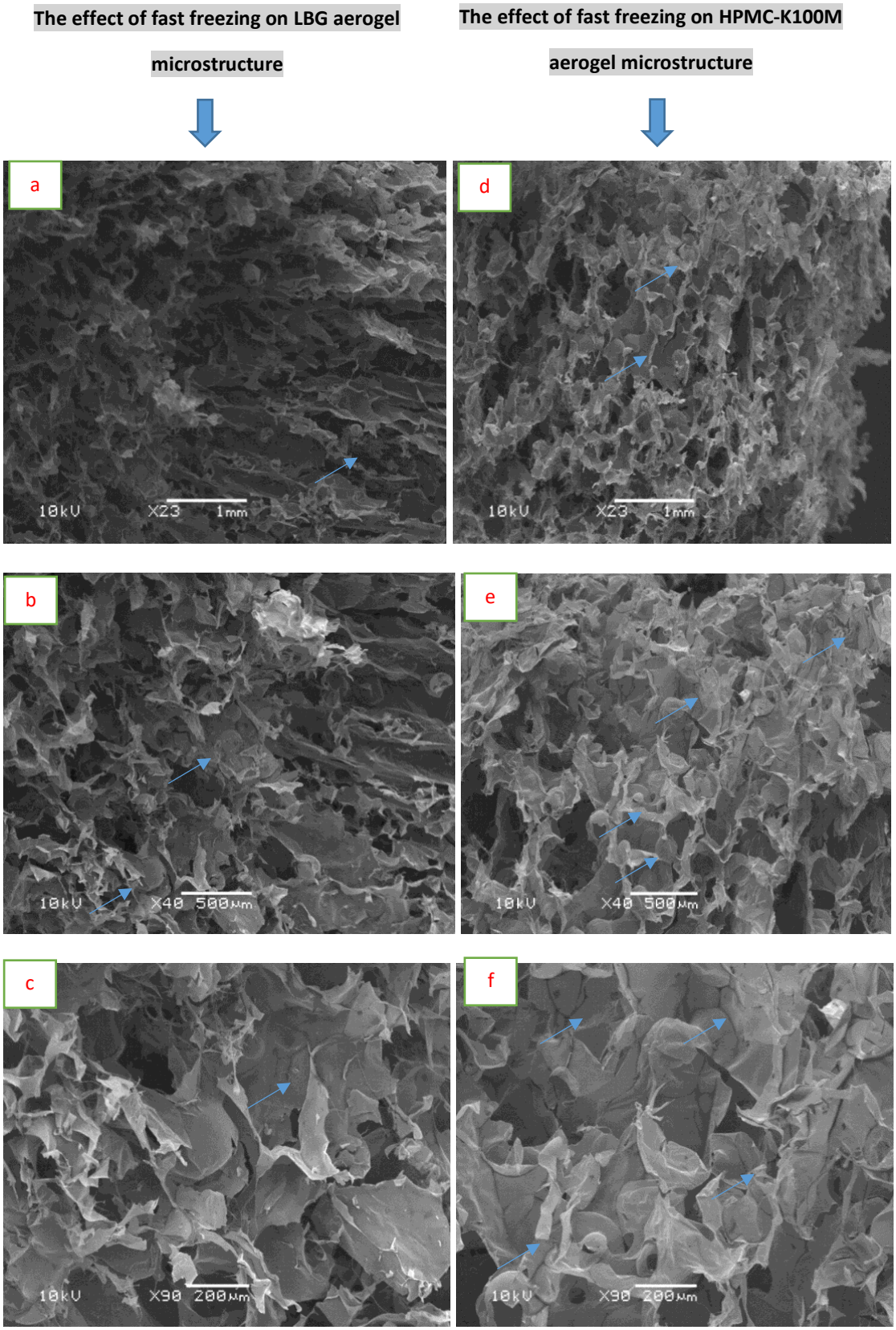

Figure 3.28. SEM images showing microstructure of LBG and K100M aerogels frozen at very low temperature (- 197 ^{0}C). Blue arrows are pointing to the intact air cells.

It has been reported that some non-gelling stabilisers (xanthan, CMC, alginate) were more effective at retarding recrystallization than gelling stabilizers (gelatin, carrageenan and LBG), suggesting that steric blocking of the interface or inhibition of solute transport to and from the ice interface caused by gelation of the polymer is not the only mechanism of stabiliser action (Bahramparvar and Tehrani, 2011). Water holding by the stabiliser and proteins, may causes a reduction in water mobility of the system, promoting ice recrystallisation mechanisms of melt–regrow instead of melt–diffuse grow. These mechanisms result in the preservation of ice crystal size and in a small span of ice crystal size distribution (Bahramparvar and Tehrani 2011).

In order to quantify the microstructure in more detail x-ray CT was attempted, but the measurements proved too difficult to perform. Nevertheless, the SEM images reflect that freezing type affected aerogel microstructure. In general, fast freezing resulted in more homogenous microstructure and more intact air cells in, and this effect was more evident on aerogel containing K100M.

3.8. Driving forces of the aerated aerogels: created synergisms between optimised physical and chemical parameters

In this research, four driving forces for aerated hydrogels have been identified; namely ionic cross-linking and created synergism between polymers and being aeration speed and aeration mixing time. As it was explained in section 3.4, ionic cross-linking was main driving force of aerated hydrogels. It was aided by synergism that created between polymers and two optimised physical parameters; aeration time and aeration speed.

Aerogels are made of various materials and each material has different gelation mechanisms and conditions. The below table was created based on information from the literature and shows necessary parameters for inducing gelation of polymers that used in this study.

Gelling parameters and gelation mechanism of individual polymers- according to literature	**WPI**	**Alginate**	**MC/HPMC**	**LBG**
^{0}C	55-90 ^{0}C	Room temperature or any temperature up to 100 ^{0}C. However, above 50 ^{0}C viscosity decrease.	35-55 ^{0}C for MC 70-90 for HPMC Gelation is due to hydrophobic interaction between glucose units	Can form weak gel upon freeze-thaw treatment in the presence of large amount of sucrose
pH	5-6-7	Usually between 3-4 or at 5 if solutions contain residual calcium	pH stable 3-11	pH stable
Salt	NaCl and $CaCl_2$	Calcium ions	NA	NA
Time	Depends on WPI and other physical and chemical parameters	Depends on Alginate %	Depends on physical and chemical parameters	Not known
%	2-12	0.5-2 % or more	1-2 %	2 % or 43% for maximum gel strength

Table. 3.7. According to literature gelling parameters and gelation mechanisms of used polymers in this study, (Haque and Morris, 1993; Nussinovitch, 1996).

However, Table 3.8 shows the actual conditions that have been identified for gelation of polymers presented in Table 3.7. When both tables are compared it is very clear to see that the conditions that were provided for creating gel structure, do not meet the criteria suggested by literature. This study has progressed the understanding of creating hydrogels and aerogels under normal conditions, it is not possible to form a gel structure with any of these polymers individually.

Gelling parameters and gelation mechanism of used polymers- introduced parameters	**WPI**	**Alginate**	**MC/HPMC**	**LBG**
^{0}C	50 ^{0}C (maximum reached temperature after aeration). No heat treatment before aeration	50 ^{0}C (maximum reached temperature after aeration). No heat treatment before aeration	50 ^{0}C (maximum reached temperature after aeration). No heat treatment before aeration	50 ^{0}C (maximum reached temperature after aeration) Blend dry materials hydrated at 40 ^{0}C for 2 hours
pH	6-7	6.7	6.7	6.7
Salt	$CaCO_3$	$CaCO_3$	NA	NA
Time	2 hours	2 hours	2 hours	2 hours
%	0.15 %	0.20 %	0. 15%	0.15 %

Table 3.8. Showing introduced gelation conditions for used polymers in aerogel production.

Based on 0.70 % dry mass, (99.3 % H_2O) (Figure 3.29a), MC/HPMC had important role in creating aerated hydrogels; without MC/HPMC it is not possible to form self-supporting uniform aerated hydrogel, where soon, after mixing was stopped there was phase separation

by means of air bubbles migrating to the surface while the liquid drained (Figure 3.29b). With the same solid mass ratio, alginate was another key polymer in gelation of the aerated media. When the amount of alginate was reduced by 50 %, the formed hydrogel was very weak, not self-supported and was difficult to handle. It was easily deformed upon removal from the mixing vessel (Figure 3.29c). When WPI was taken out of the formulation, a self-supported uniform aerated gel was able to be formed (Figure 3.29d). However, without WPI, the overrun was reduced, especially on prolonged aeration time. The effect of polymers on aerated gel characteristics will be further explained in detail in Chapter 4.

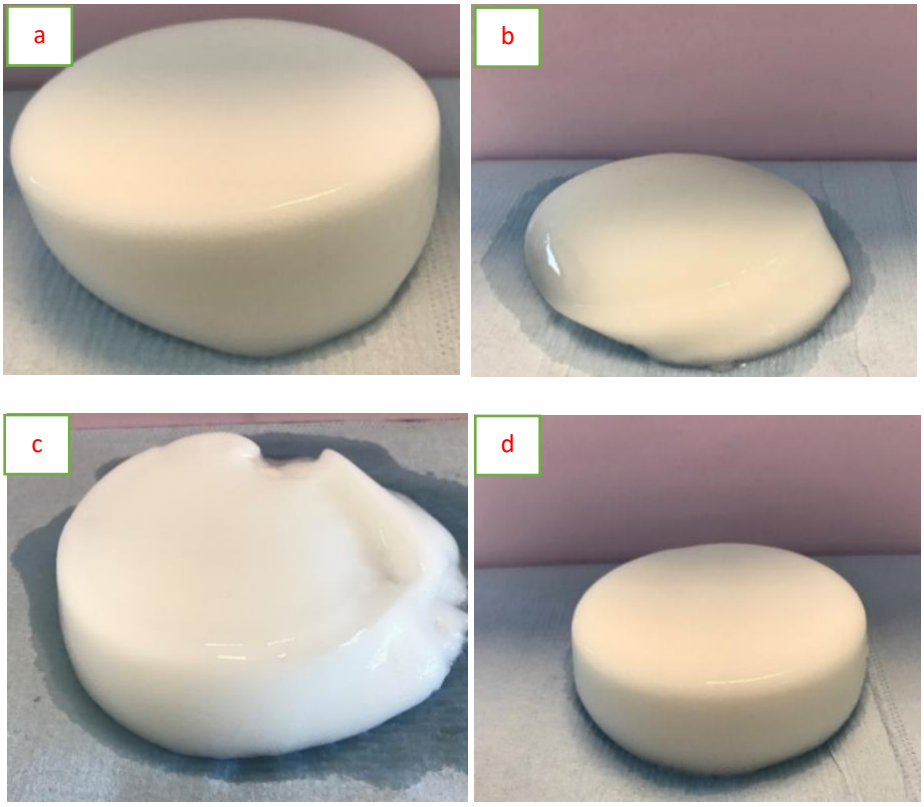

Figure 3.29. The effect of polymers on aerated gel formation; with 0.70 % solid mass content- including WPI, alginate and K100M (a), without MC/HPMC (b) with reduced alginate (c) and without WPI-0. 55 % solid mass content (d).

Used polymers	Functionality in the aerated hydrogel formation
Alginate	Gelling agent
WPI	Foaming agent: increased overrun
MC/HPMC	As the viscosity-enhancing agent; providing mechanical strength
LBG	Cryoprotectant: more intact air cells in the freeze dried aerogels

Table 3.9. The functionality of the used polymers in aerated hydrogels.

It can be seen on the Table 3.9, each single polymer had significant effect on aerated hydrogels. The synergisms that are created between the used polymers are the main driving force for creating aerogels.

Physical parameters also played crucial role in creating aerated hydrogel. Without aeration, it was not possible to form a self-supporting uniform gel based on 0.70 % dry mass

(Figure 3. 9 b-c).

When the polymer solution was subjected to aeration (10 minutes), a self-supporting uniform aerated hydrogel was formed (Figure 3.30d).

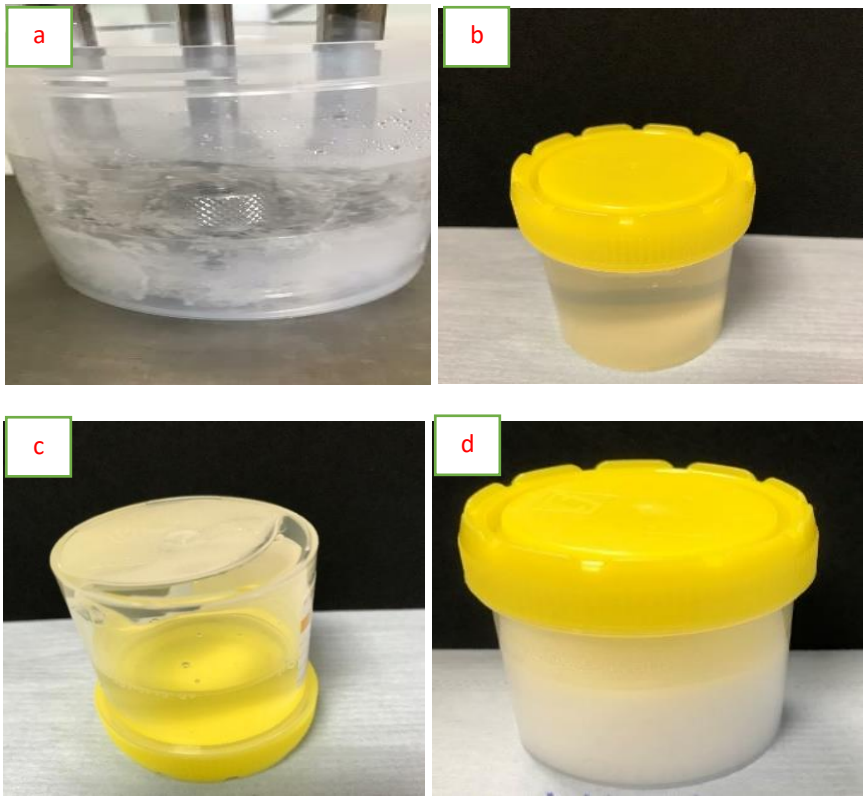

Figure 3.30. The effect of aeration (a) on hydrogel gel formation (WPI 0.15 %, Alginate 0.20%, K100M 0.15%, GDL 0.10 % and $CaCO_3$ 0.10 %). Without aeration, there was not any self-supporting uniform gel (b-c), but after 10 min aeration self-supporting aerogel formed (d).

However, not just aeration itself, but the correct aeration time and mixing speed were also of important parameters (Refer to Figure 3.8 and 3.10, respectively).

Over and under aeration were two key parameters that need to be controlled in order to form a desired hydrogel. Shorter aeration time (4 minutes) gave a two-phase non-uniform gel while an extension of aeration time resulted in the formation of a weak hydrogel. It was not well self-supporting gel and therefore it was difficult to handle for texture analysis.

Aeration (mixing) speed was also important for forming an aerated hydrogel. The minimum aeration speed for 0.70 % solid content was 6000 rpm. When aeration speed was reduced to 4000 RPM, the overrun was low, the gel was non-uniform and phase separation took place as soon as aeration was stopped. Once aeration speed was increased gradually to 8000 rpm, there was a significant improvement in gel macro structure.

Aeration (mixing) time (minutes)	**4**	**6**	**8**	**10**	**12**	**14**	**20**
Aeration (mixing) speed (rpm)	8000	8000	8000	4000[1] 6000[2] 8000[3]	8000	8000	8000
Hydrogel characteristics	Unstable	Unstable	Stable	Unstable[1] Fairly stable[2] Stable,[3] respectively	Stable	Stable	Unstable

Table 3.10. The effect of aeration time (minutes) and aeration speed (RPM) on hydrogel characteristics.

Creation of desired aerated hydrogel was a result of synergism that created between physical and chemical parameters (Table 3.10). It could have not been possible to develop a 3-dimensional self-supporting aerated hydrogel if a right relationship was not established between mentioned parameters as it is illustrated in Figure 3.31.

The effect of physical parameters aerated gel characteristic will be explained in great detail in the next chapter.

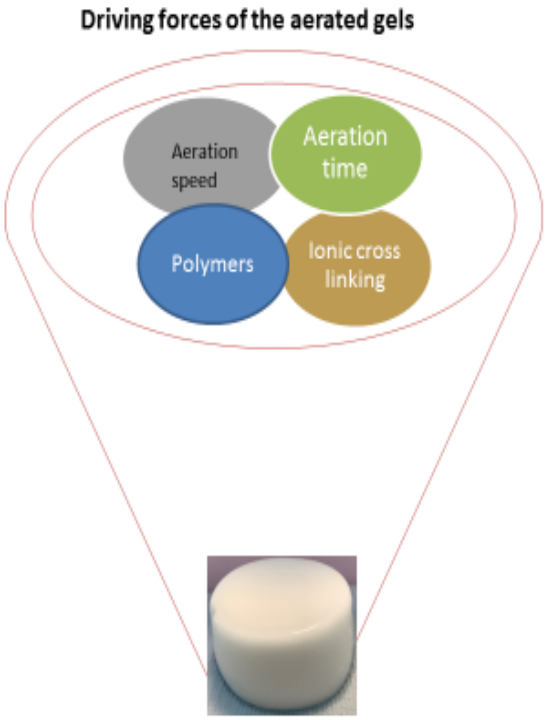

Figure 3.31. Driving forces of the aerated hydro and aerogels.

3.9. Conclusion

Hydrogels can be made of different hydrocolloids and applied in various products for improving textural characteristics, appearance and stability etc. The formation and functionality of hydrogels are dependent on some internal and external factors such as type of biopolymer, formation conditions (*e.g.*, heating), chemical conditions (*e.g.*, pH), and interactions with othe polymers.

In this this research, it was identified that time and temperature control before and also during aeration are important parameters for the formation of self-supporting aerated hydrogels. Optimization of mixing speed was another parameter that had a crucial effect to

obtain homogenous gel structure containing more air cells and higher overrun. Adding MC/HPMC to WPI + alginate hydrogels improve gel strength significantly with smaller air cells. Aerogels containing LBG had more intact air cells compare to other polymer-K100M at slow freezing temperature while fast freezing provided more intact air cells in the final aerogels made of WPI+Alginate and K100M.

In summary, a new method based on alginate ionic cross-linking gelation mechanism in the presence of calcium ions was developed for producing aerated hydro and aerogels with very low solid mass content (0.5%), which is known to be novel for producing edible aerated hydrogel with food grade materials. After setting up a novel method, there was a need to establish a relationship between processing parameters and ingredients and understand how interactions between those parameters affect gel rheology, microstructure and charactertistics (texture, cell diameter, porosity, density *etc*.). Therefore, in the next chapter the effects of physical and chemical parameters on aerated hydrogel and aerogel characteristics was explored in great detail.

CHAPTER 4

Understanding effects of physical and chemical parameters on aerated hydrogel and aerogel characteristics

4.1. Introduction

Although several studies have been focused on certain properties of HPMC, such as water affinity and gelation, there is little known concerning their behaviour in ternary systems, i.e. systems formed by water, proteins and alginate and HPMC (Pérez et al., 2006). On the gelation of whey proteins in the presence of various polysaccharides much is not known at the molecular level about the functional properties of individual biopolymers. Nevertheless, the role of protein-polysaccharide interactions, in relation to their functionality in complex multiphasic systems, such as food mixed solutions, emulsions or gels, is still not well understood (Doublier et al., 2000).

The aim of this work was to characterise the interaction of mixtures of WPI, HPMC/MC and alginate under high shearing conditions and varied mixing time and temperature changes; in order to study the impact of each polysaccharides and WPI on micro/macrostructure, texture and the dynamics of gelation and gel properties of the mixed systems.

The mixed gels can be viewed as self-assembling systems and the control of morphologies would allow to design their properties. Therefore, it is believed the results acquired from this research are important contributions to the manipulation of the physical and chemical properties for obtaining tailored aerated hydrogel and aerogels from biopolymer mixtures.

4.2. Effect of chemical parameters (polymers) on hydrogel and aerogel structure and rheology: Results and Discussion

4. 2.1. Effect of four polymers-K100M, K4M A4M and LBG on aerated hydrogel characteristics

The effect of cellulose derivatives K100M, K4M (HPMC) A4M (MC) and LBG on aerated hydrogel characteristics was studied by using various techniques; texture analyser, Cryo-Sem, X-ray computed microtomography and ImageJ.

4. 2.1.1. Overrun

Overrun was taken as increase in volume after aeration and measured using the Equation 2.1 (Refer to Chapter 2, section 2.3.1).

The effect of four different polymers (K100M, K4M, A4M and LBG) on hydrogel overrun consisting of alginate, WPI, $CaCO_3$, and GDL was studied with a fixed mixing time (10 minutes) and an aeration speed of 8000 rpm. The samples containing K100M, K4M and A4M showed a similar overrun, with no significant difference between them. Comparing the polymers tested, the lowest overrun was recorded with LBG and there was a significant difference between LBG, K100M, A4M and K4M ($P < 0.014$) (Figure 4.1).

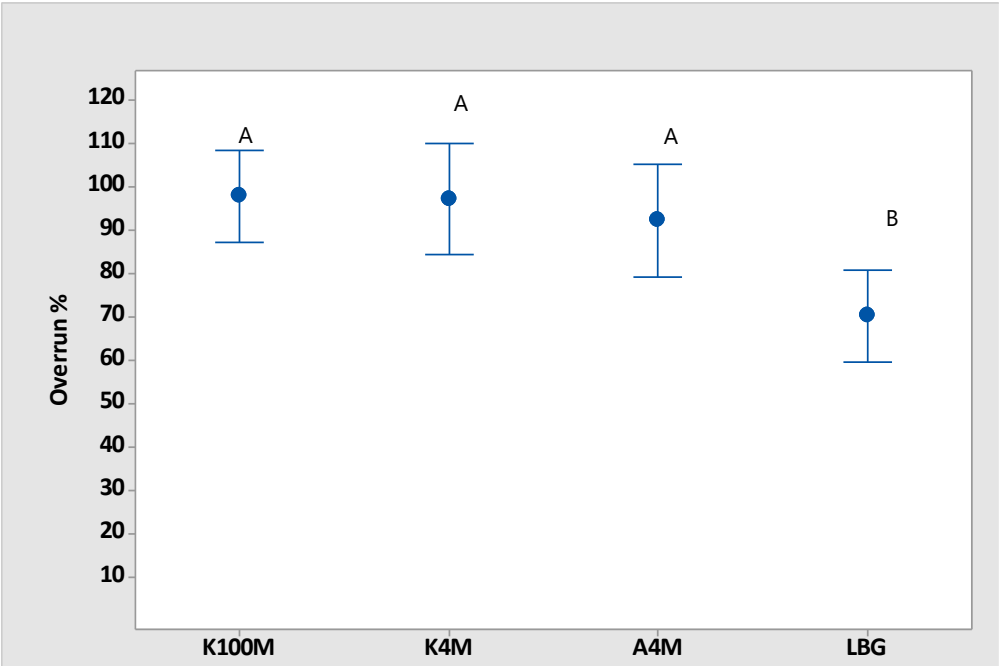

Figure 4.1. Effect of different polymers on overrun. Different letters indicate significant difference at the $p < 0.05$ level among all the tested polymers. Error bar resresents the 95 % confidence interval for the mean.

Overrun was affected by the polymers used. As it is shown in Figure 4.1 the overrun was higher with K100M and lower with LBG. This might be related to viscosity of the aerated media (Figure 4.11). It was recorded that these polymers produced viscous solutions in the following order K100M > K4M= A4M>LBG, which probably explains the difference in relative overrun. Surface active polymers play an important role in foaming and foam stability as they readily adsorb at the interface and thus reduce surface tension. In the presence of the surface-active polymers loss of gas bubbles, coalescence of liquid droplets and drainage of the liquid between films is prevented due to a viscoelastic interfacial layer and the higher continuous phase viscosity (Wallick, 2014).

4.2.1.2. Air cell count, volume and total surface area and porosity

Air cell count of aerated hydrogel samples made of K100M, A4M and LBG was measured using X-ray computed microtomography. There was a significant difference in air cell count between tested aerated hydrogels (P <0. 001). K100M has a significantly higher number of air cells, followed by A4M, while LBG samples had the lowest air cell count. Therefore, the more viscous K100M is able to retain more air as the system is aerated.

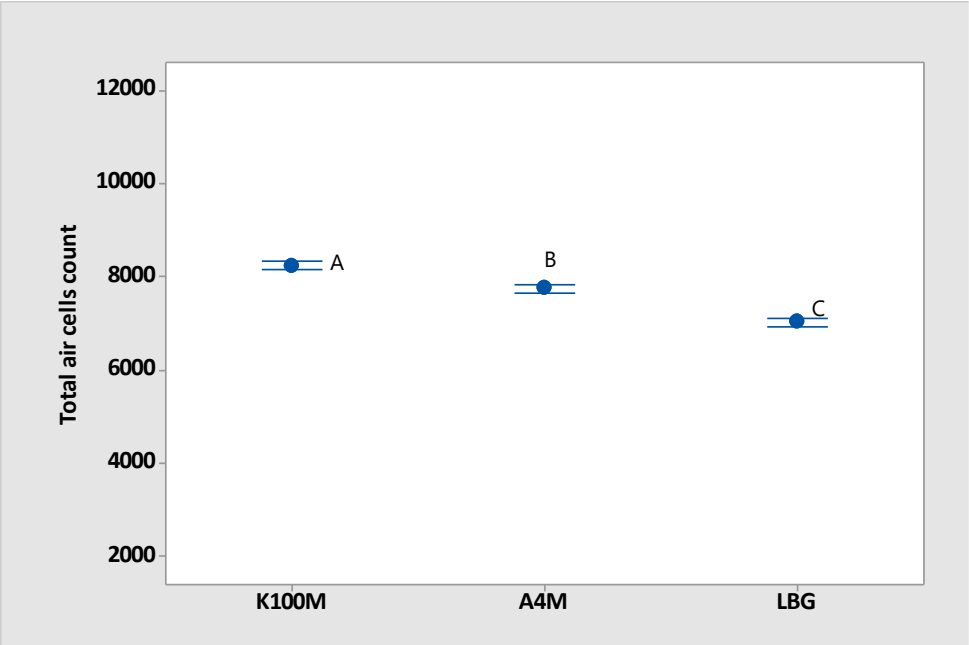

Figure 4.2. Air cells count in aerated hydrogels made of different polymers. Means that do not share a letter are significantly different. Error bar resresents the 95 % confidence interval for the mean.

The volume (mm^2), total surface area (m^3) and porosity of (%) of the aerated hydrogels was also analysed using X-ray computed microtomography. The hydrogel samples made of K100M had the highest volume (mm^2) (Figure 4.3) and total surface area (m^3) (Figure 4. 4), which is in correlation with overrun (Figure 4.1) and air cell count (Figure 4.2).

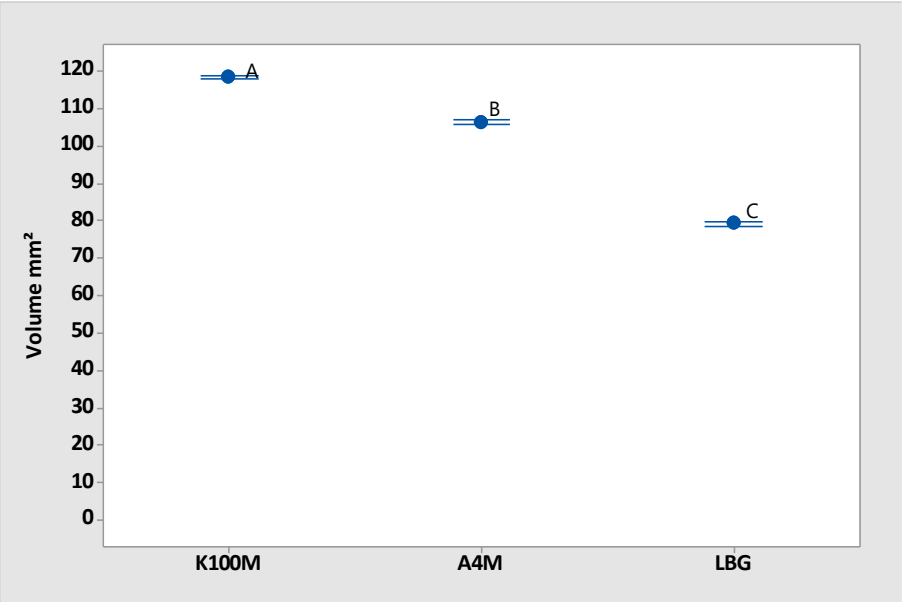

Figure 4.3. Volume of air cells in the aerated hydrogels with different polymers, P <.001. Means that do not share a letter are significantly different. Error bar resresents the 95 % confidence interval for the mean.

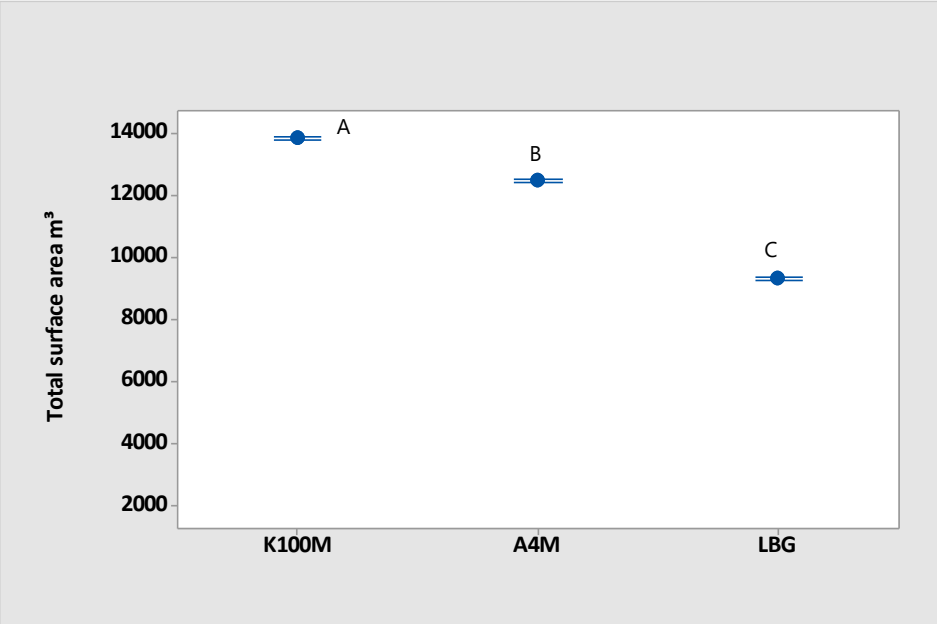

Figure 4.4. Total surface area of measured air cells in aerated hydrogels with different polymers. P < .001. Means that do not share a letter are significantly different. Error bar resresents the 95 % confidence interval for the mean.

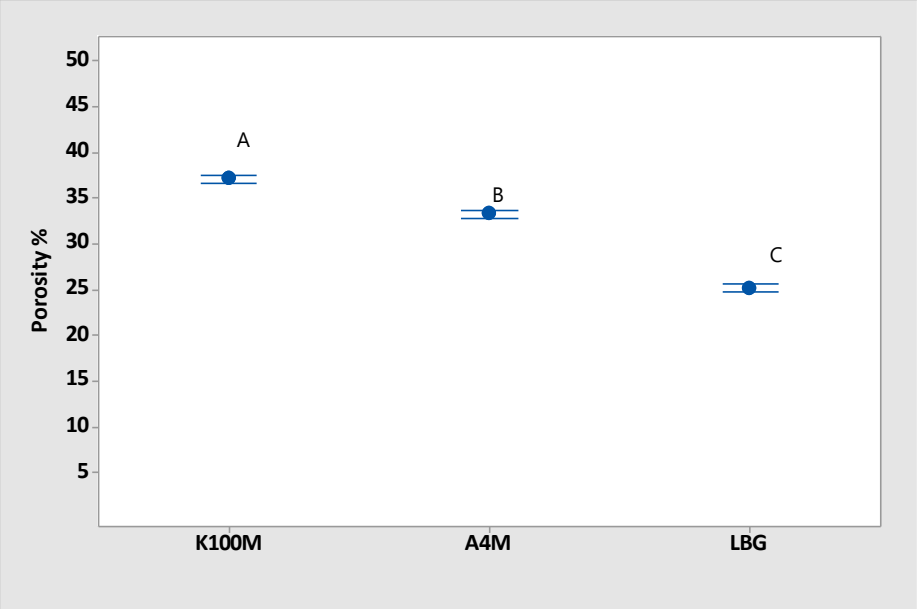

Figure 4.5. Showing porosity of aerated hydrogels containing different polymers, P < .001. Different letters indicate significant difference at the p < 0.05 level among all gel samples. Error bar resresents the 95 % confidence interval for the mean.

Thus, aerated hydrogels with different porosity (fraction of the total volume filled by air) could be obtained by varying polymer types in the mixed system.

4.2.1.3. Cell diameter

Further analysis of the aerated hydrogels was measured by using ImageJ, enabling the quantification of the mean diameter of the air cells. Initially images of hydrogels were taken soon after aeration was completed using EVOS- inverted light microscopy and then transferred to ImageJ for analysis.

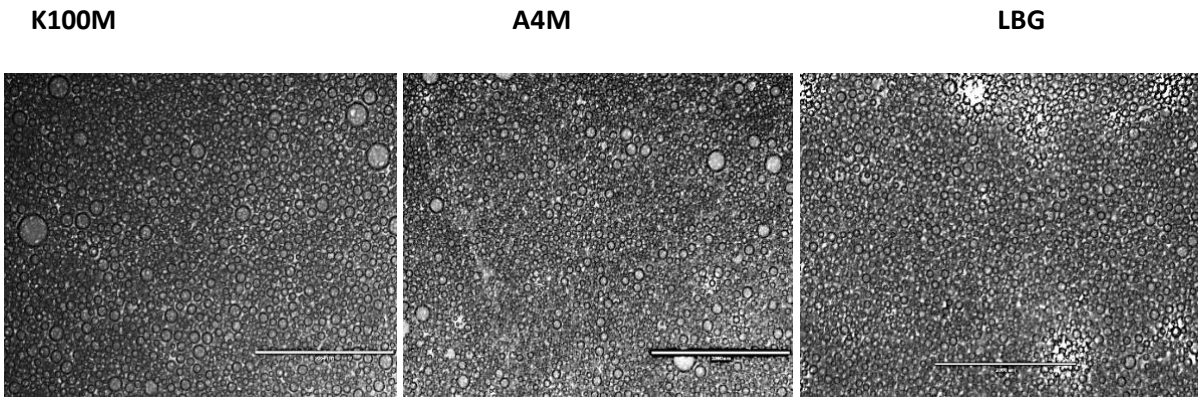

Figure 4.6. Inverted light microscopy images of aerated hydrogels at time zero with K100M, A4M and LBG, from left to right, respectively. The scale bar indicates 2000 µm.

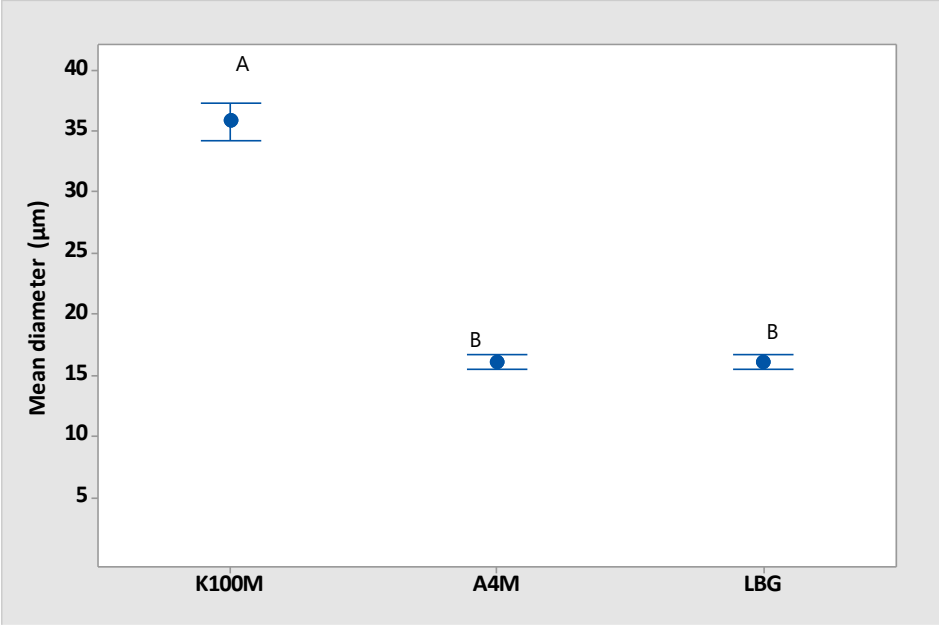

Figure 4. 7. Effect of polymers on air cells diameter. Different letters indicate significant difference at the $p < 0.05$ level among all hydrogel samples. Error bar resresents the 95 % confidence interval for the mean

Mean diameter of air cells in the aerated hydrogel containing K100M was significantly greater than A4M and LBG aerated hydrogel. A4M and LBG had similar air cells mean diameter

(Figures 4.6 and 4.7) which implies that the greater continuous phase viscosity of K100M imparts more resistance to air cell break up during the shear flow in the Silverson mixing device. Therefore, the results here suggest that an increase in continuous phase viscosity creates a greater air cell volume, but also air cells that are larger than when the viscosity is lower.

4.2.1.4. Microstructure of aerated hydrogel with different polymers

The microstructure of aerated hydrogels containing different polymers were also observed by X-ray computed microtomography and Cryo –SEM. As shown in Figure 4. 8 the K100M had more air cells than A4M and LBG aerogels, which is in correlation with overrun and air cells count results (Figure 4.1 and 4.2).

According to 3D X-ray computed microtomography images, aerated hydrogels containing K100M, displayed more heterogenous air cells with higher mean diameter value compare to A4M and LBG.

It is observable that polymer type played an important role in the enhancement of internal structure. Cellulose derivatives (K100M and A4M) enhanced the strength of the hydrogels. The aerated hydrogel prepared from SA without cellulose was too weak to hold more water (Refer to Chapter 3, Introducing new materials: MC/HPMC).

Effect of polymers on aerated hydrogel microstructure

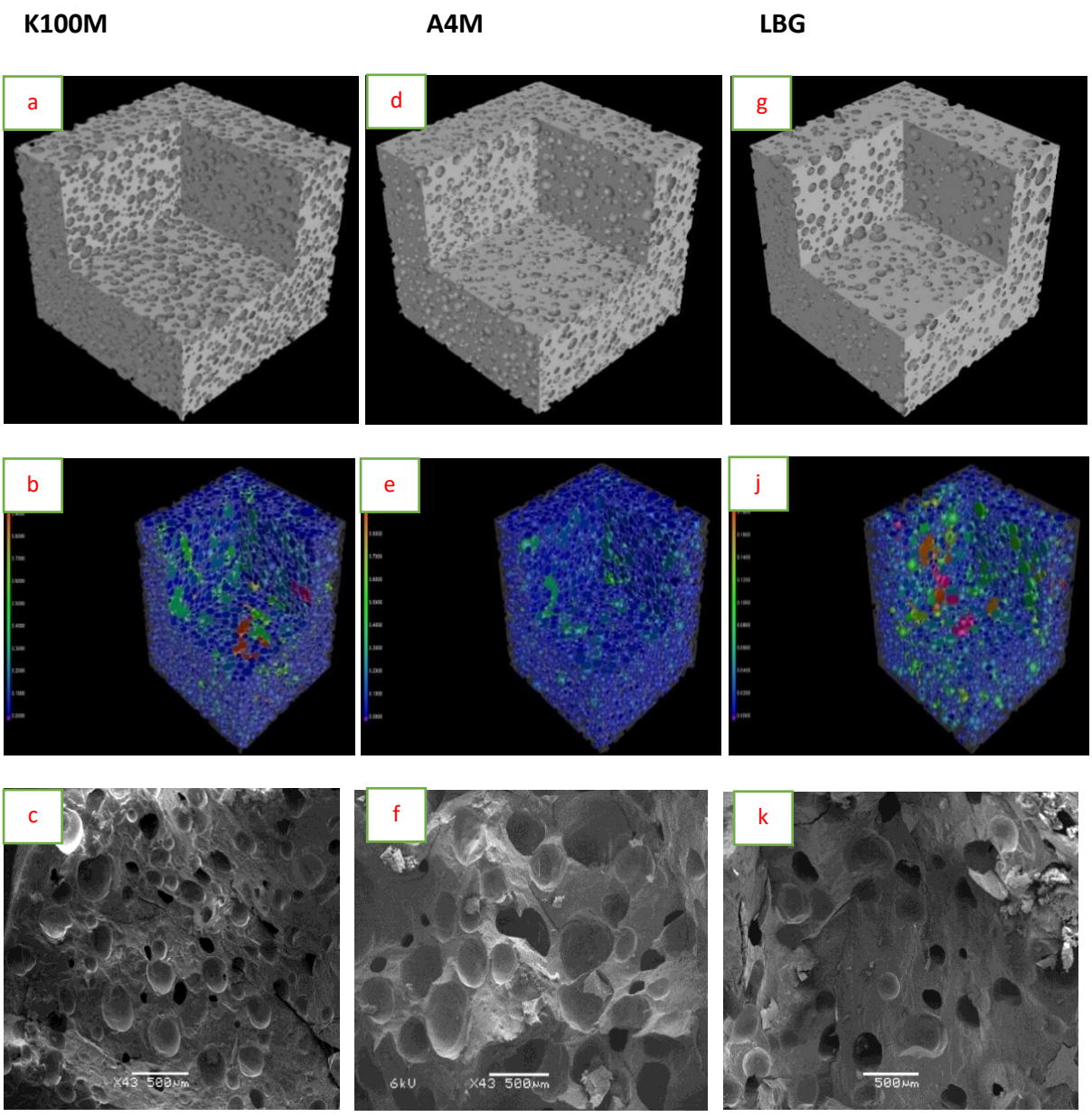

Figure 4.8. From left to right, showing effect of K100M (a-c), A4M (d-f) and LBG (g-k) on aerated hydrogel microstructure, respectively. The first and second row, 3D X-ray microtomograph images of aerated hydrogele, third row, Cryo-SEM images of aearated hydrogels.

4.2.1.5. Hydrogel texture

The aerated hydrogels containing K4M had the lowest values of the maximum force (hardness) of compression, followed by LBG. Samples made of K100M and A4M are the hardest hydrogels by exhibiting maximum force during compression. There was a significant difference between samples of K100M, K4M and LBG with $P < 0.001$.

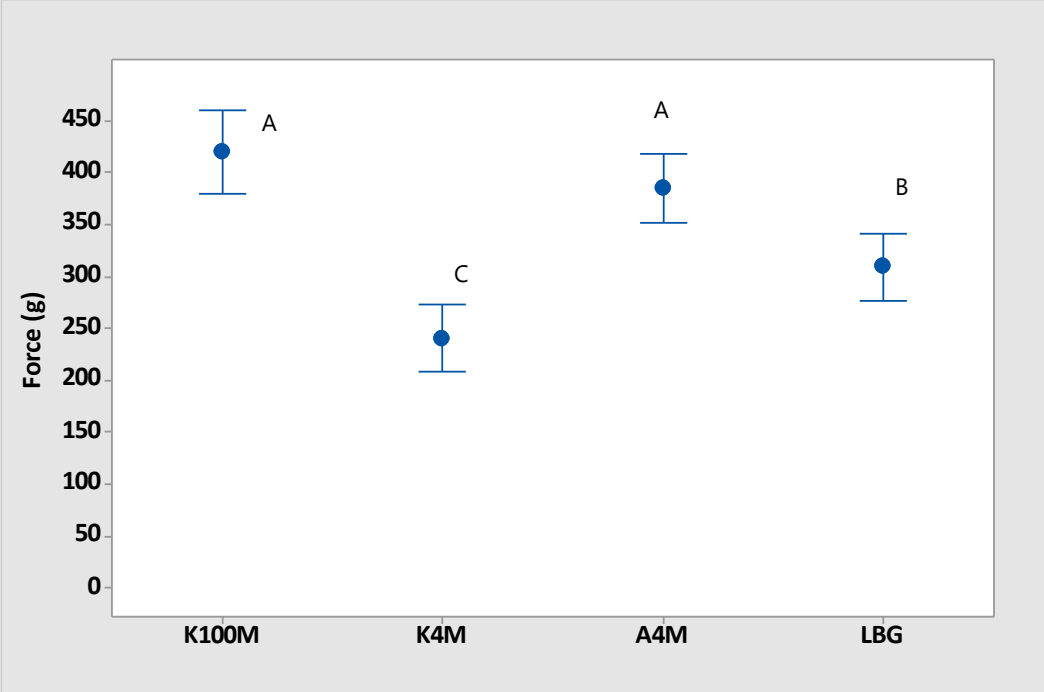

Figure 4.9. Effect of polymers on aerated hydrogel texture $P < .001$. Means that do not share a letter are significantly different. Error bar resresents the 95 % confidence interval for the mean

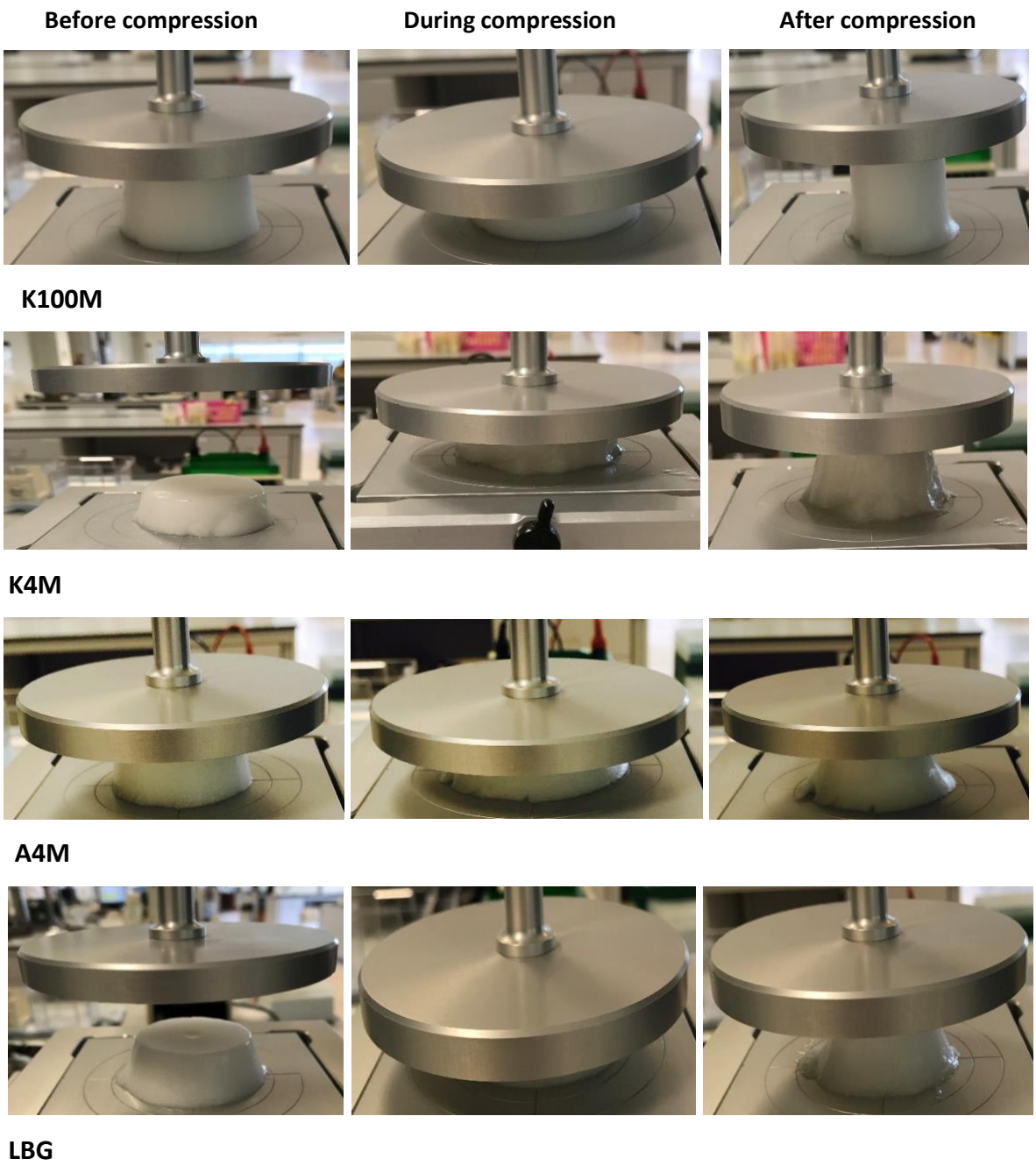

Figure 4.10. Showing stages of texture analysis of an aerated hydrogels by compression test. All the tested samples that made of different polymers showed same trend of mechanical hardness, they were slightly de-formed but kept their 3-D gel structure after the compression (40 % strain).

As it shown in Figure 4.10, all hydrogels remained uniform after the compression test. According to obtained results, cellulose derivatives (K100M, K4M, A4M) contributed to enhance the mechanical properties of the hydrogels by being viscosity enhancer in gel matrix, in which alginate could retain a lot of water and form three- dimensional gel network at very low concentration (0.20 % w/w), which is in an agreement with literature.

4.2.1.6. Effect of polymers, K100M, K4M A4M and LBG on hydrogel rheology

Initially, shear viscosity of the polymer solutions K100M, K4M, A4M and LBG with alginate, WPI, $CaCO_3$ and GDL were analyzed using rotational rheology, which was followed by oscillation for time and temperature sweep measurements. The mixture for the rheological measurements were prepared as it is explained in section 2.2.1 however, they were transferred to the rheometer prior to aeration in order to measure the properties of the matrix in which the air cells are created and stabilised.

Shear viscosity was measured at shear rate of 837s^{-1}, which is equal to 8000 rpm of the high-speed mixer, by increasing temperature from 25 to 50 ^{0}C at a heating rate of 2.5^{0}C/min. Subsequently storage modulus (G') and loss modulus (G") were measured at a frequency of 10 Hz and a strain of 0.005 % and cooling from 50 to 25 ^{0}C at a cooling rate 0.5 ^{0}C/min and then holding at 25 ^{0}C for 65 minutes. For all rheological measurements, (shear viscosity, time and temperature sweep) solution of mixed polymers was directly transferred to the rheometer just after adding $CaCO_3$ and GDL respectively.

4.2.1.6.1. Shear viscosity, time and temperature sweep

The Figure 5. 11 displays shear viscosity and Figure 5. 12 and 5.13 demonstrate viscoelastic moduli (G' and G") values of 0.70 % w/w alginate, WPI, cellulose derivatives (HPMC and MC) and LBG solutions in the presence of Ca^{2+} during heating and cooling cycle, respectively. On the both figures, the first set of data is about shear viscosity under a single constant shearing for 10 minutes. The second set of data is about time and temperature dependence of storage modulus (G') and loss modulus (G") after stopping the shearing.

4.2.1.6.1.1 Shear Viscosity

HPMC- K100M displayed the highest shear viscosity and followed by K4M, A4M and LBG, respectively.

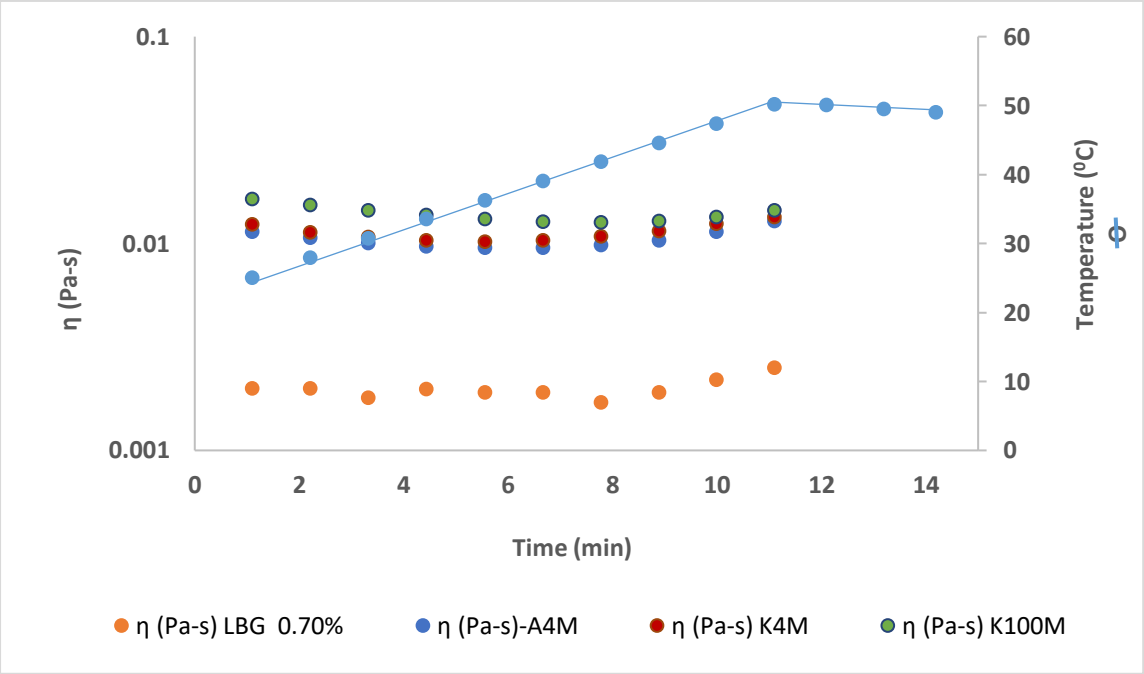

Figure 4.11. Showing shear viscosity of the polymer solutions during 10 minutes shearing at $837s^{-1}$ and temperature increase (2.5 ^{0}C/min).

It must be noted that for all the tested polymers, shear viscosity increased in a two-step fashion. Viscosity decreased during first 5 minutes of shearing, in parallel to temperature increase. However, it increased after first 5 minutes of shearing.

This viscosity decrease can be explained by the effect of temperature on polymer motion. At low temperature macromolecules are hydrated and, viscosity is dominated by simple entanglement of the molecules (Ruel-Gariépy and Leroux, 2004). Another explanation for initial viscosity decrease might be due to progressive disruption of native cellulosic 'bundles' as a result of temperature increase (Bajwa et al., 2009; Haque and Morris 1993).

The inrease in viscosity after 5 minutes of shearing, when temperature is still increasing might be explained by some occurrences such as; (a) beginning of protein aggregation, (b) cellulose derivatives begin to increase a network of swollen clusters (Alessandro et al., 2009; Haque and Morris, 1993 or (c) formation of new cross-links as a result of dissociation of $CaCO_3$ and release of Ca^{+2} to form egg-box alginate gel structures. For both a) and c) the formation of aggregates/gels corresponds with the creation fluid gel structure.

An increase in number and volume fraction of the forming particles results in an increase in viscosity (Moakes et al., 2015). After that point it seemed that the formed structure is not affected by the applied shear anymore.

According to Moakes et al. (2015), for WPI gelation in a shear field, the primary particles are held together by weak hyrophobic interaction at the beginning of the aggregation and therefore aggregates are broken down easily than later stage where more firm structure is formed because of covalent bonding. However, when heating rate is high the rate of aggregates formation is faster and therefore formed aggregate can become more resistant to

shear breakdown. Thus, at a heating rate of 10 ^{0}C min^{-1} aggregates are formed within the shear field, whereas at low heating rate (1 ^{0}C min^{-1}), larger aggregates are formed but they are broken down due to lack of resistance to shear breakdown, resulting in smaller final sizes (Moakes et al., 2015). Consequently, depends on the heating rate, size of the aggregates increased through interlinking particles and resulted in viscosity increase.

4.2.1.6.1.2 Time and temperature sweep

The Figure 4.12 demonstrates viscoelastic moduli (G$^{'}$ and G") values of 0.70 % w/w alginate, WPI and cellulose derivatives (HPMC and MC) solutions in the presence of Ca^{2+} and GDL. The storage modulus (G$^{'}$) represents the elastic portion of the viscoelastic behaviour (sample is in solid-state), while the loss modulus (G'') characterizes the viscous portion of the viscoelastic behaviour (sample is in liquid-state).

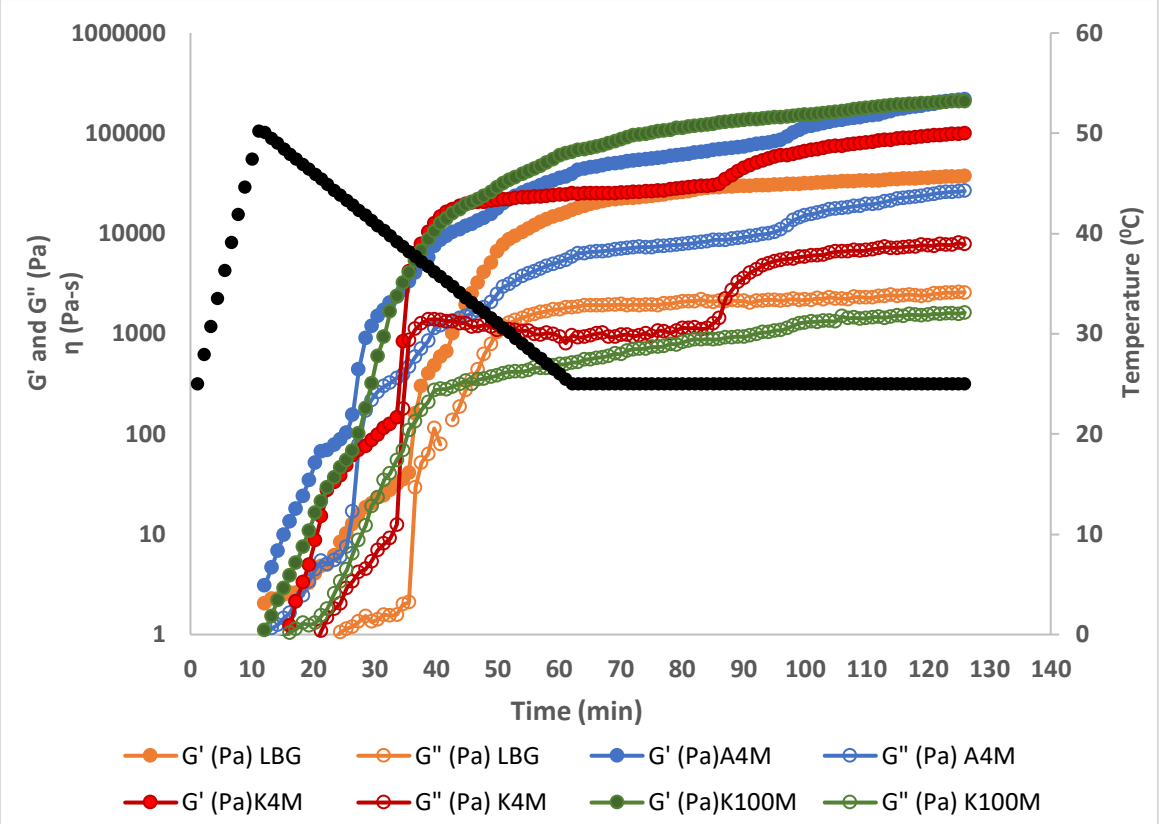

Figure 4.12. Showing elastic and loss modulus (G' and G" respectively) of the polymer solutions after 10 min shearing at 837s^{-1} and at heating rate of 2.5 ^{0}C/min, and cooling rate 0.5 ^{0}C/min and then holding at 25 ^{0}C for 65 minutes.

The G′ and G″ of the samples are depicted at time = 10minutes, upon the cessation of shearing. The storage modulus (G′) and loss modulus (G″) of hydrogels made of different polymers showed a comparable trend (Figures 4. 12 and 4. 13). The samples containing K100M and A4M displayed the highest G′ and but the lowest G″ while LBG displayed low G' moduli. There was a slight decrease in the G′ and G″ temperature between 33 and 43 ^{0}C. However, substantial increase in the both modulus at temperature above 44 ^{0}C was recorded. Further increase of G′ and G″ during cooling down to 25 ^{0}C took place. The increase in the both modulus at room temperature also occurred and only LBG reached a plateau.

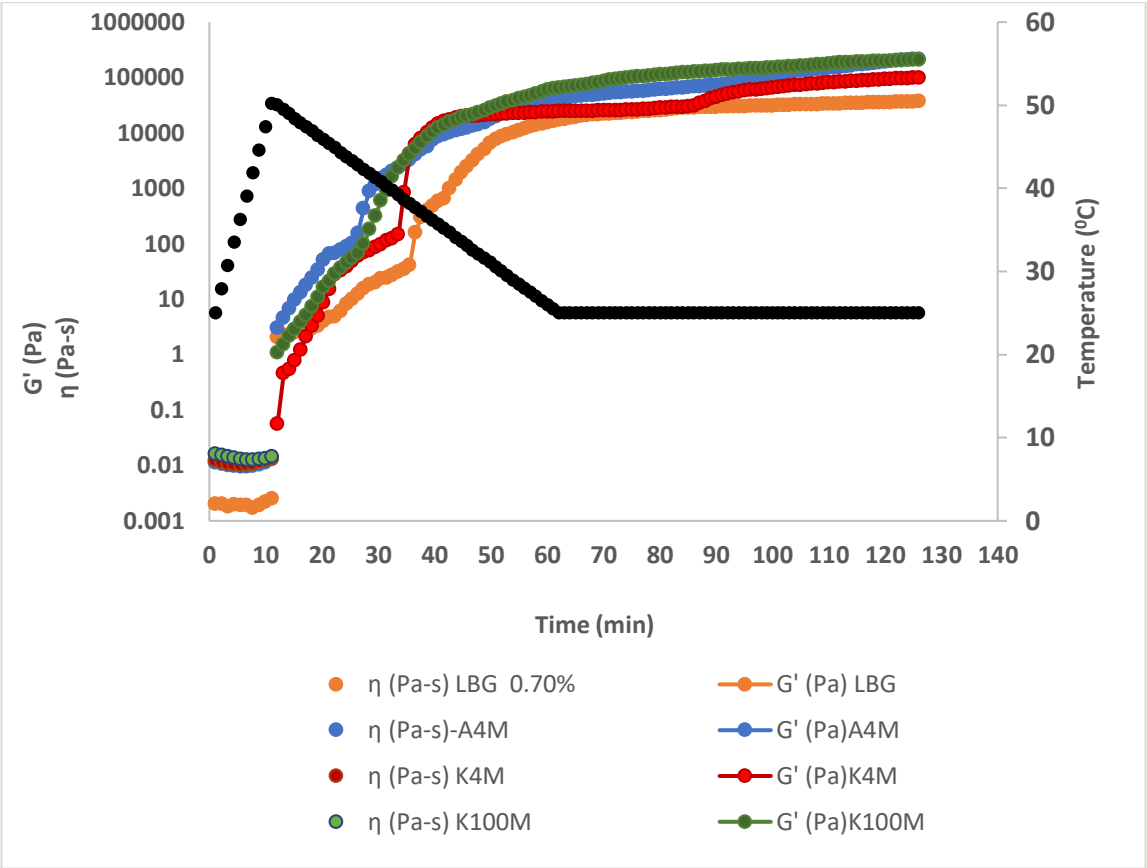

Figure 4.13. Showing elastic modulus (G') of the polymer solutions after 10 min shearing at 837s^{-1} and at heating rate of 2.5 ^{0}C/min, at a frequency of 10 Hz and a strain of 0.005 % and cooling rate 0.5 ^{0}C/min and then holding at 25 ^{0}C for 65 minutes.

According to Perez et al. (2006), when whey proteins/polysaccharide solutions are heated several events can occur simultaneously: (a) Dehydration of HPMC chains so exposition of hydrophobic groups and interaction between them; (b) After the dehydration HPMC aggregation/gelation take place (c) whey protein denaturation (d) aggregation/gelation of whey proteins and (e) phase separation. In general, there are two competitive phenomena upon heating: phase separation and gelation of both biopolymers (Perez et al., 2006).

In the literature, the temperature inflexion around 43 ^{0}C for both MC and HPMC solutions has been reported previously. So, the mentioned decrease in the G' and G" between 33 ^{0}C and

43 ^{0}C might be due to the progressive disruption of native cellulosic ‘bundles’, while the later increase in G' could be attributed to the unbundling of the constituent strands of polymer at the ends of the bundles and formation of a network of swollen clusters (Bajwa et al., 2009). According to Haque and Morris (1993), as a result of temperature increase, the ends of the bundles come apart, methyl groups (hydrophobic) are exposed to the aqueous environment, forming structured water 'cages' and causing a large increase in volume (with consequent increase in G'). A hydrophobically crosslinked network is formed at higher temperature because the methyl substituents shed structured water. Therefore, the second increase in G' can then be attributed to thermal disruption of the cage structures with consequent formation of the gel network by hydrophobic association of strands radiating from different bundles (Haque and Morris, 1993).

Similar to Haque and Morris (1993), Sammon et al. (2006) also reported that below 43 ^{0}C the G' progressively decreases as a function of temperature, which was attributed to unbundling of native cellulosic fibres and was responsible for the increase in volume of the solution. However, above 43 ^{0}C there was a gradual increase in G$^{'}$ which plateaus around 65 ^{0}C. They claimed that, this gradual increase in elastic nature is characteristic of the progressive formation of a weak structured elastic gel, held together by weak hydrophobic interactions (Sammon et al., 2006).

In addition, it has been reported that, during first stages of heating a transition from transparent to turbid solutions is observed. The temperature corresponding to this transition, the *cloud-point,* that indicates the beginning of aggregation by means of hydrophobic interactions was 30 ^{0}C and was not affected by HPMC concentration (Perez et al., 2006, Liang et al., 2004).

However, in this research aerated hydrogels are created by a rather complex mixture containing more than one hydrocolloid; cellulose derivatives (HPMC/MC), alginate, WPI and cross-linking agents $CaCO_3$ and GDL. Therefore, under high shearing conditions and increasing temperature each compound is expected to behave differently. It is very clear to see significant increase of G'(represents the elastic portion of the viscoelastic behavior) and G'' (defines the viscous portion of the viscoelastic behavior) modulus after temperature reached 50 ^{0}C (Figure 4.12). This may be attributed to increased solubility and entanglements of polymers and further formation of cross-links between alginate and Ca^{2+}. MC-A4M forms gel temperature between 35 and 55 ^{0}C while HPMC- K100 forms gel only at 70 -90 ^{0}C by hydrophobic interaction (Joshi, 2011).

The biopolymer type seemed to be only one of a number of process-formulation variables that had influence the rheological properties of the aerated alginate hydrogel. As it was mentioned earlier HPMC-K100M provided the highest shear viscosity and G' moduli due to its viscosity-enhancing assets and high swellability, which plays important role in strengthening the alginate hydrogel's mechanical properties (Liu et al., 2006; Banerjee et al., 2013; Nochos et al., 2008; Joshi, 2011).

MC-A4M, similar to K100M, provided higher G' moduli, which was followed by HPMC-K4M. MC is soluble (hydrophilic) in water due to substitution of methoxyl groups to a certain number of hydroxyl groups and breakage of some hydrogen bonds. MC forms a thermo-reversible gel but can change to a sol state at below 50 ^{0}C (Banerjee et al., 2013; Lin et al., 2007).

Hirrien et al. (1998) reported that at low concentration solutions (c<20 g/l), the sol–gel transition observed as temperature increased which was well described by a percolation process. For a polymer concentration of 0.2 g/l this critical temperature was around 55 ^{0}C, and at 60 ^{0}C. It was claimed that at low temperatures, the mechanical spectra was characteristic of a pure viscous solution. The MC solution at low temperature and low polymer concentration dissolved well in water but did not form any aggregation. However, when the temperature and concentration increase, whatever the methylcellulose samples, hydrophobic interactions due to the presence of methyl groups appear upon heating (Hirrien et al., 1998).

Haque and Morris (1993) reported that at low temperature (24 ^{0}C) MC-A4M was in the solution state and, at high temperature (85 ^{0}C) and at an intermediate temperature (49 ^{0}C) it transforms to the gel state. Although, at intermediate temperature (49 ^{0}C) there was an evidence of some gel-like character (Haque and Morris 1993).

As mentioned, with K4M, a hydroxypropyl methylcellulose (HPMC), G' moduli was lower than A4M. It has been reported by Haque et al. (1993) that thermogelation of HPMC does not occur until higher temperature and about 20 degrees higher than for A4M, due to its lower content of hydrophobic substituents which might be explained by the more polar character. Therefore, the resulting gels shows a substantially lower moduli than for corresponding concentration of A4M (by about a factor of 30). It was reported that K4M was in the solution state (at 25 ^{0}C), and in the gel state at high temperature (96 ^{0}C) and intermediate temperature (68 ^{0}C). Unlike MC, HPMC gels arises from melting and re-formation of the postulated 'bundle'

structure, and not from hydrophobic interactions until much higher temperatures (Haque et al., 1993).

It is known that contact between alginate (a polyanionic polymer) and Ca^{2+} in solution induces immediate ionic polymerization of alginate via binding of Ca^{2+} within the cavities of the guluronic residues of alginate. Thus, an interpenetrating network like structure could be formed within the methylcellulose chains when blended with divalent cations such as $CaCl_2$. According to Liang et al. (2004) at 37 ^{0}C, there was the hydrophobic interaction between methylcellulose molecules, the hydrogen-bonds formation between -COOH and –OH groups in hydrogel, and the ionic cross-links between alginate molecules within the test hydrogel (Liang et al., 2004).

Among all the tested polymers, the lowest G' moduli was recorded with LBG. It has been reported that LBG solutions with concentrations ranging from 0.5% to 2.0%, show a liquid behavior at lower frequency (G" > G') and a solid-like behavior at higher frequencies (G' > G") (Barak and Mudgil, 2014) and the relationship between alginate and LBG is described as interpenerating network (Jana et al., 2015, Madhavi et al., 2017).

It has been reported that for the WPI/LBG mixtures, at very low WPI concentration, the galactomannan had a detrimental influence on the protein network formation, but a negligible effect or even a positive influence on the gelation process at higher concentrations. WPI system alone or for LBG concentrations below 0.25% (w/w) no appreciable changes in the viscoelastic moduli were observed during the heating step 40–90 ^{0}C (Tavares and Silva, 2003). These results are indicative of transition between miscible and immiscible mixtures.

To conclude, based on above substantiations the low concentrations (0.15 % w/w) of the tested individual polymers (A4M, K4M, K100M and LBG) would not have any impact on the gelation of either WPI or alginate. In this formulation with 0.70 % (w/w) solid mass content, the seen gelation is predominantly due to alginate. However, the relationship between alginate and other polymers may be explained by semi-inter penetrating network (semi-IPN), which has been reported already (Figure 4.14) (Liang et al., 2004). In semi-IPN one polymer is linear and penetrates another cross-linked network without any other chemical bonds between them (Das, 2013).

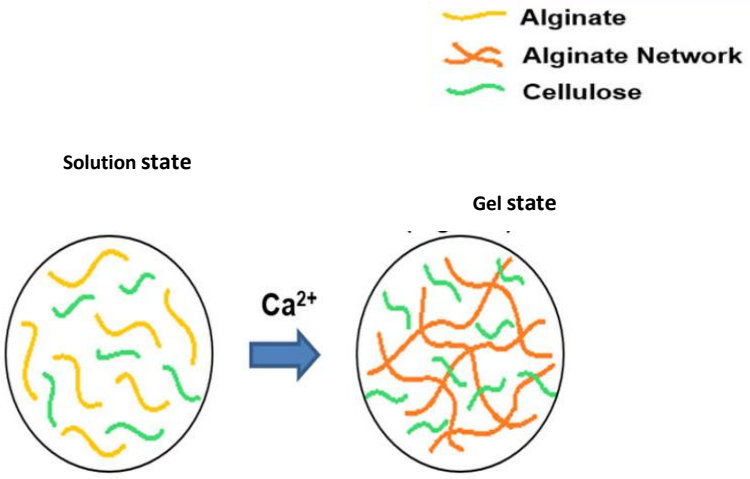

Figure 4. 14. A Schematic representation of the alginate-cellulose Semi-IPN. Adapted from Le et al. (2017).

Semi-IPN do not limit rapid kinetic response rates to pH and temperature due to lack of restricting interpenetrating network (Das, 2013). Liang et al. (2004) reported formation of a semi-interpenetrating network like structure within the methylcellulose/ alginate hydrogel when blended with divalent cations such as $CaCl_2$.

4.2.1.6.2. Fluid gel formation under high shearing

According to Figure 4.12, when shearing was stopped, the G' moduli was already greater than G", which is indication of formation of fluid gel under shearing conditions. Fluid gels are suspensions of gelled particles dispersed in a non-gelled continuous medium and formed by through mechanical break-up of clusters of the forming gel, whose properties depend on the size, number and mechanical properties of the gelled particles (Garrec and Norton, 2012; Farrés et al., 2013; Norton et al., 1999).

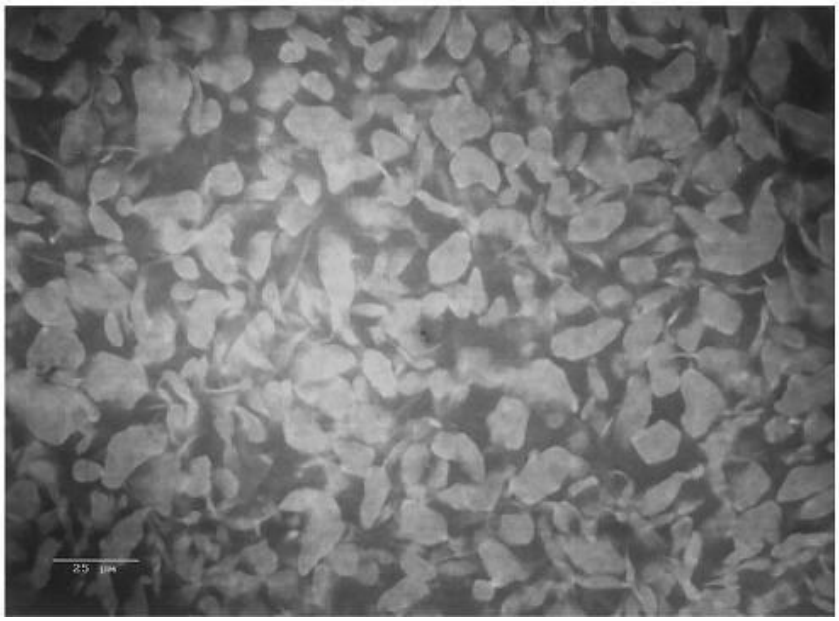

Figure 4. 15. Confocal micrograph of a 3 wt. % agarose fluid gel showing the highly anisotropic structures. The scale bar is 25 μm and the image is adapted from Norton et al., 1999.

In the complex mixed system described in this study, the early stage of the gel formation might be explained by fluid gel-formation phenomena under shearing conditions since G' moduli was greater than G" moduli.

However, the aforementioned literature indicates that if gelation is not complete during shearing then the formed particles can connect and form a three- dimensional, self-supporting gel structure.

Therefore, the final gel formed after a certain amount of aeration time is not either like a paste or a fluid, but instead it was a self-supporting three-dimensional gel.

Figure 4.16. Showing self-supporting three- dimensional gel structure formed after aeration, containing alginate, WPI, MC/HPMC, $CaCO_3$ and GDL.

Therefore, the gelation stages in the system in this research can be described in a two-step fashion (Figures 4.11, 4.12). Initially formation of alginate fluid gel in the presence of the liberated Ca^{2+} under shearing, and then the development of self-supporting hydrogel upon removal of applied shear (from fluid gel to high volume aerated hydrogel).

Hydrogels are defined as water-swollen, cross-linked polymeric network produced by two or more monomers having a three-dimensional network of polymer chains and retaining a significant amount of water within its structure (Ahmed, 2015).

After stopping shearing, according to Farrés and Norton (2014) intra-particle aggregations under shear changed into inter-particle–particle aggregations, resulting in quiescent network formation via association of particles. Formation of alginate fluid gel in the presence of Ca^{2+} and under different shearing conditions has been reported by Farrés et al. (2013). They claimed that at early stage with limited calcium ions only monocomplexes (or nucleation) formed due to binding of calcium to a single guluronate unit of the polymer chain. However, at this stage formed monocomplexes were separated from each other and therefore remained unaffected by the level of shear. But, when more calcium ions became available, formation of egg-box dimers takes place due to the pair wise association of monocomplexes. Subsequently egg-box dimers aggregate via inter-cluster association in a process that occurs simultaneously with the shear-induced break-up of the network being formed, and fluid gel particles are produced. As a result, viscosity increases due to this simultaneous increase in number and volume fraction of the forming particles (Farrés et al., 2013).

When discussing the responses of different polymers to shearing and temperature rise, care should be taken in order to make a reasonable explanation about changes in viscosity and development of G' and G" modulus. Yet, in this formula with a 0.70% dry mass content self-supporting high- volume aerated hydrogel creation is alginate driven in the presence of cross-linking agents.

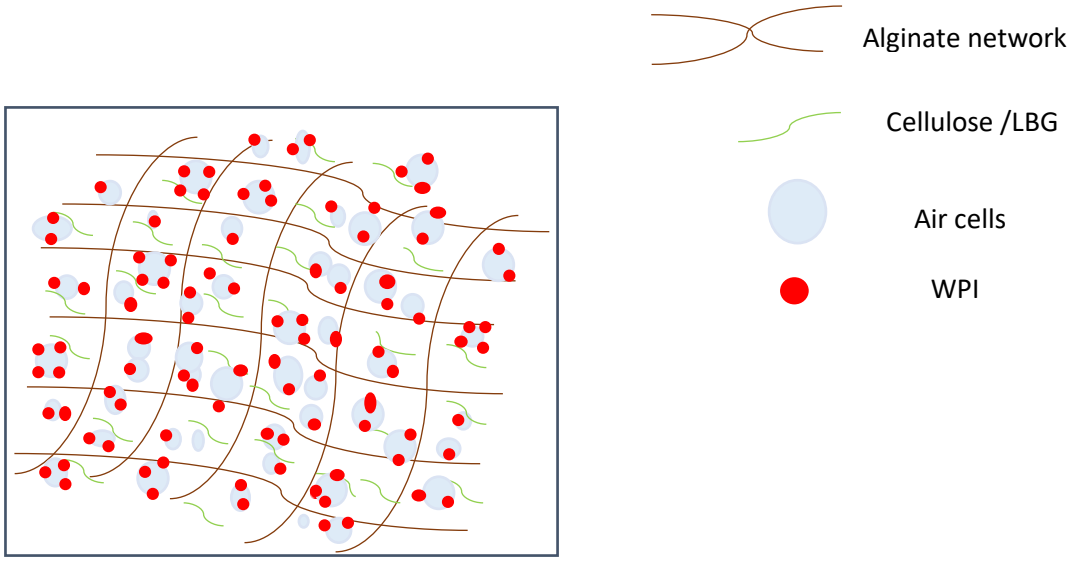

Figure 4.17. A Schematic representation of the alginate-cellulose/LBG IPN. Air cells are stabilised by WPI within an alginate network.

The proposed structure is that the cellulose derivatives acts as viscosity enhancer to support gelling and mechanical properties of low amount of alginate (0.20 % w/w) as it is illustrated in Figure 4.17, while WPI stabilise the air cells by preventing drainage and casues increase in overrun, which has been reported previosly by Lazidis et al. (2016). They claimed that foam formaton is a result of fast diffusion of smaller and mobile protein entities to the interface and reduction of interfacial tension. Therefore, the local bulk viscosity increases due to the filled free space between the air bubbles by larger protein, which improves foam stability mainly by preventing drainage (Lazidis et al., 2016).

4.2.2. Effect of chemical parameters (polymers) on aerogel structure: Results and Discussion

4.2.2.1. Effect of four polymers- K100M, K4M A4M and LBG on aerated aerogel characteristics

Upon establishing the effect of the different added viscosifying polysaccharides on the creation of aerated hydrogels, they were subsequently freeze-dried and the effect of cellulose derivatives K100M, K4M (HPMC) A4M (MC) and LBG on aerogel characteristics was studied by using texture analyser and SEM.

4.2.2.1.1. Aerogel texture

The mechanical properties of the freeze dried aerogels with different polymers was determined by texture analysis. The freeze dried aerogels were compressed with a 100 kg load cell and P/100; 100 mm diameter plate to a true strain of 0.7 %. All measurements were carried out in triplicate. Figure 4.18, represents a typical compressive force–strain curve of the four different polymers, alginate with $CaCO_3$ and GDL. The compressive force–strain of the aerogels decreased in relation to used polymers. The samples made of K100M was the strongest freeze dried aerogel.

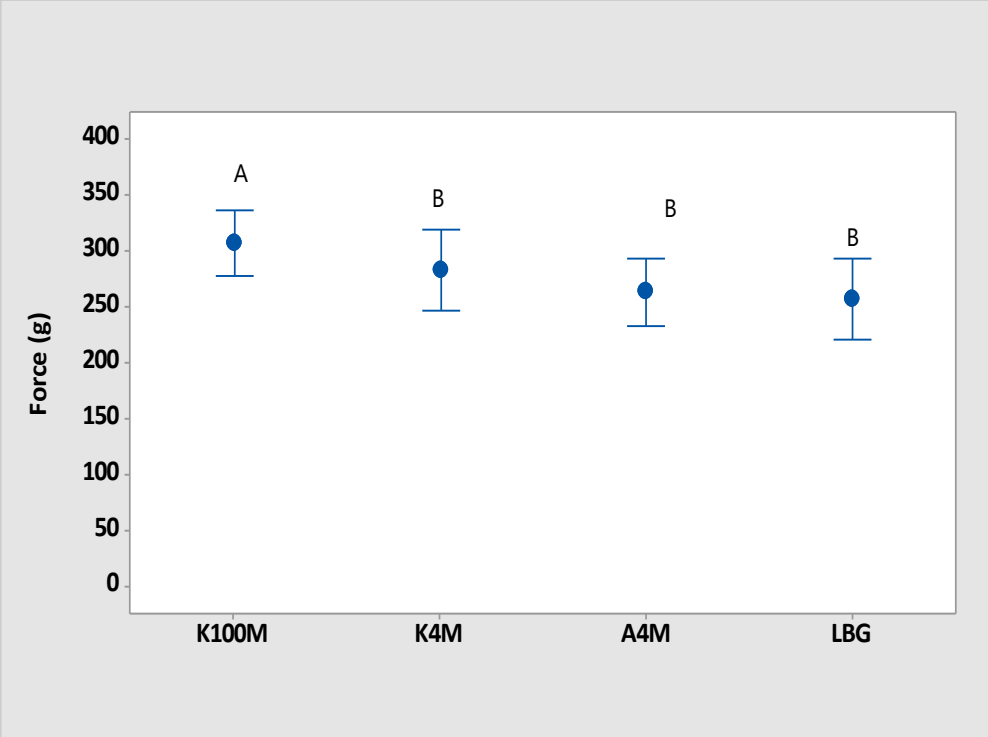

Figure 4.18. Hardness of freeze dried aerogels made different polymers. Means that do not share a letter are significantly different, ($p<0.05$). Error bar resresents the 95 % confidence interval for the mean.

Despite there being differences in the properties of aerated hydrogels, the effect of formulation change on freeze dried aerogels may indicate whether such changes in the wet state are carried forward in the dry state. Thereby indicating whether formulation and processing effects (discussed later) can have any impact on the properties of aerogels.

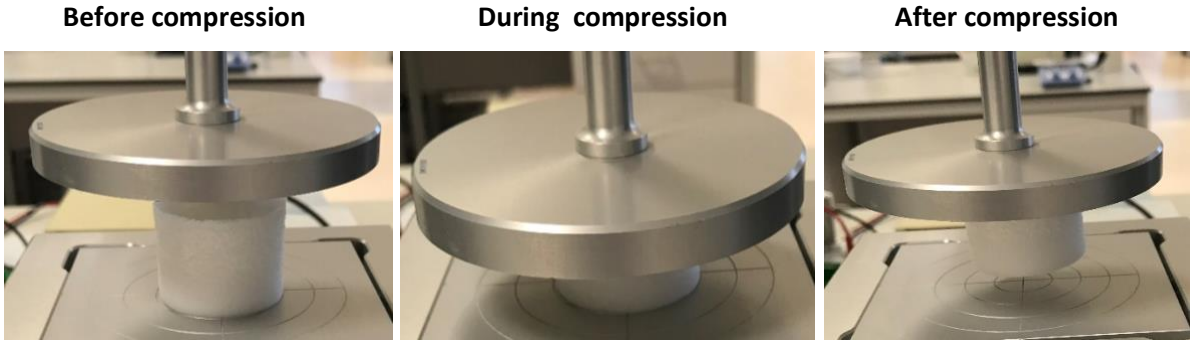

Figure 4.19. Stages of texture analysis of freeze dried aerogel by compression test.

The Figure 4.19 indicates that all the tested samples that made of different polymers were all resilient and kept their shape after compression of 70% true strain.

Aerogel containing K100M appear to be slightly firmer. This corresponds with a firmer texture (Figure 4.8) an increased solution viscosity (Figure 4.11) and greater G' values (Figure 4.12) when in the wet state (sol, hydrogel, aerated hydrogel). Therefore, the texture of the dry aerogel containing K100M seems to mirror its original from the wet state. However, the aerated hydrogels also had different microstructures (air cell size, number, porosity etc.) and therefore the microstructures of the aerogels need to be investigated to determine the origins of the differences in aerogel texture, beyond the formulation of viscosifying polymers.

4.2.2.1.2. Microstructure of aerogel with different polymers

Microstructures of a series of freeze–dried aerogels, containing different polymers are shown in the Figure 4. 20. In general, K100M showed more regular structure with more open network while the A4M displayed less regular but more compact structure. On the other hand, samples made of LBG produced an irregular structure and closed network consisted of intact air cells with very thin walls separating the pores. Freeze drying clearly changes the

structure of the aerated hydrogels (ref. Figure 4.10), which would be expected. However, the LBG sample, which had lower porosity in the wet state appears to have retained same of the air cells created in the original aeration step. The more highly aerated samples of K100M and A4M lose such structure and cell walls of their dry structures therefore influence their mechanical properties.

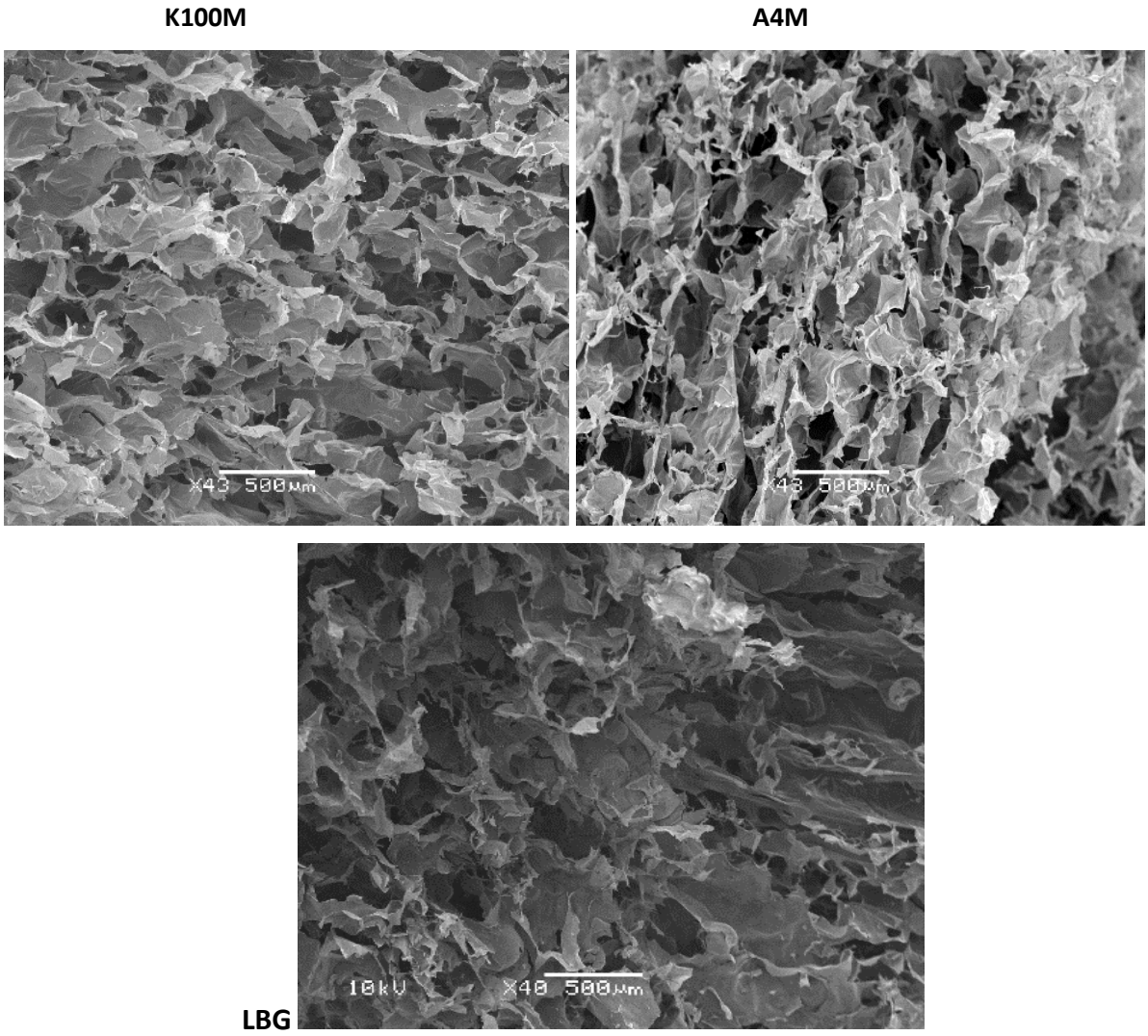

Figure 4.20. SEM images of freeze dried aerated aerogels with different polymers (K100M, A4M and LBG respectively). The scale bar indicates 500 µm.

The behaviour of freeze dried aerogels containing K100M, A4M and LBG was compared by immersing into same amount of cold water (100ml) at room temperature) for 24 hours. It was observed that K100M absorbed water slower than A4M and LBG. However, as shown in the Figure 4. 21, all the tested aerogels kept their dimensional structure even after 24 hours in water, with the LBG beginning to show disintegration.

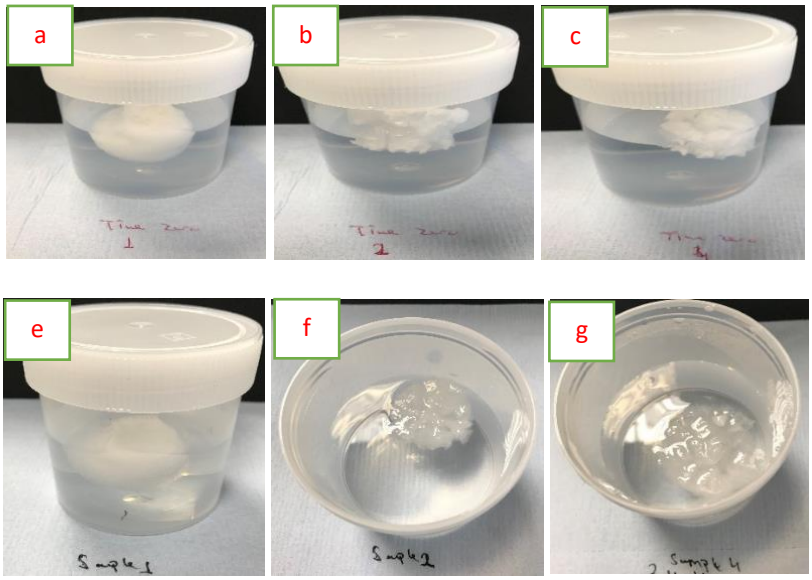

Figure 4.21. Comparison of the behaviour of freeze dried aerogel with different polymers in water at room temperature; K100M, A4M and LBG from left to right respectively. The first raw (a-c) showing initial behaviour of the tested samples in water at time zero, the second raw (e-g) showing structure of the samples after 24 hours in water.

The above results provide evidence that physical cross-linking persist after freeze drying, which has been already reported (Zhang et al., 2012). This work is providing an effective method to create stable aerated hydrogel with macroporous structure by combining a viscosifying polymer into a hydrogel network.

The partial disintegration of the LBG sample after soaking for 24 hours may indicate that the LBG decreases the effectiveness of the alginate gels to anneal after cessation of shearing (ref. Figures 4.8 and 4.13) and that its lower sol viscosity (Figure 4.11) allows it to hydrate more effectively from the dry aerogel state. Such observations may be important in an application of aerogels if they are designed to either retain an aerated structure, or disintegrate on subsequent hydration.

4.3. Effect of WPI on hydrogel characteristics and rheology: Results and Discussion

Having considered the effects of the viscosifying polymer in the complex formulation, it is also worth considering the role of the WPI, initially added to aid aeration.

4.3.1. Effect of WPI on hydrogel characteristics

Aerated hydrogels prepared with and without WPI were analysed using different analytical techniques. The mechanical properties (hardness) of wet gels were studied by texture analyser in compression mode. The microstructure of hydrogels was analysed by Cryo-SEM and by X-ray computed microtomography.

4.3.1.1. Overrun

WPI had a significant effect on overrun (Figure 4.22), as it was taken out of the formulation, all the tested polymers produced lower overruns. This effect was more pronounced for samples containing K4M and A4M. The aerated hydrogel samples containing K100M showed no significant difference with and without WPI, indicating that the higher viscosity overcomes the need for a surface- active protein.

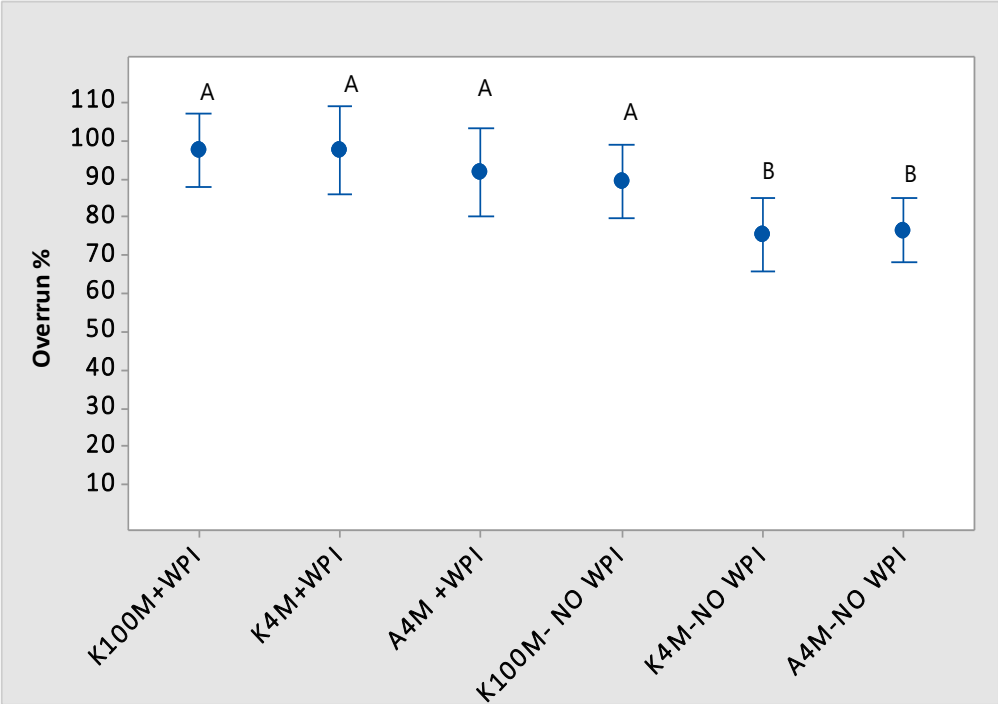

Figure 4.22. Showing overrun with and without WPI with different polymers. P- value 0.011. (At least one mean is significantly different). Error bar resresents the 95 % confidence interval for the mean.

Proteins are amphiphilic macromolecules and considered to be foaming agents due to their ability to unfold and adsorb at the interfaces between the dispersed and continuous phases, and lowering surface tension of dispersion and stabilising interfacial area (Carrera et al., 2005;

Davis and Foegeding, 2004). Nevertheless, foamability of proteins depends on various factor including temperature, pH, ionic strength, and presence and ratio of other biopolymers (Raikos et al., 2007, Dickinson 2003), viscosity and surface tension, because when the surface tension is lower, bubbles can be broken up during intense shearing or turbulent flow (Zúñiga and Aguilera, 2009, Davis and Foegeding, 2004).

Enhanced foaming properties by formation of protein and polysaccharide soluble complexes at pH higher than pI have been reported. Whey protein and polysaccharide soluble complex (e.g., WPC/pectin, WPI/guar gum, WPC/sodium alginate) at neutral pH have shown improved foaming stability due to polysaccharides, which has ability to form thicker and more viscoelastic interfacial film by increasing the viscosity of the aqueous phase and therefore limits the mobilization of aqueous phase around the bubbles by decreasing drainage (Mishra et al., 2001; Perez et al., 2009; Ercelebi and Ibanoglu, 2009), thereby retarding the break of the lamella between bubbles, and avoiding the merge of two or more bubbles into a one big bubble (coalescence) (Orrega et al., 2015).

Contrarily, polysaccharides can also have negative effect on foaming capacity of proteins due to their thickening effect. In order to generate foam, it is necessary to deliver enough energy to the system to incorporate air and create new interfaces (i.e. in the form of bubbles). If the viscosity is too high it can prevent inclusion of air and produces lower degrees of aeration. Orrego et al. (2015) reported that, there was a lower incorporation of air due to the higher resistance to flow (higher apparent viscosity) of dispersions for the same level of energy delivered from the overhead stirrer (same value of rpm). Because the large amount of energy

is used in the movement of the fluid and less energy is used for the creation of new interfaces (Orrega et al., 2015).

In addition, when viscosity is too high, it may also result in the reduced protein diffusion rate at short adsorption time which limits the foamability (Baeza et al., 2005). Because, in the foam formation process, protein has to diffuse to the interface so they form a film around the air bubbles. Higher diffusion rate and increased interfacial elasticity at short adsorption time could promote foam formation (Ercelebi and Ibanoglu 2009; Perez et al., 2009).

4.3.1.2. Air cell count, volume, total surface area of cells and porosity

Air cells count of aerated hydrogel samples made of A4M, with WPI and without WPI were compared. There was a significant difference in air cells count; aerated hydrogels samples with WPI had the highest number of air cells (Figure 4. 23). There was a correlation between overrun and air cells count (Figure 4.22 and 4.23). When the both figures are compared, it can be seen that aerated hydrogels containing WPI had higher overrun, which means there are more air cells.

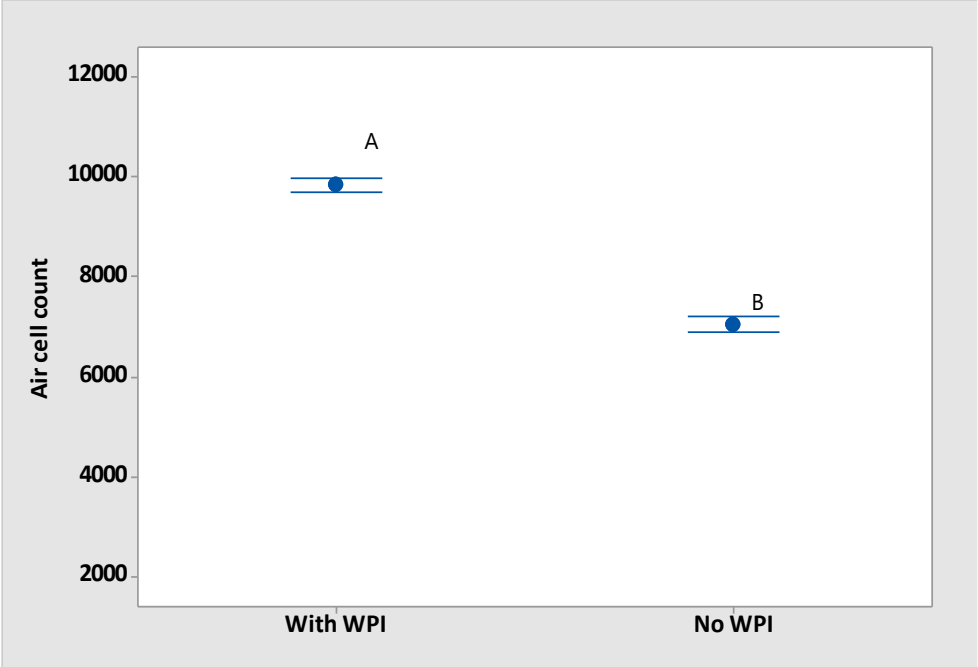

Figure 4.23. Effect of WPI on air cells count. There are more air cells in the presence of WPI. P < .001. Error bar resresents the 95 % confidence interval for the mean.

The effect of WPI on volume (mm^2) (Figure 4.24), total surface area (m^3) (Figure 4.25) of the aerated hydrogels were also analysed by X-ray computed microtomography.

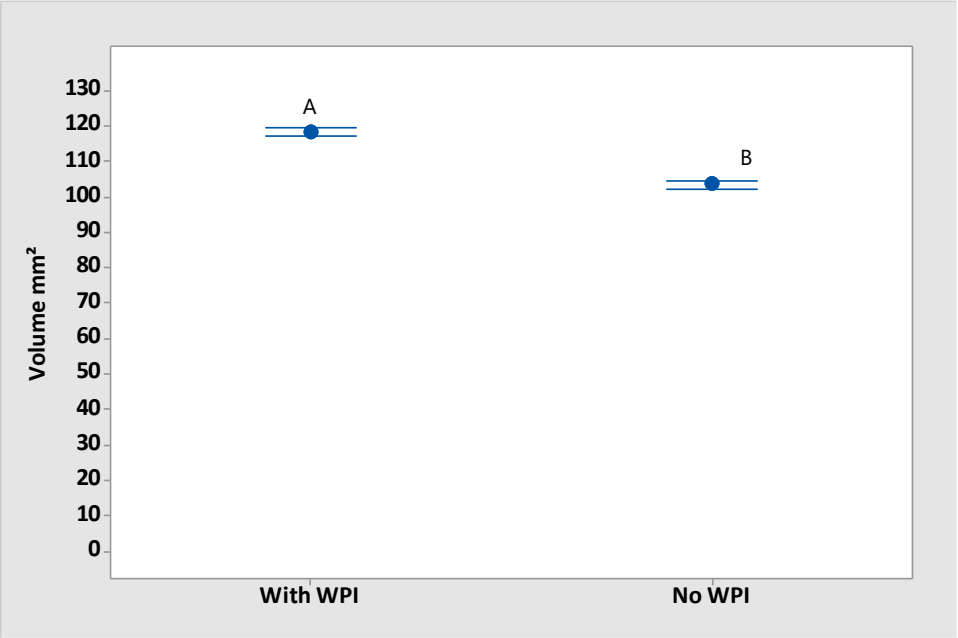

Figure 4. 24. Showing volume of aerated hydrogels with and without WPI, P < .001. Error bar resresents the 95 % confidence interval for the mean.

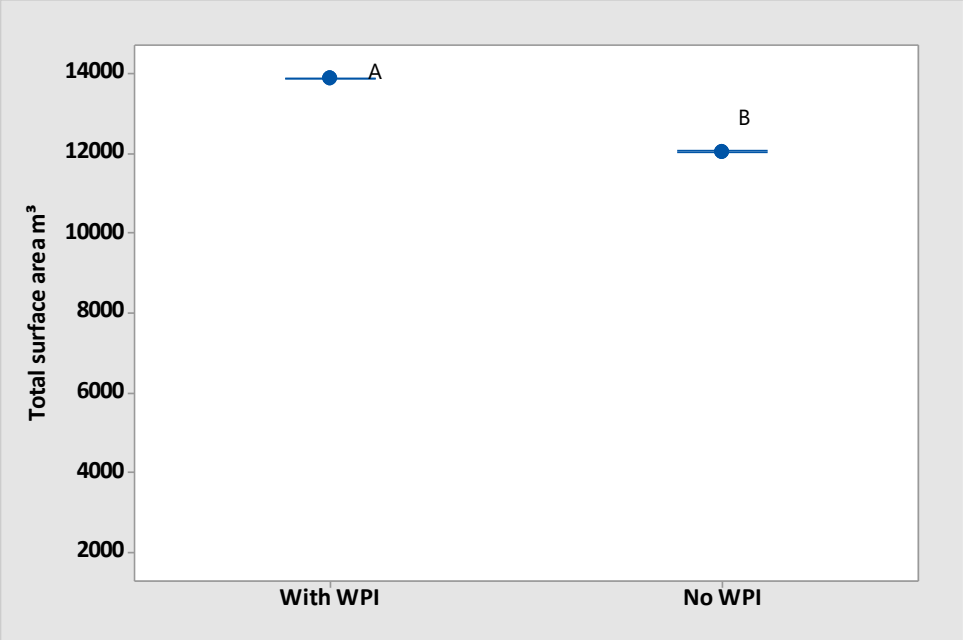

Figure 4. 25. Showing total surface area of aerated hydrogel with and without WPI. Error bar resresents the 95 % confidence interval for the mean.

The aerated hydrogel samples made of WPI had the highest volume (mm^2) and total surface area (m^3), which are in an agreement with overrun results (Figure 4.22) and air cells count (Figure 4.23).

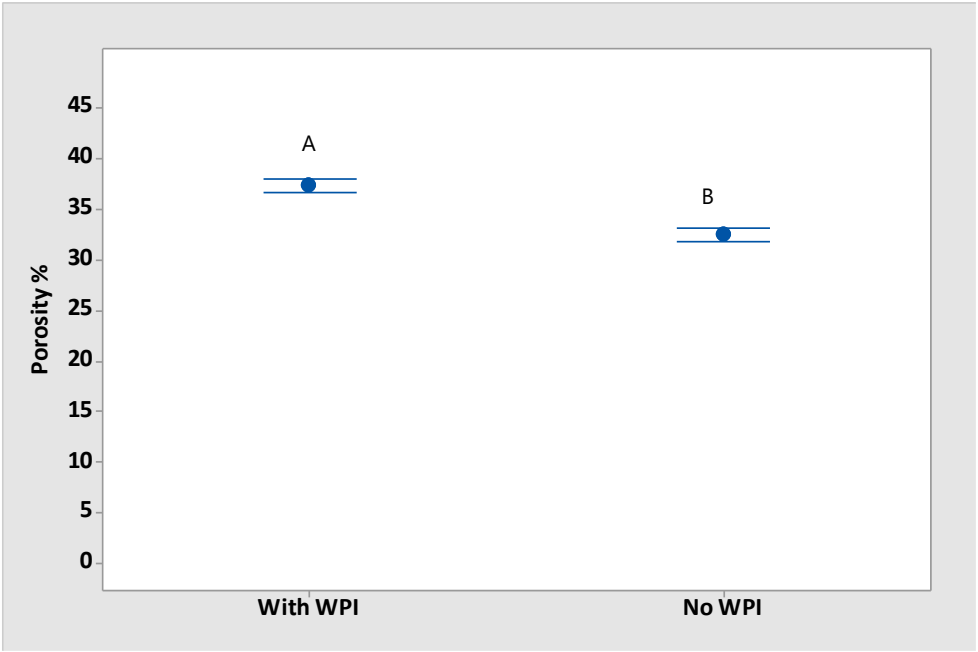

Figure 4. 26. Showing porosity of aerated hydrogels with and without WPI. More porous hydrogels were formed in the presence of WPI. Error bar resresents the 95 % confidence interval for the mean.

The porosity of aerated hydrogels prepared with WPI was higher than those without WPI ones. There was a significant difference between two aerated hydrogels (p- value 0.002).

4.3.1.3. Cell diameter

The effect of WPI on air cells diameter was measured by using ImageJ computer programme, on the basis of photos obtained from EVOS- inverted light microscopy (Figure 4.27).

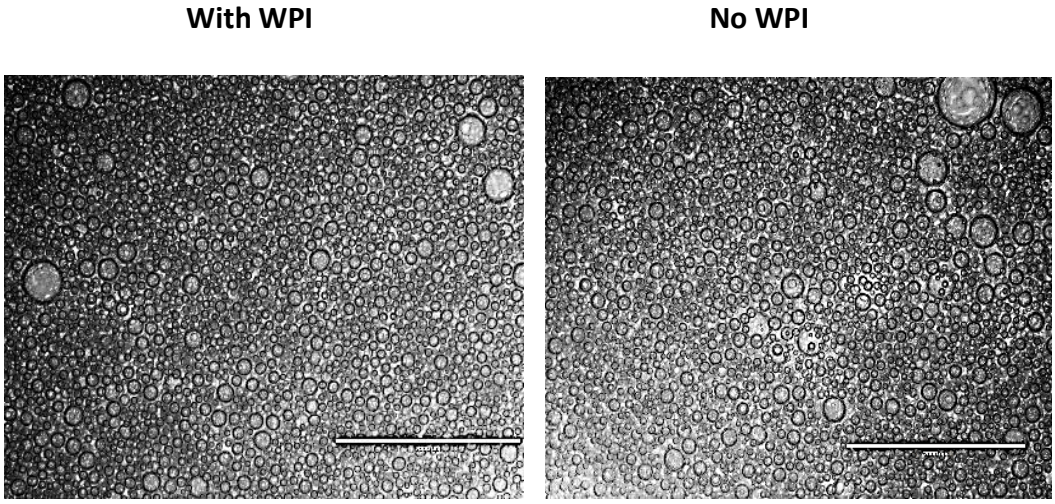

Figure 4.27. Light microscopy image of aerated hydrogel at time zero with and without WPI respectively. Scale bars represents 2000 µm.

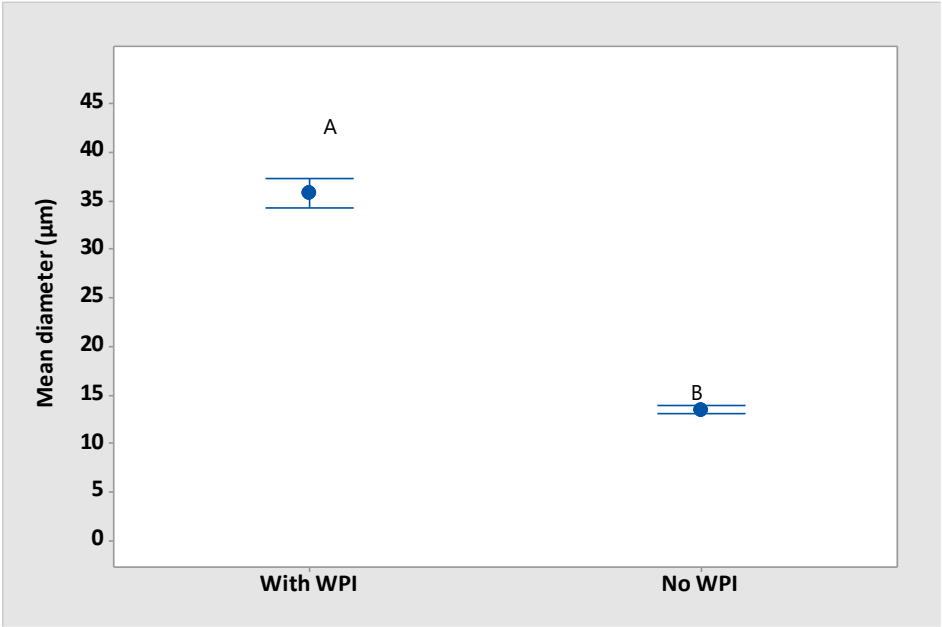

Figure 4.28. Showing air cells mean diameter of two aerated hydrogels with and without WPI respectively, P < .001. Means that do not share a letter are significantly different. Error bar resresents the 95 % confidence interval for the mean.

When 0. 15 % (w/w) WPI was taken out of the formulation, the air cells in the aerated hydrogels got smaller than those aerated hydrogels containing WPI. The mean diameter of air cells values were equal to 35 and 15 µm for WPI and No WPI, respectively (Figure 4.28).

The smaller air cells might be a reason for the lower porosity in this aerated hydrogel without WPI (Figure 4.26). In addition, the viscosity was lower with WPI (Figure 4.31), which would have some effect on the cell diameter, producing bigger air cells due to the coalesce of the air cells in a less viscous media. Thus, it could be implied that less porous aerated hydrogel with smaller air cells can be created with proper addition of WPI to alginate based aerated hydrogels.

4.3.1.4. Effect of WPI on aerated hydrogel texture

Aerated hydrogel hardness was affected significantly by the presence of WPI in the formulation. All the samples that do not contain WPI had the highest values of the maximum force (hardness) of compression. Samples containing K4M with WPI had the lowest hardness. These samples had comparable overruns to both K100M and A4M. Therefore, aeration level can not be attributed solely to the texture of aerated hydrogels. This then begins to suggest that K4M has a different effect on alginate fluid gel annealing to both K100M and A4M with $P< 0.001$. In turn this suggests that the more hydrophilic K4M impacts on alginate gelation, compared to the A4M, which is more hydrophobic, but has the same viscosity. This is perhaps similar to the effect of substituent type and distribution on binding with bile salts, shown by Torcello-Gómez and Foster (2014).

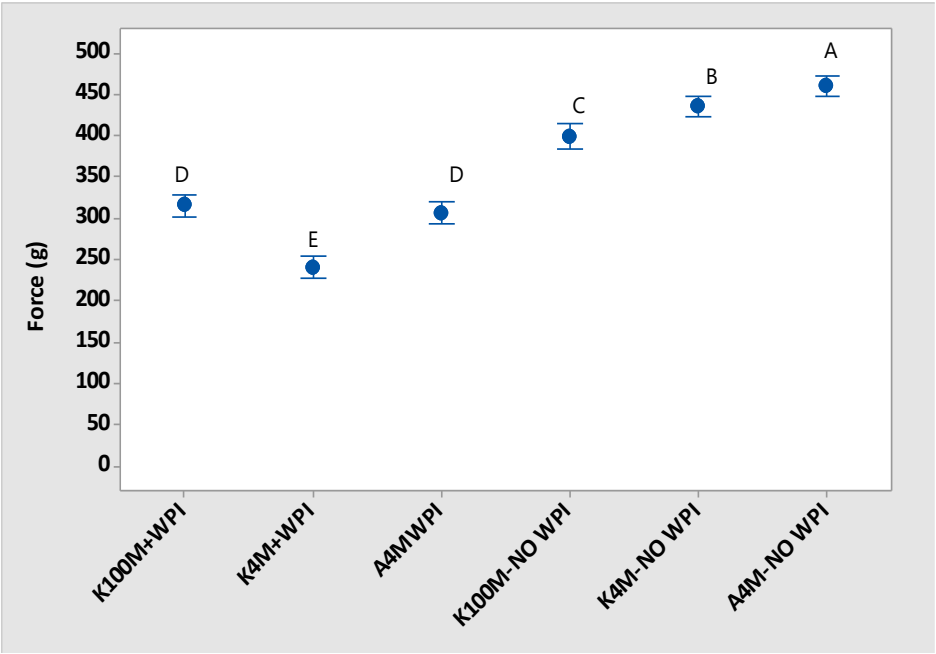

Figure 4.29. Effect of WPI on hydrogel texture (hardness). In the presence of WPI, hydrogels were less hard (softer) than with those of without WPI ones. Error bar resresents the 95 % confidence interval for the mean.

When WPI is removed the overrun for samples containing K4M and A4M is significantly lowered (refer to Figure 4.22), which now corresponds with much harder aerated hydrogels (Figure 4.8), with the more hydrophobic A4M having greatest hardness. Thus, again may imply that the more hydrophilic K4M is impacting an alginate's ability to form coherent gels. The greater viscosity of the similarly hydrophilic K100M then may compensate for such effects on alginate gelation.

All the tested aerated hydrogels containing WPI, regardless of used cellulose type, were softer than without WPI, which is in an agreement with the literature (Ciesäla et al., 2006; Chen et al., 2013). Therefore, WPI may also affect the efficiency of alginate to form a coherent gel upon cessation of shearing. In contradiction to this Leon et al. (2016) claimed that adding

protein to alginate solutions generated gels that are stronger than pure alginate gels (Leon et al., 2016).

Here softer aerated hydrogels were obtained in the presence of WPI, which might be related to some other mechanical properties of gels, depending on the balance between the kinetics of phase separation (e.g., dependent on viscosity) and gelation (e.g., competition for Ca^{2+} because of the high charge density of WPI. However, alginate binds more strongly to cations than proteins and alginate can form gel in competition with whey proteins, but the low concentrations of all polymers used in this study will affect these dynamics and compatibility of the biopolymers (Mession et al., 2013).

4.3.1.5. Effect of WPI on hydrogel microstructure

Further analysis of the effect of WPI on aerated hydrogels containing K100M, was undertaken by means of Cryo-SEM, and X-ray computed microtomography. The morphology of the aerated hydrogel made with WPI was noticeably different from that produced without WPI. In the presence of WPI air cells were larger and appeared heterogeneous in size compared to hydrogels with WPI absent (Figure 4. 30).

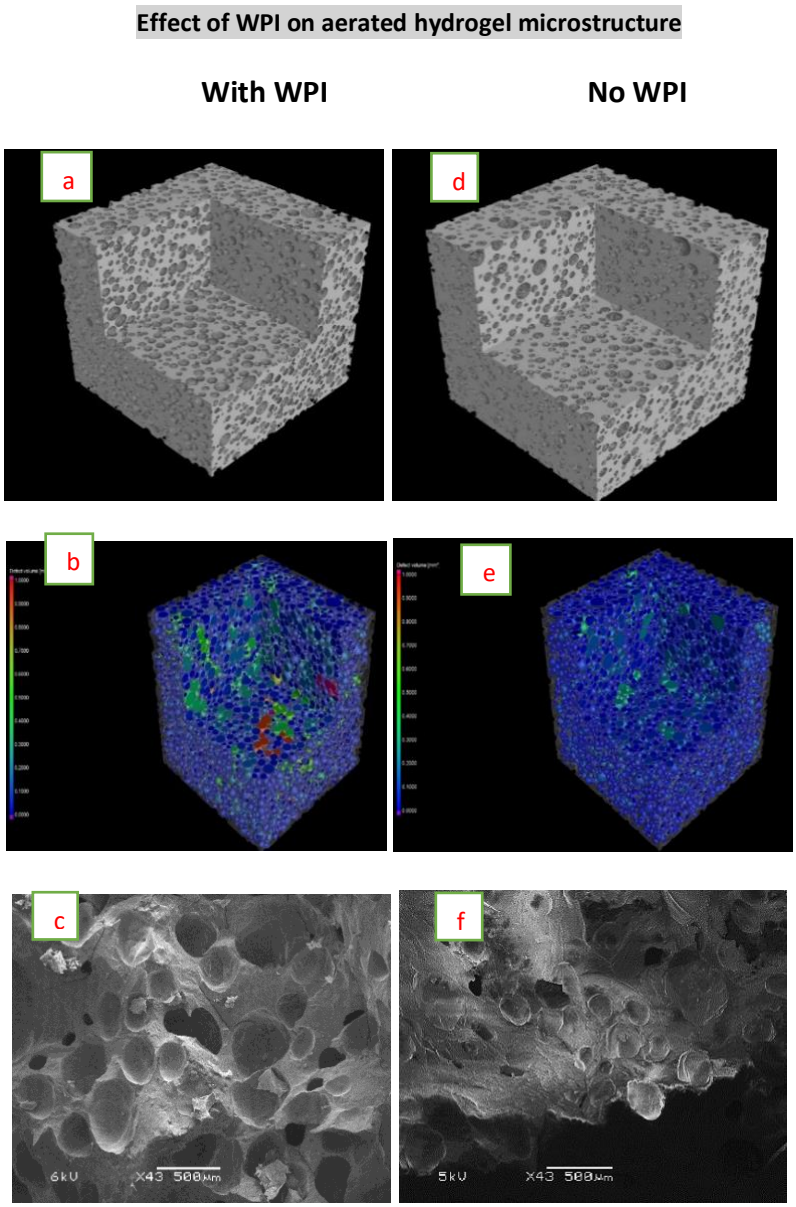

Figure 4.30. X-ray computed microtomography images show aerated hydrgel with WPI (a-b) and without WPI (d-e) and Cryo-SEM images for WPI hydrogel (c) and no WPI one (f).

Microstructure images of hydrogel samples revealed that the addition of WPI affected the gel microstructures. The ultimate gel architecture seemed to be depends on WPI. Protein/polysaccharide mixtures produced larger air cells, which is in an agreement with literature. It has been reported that interaction of alginate and whey proteins had a significant effect on microstructure of formed gels and pore sizes; bigger pores formed in the presence of alginate (Le et al., 2017).

4.3.1.6. Effect of WPI on hydrogel rheology

Effect of WPI on the rheological properties of aerated hydrogel made of alginate, K100M, $CaCO_3$ and GDL mixture was studied under and after high shearing conditions. Initially shear dependent viscosity of the solutions were measured using rotational rheology (ỳ: 837 1/s), which was followed by dynamic oscillation for time and temperature sweep measurements. The findings on the rheological properties of the WPI containing hydrogels are summarized in Figure 4.30 and 4. 31.

4.3.1.6.1. Shear viscosity

The shear viscosity of the polymer solutions with and without WPI showed two distinct behaviours. As mentioned earlier in section 4.2.1.6.1 (Effect of polymers, K100M, K4M A4M and LBG on hydrogel rheology) shear viscosity decreased during first 5 minutes of shearing and increased afterwards parallel to temperature rise. However, here it must be noted that the shear viscosity with WPI was much lower than without WPI ones. In other words, the presence of WPI caused a slight decrease in viscosity.

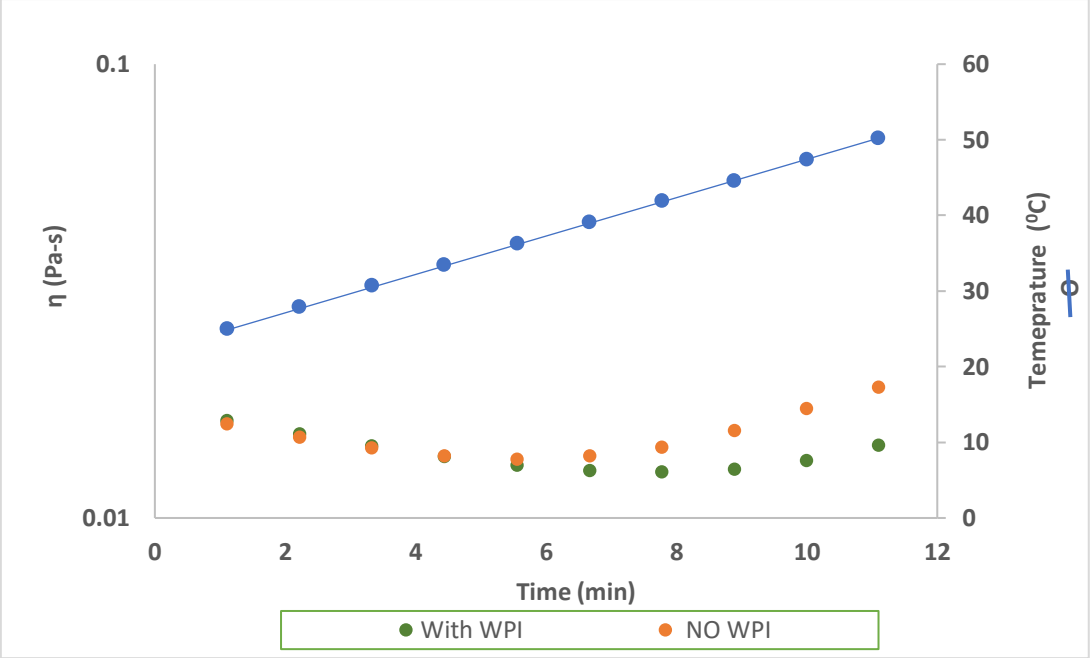

Figure 4.31. Effect of WPI on shear viscosity of alginate and K100M solution with $CaCO_3$ + GDL during shearing for 10 minutes. P value- 0.067. No significant difference between tested samples.

In the absence of WPI slightly higher viscosity was observed. However, WPI addition decreased viscosity, which might be due to the competition of WPI with alginate for Ca^{2+}. Consequently, in the presence of WPI alginate forms less junction zones, which resulted in less viscosa media.

4.3.1.6.2 Time and temperature sweep

The G' and G" of the samples are depicted at time = 10mintues, after shearing was stopped. The both dispersion (with and without WPI) had a larger G' than G". The G' and G" of the samples (with and without WPI) increased upon stopping shearing at 50 ^{0}C. When it was cooled from 50 ^{0}C to below 40 ^{0}C, the G' and G" of the both gels showed a significant further increase. However, upon prolonged cooling the G' and G" almost reached a plateau.

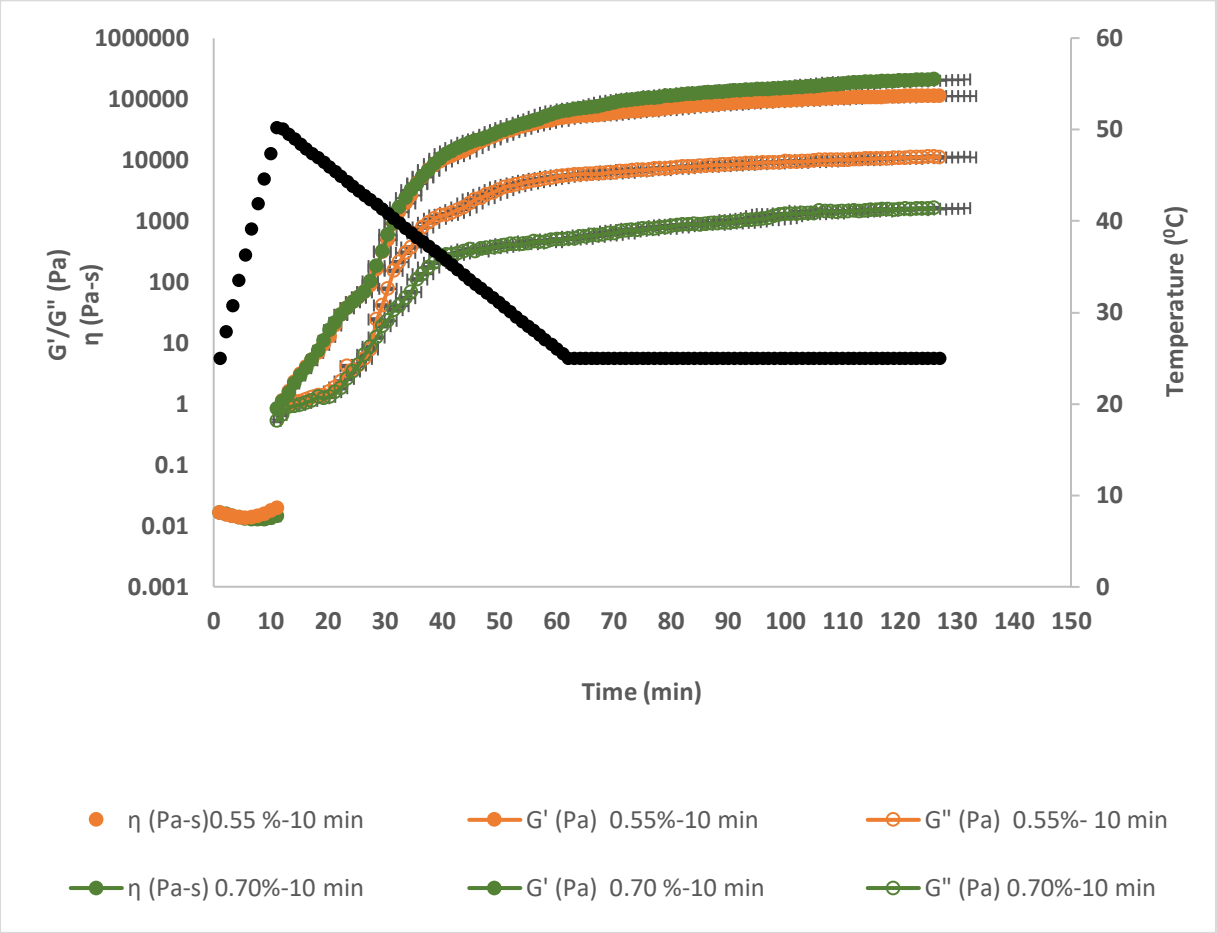

Figure 4.32. Effect of WPI on gel rheology. In the presence of WPI higher elastic modulus (G') was recorded compared to hydrogel that does not contain WPI.

Figure 4.33. Aerated hydrogels with and without WPI from left to right, respectively.

4.3.1.6.3. Discussion

The above findings (Section 4.3.1.6.2) display that addition of 0.15 % (w/w) WPI improved the rheological properties of the alginate based aerated hydrogels. The G' increased significantly while G" decreased. Strengthening of alginate microgels by the addition of whey protein has been already reported (Wichchukit et al., 2013; Mession et al., 2013).

Wichchukit et al. (2013) reported the reinforcements of alginate gel particles due to the more solid-like behavior of the formed WPI network that strengthens a weak and viscoelastic alginate gel structure (Wichchukit et al., 2013). Mession et al. (2013) has stated that a mixed gel of pea protein and calcium alginate induced by glucono- δ -lactone and calcium carbonate had a higher storage modulus than corresponding alginate gel (Mession et al. 2013).

In the protein/polysaccharide/calcium systems the components could interact in more than one way. Both the protein and the polysaccharide could interact on their own; with calcium ions; or with each other; with or without calcium involvement. Small gel strength might be connected both to the incompatibility between proteins toward polysaccharide in the presence of calcium and to the diminished capability of the examined proteins to join calcium (Ciesäla, 2006; Bernal et al., 1987).

However, in this study, the competition between gelation and phase separation might have been affected by the rate of gelation of the both polysaccharides. Therefore, increased gel strength in the presence of WPI might be attributed to lack of extensive protein- protein interaction during protein aggregation at temperatures in the 25-50 ^{0}C range which would

not prevent protein-polysaccharide associations and WPI acted as a filler polymer to strength the weak alginate gel.

However, it must be noted that there is a disagreement between rheology and texture analysis results. According to compression tests the aerated hydrogel in the absence of WPI is harder than with WPI ones. Opposing to the compression test results, according to time and temperature sweep measurements G' is higher in the presence of WPI, which means the gel is harder with WPI. This inconsistency can be explained by differences between aeration and shearing through rotational rheometer, effect of bubbles (air cells) on texture, because with WPI more air cells were included through aeration, which is not possible with rotational rheology.

On the contrary, according to literature alginate forms softer gel with proteins and easily forms a separate gel network surrounding the protein network due to being less compatible towards protein. Ciesäla (2006) stated that, it is quite possible that phase separation between WPI aggregates and alginate molecules occurred prior and during cold gelation. Therefore, two separate phases originate while an intermediate phase containing both components may arise on the border (Ciesäla, 2006).

Although it was not possible to establish a clear molecular organization of the mixed gel systems studied, it provided some insight into the forces responsible for their formation and their stability.

4.3.2 Effect of WPI on aerogel characteristics: Results and Discussion

Section 4.2.2 showed how some characteristics of wet aerated hydrogels could be translated to aerogel properties. Freeze dried aerogels were prepared with and without WPI were analysed using different analytical techniques. The mechanical properties (hardness) of freeze dried aerogels were studied by texture analyser in compression mode. The microstructure of the aerogel was studied by SEM.

4.3.2.1. Effect of WPI aerogel texture

The Figure 4.34 shows that in the presence of WPI all the tested aerogel samples displayed highest values of the maximum force (hardness) with no significant difference between the different polymers used.

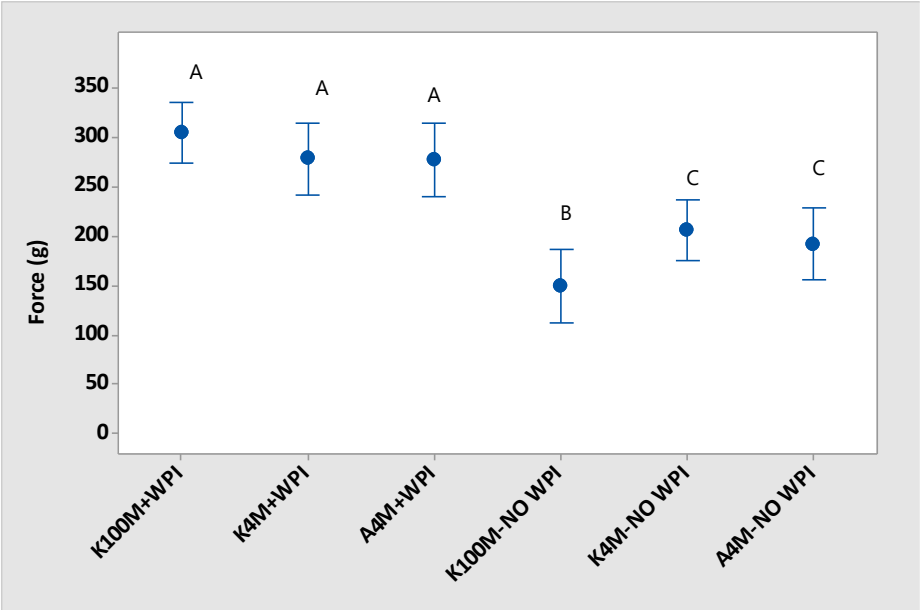

Figure 4.34. Effect of WPI on freeze dried aerogel hardness. P <0. 001. Means that do not share a letter are significantly different. Error bar resresents the 95 % confidence interval for the mean.

When comparing this data with Figure 4.29, it can be seen that this is counter to the observation of the textural properties of aerated hydrogels with and without WPI.

It has been reported that, in the absence of WPI, calcium-induced alginate gels were stiff polymeric networks with considerable flexibility. However, alginate co-gelation with whey proteins increased the flexibility of gel network, causing the gel to sustain more deformation before fractures (Roshanghias and Madadlou, 2018). In another similar research, mixing whey protein with alginate produced bio-based aerogels with higher mechanical properties than those produced with whey alone, which were brittle and collapse when compressed (Chen et al., 2013).

4.3.2.2. Effect of WPI on aerogel microstructure

The microstructure of aerogels was also determined by means of scanning electron microscope (SEM). In terms of macro morphology, the differences between two freeze-dried aerogels with and without WPI, were noticeable. The aerogels samples containing WPI have a more regular shape in comparison to the absence of WPI ones (Figure 4.35).

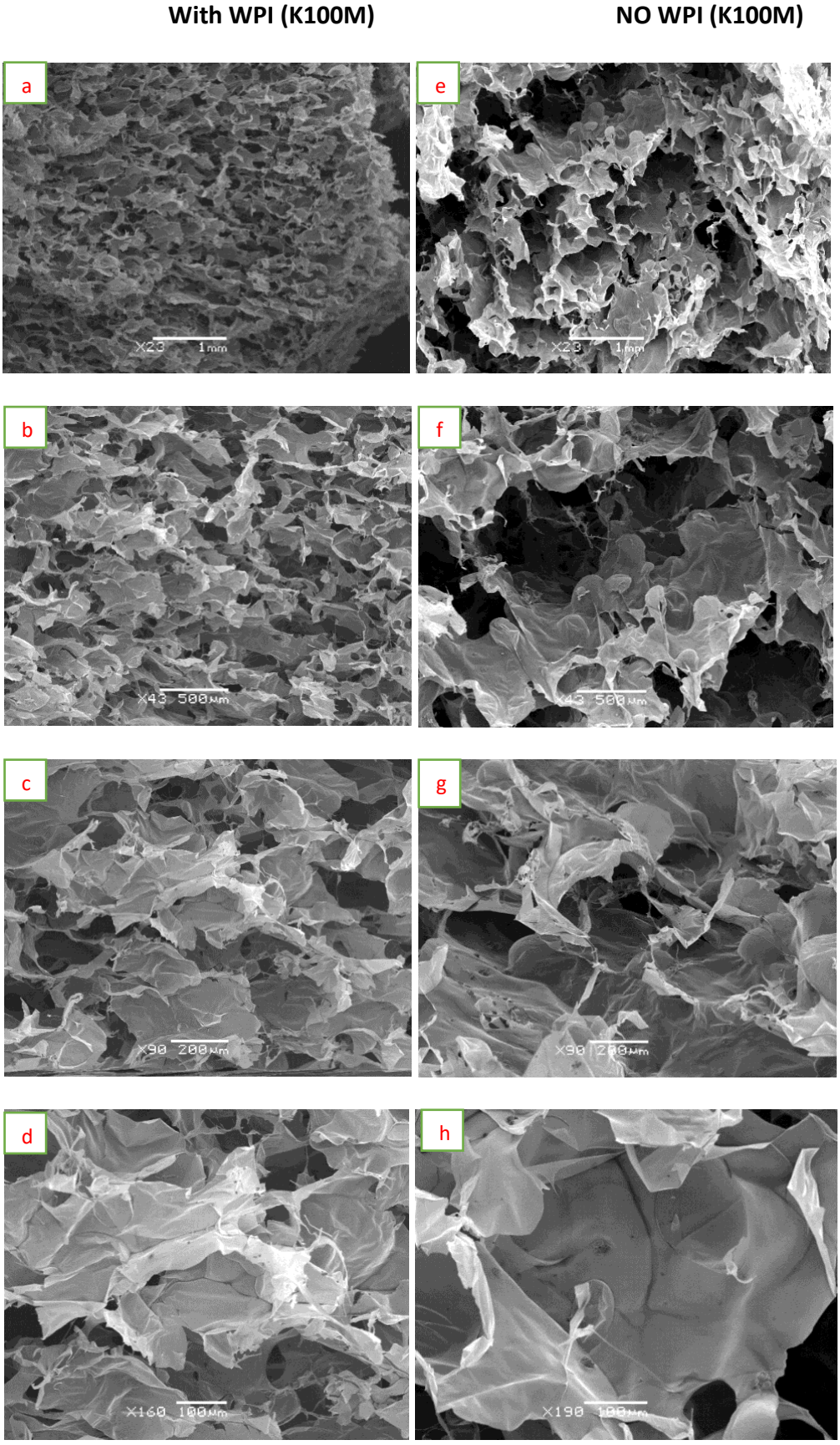

Figure 4.35. The microstructure of freeze dried aerogels with (a-d) and without WPI (e-h), respectively.

The results of SEM images show that addition of WPI leads to more robust structure with less damaged pores, which is also in correlation with texture analysis results (Figure 4.34). However, during freeze drying ice crystal growth be would expected to partly destroy the network structure, and form a micro-scale layered structure due to the increase in volume of water upon crystallation (Betz et al., 2012). The components of the aerogel complex were indistinguishable in the all micrographs. In the absence of the WPI less well- defined layered structure possessing a large number of holes were observed.

4.4. Effect of physical parameters on hydrogel characteristics: Results and Discussion

The effect of physical parameters including mixing speed (rotation speed) and aeration time, on hydrogel characteristics were studied by means of overrun measurement, texture analysis, CRYO-SEM, and X-ray computed microtomography.

A one -way ANOVA showed that all the tested physical parameters had a significant effect on formation of aerated hydrogel and on its characteristics including overrun, texture, air cells morphology, porosity and microstructure.

4.4.1. Mixing Speed

In terms physical parameters, mixing speed was an important parameter needed to be optimised for obtaining desired hydrogels and aerogels. The formulation changes have been discussed in previous sections, but the interplay between formulation and processing parameters need to be understood to ensure the maximum enhancement of air into the

hydrogel solution, during the gelation steps outlined earlier. In these experiments, the mixing time was 10 minutes, in line with the gel analyses carried out in the earlier sections.

4.4.1.1. Effect of aeration speed (shearing) on overrun

Mixing speed was found to be a key parameter in the formation of aerated hydrogels. The aerated media was very unstable when mixing speed was below 6000 rpm. This manifested itself as a phase separation soon mixing was completed with film drainage and air cell collapse. However, when mixing speed was increased to 8000 rpm, a stable self-supporting homogenous hydrogel was produced (Figure 4.36).

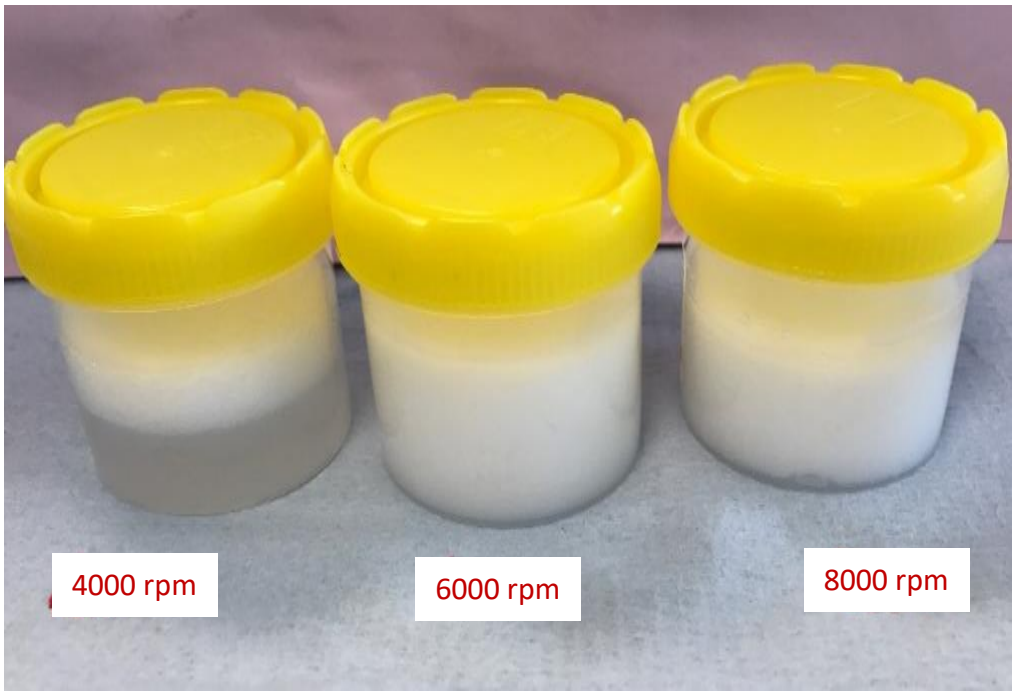

Figure 4.36. Showing effect of mixing speed on hydrogels. Mixing speed below 6000 rpm produced inhomogeneous hydrogel.

Additionally, mixing speed had a significant effect on overrun (P- value <0.001) seen in Figure 4. 37.

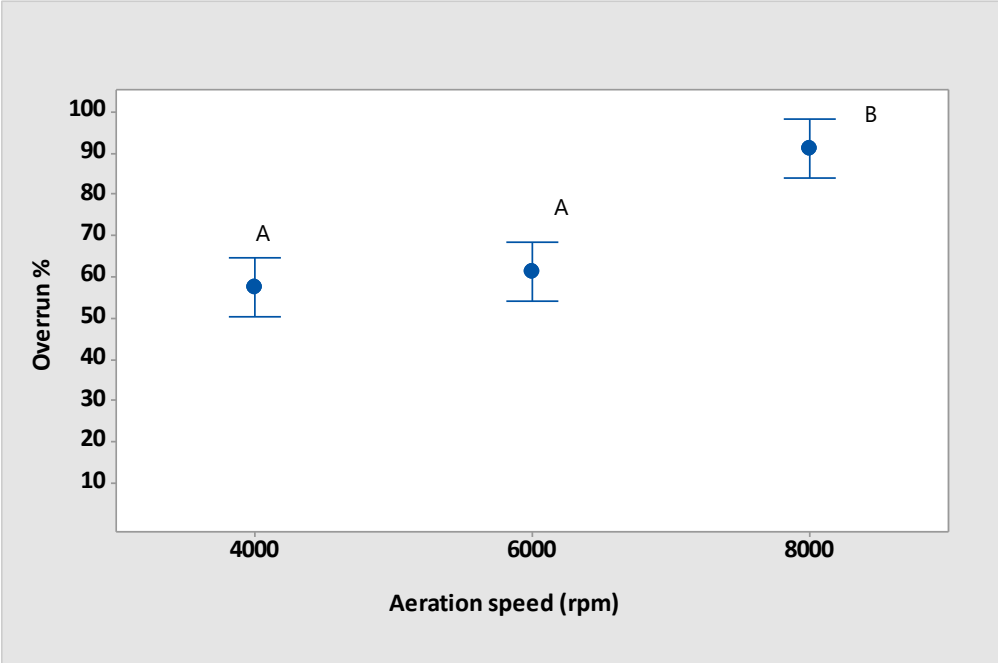

Figure. 4.37. A one -way ANOVA shows the significant effect of aeration speed on overrun (P value<-0.001). Data are the mean and standard deviation of triplicate measurements. Different letters indicate significant difference at the $p < 0.05$ level among all overrun at different aeration speed. Error bar resresents the 95 % confidence interval for the mean.

Although in this study the effect of mixing speed on gel structure was not tested, in the literature it has been reported that the structure of gels mixed at lower speed (20 rpm) showed the presence of large aggregates/particles and a very unhomogeneous distribution while the structure of fluid gels mixed at higher speeds exhibited smaller aggregates/particles and a more homogeneous structure. It was also suggested that higher shear rates can promote protein–protein interactions, resulting in stronger gels of higher G' values, structure is formed (Solar and Gunasekaran, 2010).

Ellis et al. (2017) have shown that fluid gel particles are good at plugging and preventing film drainage in foams, and therefore if the work here is indicative of partial creation and then annealing of fluid gel particles, further analysis is required to probe this effect.

Here it must be noted that aeration mixing speed and aeration time had significant effect on temperature increase in the aerated media, even though it was kept in the cold water bath. As shown below (Table 4.1), the higher the aeration time and mixing speed, the higher the temperature. The solution media temperature increased due to the heat produced by mechanical friction in the mixing head of the Silverson.

Aeration speed (rpm)	**Temperature (^{0}C)**	**OR (%)**
4000	36	57
6000	46	62
8000	50	95
Aeration time: 10 minutes		

Duration (minutes)	**Temperature (^{0}C)**	**OR (%)**
4	40	71
6	43	71
8	44	93
10	50	95
12	52	100
14	54	118
20	57	96
Mixing speed:8000 rpm		

Table 4.1. The effect of mixing speed and aeration time on temperature rise and hydrogel overrun.

There was a linear relationship between aeration speed and overrun, which is in correlation with literature (Table 4.1 first column and Figure 4.37). The effect of aeration conditions (rotation speed and aeration duration) on physical (overrun, rheological properties, bubble size) and sensory properties of aerated cake batter and biscuits has been reported by Edoura-Gaena et al. (2007). They claimed that rotation speed, duration and their interaction had significant effects on overrun. Both rotation speed and duration had significant effects on the temperature of the batter: the higher the rotation speed and duration, the higher the temperature.

Guo et al. (2013) reported that size and stability of the foam were related to the homogenizing speed. They claimed that small bubbles appeared in the bulk phase when more vigorous whipping was carried out. They also suggested that the whipping procedure might not affect the total amount of the cross-linking reactions but the porous structure. Hydrogels homogenized at 4000 and 12,000 r/min had a similar cumulative pore size distribution. Compared to the hydrogel operated at 8000 r/min, fewer pores were created in those two gels and the porosity of those two gels also decreased (Guo et al., 2013).

However, according to Laakkonen et al. (2005) the effect of stirring speed is actually complicated, where smaller bubbles are formed in the central region of the agitated vessels than close to the wall if stirring is too low. However, when stirring speed is too high small bubbles are formed above the impeller not in the centre of the vessel. When stirring speed is increased dispersion becomes more homogeneous below the impeller, and bubble size decreases with the increasing stirring speed in the impeller discharge flow.

Massey et al. (2001) showed that whisk speed has little effect on the final values of mean bubble size. Speed generall enhances the rate of bubble break up as well as bubble coalescence that is, increasing speed lowers the time required to achieve the minimum and the final mean bubble size (Massey et al., 2001).

Hanselmann and Windhab (1999) noted that mixing speed cannot be taken as a reference in bubble generation. Ross et al. (2006) reported that the effect of mixing on bubble size is dependent on the rheology of the system. They claimed that there was a greater difference in induced air bubble fraction between the slow and fast mixing treatments for the 1% agar gel than the 3% agar gel. That seemed to be a logical result as the larger viscosity of the agar pastes for the high concentration systems may avoid the formation of a larger number and large size air bubbles. They concluded that mixing speed seemed to have more of an effect on the bubble size at lower concentrations.

Therefore, the complexity of the mixed formulation in this study has shown that the rheology of the system is dynamic and dependent upon how the polymers interact with one another, and how the kinetics of phase change can impact on the structures being created while aeration in underway. Table 4.1 shows another complication is that temperature increase must be also considered. To this end, this is why a temperature up to 50 ^{0}C was included in the rheological observations described earlier.

4.4.2. Aeration Time

4.4.2.1. Effect of aeration times on hydrogel characteristics

In order to set up a most applicable aeration time, the effect of various aeration time (from 4 min to 20 minutes) on the characteristics of the aerated hydrogel containing K100M was studied.

4.4.2.1.1. Effect of aeration time on overrun and other hydrogel characteristics

Aeration time time had a significant effect on overrun ($P < .001$). An extension of aeration time from 6 to 8 minutes increased overrun significantly. Overrun peaked at an aeration time of 14 minutes and then decreased when extended to 20 minutes (Figure 4.38). As seen in Figure 4.38, phase separation was evident up to an aeration time of 10 minutes. The mixing times correspond to the minima seen in mix viscosity (Figure 4.11), and therefore it might be considered that little gel structuring has occurred at these times and therfore the matrix is not optimal for air entrainment, bubble break up and preventation of rapid film drainage.

Upon increasing aeration time it can be postulated that the increase in gel formation during shearing can produce the correct balance between fluid gel particles and particle annealing (post shear). Whereas if aeration time is extended the annealing of particles is decreased which leads to a decrease in overrun of the aerated hydrogel.

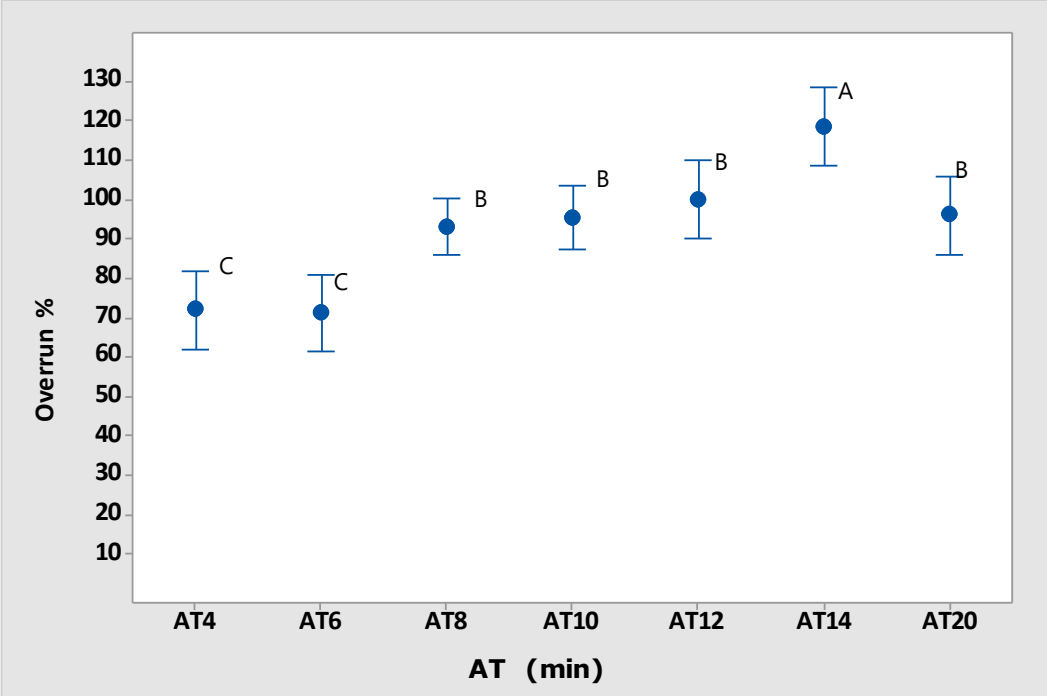

Figure 4.38. Showing the effect of aeration time (minutes) on overrun at a mixing speed of 8000 rpm. Means that do not share a letter are significantly different. AT: Aeration time. Error bar resresents the 95 % confidence interval for the mean.

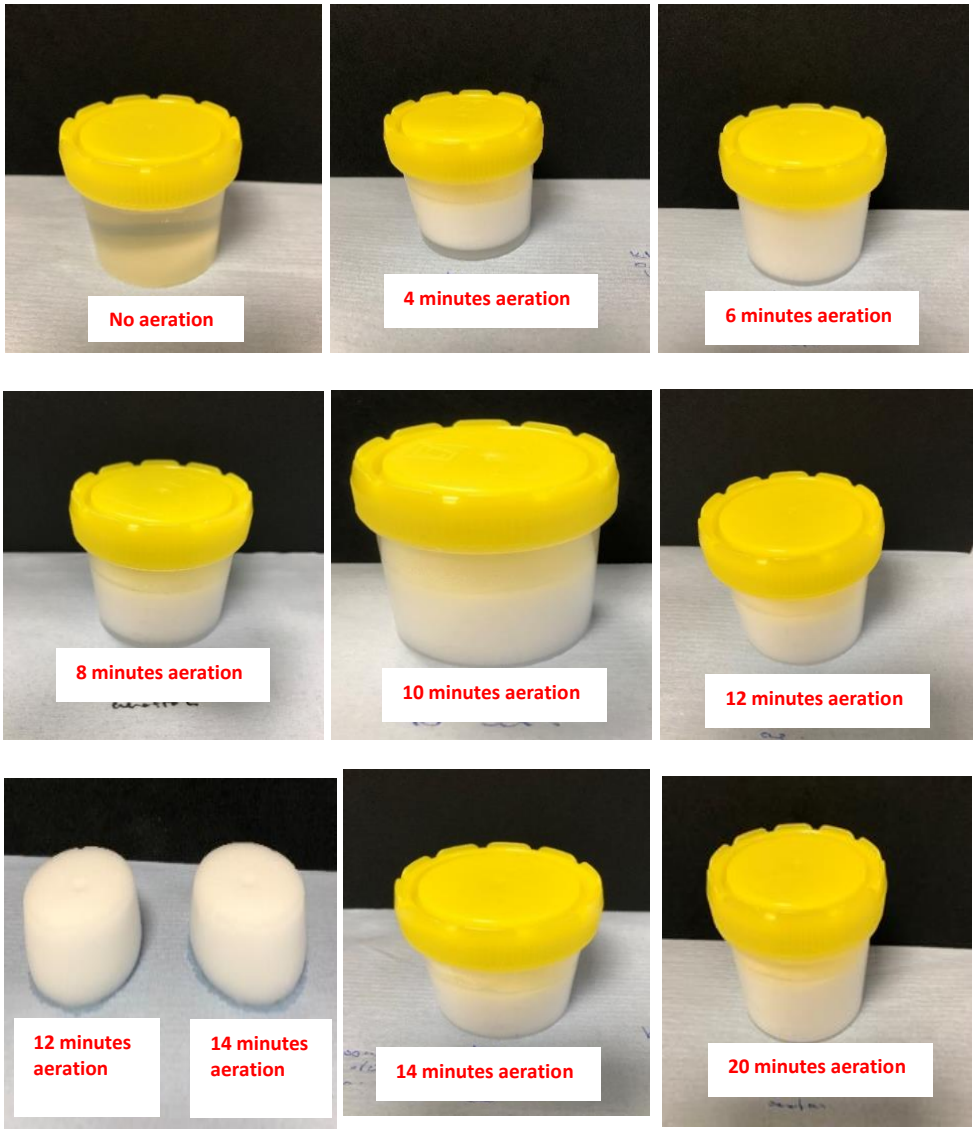

Figure 4.39. Showing sequential aeration time- Zero- time aeration to 20 minutes aeration.

The effect of aeration times on air cells count, volume (mm^2) and total surface area (m^3) were also analysed by X-ray computed microtomography (µCT).

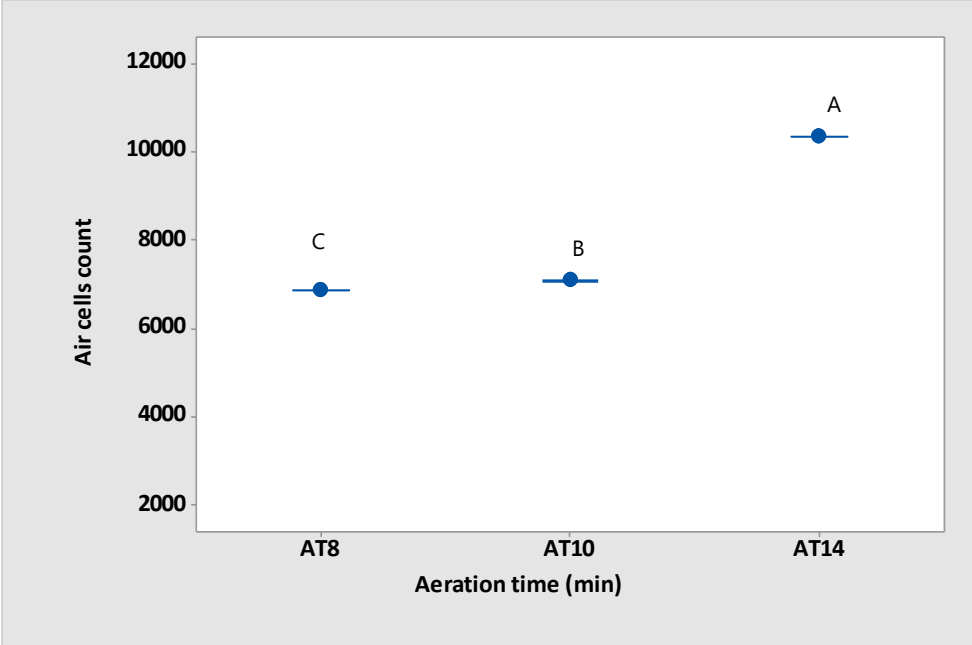

Figure 4. 40. Effect of aeration on air cells count. Aeration time had a significant effect on hydrogel air cells count; the longest the aeration time, higher the air cells count, P < .001. Error bar resresents the 95 % confidence interval for the mean.

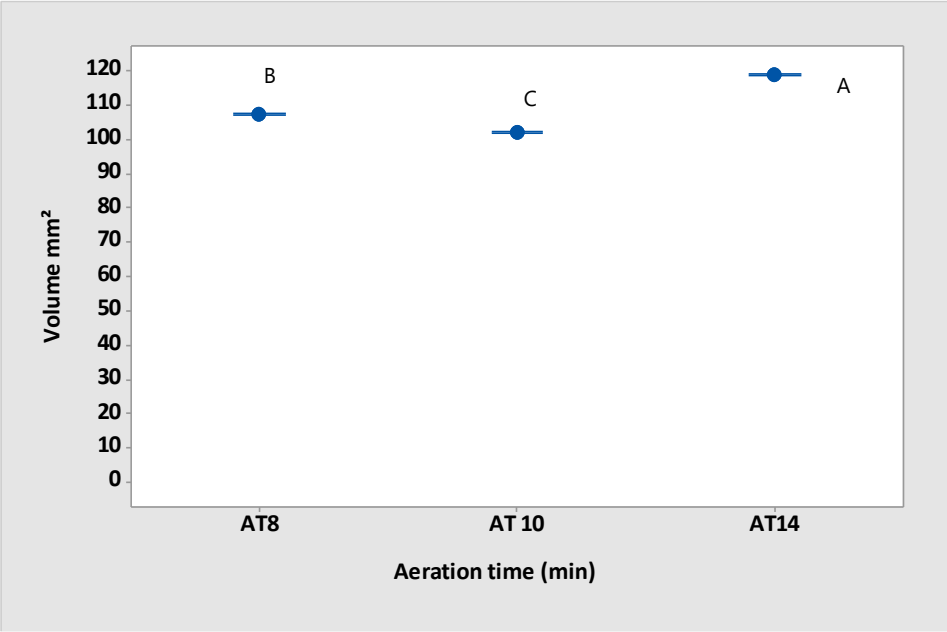

Figure 4.41. Effect of aeration on air hydrogel volume. Significant effect of aeration time on volume was recorded, so the longest the aeration time, higher the air cells count therefore higher the volume, P < .001. Error bar resresents the 95 % confidence interval for the mean.

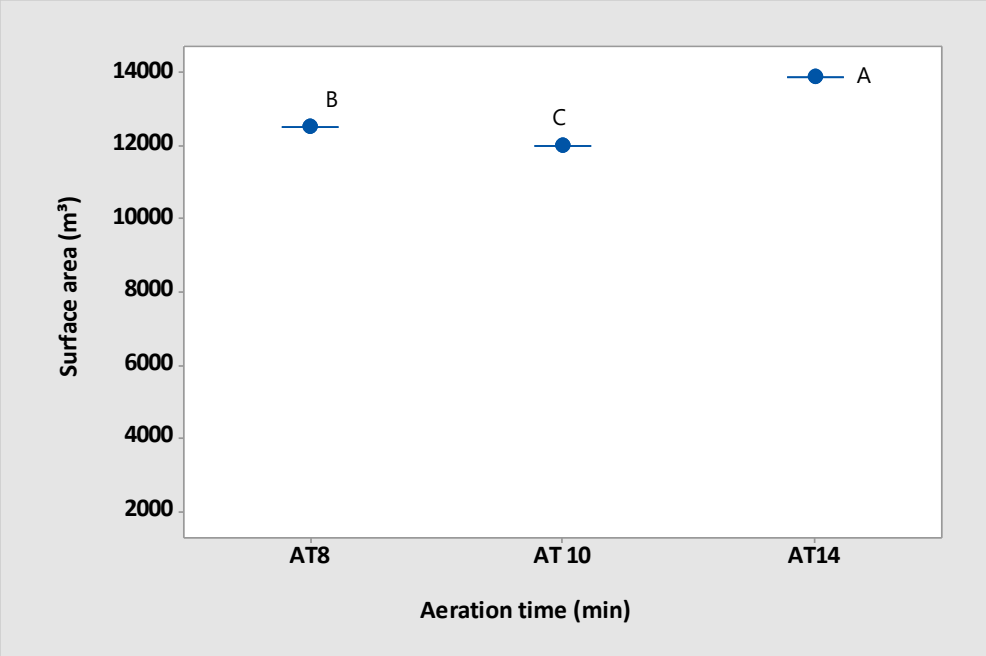

Figure 4.42. Effect of aeration time on air hydrogel surface area. Significant effect of aeration time on surface area was recorded, so the longest the aeration time, higher the air cells count therefore higher the volume and surface area, P< .001. Error bar resresents the 95 % confidence interval for the mean.

A one way-way ANOVA showed that the observations seen for overrun were confirmed in that AT14>AT10 and AT8 for air cells count (Figure 4. 40), volume (mm^2) (Figure 4.41) and total surface area (m^3) (Figure 4. 42).

Peng et al. (2018) showed that there is positive correlation between whipping time and overrun of whipped cream. The overrun increased with the increase of whipping time, from 0 to 24 min, and such increasing trend became insignificant after 16 min whipping time. With extended whipping time, larger quantity of air may be incorporated into the cream being whipped, which can result in higher overrun (Peng et al., 2018).

According to Massey et al. (2001) the reason for increased OR is due to the lower rate of bubble distrainment compared to rate of bubble entrainment. If bubble distrainment exceeds the bubble entrainment with time OR decreases. They claimed that there are two mechanisms of bubble generation in a batter. The primary mechanism is consist of the incorporation of such bubbles from the gas source or from the head- space due to the rotation of the whisk. In the secondary mechanism, the entrapped larger bubbles are broken down and smaller ones are formed. They described the primary mechanism as theoretical independent of time for a given set of operating conditions, and therefore a zero order process. On the other hand, secondary mechanism which involves the rate of bubble formation, is time dependent (Massey et al., 2001).

A decrease in overrun upon prolonged aeration time called 'overbeating', which is conventionally explained as excessive coagulation of ovalbumin at the air–water interface, with protein becoming aggregated into insoluble particles that have little water-holding capacity, thereby leading to foam collapse. At higher degrees of whipping, there is more liquid film thinning, more mechanical deformation, and also more bubble-wall rupture, all of which contribute to a decline in overrun (Lau and Dickinson, 2005).

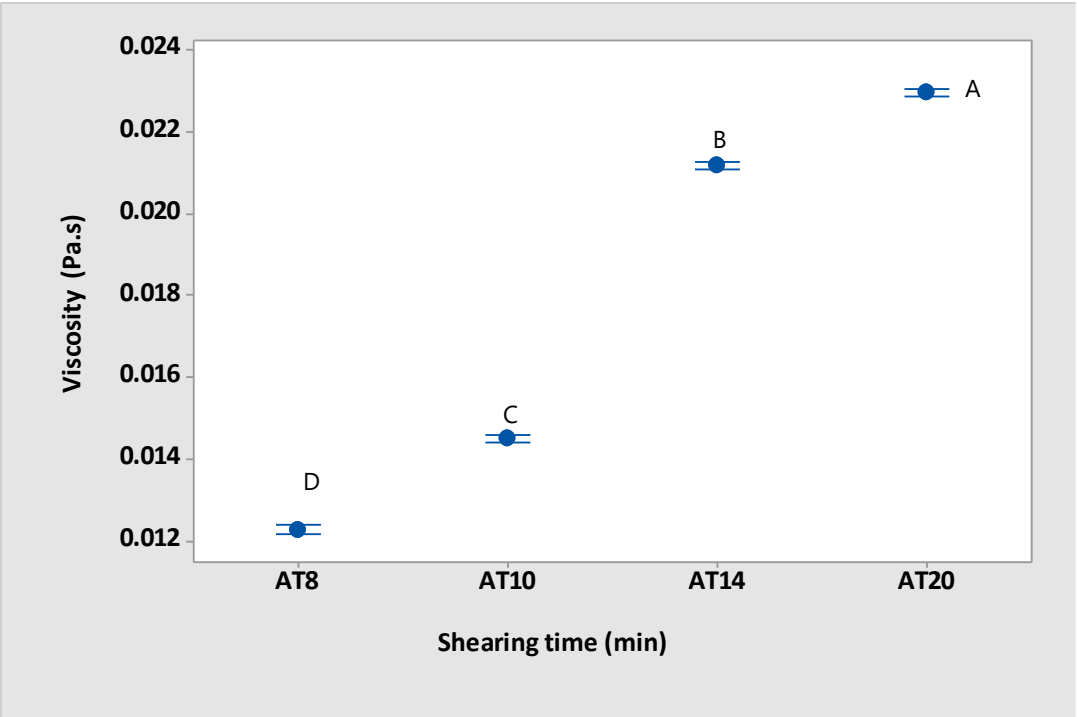

Figure 4.43. Showing effect of varied shearing time on final viscosity. There was a linear relationship between aeration time and viscosity. Error bar resresents the 95 % confidence interval for the mean.

However, here it must also be noted that similar to overrun, viscosity also increased upon prolonged aeration time. These results conflict with those of Orrego et al. (2015); Walstra (2003) and Sadahira et al. (2018), who reported that higher viscosities produced lower degrees of aeration, but in correlation with those of Lau and Dickinson (2004).

Sadahira et al. (2018) claimed that mixtures with high apparent viscosity (21.48 Pa s) resulted in foam with high density value (0.72 g/mL) and low overrun value (46.9%). They claimed that the high apparent viscosity possibly hampered the incorporation of air bubbles during whipping and also influenced molecular diffusion - decreasing the adsorption rate of proteins. In contrast, according to Lau and Dickinson (2004), the longer whipping time

presumably allows more protein to unfold at the surface of the bubbles and then to aggregate to form thicker, stronger, and stiffer lamellae, resulting in an increase in bulk foam viscosity. Though the mechanistic reason for this is not fully established, at long whipping times a rigid network of tightly packed small bubbles might be formed while at short whipping times more loose packing of large bubbles resulted in lower viscosity (Lau and Dickinson, 2005).

4.4.2.1.2. Porosity

The effect of three aeration times (8, 10 and 14 minutes) on hydrogel porosity was also measured using a non-destructive x-ray computed microtomography (µCT) technique (refer to equation 2.2). Extension of the aeration time from 8 to 14 minutes prompted a statistically significant decrease in porosity ($P < .001$) (Figure 4.44). The decrease in gel porosity upon prolonged aeration time has been reported before. According to Ciurzyńska and Lenart (2016), freeze-dried samples with low-methoxyl pectin (LMP) had an aerated structure with visibly noticeable pores, however prolongation of the aeration time induced a statistically significant decrease in porosity, which can be connected with shrinkage.

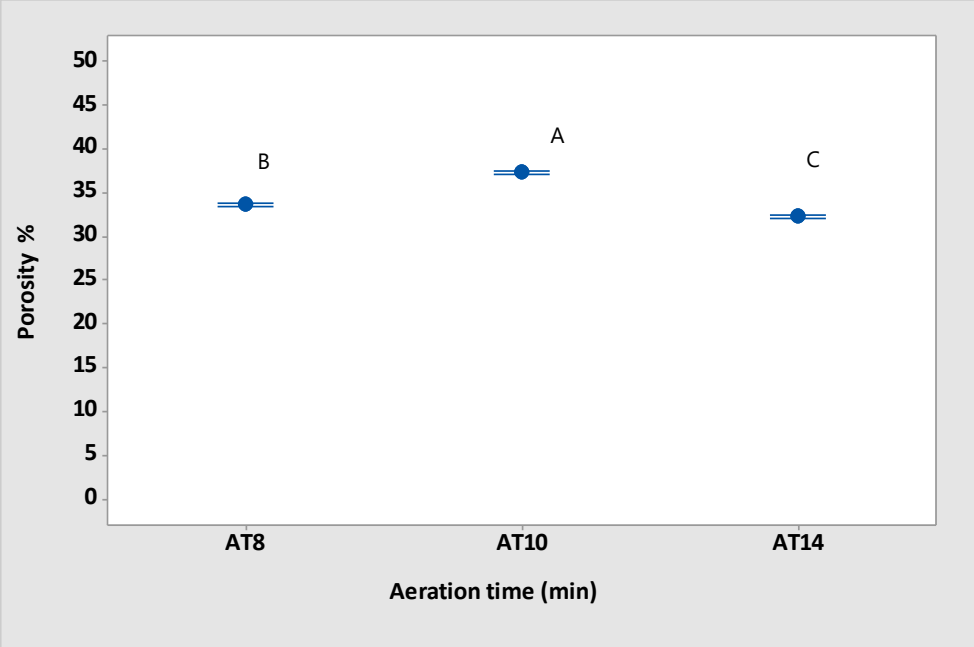

Figure 4.44. Effect of aeration time on hydrogel porosity, P< .001. Error bar resresents the 95 % confidence interval for the mean.

However, in this study, reduction in the porosity of the hydrogel upon prolonged aeration time might be related to smaller air cells, because there was a significant decrease in air cells diameter with longer aeration time (Figure 4.44). As mentioned above, according to Lau and Dickinson, when whipping is longer a rigid network of tightly packed small bubbles were formed, while more loose packing of large bubbles was formed when whipping time is short (Lau and Dickinson, 2004). Therefore, it is believed that tightly packed small air cells produced less porous structure.

4.4.2.1.3. The effect of aeration time on cell mean diameter and hydrogel microstructure

The effect of three aeration times (8, 10 and 14 minutes) on air cell mean diameter was measured by using ImageJ computer programme, on the basis of photos obtained from EVOS-inverted light microscopy. One -way ANOVA results showed a significant effect of aeration

time air cells diameter (P-value < .001). In general, extended aeration time resulted in smaller air cells. The mean diameter of air cells values were equal to 33.05, 33.06 and 28.05 for AT8, AT10 and AT14, respectively (Figure 4.45). However, there was no significant difference in mean cell diameter between AT8 and AT10. The longest aeration time (14 minutes) provided smaller air cells in diameter.

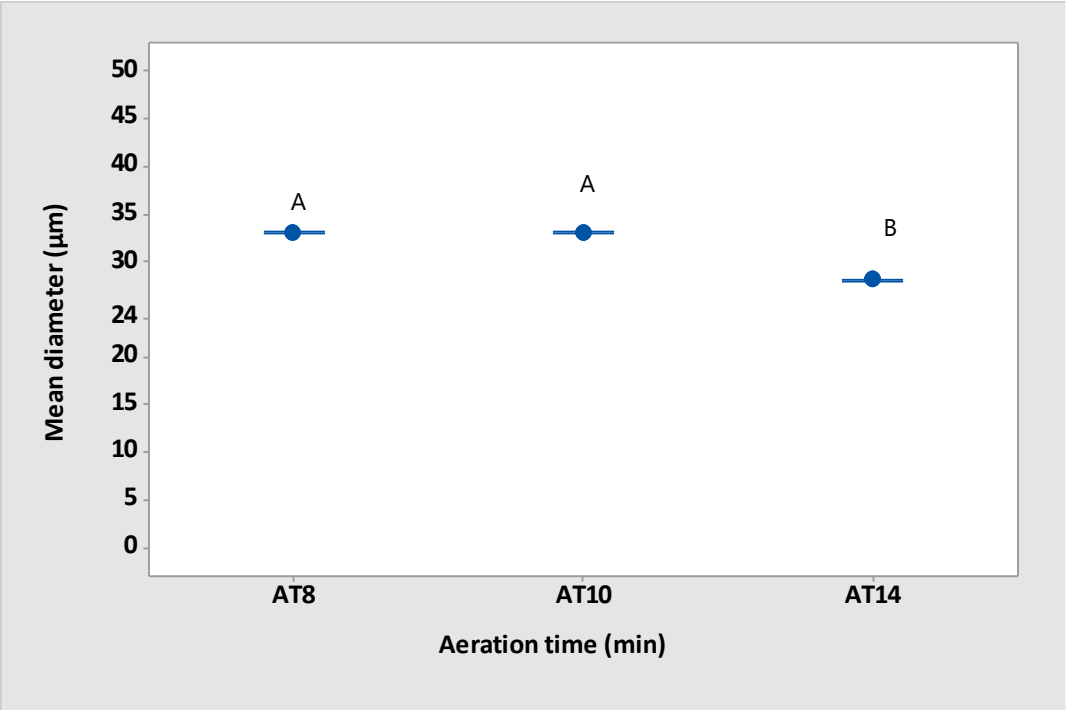

Figure 4. 45. The effect of varied aeration time on air cells mean. Error bar resresents the 95 % confidence interval for the mean.

The effect of aeration time on hydrogel morphology was also studied using X-ray computed Microtomograph. As shown in Figure 4. 45, all hydrogels were characterised by high degree of air entrainment, with numerous air cells.

However, as shown in Figure 4.46, AT8 produced less homogenous air cells compare to AT10 and AT14. As it was explained in section 4.4.4.1.1 for optimal air entrainment, bubble formation and bubble break up right aeration time is in need.

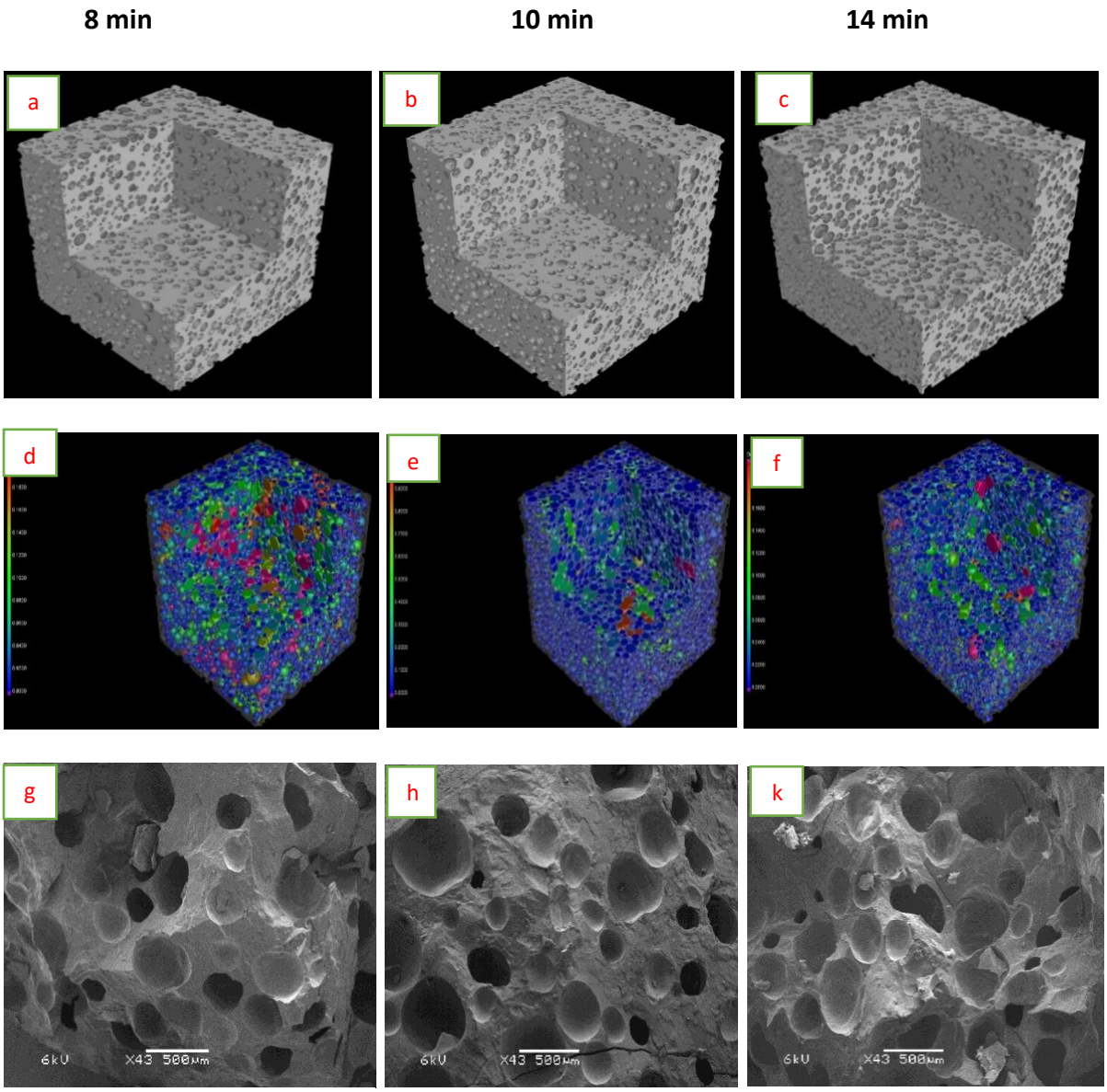

Figure 4.46. Rendered 3 D images of X-ray computed microtomograph (µCT) in greyscale (a-c) and in coloured scale (d- f) and CRYO-SEM images of (g- k) aerated hydrogels with different aeration time (AT8, AT10 and AT14), respectively.

As aeration proceeds large bubbles are broken down into smaller ones, resulting in an increase in bubble number density, but a reduction in the mean bubble size. These results in agreement with those of Laakkonen et al. (2005); Lau and Dickinson (2004); Massey et al. (2001).

Massey et al. (2001) observed that maximum overrun was corresponded to the minimum diameter because more small bubbles are formed as aeration progresses due to the turbulence induced by the rotating whisk, which initiates breakup of bubbles. They also reported that the formation of small bubbles was retained as result of surfactant migration towards the interface because of the turbulence. However, they speculated that small bubbles may also disappear if they are forced to pack closely where more bubbles accumulating within a confined volume, which actually leads to coalescence and an increase in bubble size (Massey et al., 2001).

In addition, Lau and Dickinson (2004) reported that the sample whipped for 10 minutes showed a large increase in small air bubble numbers, with the mean bubble size (5 to 15 μm) significantly reduced compared with the sample without whipping. They also claimed that the sample whipped for 15 minutes showed a further increase in bubble numbers and much finer bubbles (<5 μm) were seen to predominate, accompanied by smaller proportion of medium-sized bubbles (10 to 15 μm). However, after 15 minutes of whipping, only a small quantity of fine protein lumps could be observed (Lau and Dickinson, 2004). In general, longer aeration time resulted in an increased number density of finer bubbles.

As aeration proceeds large bubbles were broken down into smaller ones, resulting in an increase in overrun (bubble number density) and reduction in the mean bubble size. The

linear relationship was observed between elongated aeration time, overrun, air cells count, volume, surface area and air cells diameter.

4.4.2.1.4. Effect of aeration on hydrogel texture (hardness)

The effect of 5 different aeration times on hydrogel texture was revealed in texture analysis (compression). One -way ANOVA showed significant effect of aeration time on hydrogel hardness. An increase in aeration time from 8 to 12 minutes decreased hardness dramatically (P< .001). The gel structure was destroyed by the longest aeration time, which was confirmed by lowest compression force (hardness). The texture properties were strongly connected to aeration time and OR % (Figures 4.38 and 4.47).

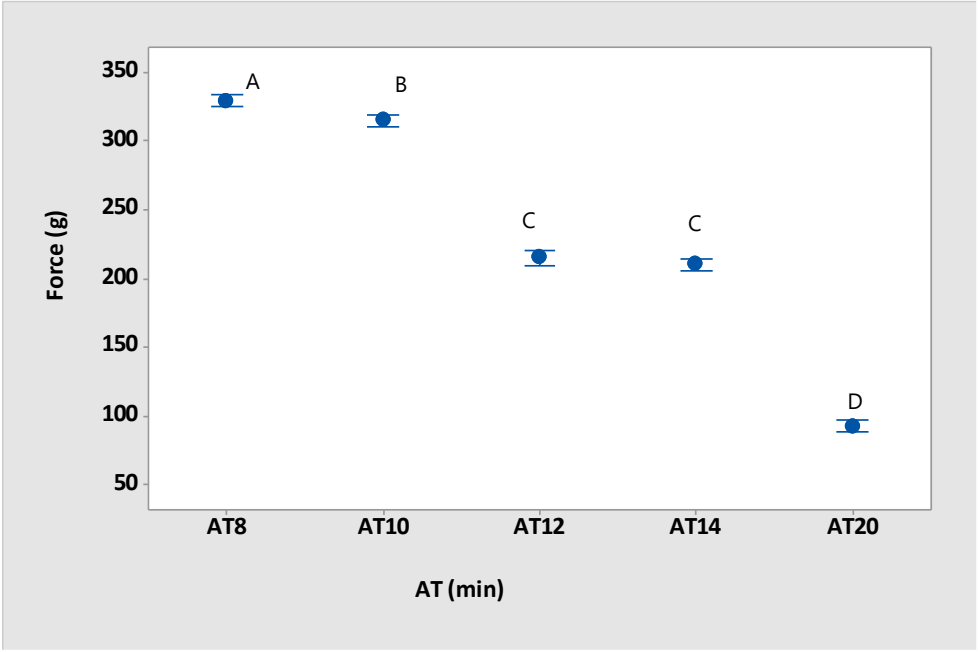

Figure 4. 47. Showing the effect of aeration time on hydrogel hardness. Means that do not share a letter are significantly different. AT: Aeration time. Error bar resresents the 95 % confidence interval for the mean.

When the overrun (Figure 4.38) and texture analysis results (Figure 4.47) are compared, it can be seen that there is a negative relationship between overrun and gel hardness; the higher the overrun, the lower the value of the hardness (softer gel), except for AT20, which exhibited effect of overbeating on the gel network.

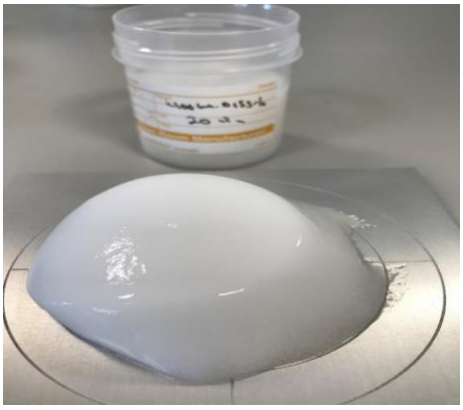

Figure 4.48. The effect of over aeration on gel structure. After 20 minutes aeration, the formed hydrogel had a very weak structure.

The above results are in an agreement with literature; the prolonged aeration time would provide higher OR, create a more delicate structure and therefore decrease gel hardness. Ciurzyńska and Lenart (2016) reported that the mixture of xanthan gum and locust-bean gum produced a delicate gel, because the aeration value was very high.

However, extended aeration time decreased porosity. It may be expected that decrease in porosity should give higher value for compression (harder gel), because it has been suggested that the increase of the pores and the decline of the pore size homogeneity were unfavorable to increasing the hardness of the gel (Guo et al., 2013).

However, these results conflict with those of Guo et al. (2013), because here a decreased porosity did not favour an increase of gel hardness. Based on these results, the degree of air inclusion (increase in overrun), which is not always related to increase of porosity, might be a key factor affecting hydrogel texture. Because according to Zúñiga and Aguilera (2009), who have studied the effect of gas (air, nitrogen and helium) on the gas-filled gelatin gels, gas-filled gels have been reported to be weaker and less ductile than control samples. However, the porous architecture that made up of pores with various sizes was also responsible for the decrease of the gel hardness.

To conclude, in general, there is a correlation between aeration time versus overrun and aeration time versus gel hardness data. When both graphs are compared, it can be seen that aeration time increased overrun but on the other side decreased the gel hardness. Thus, aerated hydrogels with different textural characteristics could be obtained by varying the aeration time; the longer the aeration time higher the overrun and less hard gel. Porosity is more related to air cells diameter rather than aeration time and overrun. With AT14 smaller air cells were produced, which formed more compact and less porous structure due to close pack of small air cells. In order to gain further information on the effect of aeration time on the gel characteristics in the complex mixture in this study rheological tests are needed.

4.4.2.2. Effect of aeration time on gel rheology. Understanding mechanism of gelation with different aeration times.

The effect of varied shearing times on gel rheology was also studied. Figure 4. 49 shows the changes in viscosity at fixed shear rate (837 s^{-1}) while temperature was increasing from 25 to

50 ^{0}C at 3.25, 2.5, 1.78 and 1.25 ^{0}C min^{-1} in relation to AT8, AT10, AT14 and AT20 minutes, respectively in order to reach final temperature of 50 ^{0}C after each aeration time.

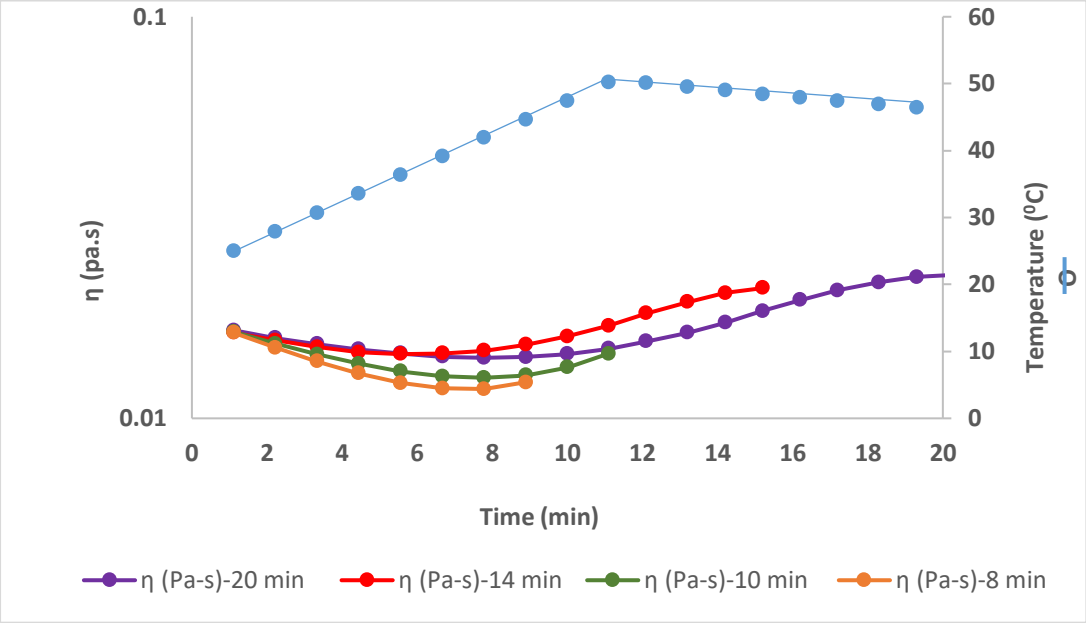

Figure 4. 49. Viscosity change during sol-gel transition upon prolonged shearing times from 8 to 20 min.

In Figure 4.49, the viscosity decreased after around 5 minutes of shearing, with then an increase, particularly noticeable when the system is cooled, after 10 minutes. It can be seen that the viscosity increased with shearing time, even up to 20 minutes.

According to Lau and Dickinson (2004), the longer whipping time presumably allows more protein to unfold at the surface of the bubbles and then to aggregate to form thicker, stronger, and stiffer lamellae, resulting in an increase in bulk foam viscosity. Too add, long whipping times the structure consists of a rigid network of tightly packed small bubbles, compared with more loose packing of large bubbles at short whipping times a therefore the viscosity is higher (Lau and Dickinson, 2004).

However, what is important to note is when this information is compared to Figures 4.50 and 4.51, which show the development of G’ and G" moduli after the varied shearing times. Now, G’ and G" moduli decreased as shearing time is increased, unlike viscosity. Shearing caused increased gel strength (G'-elasticity) compare to non-sheared ones. However, with longer shearing time there was a significant decrease in G' and G".

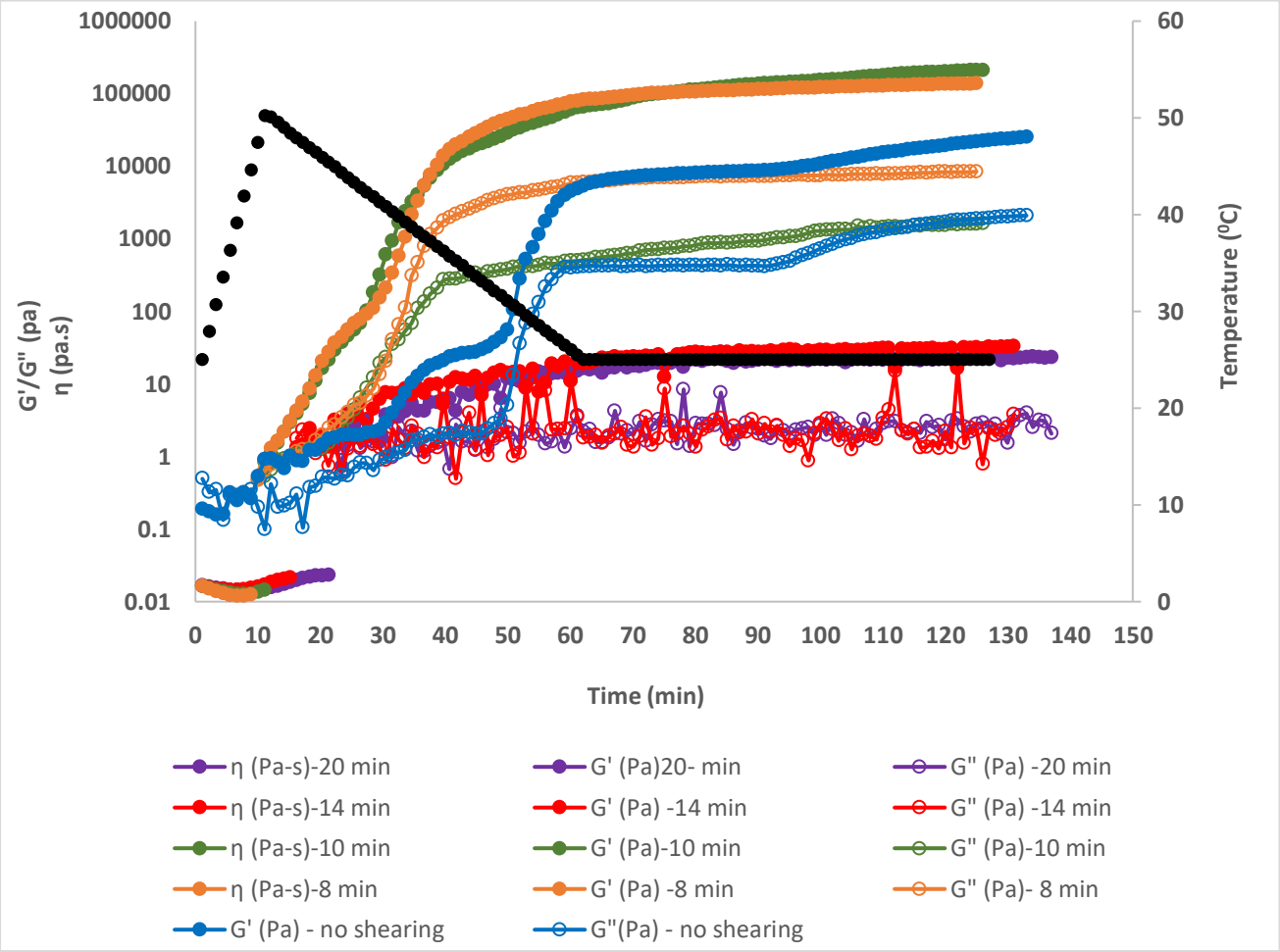

Figure 4. 50. G' and G" after varied aeration time and temperature sweep. The strongest gel was seemed to be formed after 8 and 20 minutes of shearing, while prolonged shearing caused breakdown in gel network.

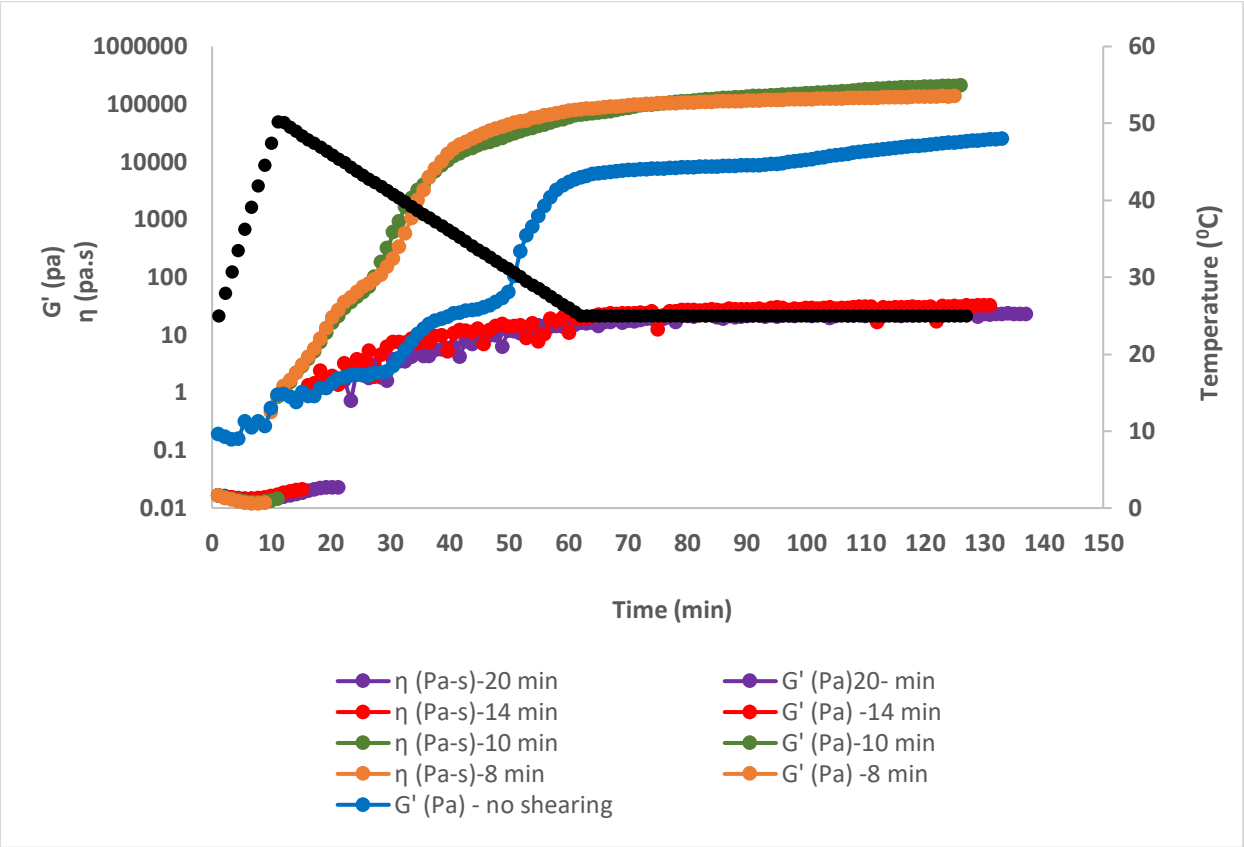

Figure 4.51. Showing G’ after varied aeration time and temperature sweep. The strongest gel was seemed to be formed after 8 and 10 minutes of shearing, while prolonged shearing caused breakdown in gel network.

The significant decrease in G’ when shearing time was prolonged to 14 and 20 minutes, can be related to nearing the completion of fluid gel particle production, and a subsequent lack of annealing upon the cessation ofshearing.

4.5. Understanding the effect of physical and chemical parameters on ionic cross linking under high shearing conditions with $CaCO_3$ and GDL: Results and Discussions

4.5.1. The effect of shearing on $CaCO_3$ particle size and dissolution rate with and without GDL

The main issue to produce aerated hydrogels from alginate is fast and temperature independent sol–gel transition of the polymer due to the "egg-box model", where inter-chain association takes place in the millisecond or microsecond timescale. Therefore, slow release of calcium salt is critical for the gelation rate and also for the resulting aerated hydrogel microstructure (Farrés et al., 2013).

In this research in order to optimise aeration time, there was need to control gelation rate. When gelation is too quick it is not easy to control in the process, which leads the resulting hydrogel to non-uniformity and weak mechanical strength. It has been reported that alginate hydrogels formed with slower rates of gelation tend to exhibit greater structural homogeneity and therefore larger moduli than those gelled rapidly. The elastic modulus also depends on the number density of physical crosslinks between chains, which is directly related to presence of cations (Kaklamani et al., 2014).

Fárres and Norton (2014) reported that by directly introducing an active form of calcium into the alginate solution and under shear, the rapid crosslinking reaction between the carboxyl groups of the polymer chain and the cations leads to the formation of anisotropic gelled particles with broad size distributions.

Therefore, in this research $CaCO_3$–GDL binary system was chosen, which can make the gelation process slow and gave homogeneous structure to alginate hydrogel. However, under the high shearing conditions and rising temperature it was important to understand the effect of high speed mixing on the $CaCO_3$- GDL interaction and its effect on gel formation.

As explained in Chapter 3, without adequate mixing time and mixing speed it was not possible to form a self-supported aerated hydrogel. It is assumed particle size distribution, which indicates particle size and its volume percentage, can strongly influence the stability and property of aerated hydrogels (Ström and Williams, 2003). For that reason, it was postulated that $CaCO_3$ particle sizes get smaller due to high speed shearing and temperature increase, and consequently interaction with GDL will be faster and form a gel network.

Initially, the effect of shearing on $CaCO_3$ particles in the absence of GDL was evaluated. In order to do that, 0.15 g of $CaCO_3$ was added to 85 g of deionized water at room temperature and mixed for 5 min at 400 rpm with a magnetic stirrer. Then it was sheared (mixed) at 8000 rpm for different time lengths with an overhead mixer (Silverson). As soon as aeration was completed the particle size distribution was analyzed using Delsa Nano particle sizer.

In another experiment, the effect of high speed shearing on $CaCO_3$ particles in the presence of GDL was examined. The $CaCO_3$ +GDL solution was prepared as follows: 0.15 g of $CaCO_3$ was dissolved in 85 g of water as explained above, and 5 minutes later 0.15 g of GDL was added, the mixture was left on the stirrer for further 5 minutes and then was sheared and analysed for the particle size distribution through the same method of $CaCO_3$ mixture.

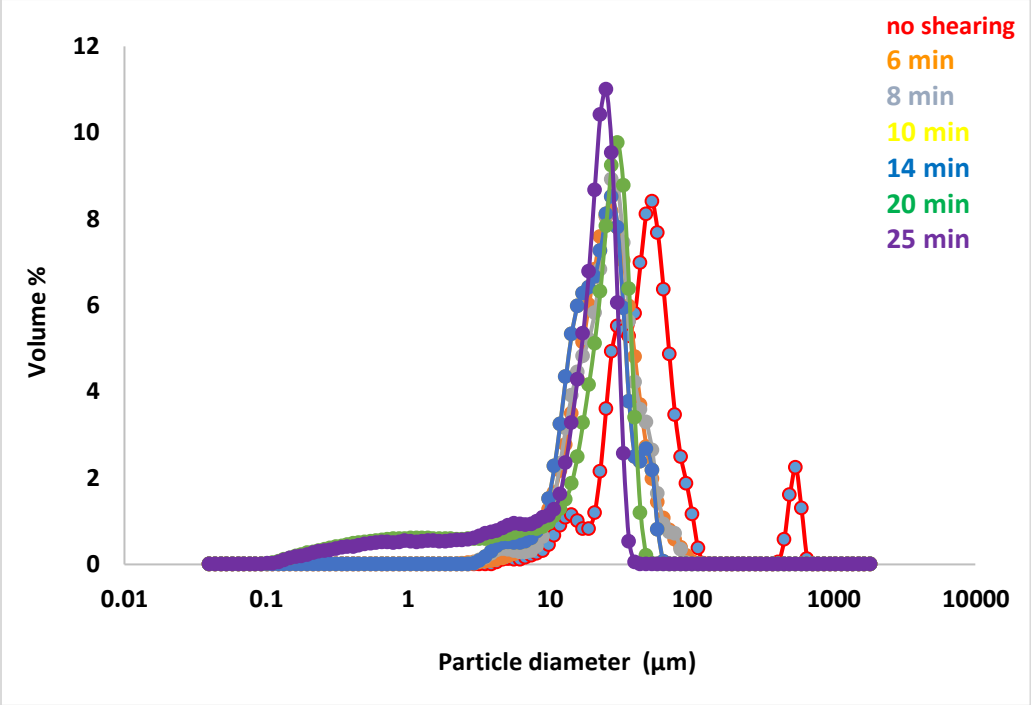

Figure 4.52. Showing particle size distribution of $CaCO_3$ after varied shearing time. The longer shearing time, the smaller the particle sizes.

Particle size distribution results showed that there were smaller particles produced when shearing time was longer. The particle size distribution curve showed two distinguishable peaks at approximately 58 µm and 541 µm without shearing (time zero shearing). In addition, the particle size of the longest aeration time, which was 25 minutes, displayed a peak at particle size of 25 µm and a long broad tail down to 0.1 µm (Figure 4.52).

In the presence of GDL, the particle size of $CaCO_3$ got progressively smaller of 20 and 25 minutes the peak moved from 7 µm to 0.07 µm (Figure 4.53).

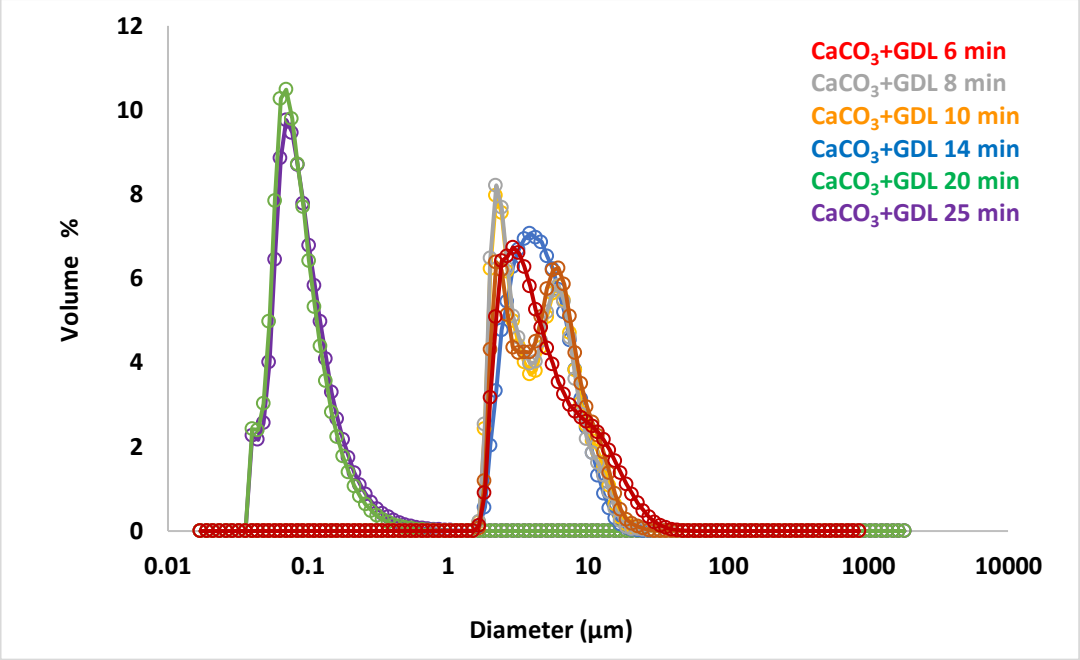

Figure 4.53. Showing particle size distribution of $CaCO_3$ after varied shearing time in the presence of GDL. The particle sizes were got even smaller upon adding GDL.

In general, average particle size of $CaCO_3$ went down significantly from 78 to 50 µm when GDL was added even if when there is no any shearing. However, the effect of GDL on $CaCO_3$ particle sizes was almost diminished when shearing time was increased to 20 and 25 minutes (Figure 4.54).

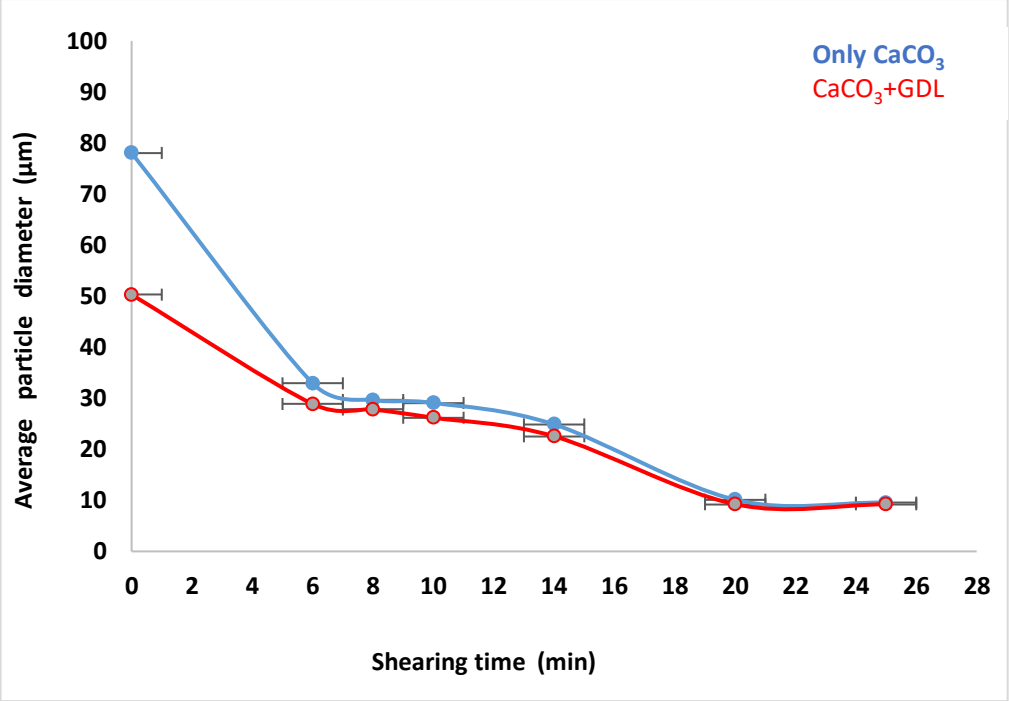

Figure 4.54. Average particle size of $CaCO_3$ after shearing for varied time length and also without shearing; with and without GDL. The error bars give an indication of the uncertainty in the measurement as assessed from a number of repeats.

Figure 4.54, first column, shows the pysical state of the $CaCO_3$ particles in water in the presence of GDL, without shearing and after shearing for 25 minutes, respectively. As it is seen without shearing there are significant amount of undissolved $CaCO_3$ particles at the bottom of the container even if in the presence of GDL. However, when the mixture was sheared for 25 minutes at 8000 rpm, fever undissolved particles at the bottom was observed.

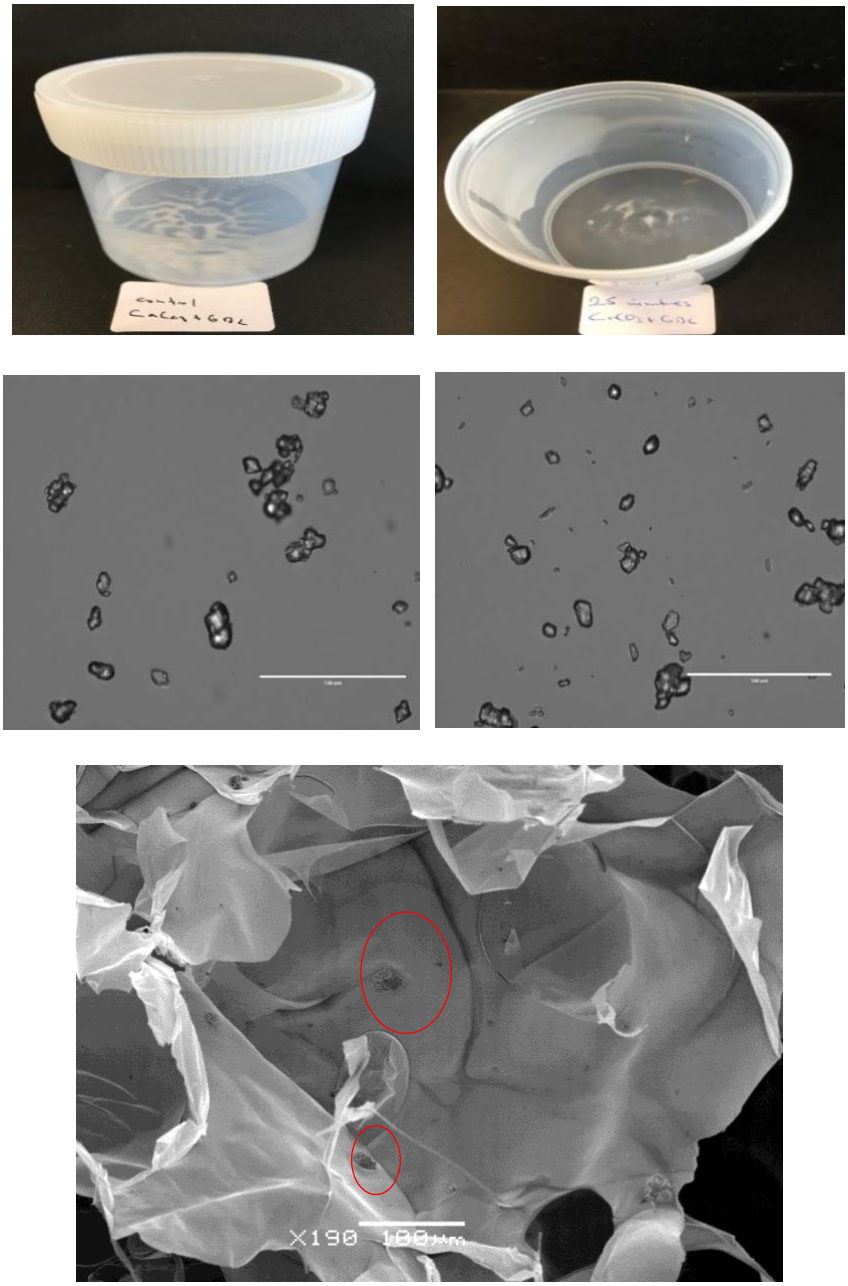

Figure 4.55. First column, from left to right: $CaCO_3$ particles without shearing and after shearing for 25 minutes, respectively. Second column from left to right: Light microscope image of $CaCO_3$ particles without shearing and after shearing for 25 minutes, respectively. Third column: SEM image of aerated hydrogel, red circles show undissolved $CaCO_3$ particles.

4.5.2. Discussion

In this study, $CaCO_3$-GDL system was used to form alginate based gels through internal gelation method. In this work it was demonstrated that shearing and also presence of GDL had a significant effect on $CaCO_3$ particle size, which potentially can affect the dissolution rate of $CaCO_3$ and rate of gelation rate (Numamaker et al., 2011; Ström and Williams, 2003; Fárres and Norton, 2014; Shchipunov and Koneva, 2002).

It has been reported by Ström and Williams (2003) that, the release of calcium via the controlled dissolution of $CaCO_3$ by GDL can be rate limited either by GDL hydrolysis or by $CaCO_3$ dissolution, dependent on the particle size. They also reported that presence of the pectin (in their case) does not significantly influence the dissolution rate of $CaCO_3$.

They also studied the effect of particles size on gelation rate. They showed that the gel point occurred almost immediately for the 1.7-µm particles and after approximately 15 and 47 min for the 5 and 20-μm mean particle sizes, respectively. So, the smaller the particles induce shorter gelation times (Ström and Williams, 2003).

Similar to the Ström and Williams (2003) and Fárres and Norton (2014) observations, here there was a linear relationship between mixing time, particle size of $CaCO_3$ and viscosity (Figure 4.54). This is might be related to the proportional increase in the the dissolution rate of $CaCO_3$ and release of calcium ions because of smaller particle size, which in turn could increase chain interaction with alginate and therefore causes an increase in viscosity and ultimately form cross links. It has been shown that when mixing time was less than 8 minutes

there was phase a separation (refer to Figure 4.39), which seems likely to be due to the formation of weak cross-links, related to limited Ca^{2+} ions available to interact with alginate.

According to Numamaker et al. (2011) the concentration of $CaCO_3$ was an important factor for the gelation time. The gel time was decreased with increasing $CaCO_3$ concentration. Cheng et al. (2012) also reported that the increase of Ca^{2+} content enhanced the inter- and intra-molecular interactions between alginate molecules, shortened the average distance of ionic crosslink, and resulted in the larger aggregate density (Cheng et al., 2012).

According to Farrés and Norton (2014) uniform distribution of ions throughout the system will prevent large clusters and will minimize the formation of inhomogeneous gelled networks if calcium ions are introduced into the aqueous phase progressively, which is driven by liberation of calcium ions from in soluble $CaCO_3$ by GDL protons.

As a result, association of the polyguluronate sequences of the alginate chain a by dimerisation mechanism takes place and forms ribbon-like assemblies with cavities into which calcium ions are located (i.e. egg-box dimers). A three-dimensional crosslinked network will be formed while extent of association increases through aggregation of ordered dimers and storage modulus G' will increase (Farrés and Norton, 2014).

4.6. Application of the created aerogel production strategy into real food system

According to the United Nations (UN) the world's population will increase from 7.2 billion today to 8.1 billion in 2025, and by 2050 it will reach 9.6 billion (http://www.un.org/en/development/desa/population). Due to this fast population growth and also climate change it is a real challenge for food scientists to produce adequate, safe and nutritious food products for a diverse group of consumers. Not only food scientists, food industry also have a strong focus on delivering innovation to meet market and consumer trends in health, texture, nutrition and targeted delivery solutions (Mikkonen et al., 2013; Arboleya et al., 2014).

It is very important to control portion size and reducing energy density of the meal in order to promote healthy eating habits. Producing low calorie food with modified structure would be an alternative way of controlling or reducing daily calorie intake. Including air in food might be an alternative to design satiating products. Aerated foods (incorporating air as small dispersed bubbles) are known to affect satiety and therefore reduce food intake. Recent published research has highlighted the link between applied material characteristics like viscosity or gel performance of polysaccharides in food matrices and the effect of gastric emptying and satiety (Arboleya et al., 2014).

Including air or some other gases into a food matrix affects texture and firmness and also changes the appearance, colour and mouthfeel. Therefore, it is essential to review this aspect because these products are not only consumed for health purposes, but also for enjoyment (Campbell and Mougeot, 1999; Arboleya et al., 2014).

The main objective of this section was to design an aerated product with some natural food materials. Carrot juice, orange juice and tomato puree were chosen to create aerated hydrogels. All the tested commercial products including carrot, orange juice and tomato puree were not suitable for the aerated aerogel production due to their low pH level. The changes in pH change the charge of the molecules and therefore alter the attractive and repulsive forces between molecules as well as the interactions between molecules and solvent, that is, hydration properties (Banerjee and Bhattacharya, 2012). However, fresh carrot juice with pH 6. 68 formed self-supported aerated hydrogels. This study, would be used to create aerated structure out of real food materials with better distribution of air and increase of volume.

4.6.1. Aerated aerogel in the real food system

The ultimate aim of this research was to apply the new created aerogel production strategy into a real food system. Although edible aerated aerogels made of food ingredients is a relatively new concept, aerogels have been receiving some great attention due to their health benefits and wide range of application possibilities such as packaging materials and selective carriers for drugs, nutrients, aroma compounds or additives. In this part of the research, some formulations were developed in order to create aerated hydrogels with some common food materials; carrot juice, tomato puree, orange juice. It was recorded that it is possible to produce aerated edible hydrogels. However, pH was seen to be a key parameter to optimise.

4.6.2. Concept testing

Initially some concept tests were carried out in order to determine the most suitable food materials for aerated hydrogel creation. For this purpose, orange juice, tomato puree and fresh and commercial carrot juice were used to produce an aerated hydrogel.

It was seen that there are some complications with orange juice with the main issue being its low pH, which was 3.98. After adding 25 % (w/w) orange juice to the alginate based mixture with $CaCO_3$ +GDL, where the pH of the solution went down to 4. 94 from 6.68. Upon addition of orange juice, the gelation rate was very fast and influencing the efficiency of the aeration step. The resultant foam-like hydrogel was not self-supporting and uniform, with a low overrun of 56 % (Figure 4.56).

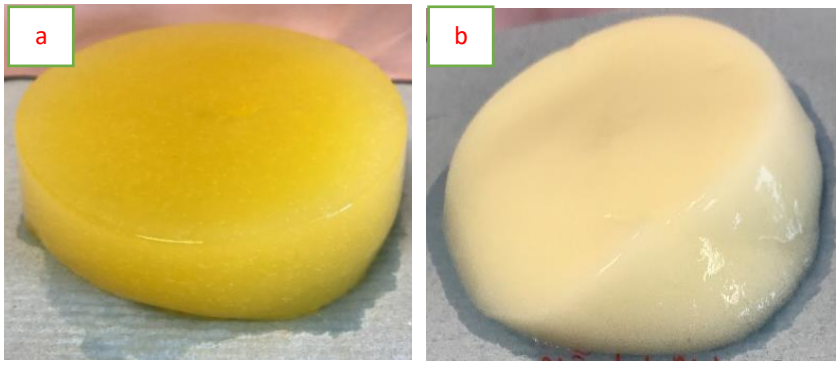

Figure 4.56 Showing alginate based non- aerated hydrogel containing 25% (w/w) orange juice (a), and upon aeration (b).

A commercial tomato puree was used and similarly to the orange juice, it was not possible to make aerated hydrogel with 25% tomato puree (Figure 4.57). The pH of the tomato puree was 4.24. Once it was added to the alginate based mixture, the pH was reduced to 4.83.

Again, it was seen that with that the low pH it was not possible to form a self supporting aerated hydrogel. The mixture was aerated but the resultant gel was like foam, it was not self-supported gel.

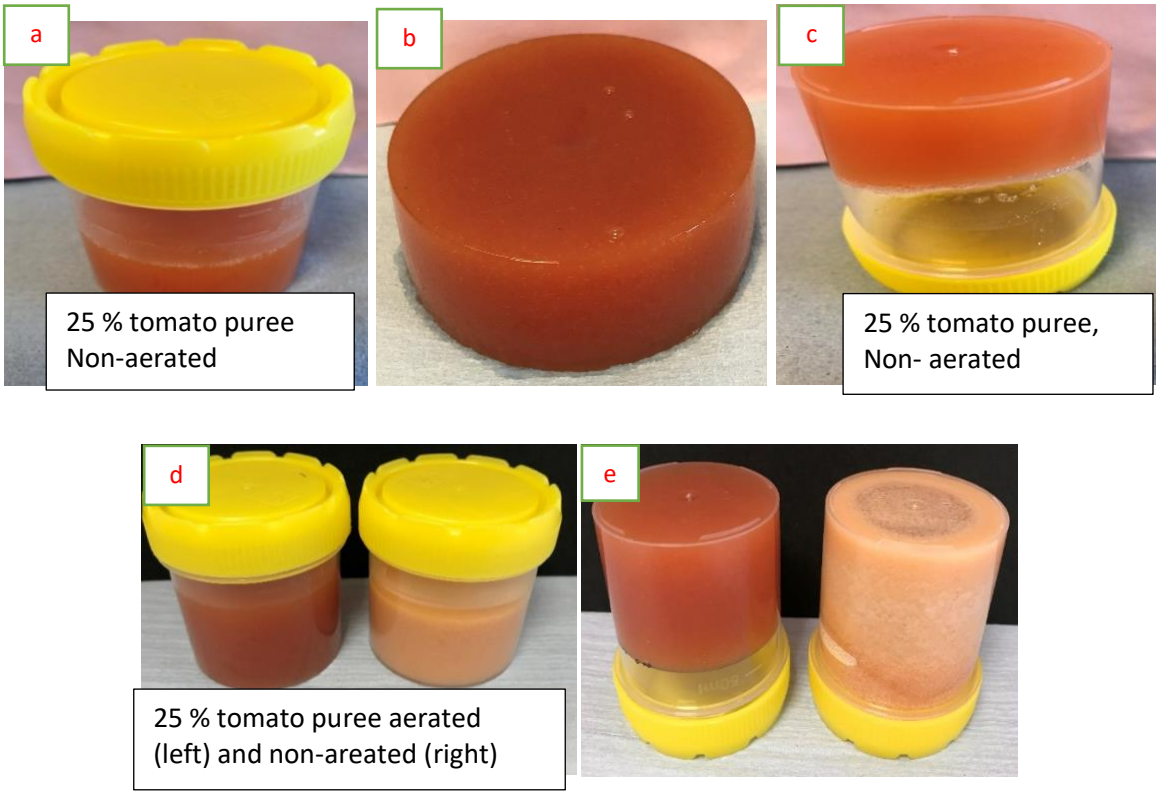

Figure 4.57. Showing alginate based non-aerated hydrogel containing 25% (w/w) tomato puree (a-c), and aerated ones (d-e), after 10 mintes aeratin at 8000 rpm, foam-like structure was formed not self-supporting gel.

In order to mitigate the effect of the pH and the fast gelation, pH of the both tomato puree and orange juice was adjusted to 6.75 by adding sodium hydroxide (1M). It was seen that it was not possible to form aerated hydrogel out of orange and tomato puree. The resultant gel was like foam and was very unstable. There was a phase separtaion soon after aeration was stopped.

4.6.3 Creation of the aerated carrot juice aerogel

Similar to commercial orange juice and tomato puree, tested commercial carrot juice also had low pH, which was measured to be 5. Therefore, it was decided not to use any commercial food materials. Subsequently carrots were bought, peeled and juiced with the pH of fresh carrot juice recorded to be 6.68. When it was added to alginate+WPI+A4M mixture containing CaCO3 and GDL, and aerated for 10 minutes at 8000 RPM, the pH of the mixture was measured to be 6.55.

With the addition 25% (w/w) fresh carrot juice it was possible to create aerated and non-aerated hydrogel (Figure 4.58). Non-aerated hydrogel, which was self-supporting gel with homogenous appearance, was formed within 30 minutes after adding the carrot juice to the alginate based hydrocolloid mixture. This time is equivalent to that seen for the creation of gels due to calcium release as a result of GDL lowering the systems' pH.

For aerated hydrogel, overrun was recorded to be 84 %. Although the formed gel was self-supporting, it was week and had homogenous appearance (Figure 5.58).

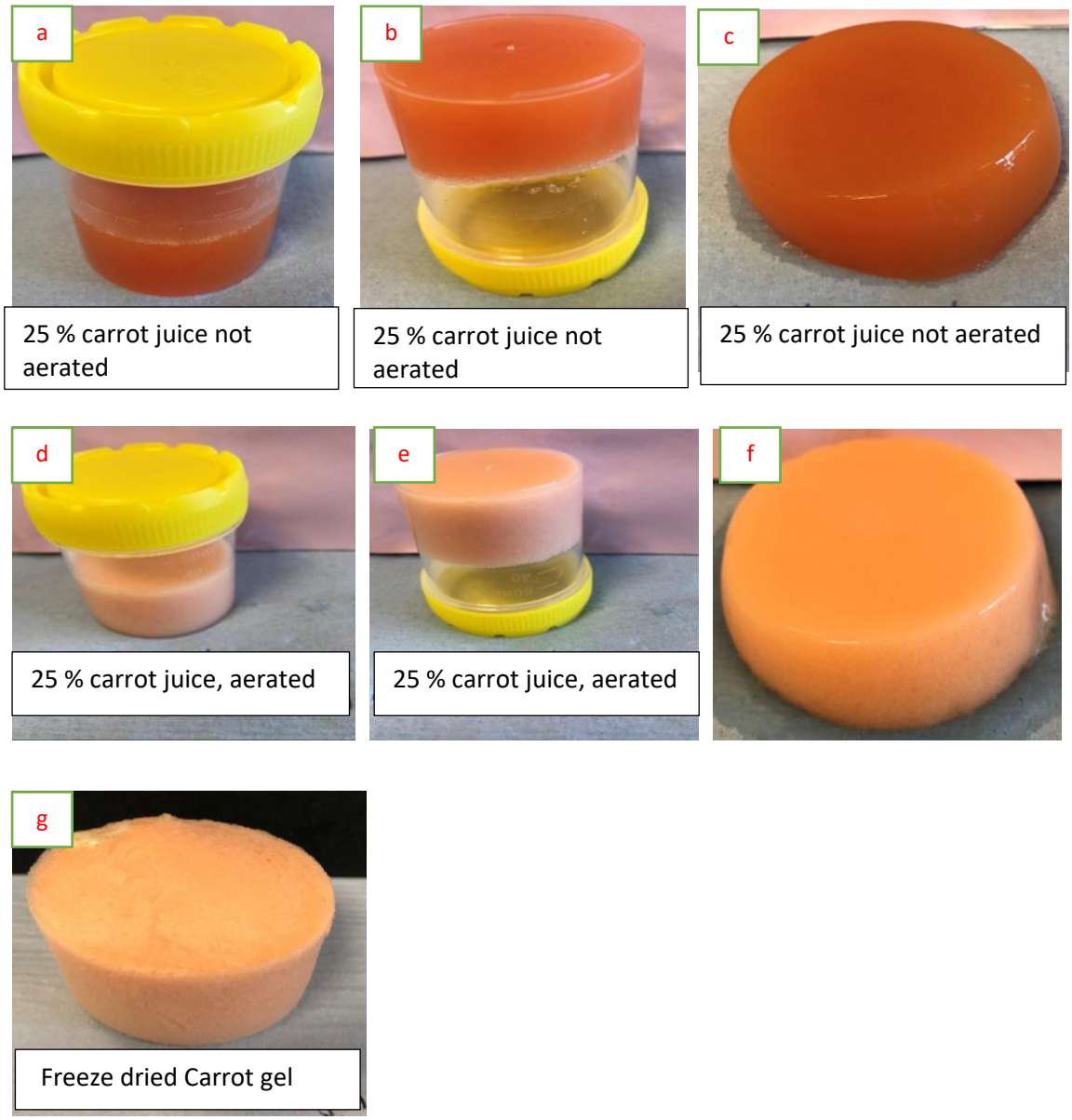

Figure 4.58. Showing alginate based non- aerated hydrogel containing 25% (w/w) fresh carrot e juice (a-c), and self-supporting aerated hydrogel after 10 min aeration at 8000 rpm. (d-f), and freeze-dried aerated carrot hydrogel (g).

4.6.4. Discussion

As it was explained earlier, pH was a critical parameter in formation of aerated hydrogels based on alginate. There are two conventional ways to gel alginates; by lowering pH below the pKa values, which was introduced as an index to express the acidity of weak acid, and by ionotropic gelation in the presence of bi- or trivalent cations.

In general, when pH of the solution is brought down below the disassociation constant (pKa) of the polymer alginic acid gels are formed. M and G residues have pKa of 3.38 and 3.65, respectively. Hence, alginate is negatively charged across a wide range of pH. The rate of pH decrease affects an alginate solution in two ways; rapid decrease results in precipitation of alginic molecules in the form of aggregates while a slow and steady drop in pH results in the formation of a continuous alginic acid bulk gel (Draget et al., 2006).

As it is shown in Figures 4.56 and 4.57 from tomato puree and orange juice respectively, with low pH, below 5, it was not possible form self-supporting gel after 10 min aeration. After adding 25% tomato puree or orange juice to the sodium alginate+WPI+A4M, $CaCO_3$ and GDL solutions, observable fast gelation was taking place. Once it is aerated, the resultant structure was foam-like rather than gel. This is might be due to the effect of pH on sodium alginate gelation mechanisms.

Cao et al. (2005) explained the pH-induced variation in the structure of cross-linked assemblies. The alginate assemblies prepared around pH 4 are comprised of the cores with large volume fraction and the shell with small volume fraction. Once such assemblies were shell-cross-linked and were dialyzed against aqueous solution at pH 7.0, owing to the

ionization of carboxylic acid groups the hydrogen bonds between carboxylic acids in the cores will be destroyed and the cores will disintegrate. Since the shells of assemblies are crosslinked, the structure of assemblies can be maintained but the expansion of assemblies is inevitable. Thus, the cavity in the centre of the assemblies occurs, and the hollow capsule structure is formed. A proposed scheme of the pH-induced self-assembly of sodium alginate and transition of cross-linked assembly to hollow capsule is shown in Figure 4.59. First, gradually partial protonation of carboxylate groups in sodium alginate chains causes the self-assembly of sodium alginate chains and forms the assemblies with the core-shell structure. Subsequently, the cross-linking reaction fixes the shape of the assemblies, which makes the assemblies yield a hollow capsule structure when they are in the medium with relatively high pH value (Cao et al., 2005).

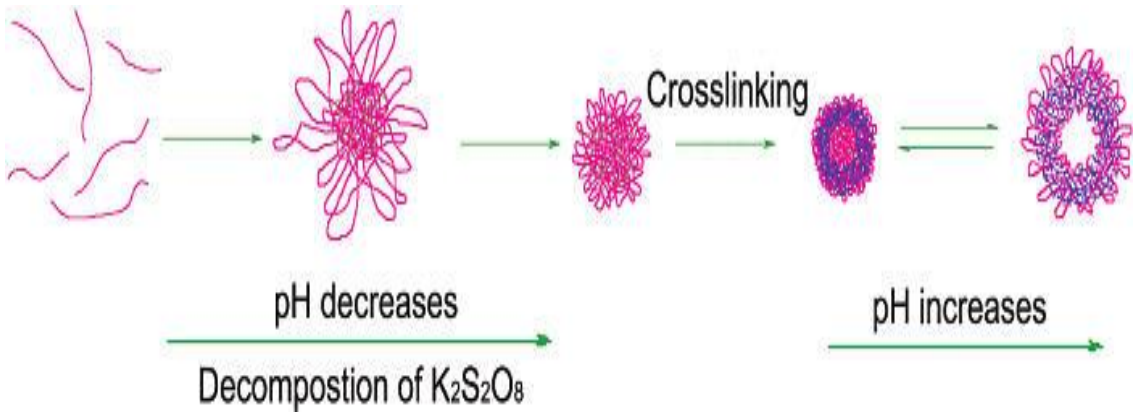

Figure 4.59 Schematic representation of pH-induced formation of sodium alginate assemblies, and the transition from the compact structure to hollow structure (from Cao et al., 2005).

Zazzali et al. (2019) reported the effect of pH on the structural properties of Ca (II)-alginate beads. They claimed that the microstructure of the alginate networks obtained at acidic conditions (below pH 3.5) significantly differ from those obtained by conventional ionotropic gelation. They reported that likewise, the pH of synthesis affects the mechanical properties of the beads. Beads synthesized at pH 5.0 and 6.8 show a similar trend in the force required for compression (Figure 4.60) while those synthetized at pH 3.8 require considerably less force to obtain the same compression indicating less strength. The uronic acid residues, which constitute the alginate polymer, create junction zones within the gel (Zazzali et al., 2019).

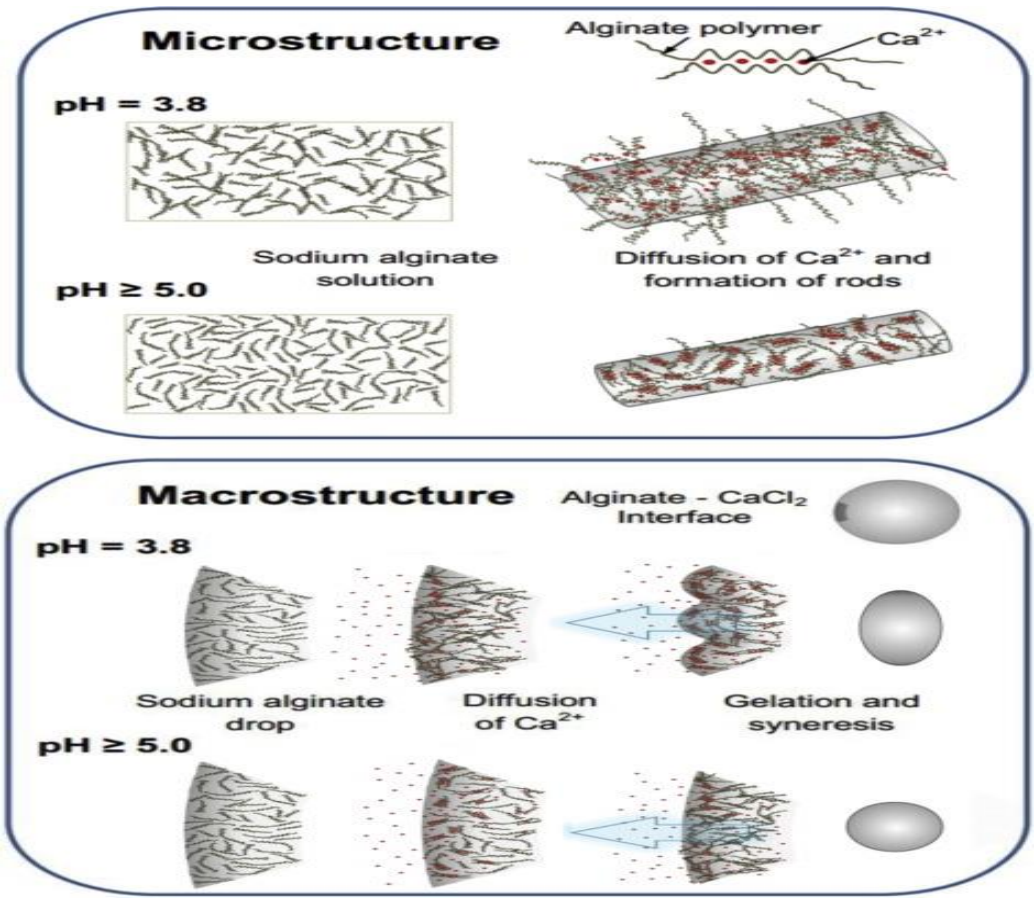

Figure 4.60. Schematic representation of the gelation process for samples synthesized at pH 3.8 and at pH values far from the pKa of the alginate polymer residues (samples synthesized at pH 5.0 and 6.8), showing details at the micro- and macroscopic scales. For samples synthesized at pH 3.8, the stronger chain-chain interactions of partially protonated alginate

polymers generate supramolecular branched blocks of construction leading to a more structured network in the front of gelation. This effect explains both, a hindered syneresis and shrinkage of the system. By the contrary, multiple events of rearrangement in the Ca(II)-alginate/solution interface are allowed in the samples synthesized at near neutral pH conditions, leading to syneresis and shrinkage of the bead, maintaining its spherical macroscopic conformation (From Zazzali et al. 2019).

As it was mentioned before, it was not possible to form any aerated hydrogel with orange juice having pH 3.98. In general, when pH was below 5 gelation did not take place after 10 minutes shearing. Because it has been reported that sodium alginate solutions for 5 and 7 pH levels shows a behaviour between Newtonian behaviour and pseudoplastic behavior (non-Newtonian-shear thinning), while in pH value of 3 they show Newtonian behaviour to dilatant behaviour (shear thickening). The effect may be the result of polysaccharides ionization rate increase for gum solution in pH>3 to neutral pH. Therefore, polysaccharides hydrophobic interactions among polysaccharides chains decrease (because of ionized groups in gum solution). Hence, in pH=3 ionization rate is very low and insignificant. Hydrophobic interactions between polysaccharides chains are higher, therefore, polysaccharides composite have been maintained well and solutions are more viscous (Mehmandoost et al., 2014).

Ramdhan et al. (2019) reported that gel strength and syneresis increased with the decrease of pH of alginate solution. From pH 4 viscosity of alginate solution increased with the increase in pH and a maximum viscosity was achieved at pH 6–7. After that, the viscosity decreased gradually when pH was further increased to 11. They also reported that when the pH decreased, the gel strength tended to increase even though the values show no significant difference between pH 6 and 4. In contrast, the gel strength gradually decreased as pH was

increased to 11. They claimed that at acidic pH, the carboxylate groups of alginate will be protonized resulting in the decrease of repulsion force among these groups. This creates an environment where syneresis is more dominant than water reabsorption resulting in the shrinkage of the alginate gels. In contrast, at alkaline pH, the carboxylic groups dissociate and become negatively charged carboxylate ions which create repulsion forces amongst each other. That repulsion force leads to the formation of spaces or voids so the gels tend to absorb water to fill the space regions within the alginate calcium network until they reach the equilibrium state at which the osmotic pressure equals to the crosslinking bonds force keeping the gels' structure stable (Ramdhan et al., 2019).

4.5. Conclusion

1. In this chapter, the effect of hydrocolloid type on structure and physical properties of the aerated hydrogel and freeze dried aerogels was evaluated in detail. It was confirmed that hydrocolloid type played significant role in the formation of the aerated hydro and aerogel micro -macro structure. K100M provided the higher overrun and the strongest hydro and aerogel as a viscosity enhancer and surface- active polymer.

2. The presence of WPI increased the overrun and porosity but resulted in less strong hydrogel.

3. Mixing time (aeration time- AT) 14 minutes gave the highest overrun. The air bubbles were more regular and smaller. Therefore, porosity was decreased. The longest AT (20 minutes) had 'over beating' effect on the hydrogel structure, producing less strong hydrogel. It was recorded that there is a relationship between mixing time, viscosity development and Ca^{2+} release, which consequently affects the aerated hydrogel rheleogy and microstructure.

4. The effect of shearing on $CaCO_3$ particles and consequently on gel formation, in the presence and absence of GDL, under high shearing conditions was evaluated. $CaCO_3$ average particle size decreased as a result of high shearing and GDL, which affects the dissolution rate of $CaCO_3$ and SA gelation rate. Therefore, it is postulated that AT less then 10 minutes was not enough for release of sufficient amount of Ca^{2+} to form stable, homogenous aerated hydrogel due to lack off formation of a gel network by SA, in where water molecules are trapped.

5. The created new method was also applied for the production of aerated hydrogel with real food materials. Altough it was possible to apply the medthod successfully, pH was one of the parameters that needed to be controlled. Fresh carrot juice with pH 6.68 was seen to be most suitable material.

CHAPTER 5

Overall Discussion

Food aeration is an important processing parameter for altering various aspects of food including texture, mouthfeel, shelf life, flavour release etc. Aerated foods are in our daily life as bread, ice cream, breakfast cereals or carbonated water. Food aeration is carried out by different methods and all include air or other gaseous within food structure and casues increase in volume. Aerogels also can be classified as aerated food since they have extremely low density but high volume. One of the most important aspect of the aerogels is having potential for being used for low calorie diets.

In this research, the main aim was to develop a novel method to create low solid mass content aerated hydro and aerogels. Based on one pot approach and ionic cros linking gelation system aerated hydro and aerogels were created containing as low as 0.5% dry mass content (99.5% H_2O) with food grade materials. To the best of the author's knowledge, in the literature there is no any publication regarding aerated hydro or aerogels with that low dry mass content.

Processing parameters (mixing time and speed) were fundamentals to be controlled in order to maximise the overrun and improve hydrogel and aerogel characteristics; appearance, strength etc, which was assumed to play important role in alginate gelation based on ionic gelation in the presence of calcium ions that were released by GDL hydroloysis. It was postulated that $CaCO_3$ particle sizes get smaller due to high speed shearing and temperature increase, and consequently interaction with GDL will be faster and form a gel network and therefore can strongly influence the stability and property of aerated hydrogels (Ström and Williams, 2003). Consequently, as it was explained in Chapter 4 (Section 4.3) without adequate mixing time and mixing speed it was not possible to form a self-supported aerated hydrogel.

It was also noted that aeration speed and overrun had a linear relationship, which is in correlation with literature (Table 4.1, the first column). Edoura-Gaena et al. (2007) claimed that rotation speed, duration and their interaction had significant effects on overrun. Both rotation speed and duration had significant effects on the temperature of the batter: the higher the rotation speed and duration, the higher the temperature. Similar to Edoura-Gaena et al. (2007) it was also seen that there was a significant increase in temperature upon elongated mixing time and speed. Therefore, the complexity of the mixed formulation in this study has shown that the rheology of the system is dynamic and dependent upon how the polymers interact with one another, and how the kinetics of phase change can impact on the structures being created while aeration in underway.

Alginate is found to be the main gelling agent, however, MC and HPMC increased strength of alginate by increasing the viscosity while WPI increased overrun significantly. It was not possible to produce a hydrogel with a very low solid mass content (0.5%) in the absence of the MC and HPMC. It is believed that the synergism that created between mixed polymers (alginate, MC/HPMC and WPI) was main driving force for very low solid mass content aerated hydro and aerogels.

Hydrocolloid type has a significant effect on the aerated hydro and aerogel micro and macro structure; K100M provided the higher overrun and the strongest hydro and aerogel. However, mean diameter of air cells in the aerated hydrogel containing K100M was significantly bigger than A4M and LBG aerated hydrogel; the lowest overrun was recorded with LBG ($P < 0.014$).

It was clearly demonstrated that each polymer had a very specific role in the alginate gelled aerated hydrogels. Firstly, overrun was very dependent on used polymers and viscosity of the aerated media. The higher overrun was recorded with K100M and lower with LBG. It was

seen that tested polymers produced viscous solutions in the following order K100M > K4M= A4M>LBG, which probably explains the difference in relative overrun. Surface active polymers play an important role in foaming and foam stability as they readily adsorb at the interface and thus reduce surface tension. In the presence of the surface -active polymers loss of gas bubbles, coalescence of liquid droplets and drainage of the liquid between films is prevented due to a viscoelastic interfacial layer and the higher continuous phase viscosity (Wallick, 2014).

However, it was seen that viscosity development was driven by temperature changes during mixing. Initially there was a decrease in viscosity which can be explained by the effect of temperature on polymer motion. At low temperature macromolecules are hydrated and, viscosity is dominated by simple entanglement of the molecules (Ruel-Gariépy and Leroux, 2004). Another explanation for initial viscosity decrease might be due to progressive disruption of native cellulosic 'bundles' as a result of temperature increase (Bajwa et al., 2009; Haque and Morris 1993).

The viscosity increases after 5 minutes of shearing, when temperature is still increasing was postulated to be due to some occurrences such as; (a) beginning of protein aggregation, (b) cellulose derivatives begin to increase a network of swollen clusters (Alessandro et al., 2009; Haque and Morris, 1993) or (c) formation of new cross-links as a result of dissociation of $CaCO_3$ and release of Ca^{+2} to form egg-box alginate gel structures. For both a) and c) the formation of aggregates/gels corresponds with the creation fluid gel structure.

An increase in number and volume fraction of the forming particles results in an increase in viscosity (Moakes et al., 2015). After that point it seemed that the formed structure is not affected by the applied shear anymore.

For instance, WPI gelation in a shear field, the primary particles are held together by weak hyrophobic interaction at the beginning of the aggregation and therefore aggregates are broken down easily than later stage where more firm structure is formed because of covalent bonding. However, when heating rate is high the rate of aggregates formation is faster and therefore formed aggregate can become more resistant to shear breakdown (Moakes et al., 2015). Consequently, depends on the heating rate, size of the aggregates increased through interlinking particles and resulted in viscosity increase.

Aerogel pore microstructure morphologies were dependent on ice crystal growth during freezing. The aerated hydrogels that frozen under the fast -freezing conditions (liquid nitrogen, -197 ^{0}C) had more regular structure and more intact air cells because at lower freezing temperature (-197 ^{0}C) a larger undercooling led to an increased rate of nucleation of ice crystals, and ice crystal growth rate was less than the nucleation rate, thus water molecules can quickly form a large number of small ice crystals. On the other hand, at slow freezing the ice crystal size can be too big, leading to a disordering aerogel pore structure with uneven ice crystal distribution (Ni et al., 2016; O'Briena et al., 2004).

The other parameter that was tested on aerogel microstructure under the fast and slow freezing method was effect of polymer types (K100M versus LBG). The analysis of SEM images of both aerated hydrogels frozen under the fast freezing conditions (liquid nitrogen, -197 ^{0}C) indicate that samples containing LBG had least regular microstructure with more delicate appearance (Figure 4.24a-c). Altough the both aerogels (with K100M and LBG) displayed large amount of intact air bubbles with thin walls separate the pores, compared to

LBG, the samples made of K100M seemed to have more distinctive cells walls with more intact air bubbles (Figure 4.24d-f).

It was seen that pH was a critical parameter for the application of the created aerated hydrogel and aerogel production method into real food system. As it is shown in Figures 4.56 and 4.57, with low pH, below 5, it was not possible form self-supporting gel after 10 min aeration. After adding 25% tomato puree or orange juice to the sodium alginate+WPI+A4M, $CaCO_3$ and GDL solutions, observable fast gelation was taking place. Once it is aerated, the resultant structure was foam-like rather than gel. This is thought to be related to the effect of pH on sodium alginate gelation mechanism (Draget et al., 2006).

CHAPTER 6

General conclusion and future works

6.1. General conclusion

Initially, a new method, based on one pot approach and ionic cross-linking gelation, was developed for making protein-polysaccharide aerated hydro and aerogels.

Following the development of new method, aerated hydro and aerogels were improved by optimising physical and chemical parameters; including time and temperature, mixing (aeration) speed and including a new material**.** Temperature control before and during mixin) was essential for successful aeration, providing higher overrun and homogeneous gel structure.

It was cruical to carry out the aeration soon after GDL was added to the solution for the prevention of gelation that might take place before aeration step. Shorter AT (4 minutes) caused phase separation, while longer AT (20 minutes) broke down the gel structure.

The right aeration speed for the mixer was recorded to be a fundamental physical parameter. When aeration speed was below 6000 rpm, there was a quick phase separation just after aeration was stopped. It was recorded that 8000 rpm (AT 10 minutes) was a right speed to form an aerated hydrogel with high overrun and uniform structure.

MC/ HPMC was introduced as a viscosifier into hydrogel in order to increase strength and stability of the aerated hydrogel. As a result, overrun increased by 15 % and air cell diameter reduced. The mean diameter of air cells in the hydrogel containing MC-A4M were much smaller (16 μm- 0.016 mm) compared with those of air cells formed without MC-A4M. The

effect of introducing MC/HPMC was more pronounce when solid mass content was reduced to 0.70 %.

By adding either MC-A4M or HPMC-K100M, the gel structure was improved significantly ($p<0.05$). The aerated hydrogel made of only WPI, alginate and cross-linking agents (0.55 % solid mass) had a very weak and heterogeneous structure. Phase separation took place soon after aeration was completed.

During freezing cycle, the mechanical strength of the aerated hydrogels was improved in order to obtain more intact air cells in the final aerogels. Initially, HPMC-K100M and LBG were compared for their stabilizing effects in the aerated hydrogels against freezing treatment (-80 ^{0}C only). The aerogel samples made of LBG showed creamy, less dense appearance and non-uniform structure with two layers, more intact air cells, which were very visible by eye.

The aerogels samples containing K100M showed more uniform microstructure with better defined cell walls, but there were hardly any intact air cells which might have been burst during either freezing or freeze-drying process. As a result, the LBG as a cryo-protectant had impact on the polysaccharide network, and could be used to improve stability of the hydrogels with better structural uniformity.

The effect of two freezing regimes namely slow freezing (-80 ^{0}C) and rapid freezing in liquid nitrogen (- 197 ^{0}C) on aerogel microstructure made of either HPMC or LBG were also stuided. The freeze-dried aerogels obtained with fast (-197 ^{0}C) and slow (-80 ^{0}C) freezing differed in terms of structure. The fast frozen aerogels had some cracks and showed a creamy

appearance with smooth surface. Compared to fast frozen aerogels, slow frozen ones (-80 ^{0}C) did not have crack.

The samples obtained with slow freezing were characterized by heterogeneous structure, more ruptured cells. On the other hand, fast frozen aerogels samples had homogenous structure with more well-defined intact air cells. SEM images indicate that slow freezing (–80 ^{0}C) lead to macro porous materials, whereas rapid freezing in liquid nitrogen resulted in both meso and macro porous structures.

In addition, the macro and micro structure of aerated hydrogels made of alginate, WPI, LBG and cross- linking agents ($CaCO_3$ and GDL) were frozen at two different freezing temperature namely fast freezing in liquid nitrogen and slow freezing at – 80 ^{0}C was compared. LBG aeorgels frozen at two different temperature showed similar microstructure. Altough the both aerogels had irregular structure with damaged cells, the both apeared to have more intact air cells.

Similarly, the freeze dried aerogels containing either LBG or K100M were compared against their macro and micro structure after fast freezing in liquid nitrogen. Visually, the both aerogels appear to be homogenous in nature throughout the entire macrostructure. Microstructure of the both aerogels was destroyed either during freezing or during freeze-drying. However, the both aerogels displayed large amount of intact air bubbles with thin walls separate the pores. Compared to LBG, the samples made of K100M seemed to have more distinctive cells walls with more intact air bubbles. To conclude, regardless of polymer type, fast frozen aerogels had more intact air cells.

Dry mass content of the aerated hydrogels was gradually reduced to 0. 50 % (0.995 % H_2O) from 2.5 %. However, compared to high dry mass content, with low dry mass, weak aerated hydrogel with less uniform structure was formed. Reduction in the dry mass also had a negative effect on overrun. The highest overrun was recorded with 0.875 % dry mass while the lowest dry mass (0.50%) gave the lowest overrun.

The sizes and number of air cells formed in the hydrogels was also dependent on the dry mass content in addition to other physical and chemical parameters. Freeze dried aerogels with the lowest dry mass content appeared to be less dense with creamy colour, sandy texture and visible air cells. High dry mass content aerogel had white creamy appearance, more compact uniform structure. The higher dry mass content showed significantly higher amount of air cells with small pore sizes and therefore appeared to be more porous, while the lower dry mass content (0.50 %) hydrogels contained larger air cells and appeared to be less porous.

Hydrocolloid type has a significant effect on the aerated hydro and aerogel micro and macro structure; K100M provided higher overrun and strongest hydro and aerogel. However, mean diameter of air cells in the aerated hydrogel containing K100M was significantly bigger than A4M and LBG aerated hydrogel. Among all the tested polymers, the lowest overrun was recorded with LBG ($P < 0.014$).

Aerated hydrogel containing K4M had the lowest values of the maximum force (hardness) of compression and followed by LBG. However, the cellulose K100M/alginate aerogels exhibited excellent mechanical properties. K100M had more air cells than A4M and LBG aerogels, which is in correlation with overrun and air cells count results. In general, K100M showed more

regular structure with more open network while the A4M displayed less regular but more compact structure, which might be related to rheleogy of the polymer solution. In terms of hydrogel rheology, K100M displayed the highest shear viscosity followed by K4M, A4M and LBG respectively. The samples containing K100M and A4M displayed the highest G' and but the lowest G" while LBG displayed very low G' moduli.

The structure of freeze-dried aerogels with WPI well aerated. The presence of WPI increase d the overrun. Bigger pore size resulted in higher porosity but less strong hydrogel. The aerated hydrogel samples made of WPI had the highest volume (mm^2) and total surface area (m^3). The porosity of aerated hydrogels prepared with WPI was higher than those without WPI ones. There was a significant difference between two aerated hydrogels (p- value 0.002).

Shear viscosity was slightly higher with WPI, which had some effect on the cell diameter, producing bigger air cells which might have some effect on hydrogel structure. Because it was seen that aerated hydrogel hardness was affected significantly by the presence of WPI in the formulation. Without WPI, all the tested samples had the highest values of the maximum force (hardness) of compression. In addition, effect of WPI on freeze dried aerogel hardness was also measured. In the presence of WPI all the tested aerogel samples displayed the highest values of the maximum force (hardness). Samples made of alginate+K100M-NO WPI was the less hard aerogel by exhibiting minimum force during compression. In the presence of WPI air cells were bigger and heterogeneous while without WPI air cells were smaller and homogenous. With WPI higher elastic modulus (G') was recorded compared to hydrogel without WPI.

The effect of physical parameters including mixing speed (rotation speed) and aeration time (AT), on hydrogel characteristics were studied by means of overrun measurement, texture analysis, CRYO-Sem, and X-ray computed microtomography. Physical parameters had a significant effect on formation of aerated hydrogel and on its characteristics including overrun, texture, air cells morphology, porosity and microstructure.

Overrun (OR) values ranged from 57 % to 91 % depending on the aeration speed. When mixing speed was under 6000 rpm, the aerated media was very unstable. There was a phase separation soon after aeration was completed. However, when mixing speed was increased to 8000 rpm, self-supporting homogenous hydrogel with high overrun was produced.

The highest OR was obtained at 8000 rpm and the lowest OR at 4000 rpm. Slower mixing speed produced less stable foam. There was a rapid phase separation after mixing was completed. The highest overrun was recorded with AT 14 minutes. The air bubbles were more regular and smaller. The longest AT (20 minutes) had 'over beating' effect on the hydrogel structure, producing less strong hydrogel. On the other side, AT 14 minutes provided the highest air cells count, volume (mm^2) and total surface area (m^3). It was observed that increase in the mixing time from 8 to 14 minutes prompted a statistically significant decrease in porosity ($P < .001$).

The effect of varied shearing times on gel rheology was also studied. Increase in shear viscosity was function of shearing time: the longer the shearing time, the higher the viscosity. There was a significant decrease in G' and G". After the longest shearing time (20 minutes), G' and G" moduli decreased as shearing time is increased unlike shear viscosity. Similarly,

the effect of shearing on $CaCO_3$ particles in the presence and absence of GDL under high shearing conditions and its effect on gel formation was also evaluated. $CaCO_3$ average particle size decreased; the longer the shearing time the smaller gets the $CaCO_3$ particles.

A high -aerated hydrogels with carrot juice, orange juice and tomato puree were also studied. Carrot, orange juice and tomato puree were not suitable for the aerated aerogel production due to their low pH level. Only fresh carrot juice with pH 6. 68 formed self-supporing aerated hydrogel.

6.2. Future works

In this thesis, it was shown that creation of highly aerated hydrogels is possible by using ionic-cross linking method and optimisation of two important physical parameters; aeration time and aeration speed. The aeration time 10 minutes and aeration speed 8000 rpm was used as a standard operation parameters for all the tested samples. Due to time length of the project, it was not possible to test effect of shorter aeration time (4-5 minutes) but with very high aeration speed up to 12000 rpm, which could provide even higher overrun. Based on the results, it may be possible to produce highly aerated self-supporting hydrogels in a shorter time if aeration speed is increased. Similar to aeration time and aeration speed, the hydration time of dry mix might be shorter; an hour or even less rather than 2 hours 10 minutes.

Aerated hydrogels are a relatively new concept. For this research sodium alginate was chosen as a gelling polymer. It may worth using other gelling polymer for example kappa carrageenan, in combination with whey proteins in order to expand application area of the

aerated hydrogels, since kappa carrageenan is already widely used in many food applications such as in gelled milk desserts.

Aerated hydro and aerogels may be an alternative method for creating bubbles in porous food materials *i.e*. bread. Therefore, there is need to explore application area of hydro and aerogels as a novel method for creation of porous food structure.

There are different drying methods to remove water from hydrogels *i.e*. freeze drying, vacuum drying and supercritical drying. Supercritical drying is one of the most used techniques for removing the liquid within a hydrogel, which leaves behind only the linked aerogel network. In general, it is performed by venting the solvent above its critical point (generally high temperature) or by prior solvent exchange with another solvent (ethanol) followed by transferring the sample in a supercritical dryer with CO_2 as co-solvent. It would therefore be interesting to obtain aerated aerogels with properties obtained via a supercritical drying method and compare that to e.g. freeze drying.

The application of food grade aerogels as drug or flavour carrier is common. It might be beneficial to assess the encapsulation and loading capacity of one-pot aerogel production and compare to some of the most common flavour encapsulation technologies such as via spray drying.

CHAPTER 7

References

Abbas S., Hayat, K., Karangwa, E., Bashari, M. and Zhang, X. (2013) An overview of Ultrasound-Assisted Food-Grade Nanoemulsions. *Food Engineering Reviews*, **5** (3), 1-13.

Abhari, N., Madadlou, A., and Dini, A. (2017) Structure of starch aerogel as affected by crosslinking and feasibility assessment of the aerogel for an anti-fungal volatile release. *Food Chemistry*, **221**, 147-152.

Adhikari, B., M., Truong, T., Bansal, N. and Bhandari, B. (2017) Use of gases in dairy manufacturing: *A review, Critical Reviews in Food Science and Nutrition*, **58** (15) 1-14.

Adler, M., V. and Weaire, D. (2008) New Foams: Fresh challenges and opportunities. *Current Opinion in Colloid & Interface Science*, **13** (3), 141-149.

Ahmad, B., Stride, E. and Edirisinghe, M. (2012) Calcium Alginate Foams Prepared by a Microfluidic T-Junction System: Stability and Food Applications. *Food and Bioprocess Technology*, **5** (7), 2848-2857.

Ahmed, E. M. (2015) Hydrogel: Preparation, characterization, and applications: *A review. Journal of Advanced Research*, **6** (2), 105-121.

Aken, G. A.V (2001) Aeration of emulsions by whipping. *Colloids and Surfaces A: Physicochemical and Engineering Aspects*, **190**, (3), 333-354.

Alessandro, S., Demitri, C. and Madaghiele, M. (2009) Biodegradable Cellulose-based Hydrogels: Design and Applications*. Materials*, **2**, 353-373.

Alessandro, S., Demitri, C., and Madaghiele, M. (2009) Biodegradable Cellulose-based Hydrogels: Design and Applications. *Materials* **2**, 353-373.

Amagliani L., and Schmitt C., (2017) Globular plant protein aggregates for stabilization of food foams an emulsions. *Annual Review of Food Science and Technology*, **6**, 211-233.

Arboleya, J.C., García-Quiroga, M., Lasa, D., Oliva, O. and Luis-Aduriz A., (2014) Effect of highly aerated food on expected satiety. *International Journal of Gastronomy and Food Science*, **2** (1), 14-21.

Arzeni, C., K. Martínez, K., Zema P., Arias A., Perez, O.E., Pilosof, A. M. R. (2012) Comparative study of high intensity ultrasound effects on food proteins functionality. *Journal of Food Engineering,* **108** (3), 463-472.

Babu, V.R., Sairam, M., Hosamani, K. M. and Aminabhavi, T.M. (2007) Preparation of sodium alginate–methylcellulose blend microspheres for controlled release of nifedipine. *Carbohydrate Polymers*, **69** (2), 241-250.

Baeza, R., Carrera Sánchez, C., Pilosof, A. M. R. and Patino, J. M. (2005) Interactions of polysaccharides with b-lactoglobulin adsorbed films at the air–water interface. *Food Hydrocolloids*, **19**, 239–248.

Bahramparvar, M. and Tehrani, M.M. (2011) Application and Functions of Stabilizers in Ice Cream. *Food Reviews International*, **27**(4), 389-407.

Bajwa, G. S., Sammon, C., Timmins, P. and Melia, C.D. (2009) Molecular and mechanical properties of hydroxypropyl methylcellulose solutions during the sol: gel transition. *Polymer*, **50**, 4571–4576.

Bals, A. and Kulozik, U. (2003a) Effect of pre-heating on the foaming properties of whey protein isolate using a membrane foaming apparatus. *International Dairy Journal*, **13** (11), 903-908.

Bals, A. and Kulozik, U. (2003b) The influence of the pore size, the foaming temperature and the viscosity of the continuous phase on the properties of foams produced by membrane foaming. *Journal of Membrane Science*, **220** (1–2), 5-11.

Banerjee, S., and Bhattacharya, S. (2012) Food Gels: Gelling Process and New Applications, *Journal Critical Reviews in Food Science and Nutrition*, **52**, (4), 334-346.

Banerjee S., Shiv, S., Bhattacharya, S., and Chattopadhyay, P. (2013) Trivalent ion cross-linked pH sensitive alginate-methyl cellulose blend hydrogel beads from aqueous template. International Journal of Biological Macromolecules, 57, 297-307.

Barak, S. and Mudgil, D. (2014) Locust bean gum: Processing, properties and food applications—A review. *International Journal of Biological Macromolecules*, **66**, 74-80.

Barbut, S. and Foegeding, E. A. (1993) Ca^{2+} Induced Gelation of Pre-heated Whey Protein Isolate. *Food Science*, **58** (4), 867-871).

Baxter, I., Cother, L.D., Dupuy, C., Lickiss, P.D., White, A.J.P., Williams, D.J., (1997) Hydrogen bonding to silanols. In: ECTOC-3 (Elec- tronic Conference on Trends in Organometallic Chemistry). http://www.ch.ic.ac.uk/ectoc/ectoc-3/

Bergeron, V. and Walstra, P. (2005) Foams. In: Fundamental of interface and colloid science, ed. Lyklema, J. volume 5. Elsevier.

Bernal, V.M., Smajda, C.H., Smith, J.L. and Stanley, D.W. (1987) Interactions in Protein/Polysaccharide/Calcium Gels. *Journal of Food Science*, **52** (5), 1121- 1125.

Betz, M., García-González, C.A., Subrahmanyam, R.P. and Smirnova, I. and Kulozik, U. (2012) Preparation of novel whey protein-based aerogels as drug carriers for life science applications. *The Journal of Supercritical Fluids*, **72**, 111-119.

Binks, B.P. (2002) Particles as surfactants similarities and differences. *Current Opinion in Colloid & Interface Science,* **7** (1–2), 21-41.

Blom, W.A.M., Koppenol, W.P., Schuring, E.A.H., Slolmon. L., Luben, N.A., David, A.J., and Stoyanov, M.S.D. (2016) Sustained satiety induced by food foams is independent of energy content, in healthy adults. *Appetite*, **97**, 64-71.

Bokulicha, N. A. and Bamforth, C. W. (2013) The Microbiology of Malting and Brewing. *Microbiology and Molecular Biology*, **77** (2), 157-172.

Bournival, G., Ata, S. and Wanless, E.J. (2015) The roles of particles in multiphase process. Particle on bubble surfaces. *Advances in Colloid and Interface Science*, **225**, 114–133.

Boye, J.I., Ma, C.-Y and Harwalkar, V.R. (1997) Thermal Danaturation and Caogulation of Proteins. IN: Food Proteins and Their Application. Ed: Damodoran S. and Paraf A. ISBN 0-8247-9820-1, Marcel Dekker, Inc.

Bureiko. A., Trybala, A., Kovalchuk, N. and Starov, V. (2015) Current applications of foams formed from mixed surfactant-polymer solutions. *Advances in Colloid and Interface Science*, **222**, 670-677.

Campbell G.M. and Mougeot E. (1999) Creation and characterisation of aerated food products. *Trends in Food Science and Technology*, **10**, 283-296.

Campbell, G. (2008) History of Aerated Foods. *A volume in American Associate of Cereal Chemists International*, 1–21.

Carrera, C. R., Sánchez, C.C and Patino, J.M.R. (2005) Interfacial, foaming and emulsifying characteristics of sodium caseinate as influenced by protein concentration in solution. *Food Hydrocolloids*, **19,** (3), 407-416.

Cao, Y., Shen, X., Chen, Y., Gou, J., Chen., Q. and Jiang, X. (2005) pH-Induced Self-Assembly and Capsules of Sodium Alginate. *Biomacromolecules*, **6** (4), 2189-2196.

Chang, C., Duan, B. and Zhang, L. (2009) Fabrication and characterization of novel macroporous cellulose–alginate hydrogels. *Polymer*, **50** (23), 5467-5473.

Chaplin, M. (2018) Water structure and Science. http://www1.lsbu.ac.uk/water/hydrocolloids_gums. html.

Charalampopoulos, D. and Webb, C. (2013) Applications of metabolic Engineering in the Production of Fermented Foods and Food Ingredients. In “Fermentation Processes Engineering in the Food Industry.

Edited by Carlos Ricardo Soccol, Ashok Pandey and Christian Larroche, CRS Press. ISBN: 13: 978-1-4398-8768-4

Chen H-B., Wang, Y-Z. and Schiraldi, D.A. (2013) Foam-like materials based on whey protein isolate. *European Polymer Journal*, **49** (10), 3387-3391.

Chen, J., Chen, D., Xie, Y., Yuan T. and Chen, X. (2013) Progress of Microfluidics for Biology and Medicine. *Nano-Micro Letters*, **5** (1), 6-80.

Chen, L. and Subirade, M. (2006) Alginate–whey protein granular microspheres as oral delivery vehicles for bioactive compounds. *Biomaterials*, **27** (26), 4646-4654.

Cheng, Y., Lu, L., Zhang, W., Jun, J. and Yang, S. (2012) Reinforced low density alginate-based aerogels: Preparation, hydrophobic modification and characterization. *Carbohydrate Polymers*, **88** (3), 1093-1099.

Chiu, N., Hewson, L., Yang, N., Linforth, R. and Fisk, I. (2015) Controlling salt and aroma perception through the inclusion of air fillers. *Food Science and Technology*, **63** (1), 65-70.

Ciesäla, K., Salmieri, S. and Lacroix, M. (2006) *γ*-Irradiation Influence on the Structure and Properties of Calcium Caseinate and Whey Protein Isolate Based Films. Part 2. Influence of Polysaccharide Addition and Radiation Treatment on the Structure and Functional Properties of the Films. *Journal of Agricultural and Food Chemistry*, **54**, 8899-8908.

Ciurzyńska, A. and Lenart, A. (2016) Effect of the aerated structure on selected properties of freeze-dried hydrocolloid gels. *International Agrophysics*, **30**, 9-17.

Ciurzyńska, A., MieszkowskaIgnacy, A. and Lenart , J.A (2017) The effect of composition and aeration on selected physical and sensory properties of freeze-dried hydrocolloid gels. *Food Hydrocolloids*, **67**, 94-103.

Das, N. (2013) Preparation methods and properties of hydrogel: a review**.** *International Journal of Pharmacy and Pharmaceutical Sciences*, **5** (3), 112-117.

Davis, J.P. and Foegeding, E.A. (2004) Foaming and interfacial properties of polymerized whey protein isolate. *Journal of Food Science*, **69** (5), 404-410.

Denkov, D., Tcholakova, S., Golemanov, K., Ananthpadmanabhab, K.P. and Lips A. (2009) The role of surfactant type and bubble surface mobility in foam rheology. *Soft Matter*, **5**, 3389–3408.

Desbrieres, J., Hirrien, M., Ross-Murphy, S.B. (2000) Thermogelation of methylcellulose: rheological considerations. *Polymer*, **41**, 2451-2461.

Dickinson, E. (2003) Hydrocolloids at interfaces and the influence on the properties of dispersed systems. *Food Hydrocolloids*, **17** (1), 25-39.

Dickinson, E. (2010) Food emulsions and foams: Stabilization by particles. *Current Opinion in Colloid & Interface Science*, **15**, 40–49.

Dickinson, E. (2016) Colloids in food: Ingredients, structure and stability. *Annual Review of Food Science and technology*, **6**, 211-233.

Dickinson, E. (2017) Biopolymer-based particles as stabilizing agents for emulsions and foams. *Food Hydrocolloids*, **68**, 219-231.

Dickinson, E., Ettelaie, R., Murray, B.S. and Du, Z. (2002) Kinetics of disproportionation of air bubbles beneath a planar air–water interface stabilised by food proteins. *Journal of Colloid Interface Science*, **252**, 202-214.

Dissanayake, M and Vasiljevic, T. (2009) Functional properties of whey proteins affected by heat treatment and hydrodynamic high-pressure shearing. *Journal of Dairy Science*, **92** (4), 1387-1397.

Donovan, M. and Mulvihill, D.M. (1987) Thermal Denaturation and Aggregation of Whey Proteins. *Irish Journal of Food Science and Technology*, **11**, (1), 87-100.

Doublier, J-L., Garnier, C., Renarda, D. and Sanchez, C. (2000) Protein-polysaccharide interactions. *Current Opinion in Colloid & Interface Science*, **5**, 202-214.

Dutta, A., Chengara, A., Nikolav, A.D., Wasan, D.T., Chen, K. and Campbell, B. (2004) Destabilization of aerated food products: Effects of Ostwald ripening and gas diffusion. *Journal of Food Engineering*, **62** (2), 177-184.

Draget, K.I., Gudmund, Skjåk-Bræk, G. and Stokke, B.T. (2006) Similarities and differences between alginic acid gels and ionically crosslinked alginate gels. *Food Hydrocolloids*, **20** (2–3), 170-175.

Edoura-Gaena, R.B., Allais, I., Trystram, G. and Gros, J-B. (2007) Influence of aeration conditions on physical and sensory properties of aerated cake batter and biscuits. *Journal of Food Engineering*, **79** (3), 1020-1032.

Ellis A.L., Norton A. B., Mills T.B., and Norton I.T. (2017) Stabilisation of foams by agar gel particles. *Food Hydrocolloids*, **73**, 222-228.

Ercelebi, E. A., Ibanoglu, E. (2009) Effects of ionic strength on the foaming properties of whey protein isolate and egg white in the presence of polysaccharides. *Journal of Food Processing and Preservation*, **33** (4), 513-26.

Fameau A-L. and Jalmes A-S. (2017) Non-aqeous foams: Current understanding on the formation and stability mechanisms. *Advances in Colloid Interface Science*, **247**, 454-464.

Farrés, I.F., DouaireI, M. and Norton, I.T. (2013) Rheology and tribological properties of Ca-alginate fluid gels produced by diffusion-controlled method. *Food Hydrocolloids*, **32** (1), 115-122.

Farrés, I.F. and Norton, I.T. (2014) Formation kinetics and rheology of alginate fluid gels produced by in-situ calcium release. *Food Hydrocolloids*, **40**, 76-84.

Farrés, I.F., Moakes, R.J.A. and Norton, I.T. (2014) Designing biopolymer fluid gels: A microstructural approach. *Food Hydrocolloids*, **42** (3), 362-372.

Feng, Y., Kopplin, G., Sato, K., Draget, K. and Vårum, K. M. (2017) Alginate gels with a combination of calcium and chitosan oligomer mixtures as crosslinkers. *Carbohydrate Polymers*, **156**, 490-497.

Fernandez, P., Andre, V., Rieger, J. and Kuhnle, A. (2004) Nano-emulsion formation by emulsion phase inversion. Colloids and Surfaces A: *Physicochemical Engineer Aspects*, **251**, 53–58.

Fernández, P.P., Martino, M.N., Zaritzky, N.E., Guignon, B. and Sanza, P.D. (2007) Effects of locust bean, xanthan and guar gums on the ice crystals of a sucrose solution frozen at high pressure. *Food Hydrocolloids*, **21**, 507–515.

Field R. and Lipnizki, F. (2017) Basic Principles of Membrane Process. In: Engineering Aspects of Membrane Separation and Application in Food Processing. Edited by Robert Field, Erika Bekassy-Molnar, Frank Lipnizki and Gyula Vataio. Taylor &Francis Group.

Foegeding, E.A., Luck, P.J. and Davis, J.P. (2006) Factors determining the physical properties of protein foams. *Food Hydrocolloids*, **20** (2–3), 284-292.

Foegeding, E.A., Stieger M., Velde F., (2017) Moving from molecules, to structure, to texture perception. *Food Hydrocolloids*, **68**, 31-42.

Forslund, B., Torgerson, H., J.S., Sjöström, Lindroos, L. (2005) Snacking frequency in relation to energy intake and food choices in obese men and women compared to a reference population. *International Journal of Obesity*, **29** (6), 711-719.

Fundo, J.F., and Silva, C.L.M. (2018) 2- Microstructure, composition and their relationship with molecular mobility, food quality and stability. In: Food Microstructure and Its Relationship with Quality and Stability, Woodhead Publishing Series in Food Science, Technology and Nutrition, 29-41.

Fyen, W., Paul W. Mertens, P.W (2008) Developments in Surface Contamination and Cleaning (Second Edition).

Garrec, D. A. and Norton, I.T. (2012) Understanding fluid gel formation and properties. *Journal of Food Engineering*, **112**, 175-182.

Goff, H.D., Ferdinando, D. and Schorsch, C. (1999) Fluorescence microscopy to study galactomannan structure in frozen sucrose and milk protein solutions. *Food Hydrocolloids*, **13**(4), 353-362.

Gonzenbach, U. T., Studart, A. R. and Tervoort, E. (2006) Stabilization of Foams with Inorganic Colloidal Particles. *Langmuir*, **22** (26), 10983–10988.

Gun'ko, V.M., Savina, I.N. and Mikhalovsky, S.V. (2013) Cryogels: Morphological, structural and adsorption characterisation. *Advances in Colloid and Interface Science*, **187–188**, 1-46.

Guo, J., Jin, Y., Yang, X-O., Yu, S-J., Yin, S-W. and Qi, J-R. (2013) Computed microtomography and mechanical property analysis of soy protein porous hydrogel prepared by homogenizing and microbial transglutaminase cross-linking. *Food Hydrocolloids*, **31** (2), 220-226.

Haedelt, J., Beckett, S.T. and Niranjan, K. (2007) Bubble-Induced Chocolate: Relation Structure with Sensory Response. *Journal of Food Science*, **72**, (3), 138-142.

Haffner, B., Khidas Y., and Pitois O. (2015) The drainage of foamy granular suspensions. *Journal of Colloid and Interface*, **458**, 200-208.

Hanselmann, W. and Windhab, E. (1999) Flow characteristics and modeling of foam generation in a continuous rotor/stator mixer. *Journal of Food Engineering*, **38**, 393-405.

Haque, A. and Morris, E. R. (1993) Thermogelation of methylcellulose. Part I: Molecular structures and processes. *Carbohydrate Polymers*, **22**, 161-173.

Haque, A., Richardson, R.K., Morris, E.R., Gidley, M.J. and Caswell, D.C. (1993) Thermogelation of methylcellulose. Part II: Effect of hydroxypropyl substituents. *Carbohydrate Polymers*, **22** (3), 175-186.

Harper, E. K., and Shoemaker, C. F. (1983). Effects of locust bean gum and selected sweetening agents on ice recrystallization rates. *Journal of Food Science*, **48**, 1801–1803.

Hilgenfeldt, S., Koehler, S.A. and Stone, H.A. (2001) Dynamics of coarsening foams. Accelerated and Self-Limiting Drainage. *Physical Review Letters*, **86**, 4704.

Hirrien, M., Chevillard, C., Desbrières, J., Axelos, M.A.V, Rinaudo, M. (1998) Thermogelation of methylcelluloses: new evidence for understanding the gelation mechanism. *Polymer*, **39** (25), 6251-6259.

Holmes, A.S. (2000) Microenginering- The next revolution. Proc. 12th IFHTSE Congress, 3, 1-8.

Horozov, T.S. (2008) Foams and foam films stabilised by solid particles. *Current Opinion in Colloid & Interface Science*, **13**, (3), 134-140.

Hu, H., Fan, X., Zhou, Z., Xu, X., Fan, G., Wanga L., Huang, X., Pan, S. and Zhu, L. (2013) Acid-induced gelation behaviour of soybean protein isolate with high intensity ultrasonic pre-treatment. *Ultrasonic Sonochemistry*, **20**, 187-195.

Hunter, T.N., Pugh, R.J., Franks, G.V. and Jameson, G.J. (2008) The role of particles in stabilising foams and emulsion. *Advances in Colloid and Interface Science*, **137** (2), 57-81.

Husing N. and Schubert, U. (1998) Aerogels–Airy Materials: Chemistry, Structure, and Properties. *Angewandte Chemie, International edition*, **37**, 22 -45.

Jana, S., Gandhi, A., Sheet, S. and Sen, K.K. (2015) Metal ion-induced alginate–locust bean gum IPN microspheres for sustained oral delivery of aceclofenac. *International Journal of Biological Macromolecules*, **72**, 47–53.

Jiang, L., Li, Y., Wang, Z., Liang J., Wanga R., Chena, Y W., Qi, B. and Zhang, M. (2014) Effects of ultrasound on the structure and physical properties of black bean protein isolate. *Food Research International*, **62**, 595-601.

Jiang, S., Hussain, M. A., Cheng, J., Jiang, Z., Geng, H., Sun, Y., Sun, C. and Hou, J. (2018) Effect of heat treatment on physicochemical and emulsifying properties of polymerized whey protein concentrate and polymerized whey protein isolate. *LWT- Food Science and Technology*, **98**, 134-140.

Joshi, S. C. (2011) Sol-Gel Behaviour of Hydroxypropyl Methylcellulose (HPMC) in ionic Media Including Drug Release. *Materials*, **4**, 1861-1905.

Ju, Z.Y. and Kilara, A. (1998) Properties of Gels Induced by Heat, Protease, Calcium Salt, and Acidulant from Calcium Ion-Aggregated Whey Protein Isolate. *Journal of Dairy Science*, **81** (5), 1236-1243.

Kaklamani, G., Cheneler, D., Grover, L.M., Adams, M.J. and Bowen, J. (2014) Mechanical properties of alginate hydrogels manufactured using external gelation. *Journal of the Mechanical Behavior of Biomedical Materials*, **36**, 135-142.

Kamath, S., Hupper, T., Houlihan, A.V. and Deeth, H.C. (2008) The influence of temperature on the foaming of milk. *International Dairy Journal*, **18**, 994–1002.

Kang, H-W., Tabata, Y. and Ikada, Y. (1999) Fabrication of porous gelatin scaffolds for tissue engineering. *Biomaterials*, **20**, 14, 1339-1344.

Karim, M. A. and Favzia S., (2018) Food Microstructure as affected by processing and its effect on quality and stability. In: Food Microstructure and Its Relationship with Quality and Stability, Woodhead Publishing, Hardcover ISBN: 9780081007648.

Kato, T., Yokoyama, M., Takahashi, A. (1978) Melting temperatures of thermally reversible gels IV. Methyl cellulose-water gels. C*olloid and Polymer Science*, **56** (1), 15–21.

Kim, H., Min, K-I., Inoue, K., Im, D. J., Kim, D-P, and Yoshida J-I. (2016) Submillisecond organic synthesis: Outpacing Fries rearrangement through microfluidic rapid mixing. *Science*, **352** (6286), 691-694.

Kinsella, J.E. (1981) Functional properties of proteins: Possible relationships between structure and function in foams. *Food Chemistry*, **7** (4), 273-288.

Kleemann, C., Selmer I and Smirnova I. (2018) Tailor made protein based aerogel particles from egg white protein, whey protein isolate and sodium caseinate: Influence of the preceding hydrogel characteristics. *Food Hydrocolloids*, **83**, 365-374.

Kokini, J. and Aken, G.V. (2006) Discussion session on food emulsion and foams. *Food Hydrocolloids*, **20**, 438–445.

Kolfschoten, R.C. (2011) Reaction and separation opportunities with microfluidic devices. Thesis, Wageningen University, Wageningen, NL. ISBN 978-90-8585-864-5

Kukizaki, M. and Goto M. (2006) Size control of nanobubbles generated from Shirasu-porous-glass (SPG) membranes. *Journal of Membrane Science*, **281**, 386-396.

Laakkonen, M., Moilanen, P. and Aittamaa, J. (2005) Local bubble size distributions in agitated vessels. *Chemical Engineering Journal*, **106**, 133-143.

Langevin. D. (2017) Aqueous foams and foam stabilised by surfactant. Gravity-free study. *Comptes Rendus Mécanique*, **345** (1), 47-55.

Laporte M., Montillet, A., Valle, D.D., Loisel C. and Riaublanc, C. (2016) Characteristics of foams produced with viscous shear thinning fluids using microchannels at high throughput. *Journal of Food Engineering*, **173**, 25-33.

Lau, K. and Dickinson, E. (2004) Structural and Rheological Properties of Aerated High Sugar Systems Containing Egg Albumen. *Journal of Food Science*, **69** (5), 232-239.

Lau, C.K. and Dickinson, E. (2005) Instability and structural change in an aerated system containing egg albumen and invert sugar. *Food Hydrocolloids*, **19** (1), 111-121.

Lazidis, A., Hancocks, R.D., Spyropoulos, F., Kreuß, M., Berrocal, R. and Norton, I.T. (2016) Whey protein fluid gels for the stabilisation of foams. *Food Hydrocolloids*, **53**, 209-217.

Lazidis, A., Parizotto, L.A., Spyropoulos, F., Norton, I.T. (2017) Microstructural design of aerated food systems by soft-solid materials. Microstructural design of aerated food systems by soft–solid. *Food Hydrocolloids*, **73**, 110-119.

Lazidis A., Parizotto, L.A., Spyropoulos F. and Norton, I.T (2018) Microstructural design of aerated food systems by soft-solid materials. *Food Hydrocolloids*, **78**, 26-35.

Le, X. T. and Turgeon, S.L. (2015) Textural and water binding behaviours of β -lactoglobulin-xanthan gum electrostatic hydrogels in relation to their microstructure. *Food Hydrocolloids*, **49**, 216 -223.

Le, X.T., Rioux, L-E and Turgeon, S.L. (2017 Formation and functional properties of protein–polysaccharide electrostatic hydrogels in comparison to protein or polysaccharide hydrogels. *Advances in Colloid and Interface Science*, **239**, 127-135.

Lee, K.Y. and Mooney, D.J. (2012) Alginate: Properties and biomedical applications. *Progress in Polymer Science*, **37** (1), 106-126.

Lee, M.H., Baek, M.H, Cha, D.S., Park, H.J and Lim, S.T. (2002) Freeze–thaw stabilization of sweet potato starch gel by polysaccharide gums. *Food Hydrocolloids*, **16** (4), 345-352.

Lee, T., Neethling, S.J. and Cilliers, J.J. (2005) Particle and liquid dispersion in foams. Colloids and Surfaces A: *Physicochemical and Engineering Aspects***, 263**, 320–329.

Leo, W.J., McLoughlin, J. and Malone, D. (1990) Effects of Sterilization Treatments on Some Properties of Alginate Solutions and Gels. *Biotechnology Progress*, **6**, 51-53.

Liang, H-F., Hong, M-H., Ho, R-M., Chung, C-K., Lin, Y-H., Chen, C-H. and Sung, H-W. (2004) Novel Method Using a Temperature-Sensitive Polymer (Methylcellulose) to Thermally Gel Aqueous Alginate as a pH-Sensitive Hydrogel. *Biomacromolecules*, **5**, 1917-1925.

Liang, H-F., Hong, M-H., Ho, R-Mi., Chung, C-K., Lin, Y-H, Chen, C-H. and Sung, H.-W. (2004) Novel Method Using a Temperature-Sensitive Polymer (Methylcellulose) to Thermally Gel Aqueous Alginate as a pH-Sensitive Hydrogel. *Biomacromolecules*, **5** (5), 1917-1925.

Liehr, M. and Kulicke, W. M. (1996). Rheological examination of the influence of hydrocolloids on the freeze–thaw stability of starch gels. *Starch*, **48**, 52–57.

Lin, S-Y., Wang, S-L., Wei, Y-S. and Li, M-J. (2007) Temperature effect on water desorption from methylcellulose films studied by thermal FT-IR microspectroscopy. *Surface Science*, **601,** 781–785.

Lioumbas, J.S., Georgiou, E., Kostoglou, M. and Karapantsios, T.D. (2015) Foam free drainage and bubbles size for surfactant concentrations below the CMC. *Colloids and Surfaces A: Physicochemical and Engineering Aspects,* **487***, 92-103.*

Liu, Z., Li, J., Nie, S., Liu, H., Ding, P. and Pan, P. (2006) Study of an alginate/HPMC-based in situ gelling ophthalmic delivery system for gatifloxacin. *International Journal of Pharmaceutics*, **315** (1–2), 12-17.

Long, L.Y., Weng, Y.X. and Wang, Y.Z. (2018) Cellulose Aerogels: Synthesis, Applications, and Prospects. *Polymers*, **10**, 1-28.

Madhavi, C., Babu, K., Maruthi, Y., Parandhmama, A., Reddy, O.S., Rao K.C., Subha, MC.S. and Kumar, J. (2017) Sodium alginate -locust bean gum IPN hydrogel beads for the controlled delivery of nimesulide-anti-inflammatory drug. *International Journal of Pharmacy and Pharmaceutical Sscience*, **6** (20), 245-252.

Magrabi, S.A. and Dlugogorski, B.Z. (2002) Foam drainage, coarsening and evaporation. Chapter 6, in: Transport processes in bubbles, drops and particles, ed. Kee, D.D. and Chhabra, Second edition, by Taylor&Francis. ISBN 1-56032-906-8.

Maleki, H. and Kulozik, U. (2016) Recent advances in aerogels for environmental remediation applications. *Chemical Engineering Journal*, **300**, 98–118.

Maleki, H., Durães, L., García-González, C.A., Gaudio, P. Portugal, A., Mahmoudi, M. (2016) Synthesis and biomedical applications of aerogels: Possibilities and challenges. *Advances in Colloid and Interface Science*, **236**, 1-27.

Malik, M.A. Sharma, H. K. and Saini, C. S. (2017) High intensity ultrasound treatment of protein isolate extracted from dephenolized sunflower meal: Effect on physicochemical and functional properties. *Ultrasonics Sonochemistry*, **39**, 511–519.

Manoi, K. (2009) Physico-chemical properties of whey protein concentrate texturized by reactive supercritical fluid extrusion. A Dissertation. Present to the Faculty of the Graduate School of Cornwell University. In partial fulfilment of the requirements for the degree of Doctor of Philosophy.

Marco, I. and Reverchon, E. (2017) Starch aerogel loaded with poorly water–soluble vitamins through supercritical CO2 adsorption. *Chemical Engineering Research and Design*, **119**, 221-230.

Massey, A.H., Khare, A.S. and Niranjan, K. (2001) Air inclusion into a model cake batter using a pressure whisk: Development of gas hold-up and bubble size distribution *Journal of Food Science*, **66** (8), 1152-1157.

McClements, D.J. and Keogh, M. K. (1995) Physical properties of cold-setting gels formed from heat-denatured whey protein isolate. *Journal of the Science of Food and Agriculture*, **69** (1), 7-14.

Mehling, T., Smirnova, I., Guenther, U. and Neubert, R.H. (2009) Polysaccharide –based aerogles as drug carriers. *Journal of Non-Crystalline Solids*, **355** (50–51), 2472-2479.

Mehmandoost, F., Hojjatoleslamy, M., Keramat, J., Behzadniya, A., Shahbazpour, N. and Ghafari, Z. (2014) Effect of pH and salts on rheological properties of sodium alginate-hydroxypropyl cellulose mixture solutions. *International Journal of Biosciences*, **4**, (1), 82-92, 2014.

Melnikov S.A., Stoyanov S. D., Kovacs E.M.R., Arnaudov L., Groot P., Schuring E.A.H., Wiseman S.A., Mela D.J. and Peters H.P.F. (2014) Sustained Hunger Suppression from Stable Liquid Food Foams. *Obesity*, **22** (10), 2131-2136.

Message, J-C., Blanchard, C., Vall-Mint-Dah, F., Lafarge, C., Assifaoui, A. and Saurel, R. (2013) The effects of sodium alginate and calcium levels on pea proteins cold-set gelation. *Food Hydrocolloids*, **31** (2), 446-457.

Mikkonen, K.S., Parikka K., Ghafar, A., Tenkanen, M. (2013) Prospects of polysaccharide aerogels as modern advanced food materials. *Trends in Food Science & Technology*, **34**(2), 124-136.

Miller-Livney, T. and Hartel, R.W. (1997) Ice Recrystallization in Ice Cream: Interactions between sweeteners and stabilizers. *Journal of Dairy Science*, **80** (3), 447-456.

Mishra, S., Mann, B. and Joshi, V.K. (2001) Functional improvement of whey protein concentrate on interaction with pectin. *Food Hydrocolloids*, **15** (1), 9-15.

Moakes, R.J.A., Sullo, A. and Norton, I.T. (2015) Preparation and characterization of whey protein fluid gels: The effects of shear and thermal history. *Food Hydrocolloids*, **45**, 227-235.

Morales, R., Martinez, K., D., Pizones, V. M., Ana, R-H., and Pilosof, A. S. (2015) Modification of foaming properties of soy protein isolate by high ultrasound intensity: Particle size effect. *Ultrasonic Sonochemistry*, **26**, 48-55.

Müller-Fischer, N., Bleuler, H. and Windhab, E.J. (2007) Dynamically enhanced membrane foaming. *Chemical Engineering Science*, **62** (16), 4409-4419.

Murray, B.S. and Ettelaie, R. (2004) Foam stability: proteins and nanoparticles. *Current Opinion in Colloid & Interface Science*, **9** (5), 314-320.

Murray, B.S. (2007) Stabilisation of bubbles and foams. *Current Opinion in Colloid & Interface Science*, **12** (4–5), 232-241.

Murray, K., Placidi, E., Schuring., E.A., Hoad, C.L., Koppenol, W., Arnaudov, L.N., Blom W.A., Pritchard, S.E., Stoyanov, S.D., Gowland, P.A., Spiller, R.C., Peters, H.P., Marciani, L. (2014) Aerated drinks increase gastric volume and reduce appetite as assessed by MRI: a randomized, balanced, crossover trial. *America Journal of Clinical Nutrition*, **101** (2), 270-278.

Narchi I., Vial C. and Djelveh G., (2009) Effect of protein-polysaccharide mixtures on the continuous manufacturing of foamed food products. *Food Hydrocolloids*, **23** (1), 188-201.

Nešić A., Gordić, M., Davidović, S., Radovanović, Z., Nedeljković J. and Smirnova I. (2018) Pectin-based nanocomposite aerogels for potential insulated food packaging application. *Carbohydrate Polymers*, **195**, 128-135.

Ni, X., Ke, F., Xiao, M., Wu, K., Kuang, Y., Corke, H. and Jiang, F. (2016) The control of ice crystal growth and effect on porous structure of konjac glucomannan-based aerogels. *International Journal of Biological Macromolecules,* **92**, 1130-1135.

Nishinari, K., Fang, Y., Yang, N., Yao, X., Zhao, M., Zhang, K. and, Gao, Z. (2018) Gels, emulsions and application of hydrocolloids at Phillips Hydrocolloids Research Centre. *Food Hydrocolloids*, **78**, 36-46.

Nochos, A., Douroumis, D. and Bouropoulos, N. (2008) In vitro release of bovine serum albumin from alginate/HPMC hydrogel beads. *Carbohydrate Polymers*, **74** (3), 451-457.

Norton, I.T, Jarvis, D.A. and Foster, T.J. (1999) A molecular model for the formation and properties of fluid gels. *International Journal of Biological Macromolecules*, **26**, 155-261.

Norton J.E., Gonzalez Espinosa Y., Watson R.L., Spyropoulos, F., and Norton, I.T. (2015) Functional food microstructures for macronutrient release and delivery. *Food & Function*, **6**, 663-678.

Nunamaker, E.A., Otto, K.J., Kipke, D.R. (2011) Investigation of the material properties of alginate for the development of hydrogel repair of dura mater. *Journal of the Mechanical Behavior of Biomedical Materials*, **4** (1), 16-33.

O'Briena, F. j., Harley, B. A., Yannas, L.V. and Gibsona, L. (2004) Influence of freezing rate on pore structure in freeze-dried collagen-GAG scaffolds. *Biomaterials*, **25**, 1077–1086.

Orrego, M., Troncoso, E. and Zúñiga, R.N. (2015) Aerated whey protein gels as new food matrices: Effect of thermal treatment over microstructure and textural properties. *Journal of Food Engineering*, **163**, 37-44.

Osterholt, M., Liane, S. R. and Roll, B. J. (2007) Incorporation of air into a snack food reduces energy intake. *Appetite*, **48** (3), 351-358.

O'Sullivan, J.J., Murray, B. A., Flynn, Cal, and Norton I.T (2016) The effect of ultrasound treatment on the structural, physical and emulsifying properties of animal and vegetable proteins. *Food Hydrocolloids*, **53**, 141-154.

Park, S. H., Hong, G. P., Kim, J. Y., Choi, M. J. and Min, S. G. (2006) The influence of food hydrocolloids on changes in the physical properties of ice cream. *Food Science and Biotechnology*, **15** (5), 721–727.

Patino J. M.R., Delgado, M-D, and Fernández N. (1995) Stability and mechanical strength of aqueous foams containing food proteins. Colloids and Surfaces A: *Physicochemical and Engineering Aspects*, **99** (1), 65-78.

Pei, E.X. and Schmidt, Z.J. (2010) Ice cream: Foam formation and stabilisation. *Food Reviews International*, **26** (2), 122-137.

Peng, F., He, S., Yi, H., Li, Q., Xu, W., Wang, R. and Ma, Y. (2018) Physical, textural, and rheological properties of whipped cream affected by milk fat globule. Membrane protein. *International Journal of Food Properties*, **21** (1), 1190–1202.

Perez, A. A., Carrara, C.R., Sánchez, C.C., Liliana, G. Santiago, L.G. and Patino, J. M.R. (2009) Interfacial dynamic properties of whey protein concentrate/polysaccharide mixtures at neutral pH. *Food Hydrocolloids*, **23** (5), 1253-1262.

Pérez, O.E., Wargon, V. and Pilosof, A.R. (2006) Gelation and structural characteristics of incompatible whey proteins/hydroxypropylmethylcellulose mixtures. *Food Hydrocolloids*, **20** (7), 966-974.

Peters, H.P.F, Koppenol, W.P., Schuring, E.A.H., Abrahamse, S.L. and Mela, D.J (2015) The effect of a low-energy food foam on appetite measures during a 1-day reduced-energy meal. *International Journal of Obesity*, **39** (2), 361-367.

Pierre, A.C. and Pajonk, G.M. (2002) Chemistry of Aerogels and Their Applications. *Chemical Reviews*, **102** (11), 4243–4266.

Plazzotta, S., Calligaris, S. and Manzocco, L. (2018) Innovative bioaerogel-like materials from fresh-cut salad waste via supercritical-CO_2-drying. *Innovative Food Science & Emerging Technologies*, **47**, 485-492.

Rabiey, L. and Britten, M. (2009) Effect of protein composition on the rheological properties of acid-induced whey protein gels. *Food Hydrocolloids*, **23** (3), 973-979.

Raikos, V. (2010) Effect of heat treatment on milk protein functionality at emulsion interfaces: A review. *Food Hydrocolloids*, **24**, 259-265.

Raikos, V., Campbell, L. and Euston, S. (2007) Effects of sucrose and sodium chloride on foaming properties of egg white proteins. *Food Research International*, **40,** 347-54.

Ramachandran, S., Fontanille, P., Pandey, A., and Larroche, C. (2006) Gluconic Acid: Properties, Applications and Microbial Production. *Food Technology and Biotechnology*, **44** (2), 185–195.

Ramdhan, R., Ching, S.H., Prakash, S. and Bhandari, B. (2019) Time dependent gelling properties of cuboid alginate gels made by external gelation method: Effects of alginate-CaCl2 solution ratios and pH. *Food Hydrocolloids*, **90**, 232-240.

Ranken M.D, Kill R.C., and Baker C.G.J. (1997) Snack Food and Breakfast Cereal. In: Food Industries Manual, 24th edition. Blackie Academic& Professional.

Rinaudo, M. (2014) Biomaterials based on a natural polysaccharide: alginate. *TIP***, 17** (1), 92-96.

Rio, E., Drenckhan, W., Salonen, A. and Langevin, D. (2014). Unusually stable liquid foams. *Advances in Colloid and Interface Science*, **205**, 74-86.

Rolls, B.J., and Roe, L.S. (2002) Effect of the volume of liquid food infused intragastrically on satiety in women. *Physiology and Behaviour*, **76** (4-5), 623-631.

Rolls, B.J., Bell, E.A., and Waugh, B.A. (2000) Increasing the volume of a food by incorporating air affects satiety in men. *American Journal of Clinical Nutrition*, **72** (2), 361-368.

Roshanghias, S. and Madadlou, A. (2018) Functional and gel properties of whey protein nanofibrils as influenced by partial substitution with cellulose nanocrystal and alginate. *International Dairy Journal*, **81,** 53-61.

Ross, K.A, Pyrak-Nolte, L.J and Campanella, O.H. (2006) The effect of mixing conditions on the material properties of an agar gel—microstructural and macrostructural considerations. *Food Hydrocolloids*, **20,** 79–87.

Ruel-Gariepy, E. and Leroux, J-C. (2004) In situ-forming hydrogels—review of temperature-sensitive systems. *European Journal of Pharmaceutics and Biopharmaceutics*, **58** (2), 409-426.

Sadahira, M.S., Rodrigues, M.I., Akhtar, M., Murray, B.S. and Netto, F.M. (2018) Influence of pH on foaming and rheological properties of aerated high sugar system with egg white protein and hydroxypropylmethylcellulose. *LWT- Food Science and Technology*, **89**, 350-357.

Sammon, C., Bajwa, G., Timmins, P. and Melia, C.D. (2006) The application of attenuated total reflectance Fourier transform infrared spectroscopy to monitor the concentration and state of water in solutions of a thermally responsive cellulose ether during gelation. *Polymer*, **47**, 577–584.

Savina, I.N., Gun'ko, V.M., Turov, V.V., Dainiak, M., Phillips, G.J., Galaevd, I.Y. and Scanlon M.G. and Zghal. M.C. (2001) Bread properties and crumb structure. *Food Research International*, **34**, 841-864.

Scanlon, M.G. and Zghal, M.C. (2001) Bread properties and crumb structure. *Food Research International*, **34**(10), 841-864.

Schmitt, C. and Turgeon, S.L. (2011) Protein/polysaccharide complexes and coacervates in food systems. *Advances in Colloid and Interface Science*, **167** (1-2), 63-70.

Selmer, I., Kleemann, C., Kulozik U., Heinrich, S. and Smirnova. I. (2015) Development of egg white protein aerogels as new matrix material for microencapsulation in food. *Journal of Supercritical Fluids*, **106**, 42-49.

Shchipunov, Y.A. and Koneva, E.L. (2002) Homogeneous alginate gels: Phase behavior and rheological properties. *Polymer Science Series A*, **44** (7), 758-766.

Sheng, L., Wang Y., Chen J., Zou J., Wang Q. and Ma, M. (2018) Influence of high-intensity ultrasound on foaming and structural properties of egg white. *Food Research International*, **108**, 604-610.

Skurtys, O. and Aguilera, J.M. (2008) Applications of microfluidic devices in food engineering. *Food Biophysics*, **3** (1), 1-15.

Smirnova, I. and Gurikov, P. (2018) Aerogel production: Current status, research directions, and future opportunities. *The Journal of Supercritical Fluids*, **134**, 228-233.

Solar, O. and Gunasekaran, S. (2010) Rheological properties of rennet casein-whey protein gels prepared at different mixing speeds. *Journal of Food Engineering*, **99**, 338–343.

Souidi, K., Mardaru A., Roudet, M., Marcati, A., Valle, D.D. and Dveljeh, G. (2012) Effect of impellers configuration on the gas dispersion in high-viscosity fluid using narrow annular gap unit. Part 1: Experimental approach. *Chemical Engineering Science*, **74**, 287-295.

Stergar, J. and Maver, U. (2016) Review of aerogel-based materials in biomedical applications. *Journal of Sol-Gel Science and Technology*, **77**, 738–752.

Ström, A. and Williams, M.A.K. (2003) Controlled Calcium Release in the Absence and Presence of an Ion-Binding Polymer. *Journal of Physical Chemistry*, **107**, 10995-10999.

Sudhakar, K., Naryana, Reddy N., Jayaramudu, T., Jayaramudu, J., Babul Reddy, A., Manjula, A and Emmanuel Rotimi, S. (2016) Chapter 5- Aerogels and Foamed Nanostructured Polymer Blends. In: Design and Applications of Nanostructured Polymer Blends and Nanocomposite Systems: A volume in Micro and Nano Technologies. ISBN: 978-0-323-39408-6.

Talansier, E., Dellavalle, D., Loisel C., Desremaux, A. and Legrand, J. (2013) Elaboration of Controlled Structure Foams with the SMX Static Mixer. *AIChE Journal*, **59**(1), 132-145.

Tan, M.C., Chin, N. L., Yusof, Y.A., Taip, F.S. and Abdullah, J. (2015) Characterisation of improved foam aeration and rheological properties of ultrasonically treated whey protein suspension. *International Dairy Journal*, **43**, 7.14

Tang, C.H., Wang, X.Y., Yang, X.Q. and Li, L. (2009) Formation of soluble aggregates from insoluble commercial soy protein isolate by means of ultrasonic treatment and their gelling properties, *Journal of Food Engineering*, **92**, 432–437.

Tannahill, R. (1998) Food in History. Three Rivers Press: New York, 48.

Tavares, C., and Lopes da Silva, J.A. (2003) Rheology of galactomannan–whey protein mixed systems. *International Dairy Journal*, **13**, 699–706.

Tolstoguzov, V. B. (1991) Functional properties of food proteins and role of protein-polysaccharide interaction. *Food Hydrocolloids*, **4** (6), 429-468.

Torcello-Gomez, A., and Foster, T.J. (2014) Interactions between cellulose ethers and a bile salt in the control of lipid digestion of lipid-based systems. *Carbohydrate Polymers*, **113**, 53-61.

Torcello-Gomez, A., and Foster, T.J. (2016) Influence of interfacial and bulk properties of cellulose ethers on lipolysis of oil-in-water emulsions. *Carbohydrate Polymers*, **144**, 495–503.

Turgeon, S.L. and Beaulieu, M. (2001) Improvement and modification of whey protein gel texture using polysaccharides. *Food Hydrocolloids*, **15** (4–6), 583-591.

Ubeyitogullari, A. and Ciftci, O.N. (2016) Formation of nanoporous aerogels from wheat starch. *Carbohydrate Polymers*, **147**, 125-132.

Ulker, Z. and Erkey, C. (2014) An emerging platform for drug delivery: Aerogel based systems. *Journal of Controlled Release*, **177**, 51-63.

Velasco, A.M., Calleros, C L., Hernandez-Rodriguez, B. E., Guerrero, A.R., Ramirez, J.A. and Carter, E.J.V. (2018) High intensity ultrasound treatment of faba bean (Vicia faba L.) protein: Effect on surface properties, foaming ability and structural changes. *Ultrasonics Sonochemistry*, 44, 97-105.

Vera, M.U. and Durian, D.J. (2002) Enhanced drainage and coarsening in Aqueous Foams. *Physical Review Letter*, **88** (8), 088304-1 -088304-4.

Vyakaranam, K. and Kokini, J.L. (2008) Study of Dynamics and Size Distribution of air bubbles during mixing in a continuous food mixer. In Bubbles in Food 2: Novelty, Health and Luxury. Editor, Grant Campbell.

Wallick, D. (2014) Chapter 17 - Cellulose Polymers in Microencapsulation of Food Additives. Microencapsulation in the Food Industry, A Practical Implementation Guide, 181-193.

Wang, J., Nguyen A.V., and Farrokpay (2016) A critical review of the growth, drainage and collapse of foams. *Advances in Colloid and Interface Science*, **228**, 55-70.

Wichchukit, S., Oztop, M.H., McCarthy, M.J., and McCarthy, K.L. (2013) Whey protein/alginate beads as carriers of a bioactive component. *Food Hydrocolloids,* **33**, 66-73.

Wilde P.J. (2000) Interfaces: their role in foam and emulsion behaviour. *Current Opinion in Colloid & Interface Science*, **5** (3–4), 176-181.

Wu, T.Y., Guo, N., The, C.Y. and Hay, J.X.W. (2013) Theory and Fundamentals of Ultrasound. IN: Advances in Ultrasound Technology for Environmental Remediation, Springer Briefs in Green Chemistry for Sustainability.

Xiong, T., Xiong, W., Ge, M., Xia, J., Li, B. and Chen, L. (2018) Effect of high intensity ultrasound on structure and foaming properties of pea protein isolate. *Food Research International*, **109**, 260-267.

Zazzali, I., Calvo, T.R A., Ruíz-Henestrosa, V.M.P., Santagapita, P.R. and Perullini, M. (2019) Effects of pH, extrusion tip size and storage protocol on the structural properties of Ca (II)-alginate beads. Carbohydrate Polymers, 206, 749-756

Zhang, W., Zhang, Y., Lu, C. and Deng, Y. (2012) Aerogels from crosslinked cellulose nano/micro-fibrils and their fast shape recovery property in water. *Journal of Materials Chemistry*, **22**, 11642-11650.

Zúñiga, R. N. and Aguilera J.M. (2008) Aerated food gels: fabrication and potential applications. *Trends in Food Science & Technology*, **19** (4), 176-187.

Zuñiga, R.N and Aguilera, J.M. (2009) Structure–fracture relationships in gas-filled gelatin gels. *Food Hydrocolloids*, **23**, 1351–1357.

Zúñiga, R.N., Kulozik, U., and Aguilera, J.M. (2011) Ultrasonic generation of aerated gelatin gels stabilized by whey protein b-lactoglobulin. *Food Hydrocolloids*, **25**, 958-967

Cited web sites

Dow Chemical web site (2018). Chemistry of METHOCEL™. Cellulose Ethers - A Technical Review. METHOCEL™ - Technical Bulletin. 10-2013

http://www.foodtimeline.org/foodbreads.html. 2018

http://winehistory.com.au/wiki/Wine_History/Ancient_winemaking_spreads_from_Egypt_and_Phoenicia

The History of Ice Cream (2008) http://www.idfa.org/news-views/media-kits/ice-cream/the-history-of-ice-cream

History of Chantilly Cream (2008) ttps://ifood.tv/cream/whipped-cream, 2018).

Introduction to Pop - The History of Soft Drinks (2008) https://www.thoughtco.com/introduction-to-pop-the-history-of-soft-drinks-1991778.

The Amazing History of Soft Drinks.http://brandstories.net/2016/01/15/the-amazing-story-of-soft-drinks/.

Our Best Days Are Yours https://www.kelloggs.com/en_US/who-we-are/our-history.html.

Statistics on Obesity, Physical Activity and Diet (2018) NHS
https://files.digital.nhs.uk/publication/0/0/obes-phys-acti-diet-eng-2018-rep.pdf

http://www.un.org/en/development/desa/population. U.N.: World population to reach 8.1B in 2025.